

Green Chemistry

Cutting-edge research for a greener sustainable future

www.rsc.org/greenchem

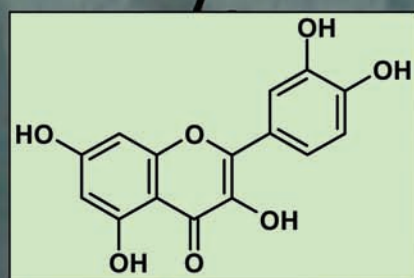
Volume 8 | Number 11 | November 2006 | Pages 929–1008



Remaining
waste



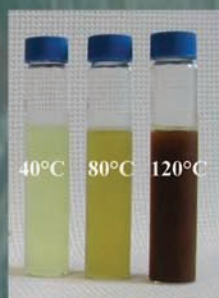
Onion waste



High-value
antioxidant
- quercetin



Subcritical water
extraction



Enzymatic
product
conversion

ISSN 1463-9262

RSC Publishing

Turner *et al.*
Subcritical water extraction and
hydrolysis of quercetin glycosides

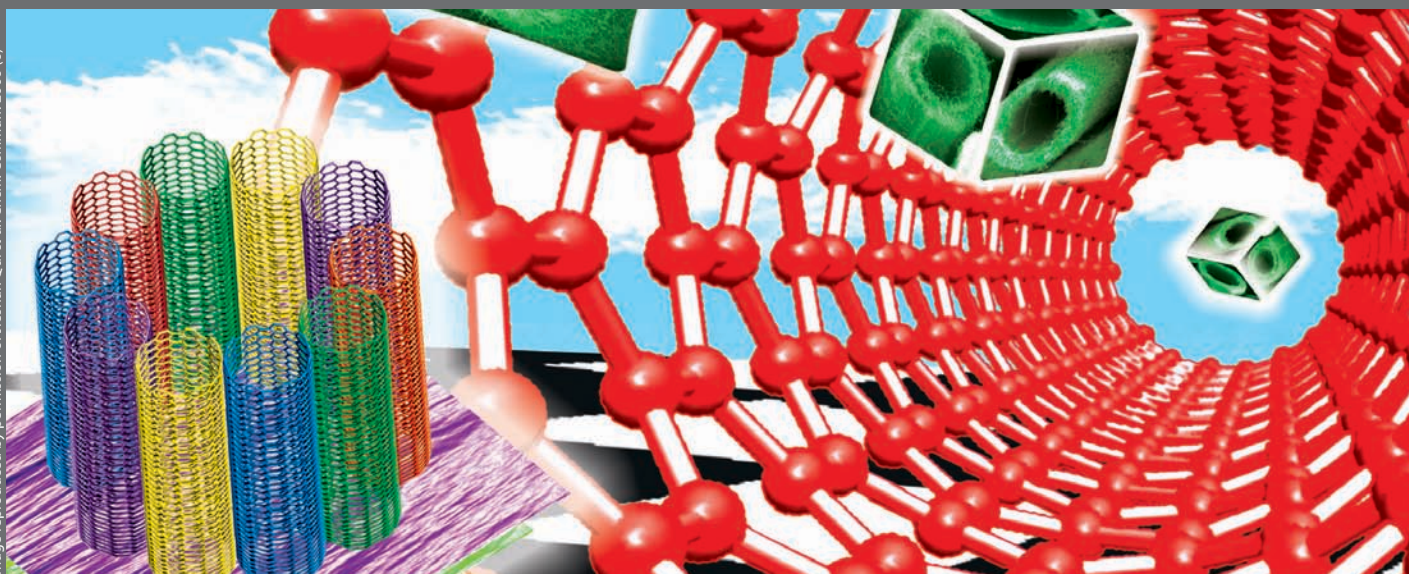
Jain and Sain
Ionic liquid promoted aziridination
of alkenes

Izák *et al.*
Stability and selectivity of a
multiphase membrane

Böing and Minnich
Green chemistry at the 1st European
Chemistry Congress



1463-9262 (2006) 8:11;1-Y



ChemComm

A leading international journal for the publication of communications on important new developments in the chemical sciences.

- Weekly publication
- Impact factor: 4.426
- Rapid publication – typically 60 days
- 3 page communications – providing authors with the flexibility to develop their results and discussion
- More than 40 years publishing excellent research
- High visibility – indexed in MEDLINE



Green Chemistry

Cutting-edge research for a greener sustainable future

www.rsc.org/greenchem

RSC Publishing is a not-for-profit publisher and a division of the Royal Society of Chemistry. Any surplus made is used to support charitable activities aimed at advancing the chemical sciences. Full details are available from www.rsc.org

IN THIS ISSUE

ISSN 1463-9262 CODEN GRCHFJ 8(11) 929-1008 (2006)



Cover

Onion waste is the source of antioxidants in a new procedure based on subcritical water extraction and β -glucosidase-catalyzed conversion of quercetin glycosides to quercetin. Image reproduced by permission of Charlotta Turner, from *Green Chem.*, 2006, **8**(11), 949.

CHEMICAL TECHNOLOGY

T41

Chemical Technology highlights the latest applications and technological aspects of research across the chemical sciences.

Chemical Technology

November 2006/Volume 3/Issue 11

www.rsc.org/chemicaltechnology

NEWS

939

Green chemistry at the 1st European Chemistry Congress

Christian Böing and Clemens B. Minnich recall the Green and Sustainable Chemistry and Processes symposium of the 1st European Chemistry Congress.



EDITORIAL STAFF

Editor

Sarah Ruthven

News writer

Markus Hölscher

Publishing assistant

Emma Hacking

Team leader, serials production

Stephen Wilkes

Technical editor

Edward Morgan

Administration coordinator

Sonya Spring

Editorial secretaries

Lynne Braybrook, Jill Segev, Julie Thompson

Publisher

Emma Wilson

Green Chemistry (print: ISSN 1463-9262; electronic: ISSN 1463-9270) is published 12 times a year by the Royal Society of Chemistry, Thomas Graham House, Science Park, Milton Road, Cambridge, UK CB4 0WF.

All orders, with cheques made payable to the Royal Society of Chemistry, should be sent to RSC Distribution Services, c/o Portland Customer Services, Commerce Way, Colchester, Essex, UK CO2 8HP. Tel +44 (0) 1206 226050; E-mail sales@rscdistribution.org

2006 Annual (print + electronic) subscription price: £859; US\$1571. 2006 Annual (electronic) subscription price: £773; US\$1414. Customers in Canada will be subject to a surcharge to cover GST. Customers in the EU subscribing to the electronic version only will be charged VAT.

If you take an institutional subscription to any RSC journal you are entitled to free, site-wide web access to that journal. You can arrange access via Internet Protocol (IP) address at www.rsc.org/ip. Customers should make payments by cheque in sterling payable on a UK clearing bank or in US dollars payable on a US clearing bank. Periodicals postage paid at Rahway, NJ, USA and at additional mailing offices. Airfreight and mailing in the USA by Mercury Airfreight International Ltd., 365 Blair Road, Avenel, NJ 07001, USA.

US Postmaster: send address changes to Green Chemistry, c/o Mercury Airfreight International Ltd., 365 Blair Road, Avenel, NJ 07001. All despatches outside the UK by Consolidated Airfreight.

PRINTED IN THE UK

Advertisement sales: Tel +44 (0) 1223 432246; Fax +44 (0) 1223 426017; E-mail advertising@rsc.org

Green Chemistry

Cutting-edge research for a greener sustainable future

www.rsc.org/greenchem

Green Chemistry focuses on cutting-edge research that attempts to reduce the environmental impact of the chemical enterprise by developing a technology base that is inherently non-toxic to living things and the environment.

EDITORIAL BOARD

Chair

Professor Martyn Poliakoff,
Department of Chemistry
University of Nottingham,
Nottingham, UK
E-mail martyn.poliakoff@nottingham.ac.uk

Scientific editor

Professor Walter Leitner,
RWTH-Aachen, Germany
E-mail leitner@itmc.rwth-aachen.de

Members

Professor Joan Brennecke,
University of Notre Dame, USA

Dr Janet Scott, Centre for Green
Chemistry, Monash University,
Australia

Dr A Michael Warhurst,
University of Massachusetts,
USA
E-mail michael-warhurst@uml.edu

Professor Tom Welton,
Imperial College, UK
E-mail t.welton@ic.ac.uk

Professor Roshan Jachuck,
Clarkson University, USA
E-mail rjchuck@clarkson.edu

Dr Paul Anastas, Green Chemistry
Institute, USA
E-mail p_anastas@acs.org

Professor Buxing Han, Chinese
Academy of Sciences
E-mail hanbx@iccas.ac.cn

Associate editors

Professor C. J. Li, McGill
University, Canada
E-mail cj.li@mcgill.ca
Professor Kyoko Nozaki
Kyoto University, Japan
E-mail nozaki@chembio-tu-tokyo.ac.jp

INTERNATIONAL ADVISORY EDITORIAL BOARD

James Clark, York, UK
Avelino Corma, Universidad
Politécnica de Valencia, Spain
Mark Harmer, DuPont Central
R&D, USA

Herbert Hugl, Lanxess Fine
Chemicals, Germany
Makato Misono, Kogakuin
University, Japan
Colin Raston,
University of Western Australia,
Australia

Robin D. Rogers, Centre for Green
Manufacturing, USA
Kenneth Seddon, Queen's
University, Belfast, UK
Roger Sheldon, Delft University of
Technology, The Netherlands
Gary Sheldrake, Queen's
University, Belfast, UK
Pietro Tundo, Università ca
Foscari di Venezia, Italy
Tracy Williamson, Environmental
Protection Agency, USA

INFORMATION FOR AUTHORS

Full details of how to submit material for publication in Green Chemistry are given in the Instructions for Authors (available from <http://www.rsc.org/authors>). Submissions should be sent via ReSource: <http://www.rsc.org/resource>.

Authors may reproduce/republish portions of their published contribution without seeking permission from the RSC, provided that any such republication is accompanied by an acknowledgement in the form: (Original citation) – Reproduced by permission of the Royal Society of Chemistry.

© The Royal Society of Chemistry 2006. Apart from fair dealing for the purposes of research or private study for non-commercial purposes, or criticism or review, as permitted under the Copyright, Designs and Patents Act 1988 and the Copyright and Related Rights Regulations 2003, this publication may only be reproduced, stored or transmitted, in any form or by any means, with the prior permission in writing of the Publishers or in the case of reprographic reproduction in accordance with the terms of

licences issued by the Copyright Licensing Agency in the UK. US copyright law is applicable to users in the USA.

The Royal Society of Chemistry takes reasonable care in the preparation of this publication but does not accept liability for the consequences of any errors or omissions.

Ⓢ The paper used in this publication meets the requirements of ANSI/NISO Z39.48-1992 (Permanence of Paper).

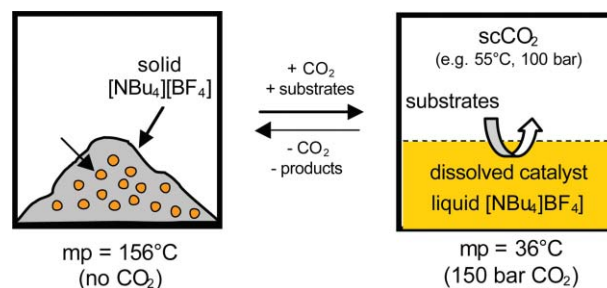
Royal Society of Chemistry: Registered Charity No. 207890

HIGHLIGHT

941

Highlights

Markus Hölscher reviews some of the recent literature in green chemistry.



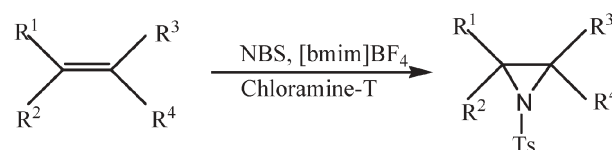
COMMUNICATIONS

943

Ionic liquid promoted highly efficient aziridination of alkenes with Chloramine-T using *N*-bromosuccinimide as catalyst

Suman L. Jain and Bir Sain*

Ionic liquids $[\text{bmim}]\text{BF}_4$ and $[\text{bmim}]\text{PF}_6$ were found to be recyclable reaction media for the aziridination of alkenes in excellent yields and at high rates using Chloramine-T as nitrene donor and NBS as catalyst.

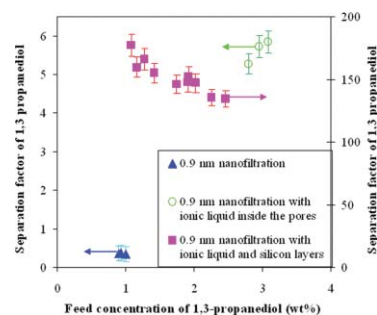


947

Stability and selectivity of a multiphase membrane, consisting of dimethylpolysiloxane on an ionic liquid, used in the separation of solutes from aqueous mixtures by pervaporation

Pavel Izák,* Martin Köckerling and Udo Kragl

A multiphase membrane consisting of a novel ionic liquid coated by dimethylpolysiloxane shows a high selectivity and stability for the separation of 1,3-propanediol from aqueous mixtures by vacuum pervaporation.



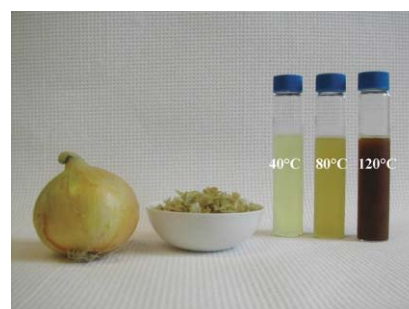
PAPERS

949

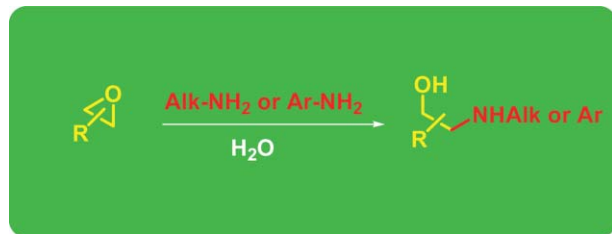
Subcritical water extraction and β -glucosidase-catalyzed hydrolysis of quercetin glycosides in onion waste

Charlotta Turner,* Pernilla Turner, Gunilla Jacobson, Knut Almgren, Monica Waldebäck, Per Sjöberg, Eva Nordberg Karlsson and Karin E. Markides

A “green” procedure to isolate valuable antioxidants—the raw material is onion waste, the extraction process uses only water as a solvent, and the hydrolysis reaction is catalyzed by enzymes.



960

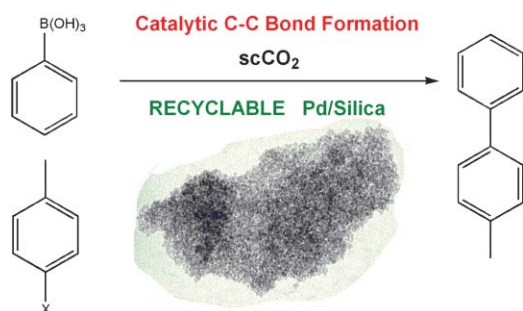


A green route to β -amino alcohols via the uncatalyzed aminolysis of 1,2-epoxides by alkyl- and arylamines

Simona Bonollo, Francesco Fringuelli,* Ferdinando Pizzo* and Luigi Vaccaro

Under mildly basic and pH-controlled aqueous conditions the aminolysis of 1,2-epoxides **1a–g** by alkyl- and arylamines **2a–k** is generally highly regioselective giving the corresponding β -amino alcohols in satisfactory to excellent yields.

965

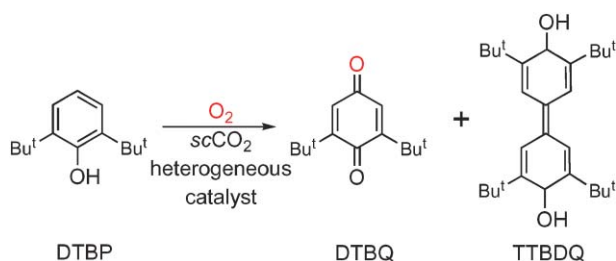


Formation and catalytic activity of Pd nanoparticles on silica in supercritical CO₂

Shohreh Saffarzadeh-Matin, Francesca M. Kerton,* Jason M. Lynam and Christopher M. Rayner

Recyclable, catalytically active palladium particles on silica were formed in supercritical carbon dioxide. During Heck and Suzuki reactions, the catalyst could be reused four times and no Pd leaching was observed.

972

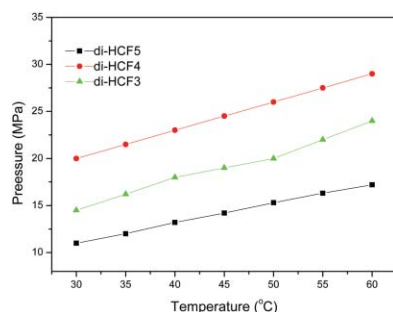


Immobilized metal complexes in porous hosts: catalytic oxidation of substituted phenols in CO₂ media

Sarika Sharma, Boris Kerler, Bala Subramaniam* and A. S. Borovik*

The highest conversion to products (~60%) is achieved in supercritical CO₂ (*scCO*₂) using dioxygen and a porous heterogeneous catalyst containing immobilized Co(II) sites.

978



Phase behavior of novel fluorinated surfactants in supercritical carbon dioxide

Zhao-Tie Liu,* Jin Wu, Ling Liu, Liping Song, Ziwei Gao, Wensheng Dong and Jian Lu

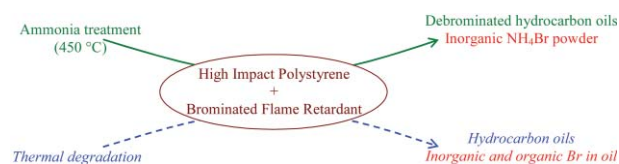
Four fluorinated surfactants were synthesized, and their properties and phase behaviors in water-in-CO₂ microemulsions were investigated.

984

Novel debromination method for flame-retardant high impact polystyrene (HIPS-Br) by ammonia treatment

Mihai Brebu* and Yusaku Sakata

Ammonia is an effective bromine scavenger during thermal degradation of flame-retardant high impact polystyrene (HIPS-Br). The process can be used for bromine recovery and feedstock recycling of plastic waste.

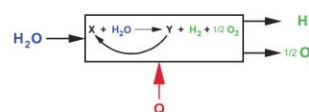


988

Limiting thermodynamic efficiencies of thermochemical cycles used for hydrogen generation

B. C. R. Ewan* and R. W. K. Allen

The production of chemical free energy by water splitting is a goal of thermochemical cycles. Some of these are examined in detail to provide a comparison with other heat-to-work processes.

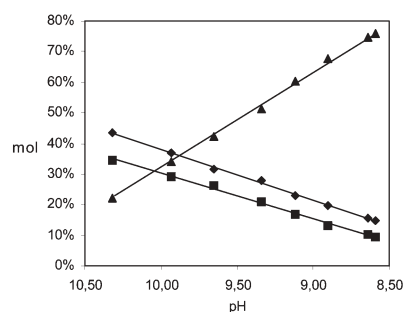


995

CO₂ absorption by aqueous NH₃ solutions: speciation of ammonium carbamate, bicarbonate and carbonate by a ¹³C NMR study

Fabrizio Mani,* Maurizio Peruzzini and Piero Stoppioni

¹³C NMR spectroscopy provides a straightforward, simple, and reliable method to evaluate the relative amounts of NH₂CO₂⁻ (◆), HCO₃⁻ (▲), and CO₃²⁻ (■) which form in the aqueous ammonia process for CO₂ capture.

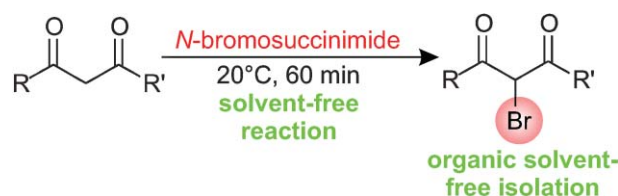


1001

Solvent-free bromination of 1,3-diketones and β-keto esters with NBS

Igor Pravst, Marko Zupan and Stojan Stavber*

Solvent-free brominations of 1,3-diketones and β-keto esters with NBS were performed, and a work-up procedure using only water to remove succinimide was employed.



AUTHOR INDEX

Almgren, Knut, 949
 Böing, Christian, 939
 Bonollo, Simona, 960
 Borovik, A. S., 972
 Brebu, Mihai, 984
 Dong, Wensheng, 978
 Ewan, B. C. R., 988
 Fringuelli, Francesco, 960
 Gao, Ziwei, 978
 Izák, Pavel, 947
 Jacobson, Gunilla, 949

Jain, Suman L., 943
 Karlsson, Eva Nordberg, 949
 Kerler, Boris, 972
 Kerton, Francesca M., 965
 Köckerling, Martin, 947
 Kragl, Udo, 947
 Liu, Ling, 978
 Liu, Zhao-Tie, 978
 Lu, Jian, 978
 Lynam, Jason M., 965
 Mani, Fabrizio, 995

Markides, Karin E., 949
 Minnich, Clemens B., 939
 Peruzzini, Maurizio, 995
 Pizzo, Ferdinando, 960
 Pravst, Igor, 1001
 Rayner, Christopher M., 965
 Saffarzadeh-Matin, Shohreh,
 965
 Sain, Bir, 943
 Sakata, Yusaku, 984
 Sharma, Sarika, 972

Sjöberg, Per, 949
 Song, Liping, 978
 Stavber, Stojan, 1001
 Stoppioni, Piero, 995
 Subramaniam, Bala, 972
 Turner, Charlotta, 949
 Turner, Pernilla, 949
 Vaccaro, Luigi, 960
 Waldebäck, Monica, 949
 Wu, Jin, 978
 Zupan, Marko, 1001

FREE E-MAIL ALERTS AND RSS FEEDS


Contents lists in advance of publication are available on the web *via* www.rsc.org/greenchem - or take advantage of our free e-mail alerting service (www.rsc.org/ej_alert) to receive notification each time a new list becomes available.

RSS Try our RSS feeds for up-to-the-minute news of the latest research. By setting up RSS feeds, preferably using feed reader software, you can be alerted to the latest Advance Articles published on the RSC web site. Visit www.rsc.org/publishing/technology/rss.asp for details.

ADVANCE ARTICLES AND ELECTRONIC JOURNAL

Free site-wide access to Advance Articles and the electronic form of this journal is provided with a full-rate institutional subscription. See www.rsc.org/ejs for more information.

* Indicates the author for correspondence: see article for details.

 Electronic supplementary information (ESI) is available *via* the online article (see <http://www.rsc.org/esi> for general information about ESI).

RSC online shop now open

And to celebrate we're having a sale...

From best selling textbooks, to games and puzzles, the RSC online shop brings you class-leading products and services from the RSC. Each sale helps us continue our work in advancing the chemical sciences. Shop online during November and December and get a huge **25% discount*** on all books, puzzles/games, videos or wall charts purchased.

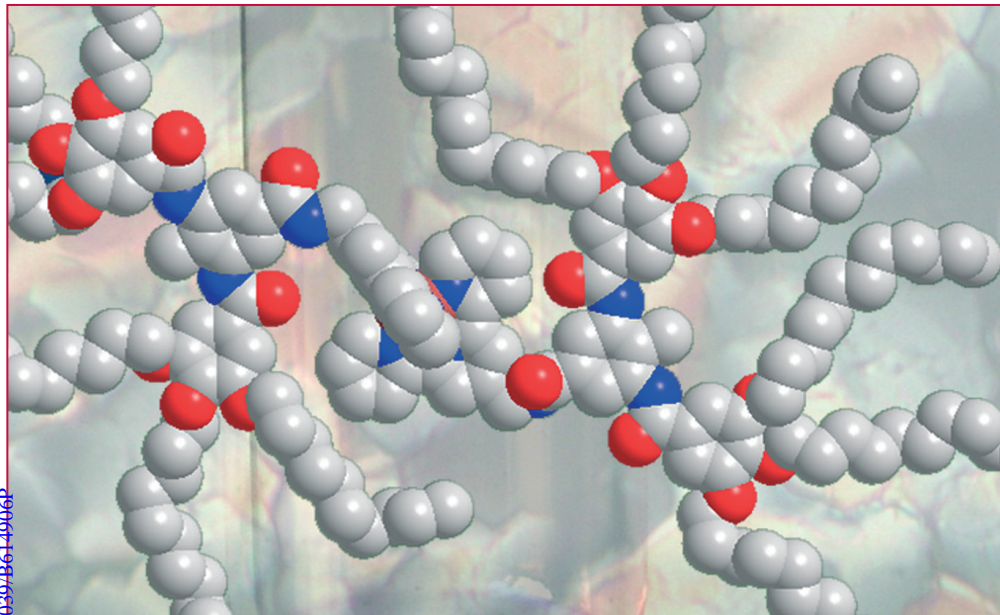
* Discount applied to your purchases when you check out. Offer ends December 31st, 2006

RSC Advancing the
Chemical Sciences

www.rsc.org/shop

Registered Charity Number: 207890

04100607



The home of new and emerging multidisciplinary work in the chemical sciences

Owned and published by learned societies

NJC (New Journal of Chemistry) publishes high-quality, original and significant work that is of wide general appeal – articles can be letters, full papers, opinions and perspectives. With an Impact factor of 2.574, fast publication and international readership, NJC is the perfect choice for multidisciplinary work from areas including: supramolecular chemistry; chemistry for materials and applications; catalysis; chemistry for biology and medicine; chemistry of polymers and dendrimers; organic synthesis of complex molecules; chemical physics and theory.

Take a look at these examples of recently published papers:

Weak paramagnetism in compounds of the type $Cp^*_2Yb(bipy)$

Marc D. Walter, Madeleine Schultz, Richard A. Andersen (USA)

A phen-terpy conjugate whose chelate coordination axes are orthogonal to one another and its zinc complex

Benoît Champin, Valérie Sartor, Jean-Pierre Sauvage (France)

A catalyst for an acetal hydrolysis reaction from a dynamic combinatorial library

Laurent Vial, Jeremy K. M. Sanders, Sijbren Otto (UK)

The first total synthesis of aeruginosamide

Zhiyong Chen, Tao Ye (China)

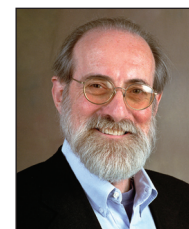
Molecular knots, links, and fabrics: prediction of existence and suggestion of a synthetic route

Dirk Andrae (Germany)

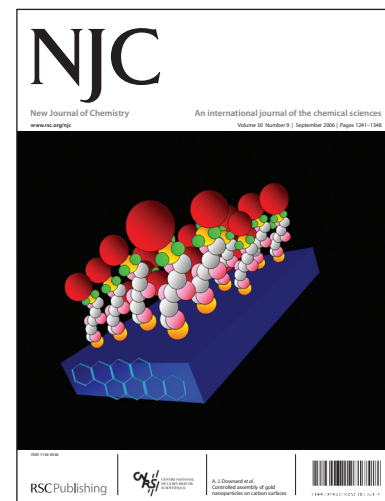
The international Editorial Board is led by:



Jean-Pierre Majoral
Co-Editor-in-Chief
Toulouse, France



Jerry Atwood
Co-Editor-in-Chief
Columbia, USA



Submit your work today at www.rsc.org/resource

Registered Charity Number: 207890

RSC Publishing



www.rsc.org/njc

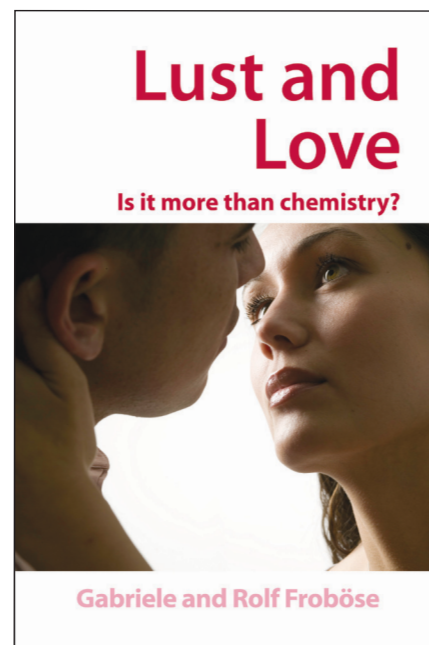
Lust and Love

Is it more than chemistry?

By Gabriele and Rolf Froböse

**Why do people fall in love? Why do we find some people attractive?
How does our physiology affect the way we feel?**

Lust and Love: Is it more than chemistry? provides answers to some of these questions through the eyes of science. Covering research from the fields of chemistry, biochemistry, neurology, psychiatry, psychology, physics and medicine the book looks at our current knowledge of the science behind these feelings.



Explores the science behind love, sex and passion

Hardback | 2006 | xii + 170 pages | £24.95 | RSC Member Price £16.50 | ISBN 10: 0 85404 867 7
ISBN 13: 978 0 85404 867 0

Registered Charity Number: 207890

RSC Publishing

www.rsc.org/lustandlove

Green chemistry at the 1st European Chemistry Congress

DOI: 10.1039/b614462b

Christian Böing and Clemens B. Minnich recall the *Green and Sustainable Chemistry and Processes* symposium of the 1st European Chemistry Congress.

Between August 27th and 31st, 2006 the 1st European Chemistry Congress was held in Budapest. It was organised by the European Association for Chemical and Molecular Sciences (EuCheMS) and featured a broad spectrum of chemistry topics covered through five plenary lectures by nobel laureates and ten special topic symposia. One of these symposia, organised by *Walter Leitner* (RWTH Aachen University, Aachen, Germany) and *István Horváth* (Eötvös University, Budapest, Hungary) and sponsored by BASF AG, focused on *Green and Sustainable Chemistry and Processes*. Since it was impossible to address all aspects of green chemistry within two days, the focus was clearly set on chemical reactions and processes. The organisers were able to invite a number of leading scientists as well as young researchers to present their recent work in that field. The symposium was well recognised by the attendees of the congress, so most of the time the lecture hall was filled completely or even overcrowded (see picture) with more than 150 listeners following stimulating talks about cutting edge research and innovation from academia as well as from industry.

After a short introduction by the symposium chairman *Walter Leitner*, *Roger Sheldon* (TU Delft, Delft, Netherlands) opened the first session with his lecture about “Multistep Catalytic Cascade Processes for Sustainable Organic Synthesis”. He reported on his recent work on one pot processes using a combination of chemocatalytic methods with biocatalysts. His group succeeded in overcoming the well known problem of incompatibility of the required surroundings for chemical catalysts and enzymes by means of compartmentalisation techniques. In particular, the coupled immobilisation of lipases for the racemisation and

deacylases for the hydrolysis of amides was presented (preparation of cross-linked enzymatic aggregates, CLEA). Furthermore, he showed highly elegant ways for the production of chiral alcohols and amines.

The second invited lecture given by *Peter Saling* (BASF AG, Ludwigshafen, Germany) was entitled “Strategies for Sustainable Development of Chemical Synthesis with the Eco-Efficiency Analysis and SEE-Balance”. He showed how BASF AG estimates the sustainability of a process by using the eco-efficiency analysis and SEE-balance. The eco-efficiency analysis was developed as a tool to visualise environmental and cost factors to decision makers, and leads to a fingerprint of a process already in an early phase of process design. As an example he compared the BASIL process, which utilises the easy separation of an ionic liquid by-product from a reaction mixture, with the original process

that instead leads to the formation of a solid ammonium salt. It was clearly shown that the BASIL process, which is well recognised in the green chemistry community, is superior to the traditional process. Finally the SEE-balance tool was introduced where societal aspects of the process are also included.

The second session of the first day continued with a lecture from industry. *Keith W. Hutchenson* (DuPont Central Research and Development, Wilmington, DE, USA) reported on “Sustainable Products and Processes from Biorenewables at DuPont”. He pointed out that DuPont committed themselves to gather 25% revenue from renewables in 2010. A key project to fulfil this target is the development of a so-called “Integrated Corn-Based BioRefinery” (ICBR), which allows the production of alternative fuels, such as bioethanol, or chemicals from renewable sources. The ICBR can convert corn grain into fermentable sugars for the production of value added products. Another example is the production of 1,3-propanediol, a building block for polyester synthesis (commercialised under the trade name Sonora), from glycerol feedstock. Levulinic acid is another important building block and platform molecule for DuPont’s strategy, and this can be synthesised from cellulose in a commercially viable way as exemplified by the Biofine process that started operation most recently in Italy.

The last invited lecture of the first day was given by *Romy Neumann* from the Weizmann Institute (Rehovot, Israel) on the “Activation of Molecular Oxygen by Binary Polyoxometalate Containing Catalysts”. He demonstrated his concept of using organometallic polyoxometalate or nanoparticle-polyoxometalate hybrid catalysts in oxidation reactions with molecular oxygen as the oxidant. This was exemplified by the aerobic oxidation



Fig. 1 Crowded lecture hall during a session (photo: László T. Mika).

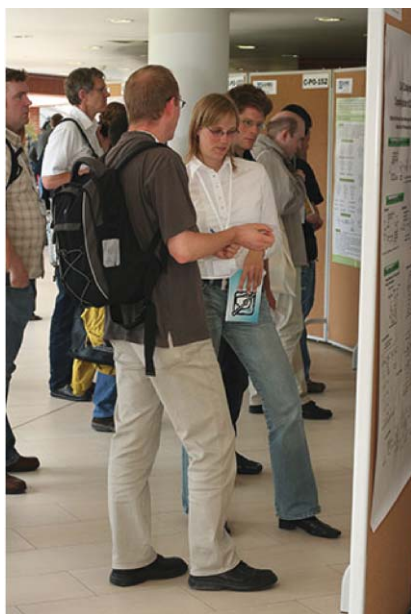


Fig. 2 Discussions in front of the posters (photo: László T. Mika).

of methane to methanol and acetaldehyde, by the aerobic epoxidation of alkenes, as well as the oxidative dehydrogenation of alkenes to alkanes.

After the last lecture of the first day, the poster session started and, despite the fact that it was located in another building, a lively discussion between the attendees started and contributed to the positive impression of the symposium.

The second day of the symposium was opened by the keynote lecture of *Walter Leitner* (RWTH Aachen University, Aachen, Germany). It was a general feature of the congress that the organiser of a special topic symposium also gave the appending keynote lecture. He presented the recent progress in utilising supercritical carbon dioxide in combination with water, poly(ethylene)glycol and ionic liquids as advanced solvent systems for catalysis. Techniques for catalyst immobilisation and continuous-flow operations with organometallic, nano-scale as well as organic catalysts

were discussed. He completed his talk with the enantioselective aza-Baylis–Hillman reaction catalysed by an achiral Lewis base in a chiral ionic liquid, providing the first example of high level chiral induction by a reaction solvent.

Shu Kobayashi (The University of Tokyo, Tokyo, Japan) described his recent work on “Lewis Acid Catalysis in Aqueous Media” and addressed the water compatibility of different Lewis acidic rare earth metals, and in particular bismuth complexes. He has developed Lewis acid catalysts based on $\text{Bi}(\text{OTf})_3$ in combination with chiral bipyridine ligands for asymmetric reactions in water. Furthermore, his group stabilised scandium-based Lewis acidic catalysts on homogeneous and heterogenised long-chain alkyl sulfonates. During this talk a multitude of impressive results were shown, and the speaker was able to convince the audience that water plays a key role in Lewis acid catalysis.

Dieter Vogt (TU Eindhoven, Eindhoven, The Netherlands) was given the opportunity to present the closing lecture of the symposium, and he talked about the “Immobilisation and Compartmentalisation of Homogeneous Catalysts” in “Shades of green”. After talks on heterogeneous systems and catalyst immobilisation in biphasic media, this presentation addressed catalyst recycling with membrane techniques. Dendritic catalysts were used to ensure that the catalyst is held back by the membrane. In the second part of his lecture Vogt showed his recent work on emulsified borate containing submicron particles as support for cationic homogeneous catalysts and their application in the rhodium catalysed hydrogenation.

Apart from the keynote and invited lectures described above, a variety of outstanding short oral contributions and poster appetisers given by young researchers and students were



Fig. 3 The BASF Prize for Sarah L. Poe (photo: André Mortreux).

contributed to the symposium. To recognise these, the Green Chemistry journal and BASF AG sponsored a prize for the best oral contribution by a young scientist and for the best poster presentation by a student, respectively. *Federica Zaccheria* (Università degli Studi di Milano, Milan, Italy) was awarded the Green Chemistry Prize for the best oral contribution and received a free one-year subscription to Green Chemistry. In her lecture, she presented her recent work on “Selective Transfer Dehydrogenation of Non-activated Alcohols over $\text{Cu}/\text{Al}_2\text{O}_3$ ”. The BASF poster prize was given to *Sarah L. Poe* (Cornell University, Ithaca, NY, USA) for her excellent poster about the development and application of a one-pot Henry reaction/Michael addition cascade.

All in all, the special topic symposium on *Green and Sustainable Chemistry and Processes* was a full success, and we are looking forward to a similarly focused symposium as part of the 2nd European Chemistry Congress in Torino 2008!

Christian Böing and **Clemens B. Minnich**.

Institut für Technische und Makromolekulare Chemie, RWTH Aachen University, Germany. *E-mail:* boeing@itmc.rwth-aachen.de, minnich@itmc.rwth-aachen.de.

Highlights

DOI: 10.1039/b614465a

Markus Hölscher reviews some of the recent literature in green chemistry.

Biphasic catalysis with high-melting ionic liquids in the presence of CO₂—rational exploitation of melting point depression

Ionic liquids have received considerable attention over the past few years as they can be potentially used as green solvents. However, to be useful in catalytic applications the ionic liquid should be a liquid at low temperatures, which is one of the original criteria that define an ionic liquid. As many organic salts consisting of an organic cation and an organic/inorganic anion exist which have high melting points, they cannot be used as ILs even though they might be very useful. Leitner and Scurto,¹ from RWTH Aachen University, have very recently exploited the depression of melting points in the presence of carbon dioxide. A variety of organic salts with melting points between moderate and high temperatures were slowly heated in the presence of CO₂ (150 bar for most experiments), and the onset of the melting process was inspected visually (Fig. 1). Interestingly, in all cases a significant depression of the melting points was observable, ranging between 20 and 120 °C.

As an example, tetrabutylammonium tetrafluoroborate [NBu₄][BF₄], which under ambient pressure in the absence of CO₂ melts at ca. 160 °C, was found to melt at 36 °C. As a result the otherwise solid compound is available for chemical reactions and was used as a prototype for the evaluation of catalytic performance. As a test reaction, 2-vinylnaphthalene was tested in hydrogenations, hydroborations and hydroformylations in the presence of common rhodium catalysts. For the hydroboration and hydroformylation, the conversions were found to be quantitative, while for the hydrogenation conversion was about 92%. Recycling of the catalyst is also possible, as was shown for the hydrogenation.

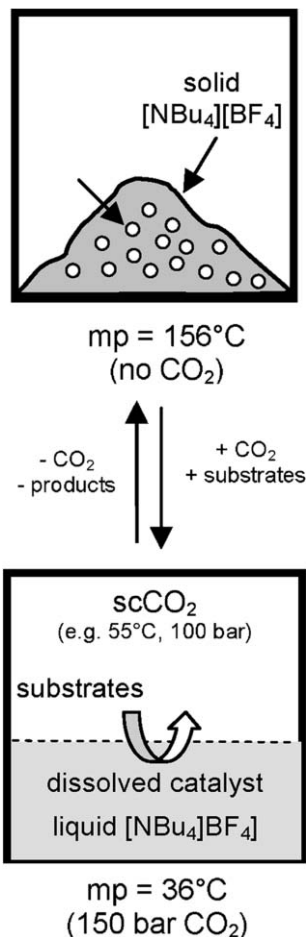


Fig. 1 CO₂-induced melting point depression to generate ionic liquids.

Taking micelles for a ride—thermoreversible transportation of polymer micelles between an ionic liquid and water

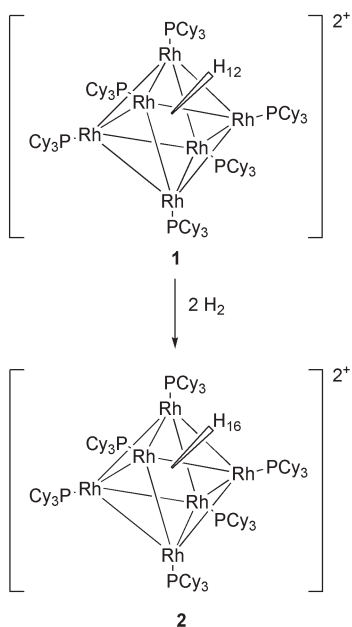
Whenever chemists think of wrapping something up, *i.e.* to shield it from unwanted influences, and transporting it to another place, with the parcel needing to travel through quite different chemical surroundings, they usually think of micelles as both the present paper and shuttle bus. Drug delivery vehicles are a common example for such applications. To date most systems only show one way transportation, while it would be

interesting to make chemical compounds as drugs or nanoparticles to be able to move back and forth between different chemical environments. Very recently He and Lodge,² from the University of Minnesota, developed block copolymers which enable round trips between an ionic liquid phase and a water phase. In self-assembly processes of polymer poly-((1,2-butadien)-block-ethylene oxide) (PB-PEO), appropriate micelles can be generated which show different solubilities in ionic liquids and water, depending on the temperature. The PEO block is soluble in water and the ionic liquid studied (1-butyl-3-methylimidazolium hexafluorophosphate [BMIM][PF₆]), while the PB blocks segregate into micellar cores. The polymer firstly was dissolved in the ionic liquid. Water was added and, as the IL and water are immiscible, two phases formed. By equilibration at ambient temperature supported by gentle agitation, the formed micelles resided in the aqueous phase. On heating the mixture to 75 °C, the micelles leave the aqueous phase and travel into the IL phase in which they remain up to 90 °C. Cooling down the mixture to ambient temperature reversed the travelling process, after which the micelles again resided in the aqueous phase. These results nicely prove the concept of micelles that can be moved around in an intact form between different phases and chemical environments.

Molecular rhodium clusters as hydrogen storage materials with redox switchability for H₂ uptake and loss

Provided hydrogen can be supplied in a clearly sustainable way in the future, the usage of H₂ as fuel, *e.g.* for automobiles, would significantly help in reducing CO₂ emissions and saving on fossil fuels in general. Within this context hydrogen storage materials are currently under intense investigation, as storing and releasing H₂ under practical conditions

is not an easy task. Weller *et al.*,³ from the University of Bath, undertook an investigation of molecular rhodium clusters with regard to H₂ storage and releasing behaviour and obtained some remarkable results. Dicationic rhodium cluster **1** was found to have a modest HOMO–LUMO gap, which suggested the compound could easily take up four more electrons.



The authors showed that these four electrons can easily be introduced into the cluster by adding two H₂ molecules to it, resulting in complex **2**. Interestingly the H₂ uptake is facile both in solution and in the solid state. Product **2** retains the H₂ absorbed for weeks with no

partial pressure of H₂, under conditions which could be useful in practical applications (1 atm Ar, 298 K). Cluster **2** can be oxidized chemically or electrochemically, which re-generates the starting complex **1**. As a result, in solution a complete uptake/release cycle can be obtained. The storage capacity is still very low, as the cluster and associated anions have a large mass compared to the mass of hydrogen. On the other hand it is unique in the way that H₂ storage is possible without the need of having a H₂ atmosphere at increased pressures.

Environmental kids club

In numerous publications, including this one, it has been repetitiously made very clear that politicians, entrepreneurs and every private individual (to name three important groups) should reconsider the way mankind is currently living (*e.g.* production and usage of energy). As the problems to overcome are complex (scientific, economic and political challenges), more adults need to think of the planet's resources and their use of them differently from the preceding generations in order to reshape modern industrial societies. But how about the following generations? Shouldn't children grow up with an awareness of these complex interactions? According to the environmental protection agency of the U.S. (EPA) they should (<http://www.epa.gov>). The EPA not only runs a website with information from all fields relevant to green topics (science,

economy, politics), it also maintains a variety of pages accessible following the link "For Kids" which brings much more information to the next generation than high school teachers can cover, even if they were to give numerous courses. Impressively 17 sub-links easily create an initial glance at the complexity of green topics while further websites explain some of the most important issues (*e.g.* greenhouse gases, garbage and recycling, water consumption). Some interactions are both simple and scary: by the end of this century, global warming, if unaddressed, is expected to ruin most of the coral reefs, which in turn destroys the initial parts of the ocean food chain. From here on the threads are spun further, helping everybody to see that the earth's species cannot live in isolation, but belong to closed cycles, which are interdependent. Teachers are also addressed and helped with information and input to create stimulating and successful lessons. And—very importantly—the necessary motivation for everyone who wants to change for the better is also generated: we can do something! Isn't this the message we all need?

References

- 1 A. M. Scurto and W. Leitner, *Chem. Commun.*, 2006, 3681–3683.
- 2 Y. He and T. P. Lodge, *J. Am. Chem. Soc.*, 2006, DOI: 10.1021/ja0655587.
- 3 S. K. Brayshaw, J. C. Green, N. Hazari, J. S. McIndoe, F. Marken, P. R. Raithby and A. S. Weller, *Angew. Chem.*, 2006, **118**, 6151–6154.

Ionic liquid promoted highly efficient aziridination of alkenes with Chloramine-T using *N*-bromosuccinimide as catalyst

Suman L. Jain and Bir Sain*

Received 12th April 2006, Accepted 27th July 2006

First published as an Advance Article on the web 10th August 2006

DOI: 10.1039/b605294k

Ionic liquids [bmim]BF₄ and [bmim]PF₆ were found to be recyclable reaction media as well as promoters for the aziridination of alkenes in excellent yields at a faster rate than previously reported methods using Chloramine-T as nitrene donor and NBS as catalyst under mild reaction conditions.

Aziridines, are highly important synthetic intermediates that are widely used as chiral auxiliaries or ligands in asymmetric synthesis, present as important structural motifs in natural products in which they show potent and diverse biological activities.¹ Various biologically important compounds such as amino acids, β -lactam, antibiotics and alkaloids are derived from aziridines.² Although the formation of aziridines from the addition of thermally or photochemically generated nitrenes to olefins is a well-known reaction, its utility is limited due to low yields and competing hydrogen abstraction and insertion reactions.³ Transition metal catalyzed reaction of *in situ* generated nitrene with olefins is an efficient and practical method for the preparation of aziridines and has received considerable attention in recent years. In this context [N-(*p*-tolylsulfonyl)imino] phenyliodine (PhI=NTs)⁴ has been widely used as a nitrene precursor for the aziridination of alkenes in the presence of several transition metal based catalysts.⁵ However, there are drawbacks with the use of PhI=NTs as a nitrene precursor,⁶ it is expensive, yields iodobenzene in equimolar amounts and oxygenated hydrocarbons are dominant by-products. Therefore, in recent years several improved methodologies using Chloramine-T as a cheap and convenient nitrene precursor have been explored in the literature.⁷ However these methods suffer from drawbacks such as use of expensive and heavy transition metals as catalyst, toxic and volatile organic solvents as reaction media, large excess of olefins and lower yields of the isolated aziridines.

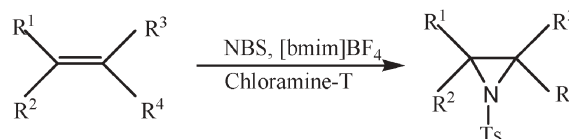
In recent years the room temperature ionic liquids owing to their unique properties such as non-volatile nature, higher solvating ability to great number of organic and inorganic compounds, high thermal stability, reusability and recyclability have been acknowledged as eco-friendly alternatives to the toxic and volatile organic solvents in various organic reactions such as Diels–Alder, Heck, alkylation, cyclopropanation, epoxidation and mannich reaction *etc.*⁸ However to the best of our knowledge there is only one literature report on the use of ionic liquids as green reaction media for the aziridination of alkenes using PhI=NTs as nitrene precursor and Cu(acac)₂ as catalyst.⁹ Herein we report for the first time the use of ionic liquids as recyclable reaction media as well as promoter for the aziridination of alkenes using Chloramine-T as

nitrene donor and *N*-bromosuccinimide (NBS) as catalyst at room temperature (Scheme 1).

At first we studied the aziridination of 4-methylstyrene (1 mmol) with Chloramine-T (1 mmol) in [bmim]BF₄ ionic liquid without using any catalyst at room temperature. We thought that due to the greater polarity of ionic liquids, it would enable polarization of the Chloramine-T in the absence of any catalyst, albeit the reaction was found to be slow and gave poor yield of the corresponding aziridine as shown in Table 1 (entry 1). Further, when we carried out the aziridination of 4-methylstyrene using Chloramine-T in 1 : 1 ratio in the presence of a catalytic amount of NBS under similar reaction conditions, the reaction was completed within 1 h and gave *N*-(*p*-tolylsulfonyl)-2-(*p*-methylphenyl)aziridine in 90% yield (Table 1, entry 2). The aziridine from the reaction mixture could be selectively separated by extraction with diethyl ether leaving the ionic liquid, succinimide and NaCl as residue. The residue was diluted with ethyl acetate and the insoluble succinimide and NaCl from the reaction mixture separated by filtration. The ethyl acetate was evaporated under reduced pressure and the ionic liquid was recovered and reused further three times for the aziridination of 4-methyl styrene, affording similar yields to the aziridine (Table 2).

The reaction was generalized by reacting a series of aliphatic and aromatic alkenes using Chloramine-T as nitrene precursor in 1 : 1 ratio and NBS (10 mol%) as catalyst in [bmim]BF₄ reaction media.¹⁰ These results are summarized in Table 1 and indicate clearly that aromatic substituted alkenes afforded better yields of aziridines as compared to aliphatic and alicyclic alkenes. Furthermore, aromatic substituted alkenes bearing electron-donating groups on the benzene ring were found to be more reactive (Table 1, entries 2 and 5).

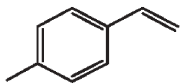
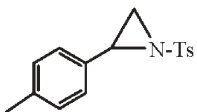
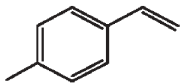
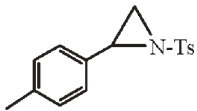
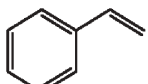
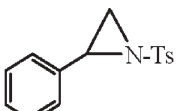
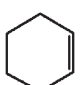
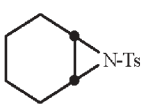
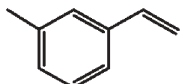
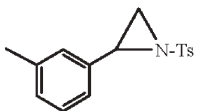
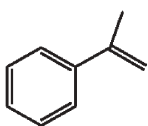
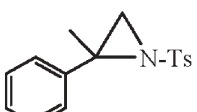
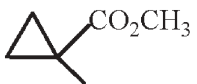
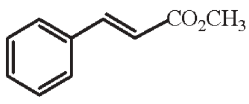
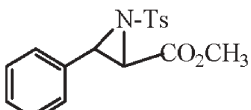
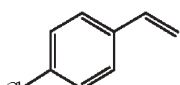
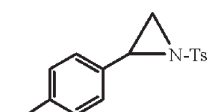
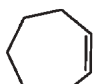

To compare the efficiency of this method, aziridination of 4-methylstyrene was carried out under similar reaction conditions in different solvents such as acetonitrile, [bmim]BF₄, [bmim]PF₆ and nitromethane (Table 1, entry 2). In general the reaction was found to be faster in ionic liquids than conventional solvents such as acetonitrile and nitromethane. However, both ionic liquids [bmim]BF₄ and [bmim]PF₆ showed similar reactivity for the aziridination of alkenes. It is assumed that this enhanced reactivity of NBS in the ionic liquid could be due to the increased polarization of the N–Br bond in the more polar ionic liquid,



Scheme 1

Chemical and Biotechnology Division, Indian Institute of Petroleum, Dehradun, 248005, India. E-mail: birsain@iip.res.in

Table 1 Ionic liquid promoted aziridination of olefins with Chloramine-T using NBS as catalyst^a

Entry	Olefin	Aziridine	Reaction time/h	Yield (%) ^{b,c}	mp/°C ^{5e}
1			6.5	40	
2			1.0	90, 62, ^d 65, ^e 88 ^f	135–6
3			4.5	75	85–86
4			2.5	75	54–55
5			1.5	88	130–1
6			1.0	92	80–82
7	CH ₂ =C(CH ₃)CO ₂ CH ₃		3.0	62	Oil
8			3.0	65	43.5
9			2.5	80	111–2
10			3.0	67	87–88

^a Reaction conditions: Substrate (1 mmol), Chloramine-T (1 mmol), NBS (10 mol%), [bmim]BF₄ (1 ml) at room temperature. ^b Isolated yields. ^c All the products were characterized by using IR and ¹H NMR. ^d Experiment carried out using acetonitrile as solvent. ^e Experiment carried out using nitromethane as solvent. ^f Experiment carried out using [bmim]PF₆ as solvent.

Table 2 Results of reuse of ionic liquid [bmim]BF₄^a

Entry	Substrate	Run	Yield ^b (%)
1	4-Methylstyrene	1	90
2	4-Methylstyrene	2	90
3	4-Methylstyrene	3	88

^a 1 mmol of substrate, 1 mmol of Chloramine-T in 1 ml of [bmim]BF₄ in the presence of 10 mol% NBS at room temperature; reaction time 1.0 h. ^b Isolated yield.

facilitating the formation of the bromonium ion, leading to the observed enhanced reactivity. The avoidance of volatile organic solvents combined with increased reaction rates, ease of recovery and reuse of this novel reaction media will make this protocol more environmentally friendly for the synthesis of aziridines.

In summary, we have described the use of ionic liquids [bmim]BF₄ and [bmim]PF₆ as recyclable reaction media as well as promoters for the aziridination of alkenes with Chloramine-T

using a catalytic amount of NBS in excellent yields within very short reaction times. The considerably enhanced reactivity due to the greater polarization of NBS in ionic liquid, use of inexpensive transition metal free catalyst, simple reaction conditions, high reaction rates, excellent yields of aziridines as compared to those obtained using Chloramine-T in conventional organic solvents make this procedure useful and attractive for aziridination of alkenes.

Experimental

The melting points were determined in open-capillaries on a Buchi apparatus and are uncorrected. The ^1H NMR spectra were recorded on 300 MHz instrument and the chemical shifts are expressed in δ parts per million relative to tetramethylsilane (TMS) as the internal standard. The IR spectra were recorded on a Perkin-Elmer FTIR X 1760 instrument.

Product characterization data

***N*-(*p*-Tolylsulfonyl)-2-(*p*-methylphenyl)aziridine (Table, entry 2).** mp 135–136 °C (Lit. 136–137 °C);^{5e} IR (cm^{-1}) 3034, 1600, 1516, 1360, 1158; ^1H NMR (δ ppm) 2.30 (s, 3H), 2.36 (d, $J = 4.2$ Hz, 1H), 2.42 (s, 3H), 2.96 (d, 7.16 Hz, 1H), 3.73 (dd, 7.16, 4.2 Hz, 1H), 7.33–7.09 (m, 6H), 7.87 (d, 2H).

***N*-(*p*-Tolylsulfonyl)-2-phenylaziridine (Table, entry 3).** mp 85–86 °C (Lit. 86–87 °C);^{5e} IR (cm^{-1}) 3017, 1600, 1520, 1327, 1162; ^1H NMR (δ ppm) 2.38 (d, $J = 4.5$ Hz, 1H), 2.43 (s, 3H), 2.98 (d, $J = 7.2$ Hz, 1H), 3.77 (dd, $J = 7.2, 4.5$ Hz, 1H), 7.27–7.33 (m, 7H), 7.86 (d, 2H).

***N*-(*p*-Tolylsulfonyl)-7-azabicyclo[4.1.0] heptane (Table, entry 4).** mp 54–55 °C (Lit. 55–56 °C);^{5e} IR (cm^{-1}) 3020, 2950, 1598, 1305, 1155; ^1H NMR (δ ppm) 1.20–1.35 (m, 4H, ring CH), 1.75–1.90 (m, 4H, ring CH), 2.42 (s, 3H), 2.95 (t, $J = 1.4$ Hz, 2H), 7.32 (d, 2 H), 7.80 (d, 2H).

***N*-(*p*-Tolylsulfonyl)-2-(*m*-methylphenyl)aziridine (Table, entry 5).** mp 130–131 °C (Lit. 131–132 °C);^{5e} IR (cm^{-1}) 3032, 1600, 1525, 1355, 1160; ^1H NMR (δ ppm) 2.31 (s, 3H), 2.34 (d, $J = 4.5$ Hz, 1H), 2.43 (s, 3H), 2.97 (d, $J = 7.4$ Hz, 1H), 3.72 (dd, $J = 7.4, 4.5$ Hz, 1H), 7.10–7.31 (m, 6H), 7.85 (d, 2H).

***N*-(*p*-Tolylsulfonyl)-2-methyl-2-phenylaziridine (Table, entry 6).** mp 80–82 °C (Lit. 83–84 °C);^{5e} IR (cm^{-1}) 3060, 2990, 1600, 1549, 1330, 1160; ^1H NMR (δ ppm) 2.01 (s, 3H), 2.43 (s, 3H), 2.71 (s, 1H), 2.79 (s, 1H), 7.27–7.34 (m, 7H), 7.85 (d, 2H).

***N*-(*p*-Tolylsulfonyl)-2-methyl-2-carbomethoxyaziridine (Table, entry 7).** colorless oil IR (cm^{-1}) 3015, 2980, 2950, 1752, 1600, 1324, 1156; ^1H NMR (δ ppm) 1.89 (s, 3H), 2.42 (s, 3H), 2.54 (s, 1H), 2.77 (s, 1H), 3.71 (s, 3H), 7.33 (d, 2H), 7.86 (d, 2H).

***trans*-*N*-(*p*-Tolylsulfonyl)-2-carbomethoxy 3-phenyl aziridine (Table, entry 8).** mp 43.5 °C (Lit. 42–44 °C);^{5e} IR (cm^{-1}) 3068, 2960, 1750, 1600, 1290, 1161; ^1H NMR (δ ppm) 2.40 (s, 3H), 3.50 (d, $J = 4.0$ Hz, 1H), 3.87 (s, 3H), 4.46 (d, $J = 3.9$ Hz, 1H), 7.25–7.30 (m, 7H), 7.75 (d, 2H).

***N*-(*p*-Tolylsulfonyl)-2-(*p*-chlorophenyl)aziridine (Table, entry 9).** mp 111–112 °C (Lit. 113–114 °C);^{5e} IR (cm^{-1}) 3052, 1596, 1370, 1182; ^1H NMR (δ ppm) 2.34 (d, $J = 4.2$ Hz, 1H), 2.45 (s, 3H), 2.85 (d, $J = 7.0$ Hz, 1H), 3.77 (dd, $J = 7.0, 4.2$ Hz, 1H), 7.15–7.37 (m, 6H), 7.83 (d, 2H).

***N*-(*p*-Tolylsulfonyl)-8-azabicyclo[5.1.0]octane (Table, entry 10).** mp 87–88 °C (Lit. 88–89 °C);^{5e} IR (cm^{-1}) 3010, 2954, 2770, 1602, 1315, 1165; ^1H NMR (δ ppm) 1.19–1.82 (m, 10H), 2.43 (s, 3H), 3.10 (m, 2H), 7.31 (d, 2H), 7.84 (d, 2H).

Acknowledgements

We are thankful to the Director, IIP for his kind permission to publish these results. SLJ is thankful to CSIR, New Delhi for the award of Research Fellowships.

Notes and references

- (a) P. Muller and C. Fruit, *Chem. Rev.*, 2003, **103**, 2905; (b) J. A. Deyrup, in *The Chemistry of Heterocyclic Compounds*, ed. A. Hassner, Wiley, New York, 1983, vol. 42, part 1, pp. 1–214; (c) A. Padwa and A. D. Woolhouse, *Aziridines and Fused Ring Derivatives*, in *Comprehensive Heterocyclic Chemistry*, ed. W. Lwowski, Pergamon, Oxford, 1984, vol. 7, pp. 47–93.
- D. Tanner, *Angew. Chem., Int. Ed. Engl.*, 1994, **33**, 599.
- For reviews, see: (a) W. Lwowski, *Carbonylnitrenes*, in *Nitrenes*, ed. W. Lwowski, Interscience, New York, 1970, pp. 185–224; (b) O. E. Edwards, *Acylnitrenes*, in *Nitrenes*, ed. W. Lwowski, Interscience, New York, 1970, pp. 225–247; (c) W. Lwowski, *Acylazides and Nitrenes*, in *Azides and Nitrenes, Reactivity and Utility*, ed. E. F. V. Scriven, Academic, New York, 1984, pp. 205–246.
- Y. Yamada, T. Yamamoto and M. Okawara, *Chem. Lett.*, 1975, 361.
- (a) A. R. Silva, J. L. Figueiredo, C. Freire and B. De. Castro, *Catal. Today*, 2005, **102**, 154; (b) D. A. Evans, M. M. Faul and M. T. Bilodeau, *J. Org. Chem.*, 1991, **56**, 6744; (c) D. A. Evans, M. M. Faul, M. T. Bilodeau, B. A. Anderson and D. M. Barnes, *J. Am. Chem. Soc.*, 1993, **115**, 5328; (d) Z. Li, K. R. Conser and E. N. Jacobsen, *J. Am. Chem. Soc.*, 1993, **115**, 5326; (e) D. A. Evans, M. M. Faul and M. T. Bilodeau, *J. Am. Chem. Soc.*, 1994, **116**, 2742; (f) D. B. Llewellyn, D. M. Adamson and B. A. Amstsen, *Org. Lett.*, 2000, **2**, 4165; (g) P. Dauban and R. H. Dodd, *Synlett*, 2003, 1571.
- L. Simkhovich and Z. Gross, *Tetrahedron Lett.*, 2001, **42**, 8089.
- (a) T. Ando, S. Minakata, I. Ryu and M. Komatsu, *Tetrahedron Lett.*, 1998, **39**, 309; (b) R. Vyas, B. M. Chanda and A. W. Bedekar, *Tetrahedron Lett.*, 1998, **39**, 4715; (c) P. Brandt, M. J. Sodergren, P. G. Anderson and P.-O. Norrby, *J. Am. Chem. Soc.*, 2000, **122**, 8013; (d) D. P. Albone, P. S. Aujla, P. C. Taylor, S. Challenger and A. M. Derrick, *J. Org. Chem.*, 1998, **63**, 9569; (e) T. Ando, D. Kano, S. Minakata, I. Ryu and M. Komatsu, *Tetrahedron*, 1998, **54**, 13485; (f) J. U. Jeong, B. Tao, I. Sagasser, H. Henniges and K. B. Sharpless, *J. Am. Chem. Soc.*, 1998, **120**, 6844; (g) S. I. Ali, M. D. Nikalje and A. Sudalai, *Org. Lett.*, 1999, **1**, 705; (h) V. V. Thakur and A. Sudalai, *Tetrahedron Lett.*, 2003, **44**, 989.
- (a) J. Muzart, *Adv. Synth. Catal.*, 2006, **348**, 275; (b) S. Pandey, *Anal. Chim. Acta*, 2006, **556**, 38; (c) C. Baudequin, D. Brégeon, J. Levillain, F. Guillen, J.-C. Plaquevent and A.-C. Gaumont, *Tetrahedron: Asymmetry*, 2006, **16**, 3921; (d) T. Welton, *Chem. Rev.*, 1999, **99**, 2071; (e) T. Welton, *Coord. Chem. Rev.*, 2004, **248**, 2459; (f) S. V. Malhotra and H. Zhao, *Aldrichimica Acta*, 2002, **35**, 75; (g) Y. Gu, J. Peng, K. Qiao, H. Yang, F. Shi and Y. Deng, *Prog. Chem.*, 2003, **15**, 222; (h) R. A. Brown, P. Pollet, E. Mckoon, C. A. Eckert, C. L. Liotta and P. G. Jessop, *J. Am. Chem. Soc.*, 2001, **123**, 1254; (i) U. R. Pillai, *Green Chem.*, 2002, **4**, 170.
- M. L. Kantam, V. Neeraja, B. Kavita and Y. Harita, *Synlett*, 2004, 525.
- Typical experimental procedure: A 25 ml round bottomed flask was charged with 4-methylstyrene (118 mg, 1 mmol), Chloramine-T (228 mg, 1 mmol), NBS (10 mol%) and [bmim]BF₄ (1 ml). The resulting reaction mixture was stirred at room temperature for 1.0 h. The

completion of the reaction was monitored by TLC (SiO_2). After completion, the product was extracted by diethyl ether and purified by passing through a small column of silica gel using ethyl acetate/hexane (4 : 6) as eluent. Evaporation of the solvent under vacuum yielded pure *N*-(*p*-tolylsulfonyl)-2-(*p*-methylphenyl)aziridine in 90% yield (258 mg),

mp 135 °C. The ionic liquid layer containing succinimide and NaCl was diluted with ethyl acetate and insoluble solids were separated by filtration through a small Buckner funnel. The ethyl acetate was evaporated under reduced pressure and ionic liquid was used for the next run.



Looking for that **special** chemical biology research paper?

TRY this free news service:

Chemical Biology

- highlights of newsworthy and significant advances in chemical biology from across RSC journals
- free online access
- updated daily
- free access to the original research paper from every online article
- also available as a free print supplement in selected RSC journals.*

*A separately issued print subscription is also available.

Registered Charity Number: 207890

RSC Publishing

www.rsc.org/chembiology

22030681

Stability and selectivity of a multiphase membrane, consisting of dimethylpolysiloxane on an ionic liquid, used in the separation of solutes from aqueous mixtures by pervaporation

Pavel Izák,^{*ab} Martin Köckerling^c and Udo Kragl^a

Received 7th June 2006, Accepted 24th August 2006

First published as an Advance Article on the web 5th September 2006

DOI: 10.1039/b608114b

A novel ionic liquid $[(C_3H_7)_4N][B(CN)_4]$ was immobilized and coated by silicon in a ceramic nanofiltration module; this multiphase membrane shows a high selectivity (separation factor up to 177) and stability (over nine months) during separation of 1,3-propanediol from aqueous mixtures by vacuum pervaporation.

Downstream processing still continues to be one of the major challenges not only in chemical and biotechnological production processes, but also in waste water treatment.¹ The aim of our work is to combine recent development in the field of membrane technology, *e.g.* in nanofiltration,² liquid membranes³ or pervaporation,⁴ with the use of ionic liquids (ILs) to provide novel solutions in downstream processing or process intensification. ILs are currently explored as new reaction media for chemical synthesis or electrochemical applications. ILs seem to have a large potential in downstream processing, especially when applied in a form that requires only a small amount of them, *e.g.* in supported liquid membranes.⁵ The special property of ILs is their negligible vapour pressure at room temperature that makes their application in liquid membranes attractive for pervaporation.⁶ Pervaporation is considered a forward looking and modern membrane process for separation of various liquids or vapour mixtures.

Supported ionic liquid membranes (SILMs) offer a range of possible advantages: molecular diffusion is higher in ionic liquids than in polymers thanks to the presence of charged ions, which are responsible for more selective and often faster transport, especially of polar permeates, through the semi-permeable membrane; the selectivity of the separation can be influenced by variation of the liquid—in particular ILs offer the advantage of a wide variety of properties;⁷ thanks to their special mixing behavior, ILs as liquid membranes easily allow three-phase systems; contrary to extraction, only a small amount of liquid is necessary to form the liquid membrane, thus also allowing the use of more expensive materials; thanks to the usage of a ceramic nanofiltration (NF) module, concentration polarization⁶ can be diminished by a rough liquid-membrane surface.

The novel hydrophobic IL tetrapropylammonium tetracyanoborate $[(C_3H_7)_4N][B(CN)_4]$, which has a quite large cation and a relatively small but stable anion, and a melting point about 60 °C, was prepared.^{8,9} The potassium tetracyanoborate was heated in water and an equal amount of tetrapropylammonium bromide was added at 50 °C. A viscous IL was obtained after extraction with, and removal of, dichloromethane on a rotary pump at 55 °C. Firstly, we evaluated the transport of the solute (1,3-propanediol) from an aqueous mixture through an empty ceramic NF module under low pressure at room temperature (22 °C). The ceramic nanofiltration module with pore size 0.9 nm was then impregnated by $[(C_3H_7)_4N][B(CN)_4]$ at 70 °C inside a burette. We performed pervaporation experiments under the same conditions with an impregnated module. The whole separation process was monitored by gas chromatography in the classical pervaporation arrangement.

The ceramic NF module with $[(C_3H_7)_4N][B(CN)_4]$ was stable under low pressure (20 Pa) in aqueous solution for 92 hours. The IL was then flushed out from the pores by water. To improve the stability and also the selectivity, the NF module with IL was immersed for 1 hour in dimethylpolysiloxane, viscosity 350 cSt (25 °C). Both sides of the NF ceramic module, made of TiO₂, got coated, and the hydrophobicity and also selectivity of this set-up increased dramatically¹⁰ as shown in Fig. 1.

The selectivity of 1,3-propanediol separation from aqueous mixtures by pervaporation can be described by the separation

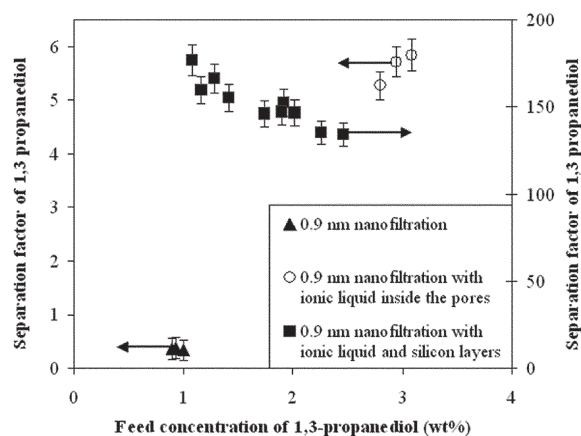


Fig. 1 Comparison of the 1,3-propanediol separation factor with its feed concentration, (▲) using the empty NF module, (○) using the NF ceramic module with the 0.9 nm pores filled with IL, (■) using the NF ceramic module with the 0.9 nm pores filled with IL and both sides coated with silicon.

^aRostock University, Institute of Chemistry, Technical Chemistry Group, Albert Einstein Str. 3a, D-18059, Rostock, Germany.

E-mail: udo.kragl@uni-rostock.de; Fax: +49 381 4986452;

Tel: +49 381 4986451

^bInstitute of Chemical Process Fundamentals, Rozvojova 135, 165 02 Prague 6, Czech Republic. E-mail: izak@icpf.cas.cz

^cRostock University, Institute of Chemistry, Inorganic/Solid State Chemistry Group, Albert Einstein Str. 3a, D-18059, Rostock, Germany. E-mail: martin.koeckerling@uni-rostock.de

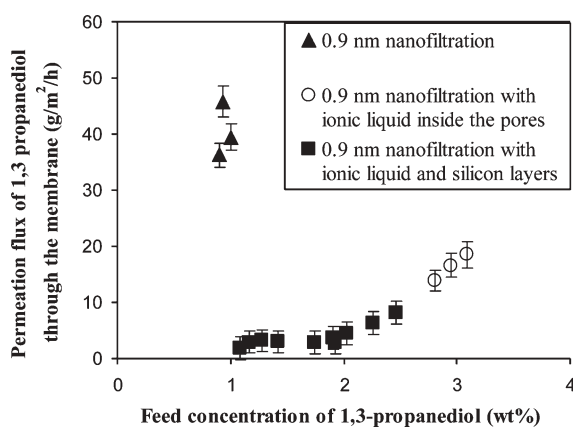


Fig. 2 Comparison of the 1,3-propanediol permeation flux with its feed concentration, (▲) using the empty NF module, (○) using the NF ceramic module with the 0.9 nm pores filled with IL, (■) using the NF ceramic module with the 0.9 nm pores filled with IL and both sides coated with silicon.

factor α , defined by $\alpha_{ij} = (w_{iP}/w_{jP})/(w_{iF}/w_{jF})$ where w_{iP} is the weight fraction of component i (1,3-propanediol) in the permeate and w_{jF} is the weight fraction of component j (water) in the feed. The separation factor of 1,3-propanediol increased from 0.4 to an average value of 5.6 when the IL was inside the pores, and to an average value of 152 when the whole ceramic module with IL was coated by dimethylpolysiloxane.

During the pervaporation with IL being present inside the pores the separation factor decreased with time and with solute concentration. This unusual behavior is caused by the decline of the 1,3-propanediol concentration in the permeate. It was actually the first sign that water was interacting with the IL. After 92 hours, the water flushed the IL out of the pores and the experiment was terminated.

When the hydrophobicity of the NF module and IL was improved by double layers of dimethylpolysiloxane (one from inside and the second from outside of the ceramic module), the separation factor was increasing with the time of experiment and also with the decreasing 1,3-propanediol feed concentration. Even after nine months we did not see any drop in selectivity or an increase of total permeation flux, which would indicate a decline of the stability of the IL–dimethylpolysiloxane selective layer. The permeation flux of 1,3-propanediol was calculated by: $J_i = Jw_{iP}$; where J is the total permeation flux through the SILM. Fig. 2, which represents the speed of the separation, shows that the NF module without IL has the highest permeation flux.

However, the preferentially permeating component is water, which has a smaller molecular size than 1,3-propanediol. The IL in this case inside the nano-pores decreases the flux of 1,3-propanediol by half. Due to its hydrophobicity the preferentially permeating component is already 1,3-propanediol. It was also observed that the flux decreases with decreasing 1,3-propanediol concentration in the feed.

Coating of the ceramic module with IL inside the pores formed two more boundary layers between dimethylpolysiloxane–[(C₃H₇)₄N][B(CN)₄]-dimethylpolysiloxane. This effect increases the separation dramatically, but it also decreased the

1,3-propanediol flux through the perm-selective barrier. The permeating flux decreased with time and with 1,3-propanediol concentration in the feed.

According to the literature, 1,3-propanediol has been recently separated from water using pervaporation through an X-type zeolite membrane,¹¹ when the membrane is selective for water. The permeation flux of 1,3-propanediol was 16 g m⁻² h⁻¹ and the separation factor about 3.6 at 35 °C. If we compare this with our multiphase membrane (MFM) data, we can see a significant improvement in selectivity (177) and a little drop in permeability (3.86 g m⁻² h⁻¹) at 22 °C. The application of liquid–liquid extraction for the downstream separation of 1,3-propanediol from dilute aqueous solutions hinders the continuous process, in which we want to remove 1,3-propanediol from the fermentation broth “*in situ*”. However, experimental verification revealed that the distribution of 1,3-propanediol into organic solvents is not good enough to make a simple extraction efficient.¹²

In conclusion, the instability of SILMs in contact with aqueous solutions, which has limited their commercial application so far, has been solved by using a dimethylpolysiloxane coating.¹⁰ By using a multiphase membrane in an NF ceramic module we increased the separation factor of the solute from 0.4 up to 177. On the other hand, the average permeating flux of the solute decreased from 34.3 g m⁻² h⁻¹ to 3.86 g m⁻² h⁻¹. Although the separation process with the MFM was one order of magnitude slower, its selectivity increased by more than two orders of magnitude, which shows a great potential for improving downstream separation processes. The pervaporation of the system was checked after nine months and we did not see any changes in transport properties, which shows the very high stability of the MFM. The binary system that we used as a case study (removal of 1,3-propanediol from aqueous solution) has a practical application in biotransformation processes, where the fermentation broth from *K. pneumoniae* is normally used.†

Notes and references

† This research was supported by a Marie Curie Intra-European Fellowships within the 6th European Community Framework Programme.

- 1 *Membrane Processes in Separation and Purification*, ed. J. G. Crespo and K. W. Böddeker, Kluwer Academic Publisher, Dordrecht, 1994, ch. 2.
- 2 J. Kröckel and U. Kragl, *Chem. Eng. Technol.*, 2003, **26**, 1166.
- 3 L. C. Branco, J. G. Crespo and C. A. M. Afonso, *Chem.–Eur. J.*, 2002, **8**, 3865.
- 4 P. Izák, N. M. M. Mateus, C. A. M. Afonso and J. G. Crespo, *Sep. Purif. Technol.*, 2005, **41**, 141.
- 5 R. Fortunato, C. A. M. Afonso, M. A. M. Reis and J. G. Crespo, *J. Membr. Sci.*, 2004, **242**, 197.
- 6 *Green Separation Processes*, ed. C. A. M. Afonso and J. G. Crespo, Wiley-VCH, Weinheim, 2005, ch. 3.6.2.
- 7 A. Heintz, *J. Chem. Thermodyn.*, 2005, **37**, 525.
- 8 T. Küppers, E. Bernhardt, H. Willner, H. W. Rohm and M. Köckerling, *Inorg. Chem.*, 2005, **44**, 1015.
- 9 U. Welz-Biermann, N. Ignatzev, E. Bernhardt, M. Finze and H. Willner, Merck Patent KGaA, Germany, *World Pat. WO 2004/072089 A1*, 2004.
- 10 P. Izák, U. Kragl and M. Köckerling, *German Pat.*, 10 2006 024 397.8, 2006.
- 11 S. Li, V. A. Tuan, J. L. Falconer and R. D. Noble, *Ind. Eng. Chem. Res.*, 2001, **40**(8), 1952.
- 12 J. J. Malinowski, *Biotechnol. Tech.*, 1999, **13**(2), 12.

Subcritical water extraction and β -glucosidase-catalyzed hydrolysis of quercetin glycosides in onion waste

Charlotta Turner,^{*a} Pernilla Turner,^b Gunilla Jacobson,^c Knut Almgren,^a Monica Waldebäck,^a Per Sjöberg,^a Eva Nordberg Karlsson^b and Karin E. Markides^a

Received 6th June 2006, Accepted 10th August 2006

First published as an Advance Article on the web 31st August 2006

DOI: 10.1039/b608011a

Onion waste is a renewable raw material, rich in different molecular species of the antioxidant quercetin. To utilize this resource, an environmentally sustainable procedure has been developed, using pressurized hot water to extract the quercetin species, followed by biocatalytic conversion of the quercetin glycosides to quercetin and carbohydrates. Two different recombinantly expressed thermostable β -glucosidases, *Thermotoga neapolitana* β -glucosidase A and B, were utilized as catalysts. These enzymes maintain activity at temperatures around 90 °C, and are therefore ideal to use in combination with hot water extraction. Our results, based on experimental design, showed that they converted quercetin glycosides to active quercetin in less than 10 min reaction time in water at 90 °C, pH 5.0. Experimental design showed that the optimal extraction conditions included three 5 min extraction cycles with water at 120 °C and 50 bars, giving a total extraction time of 15 min. Several different types of quercetin and isorhamnetin glycosides as well as kaempferol were detected in onion waste using LC-MS/MS analysis. After converting the different glycosidic compounds to their respective aglycones, the quercetin content was 10 to 50 mg g⁻¹ dry weight of onion waste (RSD 8%). In summary, our research demonstrates that subcritical water extraction followed by β -glucosidase-catalyzed hydrolysis is a rapid method to determine the content of quercetin and isorhamnetin in onion samples, and is environmentally sustainable as it only uses water as solvent and enzymes as catalysts.

Introduction

Antioxidants are compounds with electron scavenging properties that may slow down or prevent the development of cancer.^{1–4} Fruits and vegetables are rich in antioxidants,⁵ for example lycopene in tomatoes, β -carotene in carrots, anthocyanins in grapes and red onions, and quercetin in grapes, apples and onions. Furthermore, several recent studies have shown that different types of natural polyphenols may have neuroprotective effects both in vitro and in vivo,^{6–10} partly due to their electron scavenging properties. For example, it has been shown in a few studies that quercetin may prevent or slow down the development of Alzheimers disease.^{8,11–13}

Quercetin is a polyphenolic compound that occurs in vegetables and fruits mainly as different glycosides, although the skin of the fruit/vegetable commonly contains higher amounts of the quercetin aglycone. Fig. 1 shows the chemical structure of quercetin and the two most common glycosides in onion, quercetin-4'-glycoside and quercetin-3,4'-diglycoside.¹⁴ Several research projects have undertaken the isolation and identification of quercetin and its glycosides in various fruits and vegetables, including onion,¹⁵ kale,¹⁶ broccoli,¹⁷ apple

skin,¹⁸ green tea,¹⁹ and grapes and wine.^{20,21} However, most of these studies use simple liquid/solid extraction techniques combined with chemically catalyzed hydrolysis reaction followed by liquid/liquid extraction of quercetin aglycone. These procedures are tedious and require the disposal of organic solvents, such as the commonly used ethyl acetate.

The most environmentally friendly solvent that can be used for extraction of quercetin is water. However, since pure water at ambient condition is too polar to be a good solvent for quercetin, we instead use water at elevated temperatures as a solvent, *i.e.* subcritical water at temperatures above 100 °C. It is well known that the dielectric constant of water decreases significantly as the temperature of the water is increased above its atmospheric boiling point, while applying pressure to maintain water as a liquid.²² Less polar compounds such as antioxidative compounds,²³ polycyclic aromatic hydrocarbons,²² insecticides²⁴ and essential oils²⁵ have all been successfully extracted from various plant and soil samples using subcritical water at temperatures between 100 and 374 °C. Above 374 °C water is supercritical, giving too harsh conditions to use for extraction of antioxidative compounds.

In a few publications, supercritical carbon dioxide mixed with around 20% (v/v) of an alcohol such as methanol or ethanol was used to extract quercetin from fruits and agricultural samples.^{26–29} The solubility of quercetin in neat supercritical carbon dioxide is unfortunately extremely low,³⁰ otherwise this would be a viable alternative to subcritical water extraction. To the best of our knowledge, there is no previous

^aUppsala University, Department of Physical and Analytical Chemistry, Analytical Chemistry, P.O. Box 599, Uppsala, SE-75124, Sweden.

E-mail: charlotta.turner@kemi.uu.se; Fax: +46 18 471 3681

^bLund University, Department of Biotechnology, P.O. Box 124, Lund, SE-22100, Sweden

^cStanford University, Department of Chemistry, 333 Campus Drive, Stanford, CA, 94305, USA

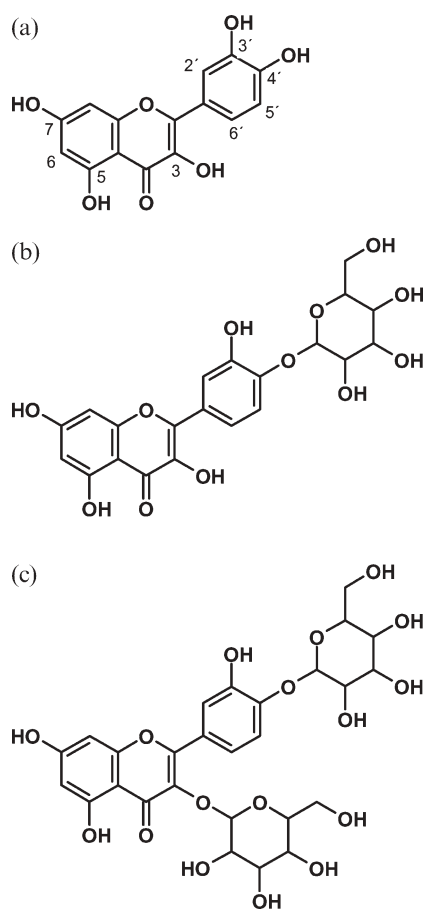


Fig. 1 Chemical structure of (a) quercetin, (b) quercetin-4'-glycoside and (c) quercetin-3,4'-diglycoside.

report on subcritical water extraction of quercetin from fruit/agricultural samples.

There are several advantages with subcritical water extraction compared to classical liquid/liquid extraction techniques, such as faster and more efficient extractions due to higher diffusion rates and lower viscosity and surface tension, environmentally safe and non-toxic extractions and easy-to-tune properties of the solvent by merely changing temperature and pressure.

Flavonoids are common and widespread secondary plant metabolites, which have a wide range of biological and physiological activities.³¹ Flavonoids occur in plants (and food products) as different glycosides, which is also the preferred form for uptake in the human intestine. After uptake, the glycosides are converted to aglycone and free carbohydrates in hydrolysis reactions mainly catalyzed by β -glucosidase and to some extent by lactase phloridzin hydrolase.³² Hence, in quantitative analysis of flavonoid content in food, β -glucosidase is a useful catalyst for transforming the several different occurring flavonoid glycosides to a single measurable aglycone. Some of these glycosidic compounds are present at concentrations below 1% of the total flavonoid content, which naturally is difficult to quantify. Furthermore, it is difficult to obtain appropriate reference standards for quantifying the different quercetin glycosides.

In this paper, we have evaluated the use of subcritical water for extraction of antioxidative quercetin and other flavonoid molecular species from onion waste. The onion waste raw material (rich in *e.g.* quercetin molecular species) was selected, being a waste product available in Sweden that could be obtained in large amounts from local restaurants and onion industries. It was also judged to be advantageous to couple the extraction to a product conversion step (deglycosylation by hydrolysis), allowing collection of the aglycone substances for quantification. To further improve the environmentally friendly profile, a biocatalytic conversion was applied.

This paper demonstrates a fully “green” procedure, where the raw material is a biodegradable and renewable agricultural waste (onion waste), the extraction process uses only water as a solvent, and the hydrolysis reaction is catalyzed by enzymes rather than by chemicals or non-renewable catalysts. Furthermore, onion waste is largely produced in Sweden as a byproduct of no value for the producer in amounts of several million kilograms per year. After quercetin extraction, the onion waste can still be used as animal feed, energy source or compost material. Hence, the herein described procedure fits well to the twelve principles of green chemistry.³³

Results and discussion

In this study, several steps were developed and optimized, including a LC-MS/MS-analysis method for quantification of the antioxidants of interest, and selection/production of a suitable catalyst, and with the analysis methodology in place, optimization of both the extraction and deglycosylation reaction steps in the procedure. Finally, the yield obtained in the newly developed procedure was compared to the yield of an established extraction/hydrolysis method for quercetin.

LC-MS/MS analysis of quercetin and isorhamnetin molecular species

A simple HPLC method was developed using a reversed phase C18 column and an isocratic mobile phase consisting of equal portions of methanol and water as well as 0.1% formic acid (giving a pH of around 3). UV detection at 350 nm was used to enable detection of smaller amounts of various glycosidic compounds, although quercetin aglycone has its maximum absorbency around 370 nm.³⁴ Fig. 2a and 2b show two representative chromatograms of yellow onion-waste samples before and after enzymatic treatment with one of the selected β -glucosidases (*TnBgl1A*, described in more detail below). At the concentration used, most of the glycosidic compounds were transformed to quercetin aglycone after only 10 minutes of reaction with the *TnBgl1A* enzyme, indicating a good potential for the enzymatic conversion.

LC-MS/MS analysis was performed to identify the different aglycone and glycosidic polyphenolic compounds. Electro-spray ionization in positive mode was applied to transfer the analytes from the liquid mobile phase from the HPLC-column to gas phase before introduction into the QTrap MS. Information dependent acquisition (IDA) was applied to allow collection of as much information as possible during each HPLC run. Fig. 3a shows MS data for the quercetin aglycone peak in a yellow onion waste extract, and Fig. 3b

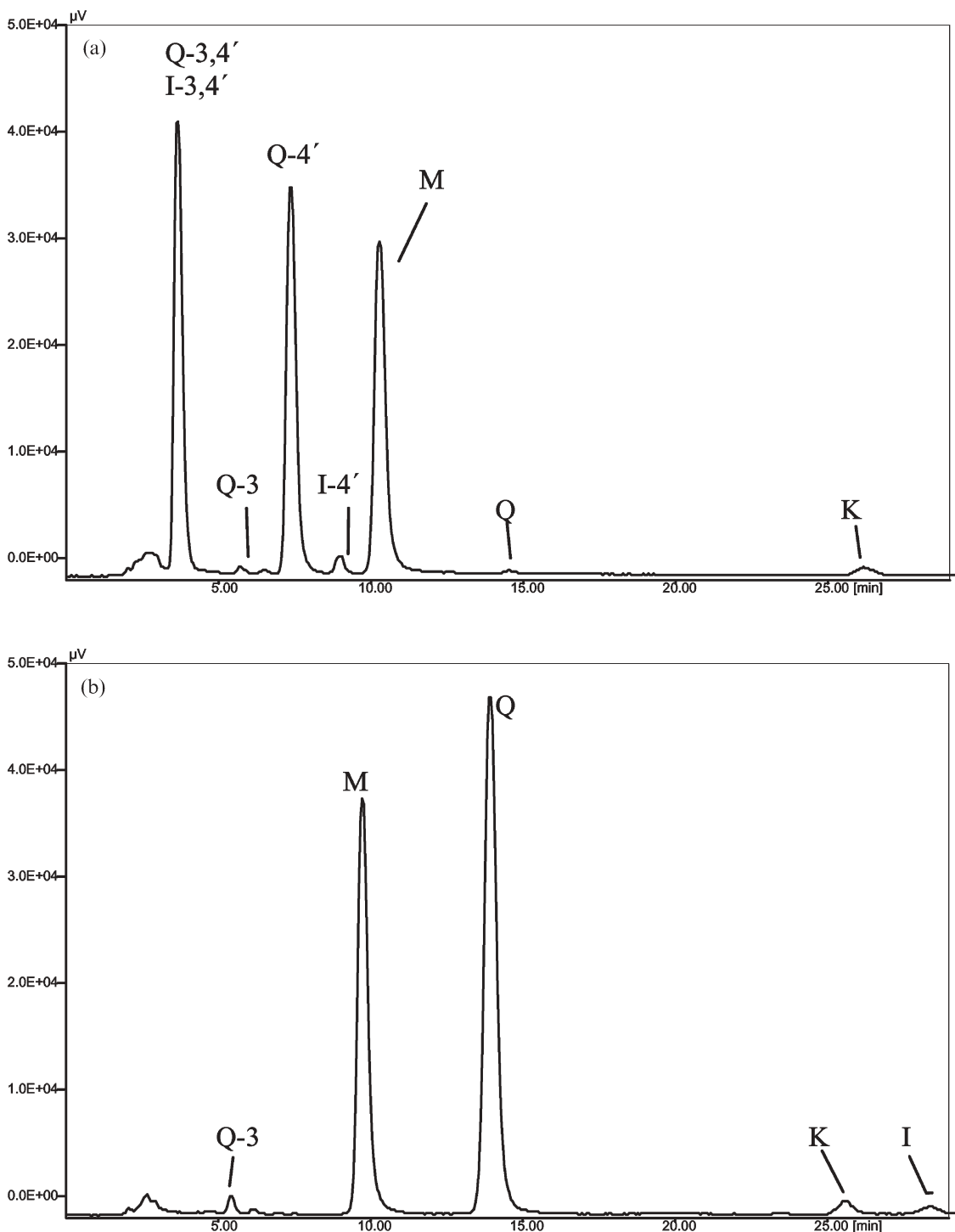


Fig. 2 HPLC chromatogram of (a) yellow onion extract and (b) β -glucosidase-treated yellow onion extract. Q-3,4' = quercetin-3,4'-diglycoside, I-3,4' = isorhamnetin-3,4'-diglycoside, Q-3 = quercetin-3-glycoside, Q-4' = quercetin-4'-glycoside, I-4' = isorhamnetin-4'-glycoside, M = morin (internal standard), Q = quercetin, K = kaempferol and I = isorhamnetin.

shows MS/MS data for the selected mother ion for quercetin (m/z 303). Fig. 3c shows the sum of the extracted mother ions m/z 303 (quercetin); 465 and 627 (mono- and diglycosides of quercetin); 317 and 479 (isorhamnetin and its monoglycosides); and finally 287 (kaempferol, *i.e.* quercetin lacking one of its hydroxyl groups).

The MS/MS data for quercetin, one of the few compounds available as a reference standard in this work, was useful for indicating the presence of possible quercetin conjugates (*e.g.* glycosides) in the sample extracts. Up-front fragmentation of the conjugates generates a fragment ion (m/z 303) corresponding to protonated quercetin aglycone that, when selected for

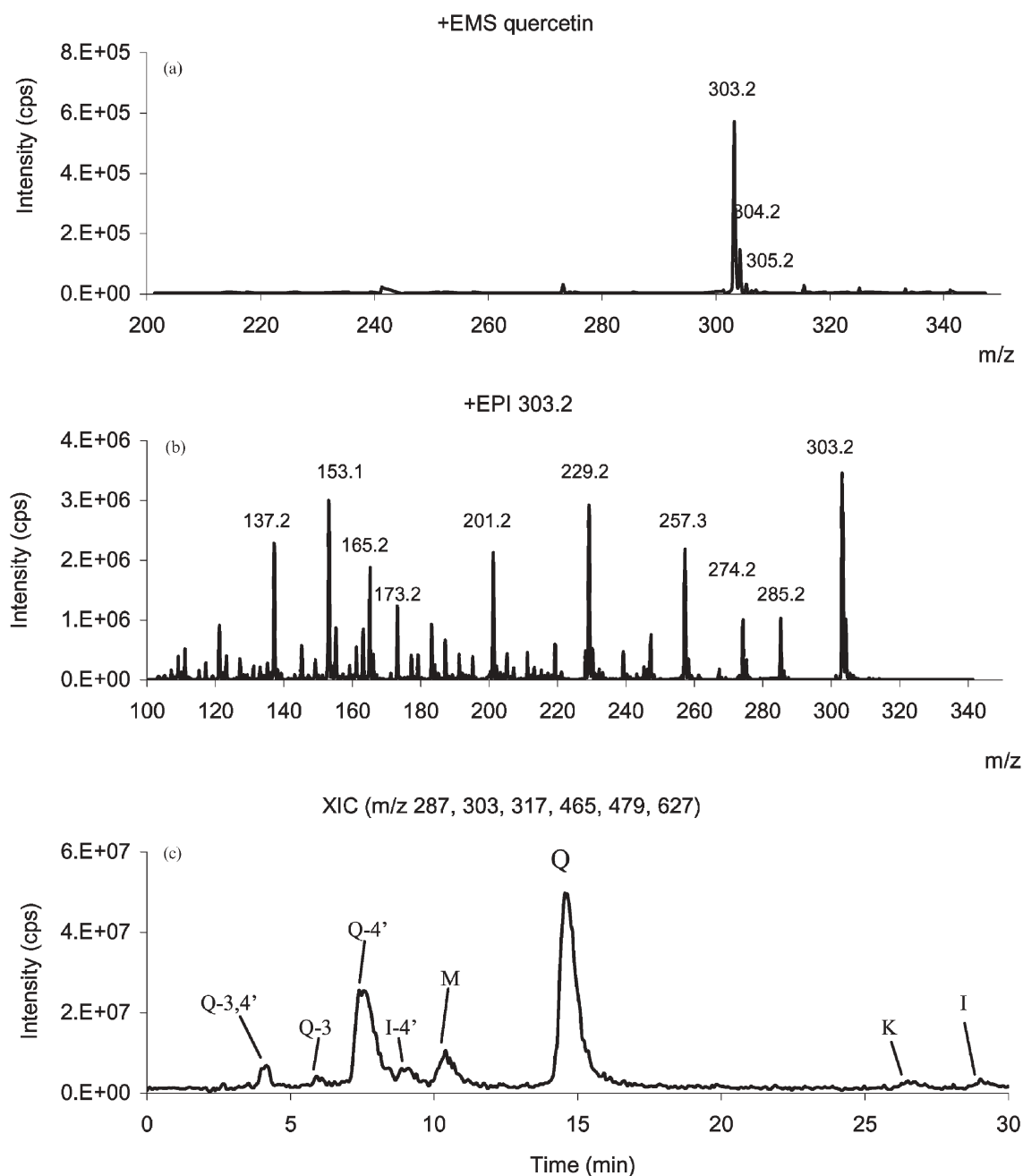


Fig. 3 (a) Enhanced MS data for quercetin, (b) enhanced product ion (MS/MS) for the selected mother ion of quercetin, m/z 303.2, and (c) a sum of the extracted ions 287, 303, 317, 465, 479 and 627 detected in a yellow onion extract. Abbreviations: see Fig. 2.

further MS/MS fragmentation, showed the same fragmentation pattern as quercetin.

The position of the glucose moieties was determined by knowing (and confirming, see Experimental, Enzyme specificity) that the β -glucosidase has a very limited activity on polyphenolic glycosides linked at position 3, but high activity on position 4' glycosides (data not shown). This, in combination with the fact that the two major polyphenolic glycosides in onion are quercetin-4'-glycoside and quercetin-3,4'-diglycoside,¹⁴ make us quite confident that the identity of the glycosides are as labeled in Fig. 2 and Fig. 3c. Typical composition of quercetin and related compounds in

one gram of wet yellow onion waste extracted by subcritical water at 120 °C and 50 bar for 15 min was 0.63 mg quercetin, 0.53 mg quercetin-4'-glycoside, 0.19 mg quercetin-3,4'-diglycoside (co-eluting with trace amount of isorhamnetin-3,4'-diglycoside), 0.06 mg isorhamnetin, 0.04 mg isorhamnetin-4'-glycoside, 0.03 mg quercetin-3-glycoside, and 0.008 mg kaempferol.

Subcritical water extraction

Extraction of quercetin molecular species from yellow onion waste was performed using pressurized hot water at 50 bar and

Table 1 Response surface coefficients for quercetin yield (mg g^{-1} onion) at different extraction conditions

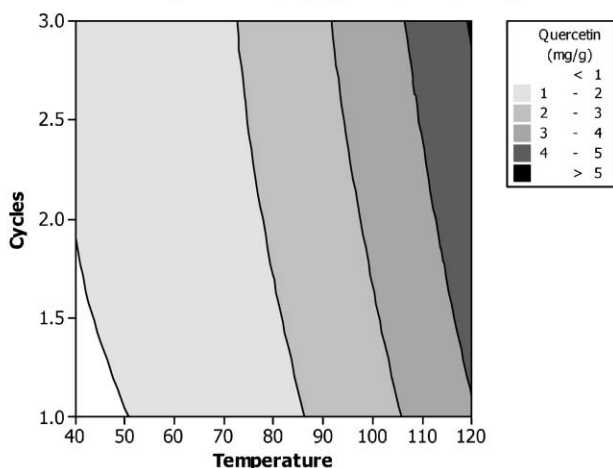
Term	Coefficient	SE Coefficient	P
Constant	2.10	0.16	<0.001
Temp.	1.77	0.09	<0.001
Cycles	0.31	0.09	0.004
Temp. \times Temp.	0.68	0.15	0.001
Cycles \times Cycles	-0.05	0.15	0.758
Temp. \times Cycles	0.26	0.11	0.032

$S = 0.30$ R-Sq = 97.4% R-Sq(adj) = 96.3%

extraction cycles of 5 min each. A response surface design was applied to investigate the effects of temperature (40, 80 and 120 °C) and number of extraction cycles (1, 2 and 3) on the yield of quercetin. The onion waste extract was thereafter hydrolyzed according to the method optimized below. The statistical data is shown in Table 1 and the response surface plot for number of cycles *versus* extraction temperature is shown in Fig. 4.

Table 1 clearly demonstrates that the response surface design was suitable for investigating number of cycles and extraction temperature (R square = 97.4%). Extraction temperature and number of cycles as well as the interaction temperature \times cycles all show significant effects on a 95% confidence level. The response surface plot shows that the highest yields are obtained at the highest temperature investigated, 120 °C, using two or preferably three cycles (Fig. 4). However, it does not seem to be crucial whether two or three cycles are used when operating at the highest temperature, 120 °C.

In order to find out if an even higher temperature would result in an improved recovery of quercetin, triplicate yellow onion waste samples were extracted at 80, 120 and 160 °C using three cycles of five minutes extraction each. The quercetin yield obtained were as follows: 0.85 mg g^{-1} at 80 °C (RSD 14%), 1.97 mg g^{-1} at 120 °C (RSD 8%), and 1.92 mg g^{-1} at 160 °C (RSD 5%), showing that 120 °C extraction temperature was sufficient.

Contour Plot of Quercetin (mg/g) vs Cycles, Temperature**Fig. 4** Response surface of quercetin yield (mg g^{-1} onion) *vs.* temperature and number of extraction cycles for the PHW extraction.

Catalyst selection, production and purification

The extraction procedure, using subcritical water, requires elevated temperatures and a biocatalyst that operates as close as possible to the extraction temperature. Therefore, a thermostable enzyme was considered as a suitable alternative. Two β -glucosidases originating from the hyperthermophilic bacterium *Thermotoga neapolitana* were selected as candidates for this purpose. *T. neapolitana* grows optimally above 80 °C, and its enzymes are therefore likely to have high thermostability. High temperature optima for activity for both enzymes have also been shown in previous works,^{35,36} making them good candidates for high-temperature applications. The two thermostable glucosidases are, despite their common origin, unrelated in primary as well as tertiary structure, and belong to glycoside hydrolase families 1 and 3, respectively (according to the classification by Coutinho *et al.*³⁷) and are termed *TnBgl1A* and *TnBgl3B* in accordance with the taxonomy proposed by Henrissat *et al.*³⁸ Both enzyme families are, however, known to share a retaining reaction mechanism.

The genes encoding the two β -glucosidases were amplified by PCR from genomic DNA, and cloned in the vector pET22b(+) under control of the T7/lac promoter for expression in *Escherichia coli*. Both enzymes were produced in the *E. coli* expression host Tuner(DE3) using a protocol developed for a GH13 enzyme where reduction in the IPTG concentration used for induction of the T7/lac promoter yielded more active and soluble protein.³⁹ *TnBgl1A* was more prone to form inclusion bodies than *TnBgl3B*, but a substantial amount of soluble protein could still be produced using the described strategy (Fig. 5a, lane 2). Production of *TnBgl1A* resulted in the recombinant enzyme constituting approximately 10% of the total soluble protein content, while for *TnBgl3B* more than 20% of the total soluble proteins consisted of the target enzyme (Fig. 5b, lane 2). Before use in the conversion, the β -glucosidases were purified using a two-step purification protocol. The extracts obtained after sonication of *E. coli* cell pellets were heat treated, which removed a large part of the *E. coli* proteins (Fig. 5, lane 3) and the subsequent affinity chromatography by immobilized metal ion chromatography

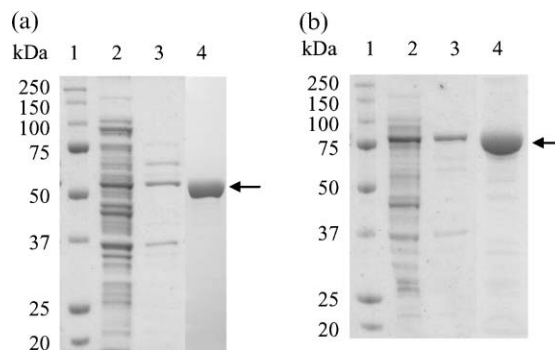
**Fig. 5** SDS-PAGE analysis of expression and purification of (a) *TnBgl1A* and (b) *TnBgl3B*. The apparent molecular weights corresponded well with the theoretically calculated values of 52.6 kDa (*TnBgl1A*), and 82.2 kDa (*TnBgl3B*). The samples in the lanes are: lane 1, molecular weight standard; lane 2, crude extract; lane 3, heat-treated protein; lane 4, protein purified by IMAC.

Table 2 Response surface coefficients for quercetin yield (mg g⁻¹ onion) using *TnBgl1A*

Term	Coefficient	SE Coefficient	P
Constant	5.93	0.23	<0.001
Temp.	0.15	0.13	0.279
pH	0.05	0.14	0.739
Temp. × Temp.	-0.04	0.23	0.879
pH × pH	-0.64	0.22	0.009
Temp. × pH	-0.27	0.17	0.123
<i>S</i> = 0.50 R-Sq = 44.8% R-Sq(adj) = 28.5%			

using copper ions further removed contaminating proteins to yield a purity of over 90% (Fig. 5, lane 4).

Optimization of deglycosylation reactions

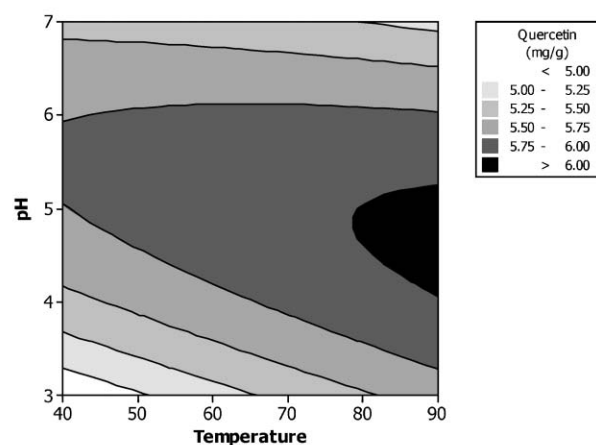
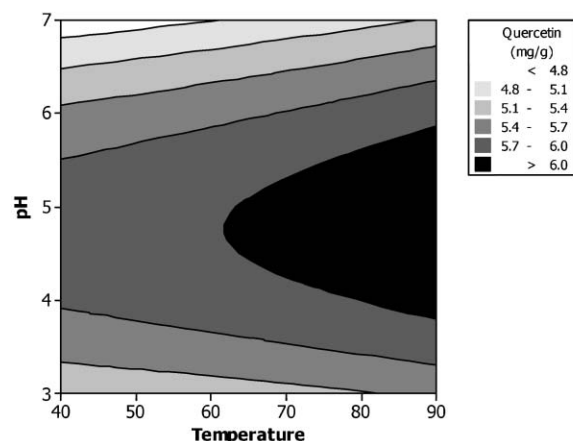
As expected, preliminary data clearly showed the advantage of using these thermostable β -glucosidases rather than the commercially available β -glucosidase from almond (classified under glycoside hydrolase family 1) obtainable from Sigma-Aldrich, as the two former enzymes showed significantly faster reaction kinetics towards polyphenolic glycosides, even well below their temperature optima (data not shown).

After confirming the improvement of the deglycosylation reaction using the thermostable enzyme representatives, an initial study was performed to find out approximately how much of the enzyme solution was needed to convert the most abundant glycoside in yellow onion waste, quercetin-4'-glycoside, into quercetin aglycone. The results showed that for a complete reaction of an onion waste extract, 28 pmol *TnBgl3B* per μ mol of quercetin-4'-glycoside was needed for the chosen conditions pH 5.6, 80 °C and a 5 min reaction time. For *TnBgl1A*, four times more of the enzyme was necessary to obtain the same result. These data were used to set up an experimental design for the optimization of glucosidase-catalyzed reactions.

A response surface design was used to investigate the effects of varying the temperature and pH on the yield of quercetin formed from quercetin glycosides in onion waste extract. Temperatures of 40, 65 and 90 °C were applied combined with pHs of 3.0, 5.0 and 7.0. The reaction time was 10 min and the amount of enzyme used was 136 pmol for *TnBgl1A* and 35 pmol for *TnBgl3B*, based on the preliminary experiments described above. The statistics in Tables 2 and 3 show that only the pH × pH term is significant on a 95% confidence level using a response surface design for the two enzymes investigated. However, the response surface plots in Fig. 6a and 6b still show that the optimal pH for the hydrolysis reaction is around 5 and the best temperature is 90 °C.

Table 3 Response surface coefficients for quercetin yield (mg g⁻¹ onion) using *TnBgl3B*

Term	Coefficient	SE Coefficient	P
Constant	6.01	0.27	<0.001
Temp.	0.21	0.17	0.231
pH	-0.22	0.17	0.203
Temp. × Temp.	0.03	0.27	0.925
pH × pH	-0.95	0.27	0.004
Temp. × pH	0.06	0.20	0.785
<i>S</i> = 0.57 R-Sq = 54.5% R-Sq(adj) = 37.1%			

(a)
Contour Plot of Quercetin (mg/g) vs pH, Temperature**(b)**
Contour Plot of Quercetin (mg/g) vs pH, Temperature**Fig. 6** Response surface of quercetin yield (mg g⁻¹ onion) vs. pH and temperature of the reaction, catalyzed by (a) *TnBgl1A* and (b) *TnBgl3B*.

The statistics, however, also show that the response surface design was less suitable for investigating reaction pH and temperature (*R* square = 44.8% and 54.5% for *TnBgl1A* and *TnBgl3B*, respectively), compared to the number of extraction cycles and the extraction temperature (*R* square = 97.4%) shown in Table 1. Higher temperatures than 90 °C were not tried, since the melting points of *Bgl1A* and *Bgl3B* are 102 and 90 °C, respectively (unpublished data). It was therefore necessary to decrease the temperature from the optimal 120 °C extraction temperature, before adding the enzyme. From the response surface plots (Fig. 6) it can be seen that *TnBgl3B* has a larger area of quercetin yield, larger than 6 mg g⁻¹ onion waste, compared to *TnBgl1A*. Hence, it seems that although less amount of *TnBgl3B* was used for the reaction, still higher yield was achieved at a wider temperature/pH range compared to *TnBgl1A*.

The effect of different enzyme/substrate ratios on the quercetin yield *versus* reaction time was investigated for both enzymes at 90 °C and pH 5.0. An addition of 50 μ L of *TnBgl1A* was needed to convert the quercetin glycosides in

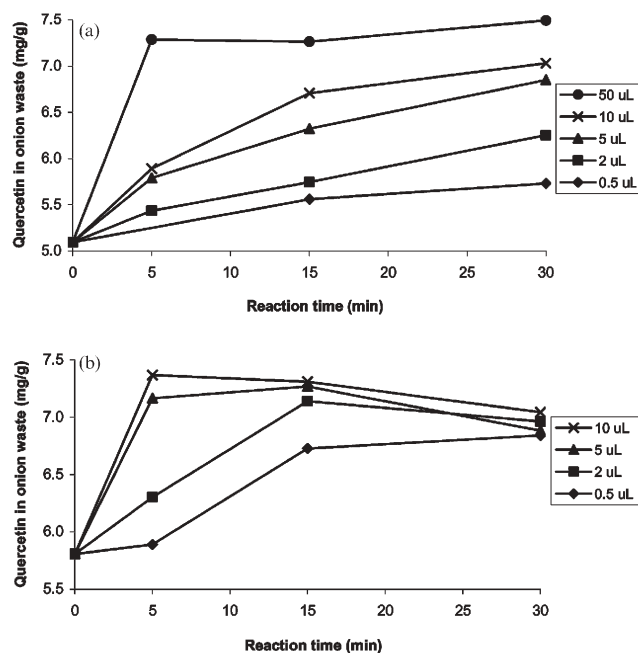


Fig. 7 Effects of enzyme amount and reaction time on the quercetin yield for (a) *TnBgl1A* and (b) *TnBgl3B*. 1 μL *TnBgl1A* equals ~ 68 pmol and 1 μL *TnBgl3B* equals ~ 69 pmol. The reaction was performed with 4 mL of yellow onion skin extract (~ 40 mg onion mL^{-1}) at 90°C and pH 5.0.

4 mL of onion waste extract (corresponding to around 40 mg of onion per mL) within 5 min of reaction (Fig. 7a), compared to *TnBgl3B* for which only 5 to 10 μL was needed to do the same job (Fig. 7b). Hence, it was decided that the optimal reaction method was to use 10 μL of *TnBgl3B* (690 pmol) per 4 mL of onion waste extract, and to perform the reaction at 90°C and pH 5.0 for 10 min. However, in all further experiments, 5 μL of *TnBgl3B* was added to 1.2 mL of onion extract in order to be able to perform the reaction in standard 1.5 mL HPLC vials, and still ensure a sufficient enzyme/substrate ratio.

Comparison of the novel extraction and conversion procedure with an established method

A common conventional methodology to extract and hydrolyze polyphenolic glycosides from fruits and plants is to use a mixture of methanol and hydrochloric acid with a final concentration of around 1.2 M and heat for one or several hours at 80 to 90°C .^{34,40} Usually, the extraction/hydrolysis step is followed by an additional extraction of quercetin into an organic solvent and/or filtration of the mixture prior to analysis. The hydrolysis procedure is relatively harsh to the sample and may result in degradation of the compounds of interest, even when a protective antioxidant has been added.⁴⁰ In fact, our initial studies showed that it is crucial to select the optimal HCl concentration to avoid degradation but still obtain complete hydrolysis (data not shown). From a green chemistry point-of-view, it is also obvious that hydrochloric acid is not as environmentally friendly a catalyst as enzymes, especially when it is used in large volumes and is not recycled. Moreover, methanol (as well as ethyl acetate if used) is an

Table 4 Comparison of the developed method with a conventional extraction/hydrolysis method ($n = 3$)

Parameter	New method	Conventional method
Quercetin yield/ mg g^{-1} onion)	1.97	1.86
Quercetin yield/ mg g^{-1} (dry weight)	13.31	12.55
RSD (%)	7.94	9.32
Total time per sample	~ 40 min	~ 150 min
Total time manual work per sample	~ 5 min	~ 30 min
Volume of organic solvent per sample	0.5 mL	~ 50 mL

organic solvent that requires disposal in addition to production and transport. Furthermore, the conventional methodology is rather tedious and requires a substantial amount of manual work. In the novel procedure developed here, the extraction is the first step, using solely water as solvent. In the following hydrolytic conversion step, the enzyme, specifically hydrolyzing the glycosidic bond, is added to the extract in a buffer assuring a suitable pH for the enzymatic reaction.

To compare the yield from both methodologies, onion waste from the same batch was extracted using both a method based on conventional extraction with methanol–2.4 M HCl (1 : 1) for two hours at 80°C followed by filtration, and using the subcritical water extraction/biocatalytic conversion. The conventional method gave a quercetin yield of 1.86 mg g^{-1} (RSD 9%), which corresponds very well to the result obtained by the new subcritical water extraction method (1.97 mg g^{-1} , RSD 8%), see Table 4. Analysis of the quercetin species composition in yellow onion skin and pulp, and red onion skin and pulp before and after enzymatic hydrolysis, proved that the enzymes efficiently hydrolyzed quercetin-glycosides linked at position 4', but it was also obvious that although the new method gave results very similar to those obtainable with a conventional method, the *TnBgl3B* enzyme was not capable of converting quercetin-3-glycoside to quercetin aglycone and glucose (Fig. 8). This effect of enzyme specificity was also confirmed in an experiment in which quercetin-3-glycoside and quercetin-4'-glycoside were used as substrates for the two studied enzymes (data not shown).

In summary, our results show that the new environmentally benign method gives not only similar results to the conventional method, but also demonstrates a faster method with less manual extractions (see Table 4). The new method consumes 100 times less organic solvents (here: methanol) using the same amount of onion waste sample, and it shows similar or better RSD values than the conventional method. Note that the conventional method used in this work for comparison was quite simple in that the extraction/hydrolysis mixture was only filtrated and injected directly into the HPLC instrument for analysis. Most other conventional methods apply an additional organic solvent extraction, *e.g.* with ethyl acetate, and washing off the acid residues from the HCl, which results in an even more tedious and hazardous method, although it is more friendly to the HPLC column.

Conclusions

In summary, the new method using subcritical water as the only extraction solvent and enzymes in the hydrolysis reaction

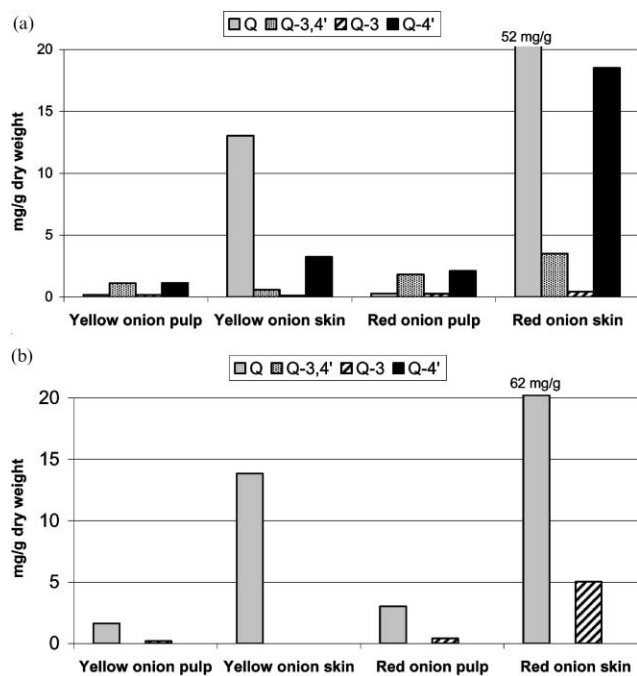


Fig. 8 Composition of quercetin molecular species in yellow onion pulp and skin, and red onion pulp and skin (mg g^{-1} dry weight), (a) before and (a) after enzymatic deglycosylation ($n = 2$). The concentration of the various components was calculated using a quercetin standard calibration curve with morin as internal standard and detection at 350 nm. Hence, the results are only approximate, since quercetin has a different absorption coefficient than its glycosides. For abbreviations, see Fig. 2.

is clearly a viable alternative to conventional organic solvent-based extractions and HCl-catalyzed hydrolysis. The raw material used in the process is renewable and biodegradable. The new method does not use or produce any hazardous or toxic compounds. Furthermore, biocatalysis is used in the hydrolysis reaction, which is environmentally more sustainable than chemical catalysis. The developed method is also faster and close to 100% automated, which allows for high sample throughput. Finally, the method could potentially be applied to other agricultural waste materials as well, such as apple skin, grape skin and berry wastes from the juice industry.

Experimental

Raw material (onion waste)

Onion (*Allium cepa*) waste was obtained from a local restaurant as well as from a Swedish onion industry. In some cases, onions were purchased in a local market and samples were thereafter prepared in the lab. Onion sample, independent from which source, was cut into small pieces ($\sim 1\text{--}10$ mm in diameter) using a food processor.

Chemicals used

Methanol and formic acid was purchased from Merck (Darmstadt, Germany). Quercetin dihydrate ($>98\%$), morin (puriss p.a.), quercetin-3-glycoside, kaempferol, citric acid monohydrate and disodium hydrogen phosphate were

purchased from Sigma-Aldrich (Steinheim, Germany). Ultrapure water (MilliQ) was used at all times.

Cloning of *Tnbg1A* and *Tnbg3B*

The genes encoding Bgl1A and Bgl3B were amplified from genomic *Thermotoga neapolitana* (DSM strain 4359) DNA. Primers were designed to amplify the coding sequences of *bgl1A* (also termed *gghA*) and *bgl3B* obtained from the NCBI server (<http://ncbi.nlm.nih.gov>) under the accession numbers AF039487 and Z77856. Primers were forward 5'- TAT TCT TAT CAT ATG AAA AAG TTT CCC GAA GGG TTC and reverse 5'- TAT TCT TAT CTC GAG ATC TGT TAG TCC GTT GTT TTT G for *bgl1A* and forward 5'- TAT TCT TAT CAT ATG GAA AAG GTG AAT GAA ATC CTG and reverse 5'- TAT TCT TTA CTC GAG CGG TTT GAA TCT TCT CTC C for *bgl3B* with the restriction sites for cloning underlined. The complete genes were PCR-amplified under standard conditions (94 °C 5 min; 25 cycles: 94 °C 30 s, 55 °C 30 s, 68 °C 2 min; 68 °C 7 min) on a Biometra T Gradient thermal cycler (Nordic BioSite, Täby, Sweden) using the Expand High Fidelity PCR System (Roche Diagnostics, Mannheim, Germany) for insertion into the expression vector pET22b(+) (Novagen, Madison, WI, USA) incorporating the C-terminal hexa-histidine tag. The PCR products were purified with QIAEXII Gel Extraction kit (Qiagen, Hilden, Germany) after gel separation. Both the PCR products and the vector were digested with appropriate restriction enzymes (New England Biolabs, Beverly, MA, USA) and the vector was treated with bacterial alkaline phosphatase before being ligated to the insert using T4 DNA ligase (Invitrogen Life Technologies, Frederick, MD, USA). The resulting plasmids were transformed into *E. coli* Nova Blue cells (Novagen) and screened by colony PCR using the T7 forward and T7 reverse primers and *Taq* DNA polymerase under standard conditions. Positive clones were transformed into the *E. coli* expression host Tuner(DE3) (Novagen). The complete genes were sequenced at MWG Biotech (Ebersberg, Germany). The *bgl1A* sequence contained a single residue change (G436V), compared to the deposited sequence. The previously deposited *bgl3B* sequence was cloned from strain Z2706-MC24,³⁶ while in this work the DSM-strain 4359 was used as template. The newly amplified gene contained several changes compared to the deposited gene, especially in the 5'-end where a deletion caused a frame shift which was restored by an insertion after a stretch encoding 24 amino acids. A few more changes further downstream were also found. The new sequence was deposited to GenBank under accession number DQ873691. The molecular weight of the respective gene (including the His-tag) was theoretically calculated using the ProtParam-tool (<http://www.expasy.org/tools/protparam.html>).

Expression and purification

The genes were expressed at 37 °C in a 2.5 L bioreactor during a probed temperature limited fed-batch cultivation as described previously.⁴¹ The expression was initiated by the addition of 0.1 mM isopropyl-1-thio- β -D-galactopyranoside and the production was continued for 6 h before the cells were harvested by centrifugation at $5000 \times g$, 4 °C, 5 min. The

obtained cell dry weight was typically 35 g L^{-1} at the end of the cultivation, with a total protein content of approximately 15 g L^{-1} . The cell pellet was dissolved in binding buffer (20 mM Tris-HCl, 0.75 M NaCl, 20 mM imidazole, pH 7.5) and lysed in a Gaulin 60 high pressure homogenizer (APV-Schröder, Lübeck, Germany) at 600 bar (3 cycles). The crude extract was obtained by centrifugation at $27\,000 \times g$, $4 \text{ }^\circ\text{C}$, 30 min. After heat treatment at $70 \text{ }^\circ\text{C}$ for 40 min, the protein fraction was centrifuged twice at $27\,000 \times g$, $4 \text{ }^\circ\text{C}$, 30 min. The His-tagged recombinant proteins were purified by immobilized metal ion affinity chromatography (IMAC). Onto a column containing 30 mL IDA-linked DEAE Sepharose CL-6B (Amersham Biosciences, Uppsala, Sweden), 60 mL of 5 mg mL^{-1} copper sulfate was applied and the matrix was subsequently washed with 120 mL ultrafiltrated deionized water. Next the column was equilibrated with 150 mL binding buffer before the heat-treated protein solution (300 mL) was loaded by gravitational flow. Unbound proteins were washed off by 90 mL binding buffer. The His-tagged β -glucosidase was eluted by passing through 80 mL 20 mM Tris-HCl, 250 mM imidazole, 0.75 M NaCl, pH 7.5, and collected in 10 mL fractions. The purified β -glucosidases were dialyzed extensively towards 20 mM citrate phosphate buffer, pH 5.6, in a Spectra/Por Membrane WMC0 3500 (Spectrum Laboratories, Rancho Dominguez, CA, USA) before protein estimation. The protein content in the purified protein sample was estimated by the BCA-copper method with BSA as standard (Sigma, Steinheim, Germany). SDS-PAGE according to Laemmli⁴² was used to analyze the purity of the enzyme, and the expected molecular weight of *TnBgl1A* (52.6 kDa) and *TnBgl3B* (82.2 kDa) was confirmed by comparing the migration with those of the protein standard Precision Plus (BioRad, Sundbyberg, Sweden).

Experimental design

Response surface designs were used to optimize both the subcritical water extraction method and the enzymatic hydrolysis method (see below). The software Minitab[®] (Release 14.1) was used to evaluate the data. Two factors were studied in both designs (extraction cycles, 1, 2 and 3; and temperature, 40, 90 and $120 \text{ }^\circ\text{C}$, in the subcritical water extraction method and pH, 3.0, 5.0 and 7.0; and temperature, 40, 65 and $90 \text{ }^\circ\text{C}$, in the enzymatic hydrolysis method). Two replicates and three central points were used, giving a total number of runs of 18 in both designs.

Subcritical water extraction

Ten grams of onion samples were weighed into 33 mL stainless steel extraction cells containing a cellulose filter at the bottom. Extractions were performed on a Dionex ASE[®]-200 pressurized fluid extraction system (Dionex, Sunnyvale, CA, USA) using water as the only solvent. The pressure was set to 50 bar and the initial heating lasted for 5 min. One to three extraction cycles (steps) of five minutes each were used in a response surface design aiming at optimizing the extraction yield of quercetin and its glycosides from onion waste. Extraction temperatures of 40 to $160 \text{ }^\circ\text{C}$ were also investigated (in the response surface design 40, 90 and $120 \text{ }^\circ\text{C}$). The optimized final

method used three extraction cycles and $120 \text{ }^\circ\text{C}$ extraction temperature. Purging between extractions was performed with nitrogen. Collection was accomplished in 100 mL clear glass vials. The volumes of the aqueous extracts were determined by weighing the collection vials before and after the extraction, and were around 40 to 50 mL.

Enzymatic hydrolysis

Enzymatic hydrolysis was achieved by taking 1.2 mL of onion extract and mixing with 300 μL citrate phosphate buffer (0.1 M). The buffer was prepared by mixing citric acid monohydrate (0.1 M) with disodium hydrogen phosphate Na_2HPO_4 (0.2 M) in different proportions depending on the pH: 79.5, 48.5 and 17.6 vol% of citric acid monohydrate for pH 3.0, 5.0 and 7.0, respectively. The effect of these pH values on the quercetin yield in the enzymatic hydrolysis reaction was investigated in a response surface design. In the same design, the effect of reaction temperature was also studied (40, 65 and $90 \text{ }^\circ\text{C}$). After heating to the desired reaction temperature for 5 min, an initial 100 μL fraction was taken and thereafter the reaction was started by adding the enzyme. The reaction took place during magnetic stirring and controlled heating, and samples of 100 μL were collected during the course of the reaction. To each collected 100 μL fraction, 400 μL formic acid (0.25%), 100 μL morin ($50 \text{ } \mu\text{g mL}^{-1}$, internal standard in methanol) and 400 μL methanol were added. These vials were analyzed by HPLC.

The optimized method used a buffer of pH 5.0 and reaction temperature of $90 \text{ }^\circ\text{C}$. Five microlitres of *TnBgl3B* was used to catalyze the reaction during a reaction time of 10 min.

Conventional extraction/hydrolysis

Conventional extraction/hydrolysis was performed by adding 30 mL of methanol–2.4 M HCl (1 : 1) and a small amount of ascorbic acid ($\sim 20 \text{ mg}$) to 5 g of onion waste and letting it boil at $80 \text{ }^\circ\text{C}$ (ambient pressure) for 2 hours with stirring and occasional shaking.⁴⁰ The extraction slurry was allowed to reach room temperature and then filtered through a Munktell's paper filter (0A, 12.5 cm). The volume was made up to 50 mL with methanol–water (1 : 1). Thereafter, 100 μL was taken and mixed with 400 μL water, 100 μL morin ($50 \text{ } \mu\text{g mL}^{-1}$, internal standard in methanol) and 400 μL methanol. These vials were analyzed by HPLC.

Enzyme specificity

Enzyme specificity of *TnBgl1A* and *TnBgl3B* were determined for two of the substrates, quercetin-3-glycosides and quercetin-4'-glycoside, of which the latter was prepared from onion extracts using preparative HPLC. Substrates dissolved in methanol ($\sim 30 \text{ } \mu\text{g}$ or $\sim 65 \text{ nmol}$ of each) were evaporated and 1 mL of citrate phosphate buffer (0.1 M, pH 5.0) was added. After stirring for 5 min at $90 \text{ }^\circ\text{C}$, an initial 50 μL fraction was taken and thereafter the reaction was started by adding the enzyme. The enzyme concentrations used in this experiment was 35.7 and $55.9 \text{ } \mu\text{g mL}^{-1}$, for *TnBgl1A* and *TnBgl3B*, respectively. Five microlitres of enzyme was used, i.e. 3.4 and 3.5 pmol, respectively. The reaction took place

during magnetic stirring, and fractions of 50 μL were collected after 5, 10, 15, 30 and 60 min of reaction. To each collected 50 μL fraction, 50 μL morin (50 $\mu\text{g mL}^{-1}$, internal standard in methanol) and 900 μL of mobile phase were added. These vials were analyzed by HPLC-UV.

HPLC analysis

Two RP-HPLC systems were used during this study, one system with UV detection and one system with both UV and MS detection in parallel.

HPLC-UV analysis was performed using a chromatographic system composed of a Jasco HPLC pump (Jasco Scandinavia, Mölndal, Sweden), an HP 1050 autosampler (Agilent Technologies, Kista, Sweden) and a Waters 490E UV detector (Waters, Söllerntuna, Sweden). A Waters Symmetry C18 column (150 \times 2.1 mm, 3.5 μm) was used for separation with a methanol–water–formic acid (50 : 50 : 0.1) mobile phase at a flow rate of 0.15 mL min^{-1} . Ten microlitre portions were injected and detection was accomplished at 350 nm. Quantification of quercetin was performed using a four-point calibration curve of a quercetin dihydrate standard (obtained from Sigma–Aldrich, Steinheim, Germany) at concentrations between 2 and 40 $\mu\text{g mL}^{-1}$. Each vial taken to analysis had a total volume of 1 mL and contained an internal standard, morin (Sigma–Aldrich), at a concentration of 5 $\mu\text{g mL}^{-1}$. Estimation of quercetin glycoside composition in different onion parts, the same quantification procedure was applied, although the absorbency of the glycosides was not identical to that obtained with quercetin.

LC-UV-MS/MS analysis was accomplished using a similar chromatographic system but with a manual Rheodyne injector instead of an autosampler. A QTrap linear ion trap mass spectrometer (Applied Biosystems, MDS Sciex, Toronto, Canada) equipped with a pneumatically assisted ESI interface was used. The effluent from the column was split in a Valco-tee connection (Valco International, Schenkon, Switzerland) using two capillaries: one 40 cm silica capillary (i.d. 51 μm) from Polymicro Technologies (Phoenix, AZ, USA) resulting in a flow rate of around 5 $\mu\text{L min}^{-1}$ into the MS, and one 15 cm peek tubing (i.d. 0.25 mm) (Scantec Lab, Partille, Sweden) giving a flow rate of slightly less than 0.15 mL min^{-1} into the UV detector. The ion spray voltage and declustering potential were typically set to 5000 and 50 V respectively. The nebulizer and curtain gas (boil off from liquid nitrogen) were set to 25 and 15 psi, respectively. An information dependent acquisition (IDA) experiment was performed in positive ion mode, which for each chromatographic run involved: (i) enhanced MS scan (EMS) covering a mass range of 200–1000 amu; (ii) enhanced product ion scan (EPI) on four selected parent ions in the above mass range with a collision energy (CE) set to 40 eV and a collision gas pressure (CAD) set to high (4×10^{-5} Torr). A scan rate of 4000 amu s^{-1} with a step size of 0.12 amu was used for both types of scans.

Acknowledgements

Gashaw Mamo is thanked for supplying us with the *T. neapolitana* genomic DNA. Rolf Danielsson is acknowledged for help with statistical evaluation. Sara Bergström is

acknowledged for her valuable help with mass spectrometric analysis. ENK and PT thank the Foundation for Strategic Environmental Research (Mistra), and the Krapperup foundation for financial support. CT acknowledges the financial support from VINNOVA (project number 2005-00322) and SSF (Ingvar Carlsson Award).

References

- S. De, R. N. Chakraborty, S. Ghosh, A. Sengupta and S. Das, Comparative evaluation of cancer chemopreventive efficacy of alpha-tocopherol and quercetin in a murine model, *J. Exp. Clin. Cancer Res.*, 2004, **23**(2), 251–258.
- U. Wenzel, A. Herzog, S. Kuntz and H. Daniel, Protein expression profiling identifies molecular targets of quercetin as a major dietary flavonoid in human colon cancer cells, *Proteomics*, 2004, **4**(7), 2160–2174.
- T. Tanaka, H. Makita, M. Ohnishi, H. Mori, K. Satoh and A. Hara, Chemoprevention of rat oral carcinogenesis by naturally-occurring Xanthophylls, Astaxanthin and Canthaxanthin, *Cancer Res.*, 1995, **55**(18), 4059–4064.
- F. Afaq, M. Saleem, C. G. Krueger, J. D. Reed and H. Mukhtar, Anthocyanin- and hydrolyzable tannin-rich pomegranate fruit extract modulates MAPK and NF-kappa B pathways and inhibits skin tumorigenesis in CD-1 mice, *Int. J. Cancer*, 2005, **113**(3), 423–433.
- P. C. H. Hollman and I. C. W. Arts, Flavonols, flavones and flavanols – nature, occurrence and dietary burden, *J. Sci. Food Agric.*, 2000, **80**(7), 1081–1093.
- S. Mandel, O. Weinreb, T. Amit and M. B. H. Youdim, Cell signaling pathways in the neuroprotective actions of the green tea polyphenol (–)-epigallocatechin-3-gallate: implications for neurodegenerative diseases, *J. Neurochem.*, 2004, **88**(6), 1555–1569.
- S. Bastianetto, W. H. Zheng and R. Quirion, Neuroprotective abilities of resveratrol and other red wine constituents against nitric oxide-related toxicity in cultured hippocampal neurons, *Br. J. Pharmacol.*, 2000, **131**(4), 711–720.
- K. Ono, Y. Yoshiike, A. Takashima, K. Hasegawa, H. Naiki and M. Yamada, Potent anti-amyloidogenic and fibril-destabilizing effects of polyphenols in vitro: implications for the prevention and therapeutics of Alzheimer's disease, *J. Neurochem.*, 2003, **87**(1), 172–181.
- E. Savaskan, G. Olivieri, F. Meier, E. Seifritz, A. Wirz-Justice and F. Muller-Spahn, Red wine ingredient resveratrol protects from beta-amyloid neurotoxicity, *Gerontology (Basel)*, 2003, **49**(6), 380–383.
- H. Zhuang, Y. S. Kim, R. C. Koehler and S. Dore, Potential mechanism by which resveratrol, a red wine constituent, protects neurons, in *Neuroprotective Agents*, 2003, vol. 993, pp. 276–286.
- S. Bastianetto and R. Quirion, Natural extracts as possible protective agents of brain aging, *Neurobiol. Aging*, 2002, **23**(5), 891–897.
- G. Zapata-Torres, F. Opazo, C. Salgado, J. P. Munoz, H. Krautwurst, C. Mascayano, S. Sepulveda-Boza, R. B. Maccioni and B. K. Cassels, Effects of natural flavones and flavonols on the kinase activity of Cdk5, *J. Nat. Prod.*, 2004, **67**(3), 416–420.
- C. M. H. Watanabe, S. Wolfram, P. Ader, G. Rimbach, L. Packer, J. J. Maguire, P. G. Schults and K. Gohil, The in vivo neuromodulatory effects of the herbal medicine ginkgo biloba, *Proc. Natl. Acad. Sci. U. S. A.*, 2001, **98**(12), 6577–6580.
- D. P. Makris and J. T. Rossiter, Domestic processing of onion bulbs (*Allium cepa*) and asparagus spears (*Asparagus officinalis*): Effect on flavonol content and antioxidant status, *J. Agric. Food Chem.*, 2001, **49**(7), 3216–3222.
- K. A. Lombard, E. Geoffriau and E. B. Peffley, Total quercetin content in onion: Survey of cultivars grown at various locations, *HortTechnology*, 2004, **14**(4), 628–630.
- J. M. Zhang, M. B. Satterfield, J. S. Brodbelt, S. J. Britz, B. Clevidence and J. A. Novotny, Structural characterization and detection of kale flavonoids by electrospray ionization mass spectrometry, *Anal. Chem.*, 2003, **75**(23), 6401–6407.
- T. Bahorun, A. Luximon-Ramma, A. Crozier and O. I. Aruoma, Total phenol, flavonoid, proanthocyanidin and vitamin C levels

- and antioxidant activities of Mauritian vegetables, *J. Sci. Food Agric.*, 2004, **84**(12), 1553–1561.
- 18 Y. R. Lu and L. Y. Foo, Identification and quantification of major polyphenols in apple pomace, *Food Chem.*, 1997, **59**(2), 187–194.
- 19 H. F. Wang and K. Helliwell, Determination of flavonols in green and black tea leaves and green tea infusions by high-performance liquid chromatography, *Food Res. Int.*, 2001, **34**(2–3), 223–227.
- 20 S. F. Price, P. J. Breen, M. Valladao and B. T. Watson, Cluster sun exposure and quercetin in Pinot-Noir grapes and wine, *Am. J. Enol. Viticul.*, 1995, **46**(2), 187–194.
- 21 H. Vuorinen, K. Maatta and R. Torronen, Content of the flavonols myricetin, quercetin, and kaempferol in Finnish berry wines, *J. Agric. Food Chem.*, 2000, **48**(7), 2675–2680.
- 22 S. B. Hawthorne, Y. Yang and D. J. Miller, Extraction of organic pollutants from environmental solids with subcritical and supercritical water, *Anal. Chem.*, 1994, **66**(18), 2912–2920.
- 23 E. Ibanez, A. Kubatova, F. J. Senorans, S. Cavero, G. Reglero and S. B. Hawthorne, Subcritical water extraction of antioxidant compounds from rosemary plants, *J. Agric. Food Chem.*, 2003, **51**(2), 375–382.
- 24 C. S. Eskilsson, K. Hartonen, L. Mathiasson and M. L. Riekkola, Pressurized hot water extraction of insecticides from process dust - Comparison with supercritical fluid extraction, *J. Sep. Sci.*, 2004, **27**(1–2), 59–64.
- 25 M. M. Jimenez-Carmona and M. D. L. de Castro, Isolation of eucalyptus essential oil for GC-MS analysis by extraction with subcritical water, *Chromatographia*, 1999, **50**(9–10), 578–582.
- 26 M. Vaher and M. Koel, Separation of polyphenolic compounds extracted from plant matrices using capillary electrophoresis, *J. Chromatogr., A*, 2003, **990**(1–2), 225–230.
- 27 K. G. Martino and D. Guyer, Supercritical fluid extraction of quercetin from onion skins, *J. Food Proc. Eng.*, 2004, **27**(1), 17–28.
- 28 E. Dimitrieska-Stojkovic and Z. Zdravkovski, Supercritical fluid extraction of quercetin and rutin from Hyperici herba, *J. Liq. Chromatogr. Relat. Technol.*, 2003, **26**(15), 2517–2533.
- 29 A. Chafer, M. C. Pascual-Marti, A. Salvador and A. Berna, Supercritical fluid extraction and HPLC determination of relevant polyphenolic compounds in grape skin, *J. Sep. Sci.*, 2005, **28**(16), 2050–2056.
- 30 A. Chafer, T. Fornari, A. Berna and R. P. Stateva, Solubility of quercetin in supercritical CO₂ plus ethanol as a modifier: measurements and thermodynamic modelling, *J. Supercrit. Fluids*, 2004, **32**(1–3), 89–96.
- 31 F. Cuyckens and M. Claeys, Mass spectrometry in the structural analysis of flavonoids, *J. Mass Spectrom.*, 2004, **39**(1), 1–15.
- 32 T. Walle, Absorption and metabolism of flavonoids, *Free Radical Biol. Med.*, 2004, **36**(7), 829–837.
- 33 P. T. Anastas, J. C. Warner, *Green chemistry: theory and practice*. Oxford University Press, Oxford, 1998, p. 135.
- 34 S. Sellappan and C. C. Akoh, Flavonoids and antioxidant capacity of Georgia-grown Vidalia onions, *J. Agric. Food Chem.*, 2002, **50**(19), 5338–5342.
- 35 D. A. Yernool, J. K. McCarthy, D. E. Eveleigh and D.-J. Bok, Cloning and characterization of the glucooligosaccharide catabolic pathway -glucan glucohydrolase and cellobiose phosphorylase in the marine hyperthermophile *Thermotoga neapolitana*, *J. Bacteriol.*, 2000, **182**(18), 5172–5179.
- 36 V. V. Zverlov, I. Y. Volkov, T. V. Velikodvorskaya and W. H. Schwarz, *Thermotoga neapolitana* bglB gene, upstream of lamA, encodes a highly thermostable beta-glucosidase that is a laminaribiase, *Microbiol.*, 1997, **143**(11), 3537–3542.
- 37 P. M. Coutinho, B. H. Henrissat, in *Recent Advances in Carbohydrate Bioengineering*, ed. H. J. Gilbert, G. Davies, B. Henrissat and B. Svensson, The Royal Society of Chemistry, Cambridge, 1999, p. 3.
- 38 B. Henrissat, T. T. Teeri and R. A. J. Warren, A scheme for designating enzymes that hydrolyse the polysaccharides in the cell walls of plants, *FEBS Lett.*, 1998, **425**(2), 352–354.
- 39 P. Turner, O. Holst and E. N. Karlsson, Optimized expression of soluble cyclomaltodextrinase of thermophilic origin in *Escherichia coli* by using a soluble fusion-tag and by tuning of inducer concentration, *Protein Expression Purif.*, 2005, **39**(1), 54–60.
- 40 A. M. Nuutila, K. Kammiovirta and K. M. Oksman-Caldentey, Comparison of methods for the hydrolysis of flavonoids and phenolic acids from onion and spinach for HPLC analysis, *Food Chem.*, 2002, **76**(4), 519–525.
- 41 L. d. Maré, S. Velut, E. Ledung, C. Cimander, B. Norrman, E. N. Karlsson, O. Holst and P. Hagander, A cultivation technique for *E. coli* fed-batch cultivations operating close to the maximum oxygen transfer capacity of the reactor, *Biotechnol. Lett.*, 2005, **27**(14), 983–990.
- 42 U. Laemmli, Cleavage of structural proteins during assembly of the head of bacteriophage T4, *Nature*, 1970, **227**(5259), 680–685.

A green route to β -amino alcohols *via* the uncatalyzed aminolysis of 1,2-epoxides by alkyl- and arylamines

Simona Bonollo, Francesco Fringuelli,* Ferdinando Pizzo* and Luigi Vaccaro

Received 30th May 2006, Accepted 18th July 2006

First published as an Advance Article on the web 10th August 2006

DOI: 10.1039/b607620c

Under mildly basic and pH-controlled aqueous conditions the aminolysis of 1,2-epoxides **1a–g** by alkyl- and arylamines **2a–k** is generally highly regioselective giving the corresponding β -amino alcohols in satisfactory to excellent yields.

Water is playing an important role in the development of new synthetic processes both by improving their chemical efficiency and by reducing their environmental impact.¹

The aminolysis of 1,2-epoxides is an important synthetic tool which furnishes the direct access to β -amino alcohols, that are an undoubtedly important class of molecules in organic synthesis.²

The oxirane ring-opening by an amine is a widely studied process and the use of a large number of metal catalysts has been investigated.³ However, the results have never been completely satisfactory due to typical limitations of these procedures (high temperatures, large amounts of catalysts, hazardous solvents, formation of bis-adducts). Surprisingly, water has been scarcely used as reaction medium for this transformation.⁴

Aminolysis of 1,2-epoxides with arylamines has been recently performed in water in the presence of 1,4-diazabicyclo[2.2.2]octane (DABCO),^{4d} triethylamine,^{4d} and β -cyclodextrin.^{4e} In addition, a kinetic study and an investigation on the distribution of mono-, di-, and trisubstituted products, carried out in water and in the absence of any catalyst, already appeared more than thirty years ago.^{4a,b} Recently, Azizi and Saidi^{4c} reported excellent results on the aminolysis of aliphatic 1,2-epoxides with aliphatic amines in water. In this paper it has also been reported that aniline and *p*-isopropylaniline reacted only with styrene oxide, while with other aryl amines and 1,2-epoxides only discouraging results were obtained.

In summary, the few data reported in the literature suggest that an efficient protocol for the uncatalyzed aminolysis of 1,2-epoxides by aromatic amines in water is desirable.

In the last few years, we have been working on the chemistry of 1,2-epoxide in water⁵ and under solvent-free conditions,⁶ and we have demonstrated that by an accurate choice of the pH-conditions of the aqueous medium, the efficiency of the oxirane ring-opening reactions can be significantly increased.^{5,6}

Accordingly, we have started a study aimed at the optimization of the aminolysis of 1,2-epoxides in water. On the basis of our previous experience,^{5,6} we have ascertained that the pH value of the aqueous medium plays a crucial role

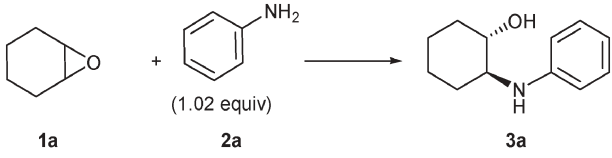
in determining the efficiency of this process. Surprisingly, in the literature devoted to the study of this reaction in aqueous medium, the pH has never been taken into account.⁴ We believe that by controlling the pH of the aqueous medium, the aminolysis of 1,2-epoxides by aryl amines can also be performed efficiently.

In our study, we have considered the reactions of 1,2-epoxides **1a–g** with the amines **2a–k**.

We have initially performed the aminolysis of cyclohexene oxide (**1a**) with aniline (**2a**) in water for which divergent results have been reported.^{4d,e} The results are reported in Table 1.

Under acidic conditions (pH 5.0) at 30 °C, even if the oxirane ring is in principle activated⁷ and the aniline (**2a**) is present in a deprotonated form at a sufficient concentration, the aminolysis reaction leading to *trans*-2-(*N*-phenylamino)-cyclohexanol (**3a**) was very slow (100 h for 90% conversion) and accompanied by the hydrolysis of **1a** with the formation of the corresponding *trans*-1,2-cyclohexanediol (20%) (Table 1, entry 1). Under neutral conditions the reaction was faster and the *trans*-1,2-cyclohexanediol was not formed (Table 1, entry 2). By performing this process under slightly basic conditions (pH 8 and 10), the reaction time, for the 90–95% conversion of **1a** to **3a**, was reduced to 25 h (Table 1, entries 3 and 5, respectively).

Table 1 Aminolysis of cyclohexene oxide (**1a**) by aniline (**2a**)



Entry	pH	T/°C	t/h	Conversion ^a (%)
1	5.0	30	100	90 ^b
2	7.0	30	45	90
3	8.0	30	25	90
4	8.30 ^c	30	25	90
5	10.0	30	25	95
6	8.0 ^c	60	14	95 ^d
7	— ^e	30	120	5
8	— (in MeCN)	30	120	<1

^a Conversion measured by GLC analyses, the remaining material was the unreacted **1a**. ^b 20% of *trans*-1,2-cyclohexanediol was formed. ^c pH obtained by mixing 1.0 mmol of **1a** and 1.02 mmol of **2a** in 2.0 mL of deionized water. ^d **3a** was isolated in 90% yield. ^e Under solvent-free conditions

CEMIN—Centro di Eccellenza Materiali Innovativi Nanostrutturati, Dipartimento di Chimica, Università di Perugia, Via Elce di Sotto, 8 06123, Perugia, Italia. E-mail: pizzo@unipg.it; frifra@unipg.it; Fax: +39 075 5855560; Tel: +39 075 5855558

It is noteworthy that when 1.0 mmol of **1a** was mixed with 1.05 mmol of **2a** in 2.0 mL of deionized water the resulting pH value was 8.30, and in addition during the progress of the aminolysis process, little change of pH was observed. Therefore, we have identified as the optimal pH reaction conditions just those resulting from the simple mixing of the reagents (pH 8.30) (Table 1, entry 4).

Finally, when the aqueous mixture of **1a** and **2a** was warmed at 60 °C the resulting pH was 8.0 and after 14 h the product **3a** was isolated in 90% yield (Table 1, entry 6). Very little conversion was obtained by performing this reaction in MeCN or under solvent-free conditions (Table 1, entries 7 and 8).

In summary, the reaction of **1a** with **2a** in water at 60 °C, performed by simply mixing the reagents, was complete in an acceptable time, avoiding the use of any catalyst and making this procedure very economical and efficient. β -Amino alcohol **3a** was the only product and no traces of bis-adduct coming from the attack of **3a** to another molecule of 1,2-epoxide **1a** was detected.

This protocol was extended to the aminolysis of alkyl 1,2-epoxides **1b–f** by aniline (**2a**) and the results are reported in Table 2.

The pH of the aqueous mixture of 1,2-epoxide **1b–f** (1.0 mmol) with **2a** (1.02 mmol) at 60 °C was already adequate for a successful aminolysis. Under these reaction conditions all the transformations proceeded with acceptable reaction times.

Table 2 Aminolysis of alkyl-1,2-epoxides **1b–f** by aniline (**2a**) (1.02 equiv.) in water at 60 °C

Entry	1,2-Epoxide	pH	t/h	3/4 ^a	Bis-adducts ^b	Y (%) ^c
1		8.0	40	93/7	5	80
2		8.1 ^c	170	93/7	5	70
3		7.8	22	—	—	78
4		8.4	17	99/1	15	70
5		8.4	17	99/1	8	80 ^d
6		8.2	10	99/1	5	90

^a Ratios evaluated by GLC analyses. ^b Evaluated by ¹H NMR analyses ^c Yield of the isolated β -amino alcohols products. ^d By using 2.0 mol equiv. of **2a**.

In the case of **1b**, **c**, and **f** the bis-adduct coming from attack of the product **3** to the β -carbon of another molecule of the 1,2-epoxide, was generally negligible (5% of the reaction mixture, Table 2, entries 1, 2, and 6), while with **1d** bis-adduct product was totally absent (Table 2, entry 3). Only in the case of **1e** the corresponding bis-adduct formed in a relevant amount (15%, Table 2, entry 4) but by using 2.0 mol equiv. of aniline (**2a**) was reduced to 8% of the reaction products mixture (Table 2, entry 5). The attack of aniline (**2a**) to alkyl 1,2-epoxides occurred regioselectively at the less substituted C- β carbon and in all the cases the β -amino alcohols were isolated in satisfactory yields (70–90%).

Our synthetic study was further completed by performing the aminolysis of **1g** by using a variety of amines (**2a–k**). The results obtained are reported in Table 3.

The aqueous mixture of **1g** and one of the alkylamines **2b–d** was strongly basic (pH 11–12) and in these cases aminolyses of **1g** with **2b–d** were very efficient giving the complete conversion to products **5b–d** and **6b–d** in reasonable times (9–19 h) and without formation of any by-products and with a preferential C- β regioselectivity (Table 3, entries 1–3).

In the case of 2-picolyamine (**2e**), when the reagents were used in equimolar amounts, 15% of the bis-adduct coming from the attack of **5e** to the β -carbon of **1g** was found (Table 3, entry 4). This product was reduced to 5% of the reaction mixture by using 2.0 mol equiv. of **2e** (Table 3, entry 5).

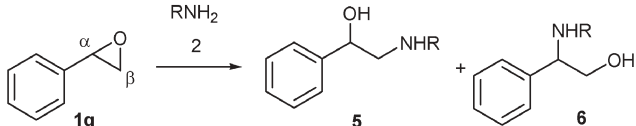
Also, the reaction of **1g** with aniline (**2a**) and with electron-rich anilines **2f** and **2g** could be performed with high yields at the pH resulting from the mixing of equimolar amounts of reagents (Table 3, entries 6–8). In these cases a reversed regioselectivity was observed with respect to that obtained in the case of aliphatic amines.

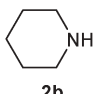
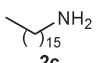
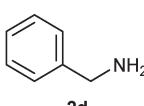
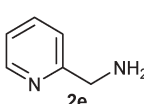
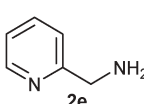
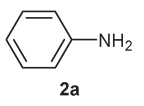
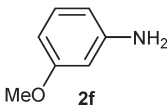
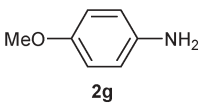
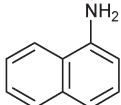
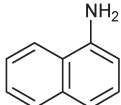
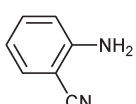
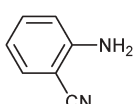
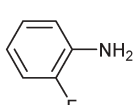
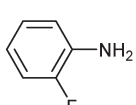
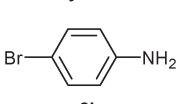
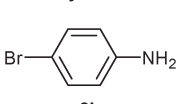
The reactions of styrene oxide (**1g**) with poorly nucleophilic amines **2h–k** at the pH resulting from the mixing of equimolar amounts of **1g** and the appropriate amines gave large amounts of the corresponding 1-phenyl-ethane-1,2-diol (36–50% of the product mixtures) (Table 3, entries 9, 11, 13, and 15). By working at pH 10.0 and by using 2.0 molar equiv. of the amine the problem was overcome and satisfactory yields of the isolated products were obtained (Table 3, entries 10, 12, 14, and 16).

As for the aminolysis by electron-rich anilines a C- α regioselectivity was observed.

The regioselectivities in the aminolysis of 1,2-epoxides in water are similar to those obtained in the azidolysis and thiolysis performed in water under basic conditions.^{5b,c,7} Arylamines preferentially attack the C- β of alkyl epoxides while in the case of styrene oxide (**1g**), the C- α benzylic carbon is preferred according to an S_N2 borderline mechanism. Alkylamines, that possess a higher nucleophilic character than aromatic amines, attack preferentially the less substituted C- β carbon of **1g** according to an S_N2 mechanism.

In conclusion, the results obtained in this study show that in water, a careful control of the pH conditions is essential for the efficiency of the aminolysis of 1,2-epoxides and a protocol for both alkyl- and arylamines has been defined. The procedure reported avoids the use of both organic solvents and catalyst, proving to be chemically efficient, economical, and environmentally-friendly.

Table 3 Aminolysis of styrene oxide (**1g**) with alkyl- and arylamines **2a–k** in water at 60 °C


Entry	Amine	pH	t/h	5/6	Yield (%) ^a
1	 2b	12	9 ^b	63/37	90
2	 2c	11	12 ^b	83/17	75
3	 2d	11	19 ^b	60/40	80
4	 2e	11	8 ^b	43/57	—
5	 2e	11	8 ^c	43/57	77
6	 2a	8.1	15 ^b	16/84	93
7	 2f	7.7	7 ^b	14/86	85
8	 2g	7.5	2 ^b	12/88	90
9	 2h	7.1	9 ^b	20/80	— ^d
10	 2h	10 ^e	7 ^c	18/82	70
11	 2i	6.1	19 ^b	8/92	— ^f
12	 2i	10 ^e	24 ^c	8/92	70
13	 2j	7.3	19 ^b	14/86	— ^g
14	 2j	10 ^e	11 ^c	14/86	90
15	 2k	7.1	35 ^b	11/89	— ^h
16	 2k	10 ^e	26 ^c	11/89	70

^a Yield of the isolated products **5/6**. ^b 1.05 molar equiv. of amine. ^c 2.0 molar equiv. of amine. ^d 36% of diol was formed. ^e Obtained by adding a few drops of NaOH 5 M aqueous solution. ^f 50% of diol was formed. ^g 43% of diol was formed. ^h 39% of diol was formed.

Experimental

General

All chemicals were purchased and used without any further purification. GC-EIMS analyses were carried out with 70 eV electron energy. ¹H NMR and ¹³C NMR spectra were recorded at 200 MHz or 400 MHz, and at 50.3 or 100.6 MHz respectively, using a convenient deuterated solvent (reported below) and the residual peak as internal standard, or TMS in the case of CDCl₃. All melting points are uncorrected. Thin layer chromatography analyses were performed on silica gel on aluminium plates and UV and/or KMnO₄ were used as revealing agents. Column chromatographies were performed by using silica gel 230–400 mesh and eluting as reported below. β-amino alcohols **3a**,¹ **3b**,² **3d**,¹ **3e**,³ **3f**,² **5b**,⁴ **5d**,⁵ **5e**,⁷ **6a**,³ **6b**,⁶ **6d**,³ **6e**,⁷ and **6g**⁶ are known compounds, β-amino alcohols **6f** and **6k** have been already prepared but spectroscopic data have not been reported, β-amino alcohols **3c**, **5c**, **6h**, **6i**, **6j** are new compounds. Characterization data (¹H NMR, ¹³C NMR, GC-EIMS, mp, and elemental analyses) for β-amino alcohols **3c**, **5c**, **6f**, **6h–k** are reported below.

Representative experimental procedure. Aminolysis of 1,2-hexadecene oxide (**1c**) by aniline (**2a**): in a screw capped vial equipped with a magnetic stirrer, aniline (**2a**) (0.190 g, 2.04 mmol) and 1,2-hexadecene oxide (**1c**) (0.481 g, 2.0 mmol) were consecutively added in water (4 mL) and the resulting mixture was left under vigorous stirring at 60 °C for 170 h. The mixture was basified with NaOH 5 M until pH 10 and extracted with AcOEt (2 × 4 mL). The combined organic layers were dried over anhydrous Na₂SO₄. The solvent was evaporated and the crude product was charged on a triethylamine pretreated silica gel column chromatography (diethyl ether/petroleum ether 3/7; silica/sample: 60 : 1). Pure 1-(phenylamino)hexadecan-2-ol (**3c**) was isolated as a white solid (70% overall yield **3c** + **4c**, 0.466 g).

1-(Phenylamino)hexadecan-2-ol (**3c**)

Isolated in 70% overall yield **3c** + **4c**. White solid, mp = 57–59 °C (diethyl ether/petroleum ether 3/7). ¹H NMR (CDCl₃) δ = 0.88 (t, 3H, *J* = 6.6 Hz); 1.20–1.40 (m, 23H); 1.40–1.60 (m, 3H); 2.99 (dd, 1H, *J* = 8.6, 12.8 Hz); 2.80–3.20 (bs, 1H); 3.26 (dd, 1H, *J* = 2.9, 12.8 Hz); 3.80–3.90 (m, 1H); 6.66 (d, 2H, *J* = 8.2 Hz); 6.74 (t, 1H, *J* = 7.2 Hz); 7.18 (t, 2H, *J* = 7.6 Hz). ¹³C NMR (CDCl₃) δ = 148.1, 129.3, 118.1, 113.5, 70.3, 50.5, 35.1, 31.9, 29.7, 29.6, 29.4, 25.6, 22.7, 14.1. Anal. calc. for C₂₂H₃₉NO: C, 79.22; H, 11.79; N, 4.20; O 4.80. Found: C, 79.19; H, 11.88; N, 4.26. GC/EIMS (*m/z*): 333 (M⁺, 16), 107 (13), 106 (100).

2-(Hexadecylamino)-1-phenylethanol (**5c**)

Isolated in 75% overall yield **5c** + **6c**. White solid, mp = 83–85 °C (diethyl ether). ¹H NMR (CDCl₃) δ = 0.88 (t, 3H, *J* = 6.8 Hz); 1.20–1.40 (m, 25H); 1.40–1.60 (m, 3H); 2.20–2.80 (bs, 2H); 2.60–2.80 (m, 3H); 2.90 (dd, 1H, *J* = 3.6, 12.2 Hz); 4.73 (dd, 1H, *J* = 3.6, 9.1 Hz); 7.20–7.45 (m, 5H). ¹³C NMR (CDCl₃) δ = 142.2, 128.4, 127.6, 125.8, 71.1, 56.9, 49.3, 31.9, 29.7, 29.4, 29.3, 27.1, 22.7, 14.1. Anal. calc. for C₂₄H₄₃NO: C,

79.72; H, 11.99; N, 3.87. Found: C, 79.93; H, 11.64; N, 3.71. GC/EIMS (*m/z*): 362 (M^+ , 1), 255 (25), 254 (100), 44 (20).

2-(3'-Methoxyphenylamino)-2-phenylethanol (6f)

Isolated in 85% overall yield **5f** + **6f**. Yellow oil. 1H NMR ($CDCl_3$) δ = 3.68 (s, 3H); 3.79 (dd, 1H, J = 7.1, 11.2 Hz); 3.94 (dd, 1H, J = 4.1, 11.2 Hz); 4.50 (dd, 1H, J = 4.1, 7.1 Hz); 6.15 (d, 1H, J = 2.0 Hz); 6.23 (dd, 1H, J = 1.4, 8.1 Hz); 6.27 (dd, 1H, J = 2.0, 8.1 Hz); = 7.01 (t, 1H, J = 8.1 Hz); 7.20–7.50 (m, 5H). ^{13}C NMR ($CDCl_3$) δ = 160.6, 148.0, 139.6, 129.9, 128.8, 127.7, 126.8, 107.3, 103.6, 100.3, 67.1, 60.4, 55.0. Anal. calc. for $C_{15}H_{17}NO_2$: C, 74.05; H, 7.04; N, 5.76. Found: C, 74.41; H, 6.82; N, 5.96. GC/EIMS (*m/z*): 243 (M^+ , 19), 137 (17), 136 (100), 77 (14).

2-(Napht-1'-ylamino)-2-phenylethanol (6h)

Isolated in 70% overall yield **5h** + **6h**. Orange solid, mp = 127–130 °C (diethyl ether/petroleum ether 3/7). 1H NMR ($CDCl_3$) δ = 1.50–2.00 (bs, 1H); 3.92 (dd, 1H, J = 6.9, 11.2 Hz); 4.10 (dd, 1H, J = 4.1, 11.2 Hz); 4.69 (dd, 1H, J = 4.1, 6.9 Hz); 6.39 (d, 1H, J = 6.7 Hz); 7.10–7.40 (m, 5H); 7.40–7.55 (m, 4H); 7.80–7.90 (dd, 1H, J = 2.6, 6.9 Hz); 8.00–8.15 (m, 1H). ^{13}C NMR ($CDCl_3$) δ = 142.0, 139.7, 134.3, 128.9, 128.7, 127.7, 126.7, 126.4, 125.7, 124.9, 123.8, 120.0, 118.0, 106.7, 67.5, 60.0. Anal. calc. for $C_{18}H_{17}NO$: C, 82.10; H, 6.51; N, 5.32. Found: C, 82.42; H, 6.38; N, 5.17. GC/EIMS (*m/z*): 263 (M^+ , 15), 233 (22), 232 (100), 127 (13).

2-(2'-Cyanophenylamino)-2-phenylethanol (6i)

Isolated in 70% overall yield **6i** + **5i**. Yellow liquid. 1H NMR ($CDCl_3$) δ = 2.30–2.55 (bs, 1H); 3.83 (dd, 1H, J = 7.0, 11.2 Hz); 3.97 (dd, 1H, J = 4.2, 11.2 Hz); 4.55–4.65 (m, 1H); 5.45 (d, 1H, J = 4.9 Hz); 6.43 (d, 1H, J = 8.5 Hz); 6.64 (t, 1H, J = 7.5 Hz); 7.15–7.50 (m, 7H). ^{13}C NMR ($CDCl_3$) δ = 149.5, 138.9, 134.0, 132.7, 128.9, 127.9, 126.5, 117.9, 117.1, 112.3, 96.4, 66.8, 59.4. Anal. calc. for $C_{15}H_{14}N_2O$: C, 75.61; H, 5.92; N, 11.76. Found: C, 75.92; H, 5.64; N, 11.79. GC/EIMS (*m/z*): 238 (M^+ , 3), 208 (21), 207 (100), 129 (24), 102 (10).

2-(2'-Fluorophenylamino)-2-phenylethanol (6j)

Isolated in 90% overall yield **5j** + **6j**. White solid, mp = 75–78 °C (diethyl ether/petroleum ether 3/7). 1H NMR ($CDCl_3$) δ = 1.60–2.00 (bs, 1H); 3.77 (dd, 1H, J = 7.0, 11.2 Hz); 3.94 (dd, 1H, J = 4.2, 11.2 Hz); 4.51 (dd, 1H, J = 4.2, 7.0 Hz); 4.60–4.90 (bs, 1H); 6.46 (dt, 1H, J = 1.5, 8.4 Hz); 6.55–6.62 (m, 1H); 6.82 (dt, 1H, J = 0.7, 7.8 Hz); 6.97 (ddd, 1H, J = 1.4, 8.0, 11.8 Hz); 7.20–7.40 (m, 5H). ^{13}C NMR ($CDCl_3$) δ = 151.8, 139.7, 135.6, 128.9, 127.7, 126.6, 124.4, 117.3, 114.4, 113.6, 67.2, 59.6. Anal. calc. for $C_{14}H_{14}FNO$: C, 72.71; H, 6.10; F 8.21; N, 6.06. Found: C, 72.32; H, 6.36; F 8.47; N, 6.28. GC/EIMS (*m/z*): 231 (M^+ , 7), 201 (20), 200 (100), 122 (24).

2-(4'-Bromophenylamino)-2-phenylethanol (6k)

Isolated in 70% overall yield **5k** + **6k**. Yellow liquid. 1H NMR ($CDCl_3$) δ = 3.66 (dd, 1H, J = 7.0, 11.1 Hz); 3.86 (dd, 1H,

J = 3.7, 11.1 Hz); 4.38 (m, 1H); 6.39 (d, 2H, J = 8.5 Hz); 7.13 (d, 2H, J = 8.5 Hz); 7.20–7.40 (m, 5H). ^{13}C NMR ($CDCl_3$) δ = 146.1, 139.5, 131.7, 128.8, 127.7, 126.6, 115.3, 109.4, 67.1, 59.7. Anal. calc. for $C_{14}H_{14}BrNO$: C, 57.55; H, 4.83; Br 27.35 N, 4.79. Found: C, 57.49; H, 4.78; Br, 27.38; N, 4.73. GC/EIMS (*m/z*): 293 (M^+ , 7), 263 (15), 262 (98), 261 (17), 260 (100), 183 (11), 181 (14), 180 (12), 157 (10), 77 (10).

Acknowledgements

The Ministero dell'Istruzione dell'Università e della Ricerca (MIUR) and the Università degli studi di Perugia (within the funding projects: COFIN, COFINLAB (CEMIN) and FIRB 2001) are thanked for financial support.

References

- (a) P. T. Anastas, *Green Chemistry: Theory and Practice*, Oxford University Press, Oxford, 1998; (b) C. J. Li and T. H. Chang, *Organic Reactions in Aqueous Media*, Wiley, New York, 1997; (c) *Organic Synthesis in Water*, ed. P. A. Grieco, Blackie Academic and Professional, London, 1998; (d) F. Fringuelli, O. Piermatti, F. Pizzo and L. Vaccaro, *Eur. J. Org. Chem.*, 2001, 439–455; (e) U. M. Lindström, *Chem. Rev.*, 2002, **102**, 2751–2772; (f) C. J. Li, *Chem. Rev.*, 2005, **105**, 3095–3165.
- (a) D. J. Ager, I. Prakash and D. R. Schaad, *Chem. Rev.*, 1996, **96**, 835–876; (b) S. C. Bergmeier, *Tetrahedron*, 2000, **56**, 2561–2576; (c) H. -S. Lee and S. H. Kang, *Synlett*, 2004, 1673–1685.
- (a) G. H. Posner and D. Z. Rogers, *J. Am. Chem. Soc.*, 1977, **99**, 8208–8214; (b) M. Chini, P. Crotti and F. Macchia, *Tetrahedron Lett.*, 1990, **31**, 4661–4664; (c) Y. Yamamoto, N. Asao, M. Meguro, N. Tsukade, H. Nemoto, N. Adayari, J. G. Wilson and H. Nakamura, *J. Chem. Soc., Chem. Commun.*, 1993, 1201–1203; (d) U. M. Lindström and P. Somfai, *Synthesis*, 1998, 109; (e) G. Sekar and V. K. Singh, *J. Org. Chem.*, 1999, **64**, 287–289; (f) S. Sagava, H. Abe, Y. Hase and T. Inaba, *J. Org. Chem.*, 1999, **64**, 4962–4965; (g) M. Curini, F. Epifano, M. C. Marcotullio and O. Rosati, *Eur. J. Org. Chem.*, 2001, 4149–4152; (h) K. Fagnou and M. Lautens, *Org. Lett.*, 2000, **2**, 2319–2321; (i) L. D. Pachón, P. Gamez, J. J. van Bassel and J. Reedijk, *Tetrahedron Lett.*, 2003, **44**, 6025–6027; (j) A. K. Chakraborti and A. Kondaskar, *Tetrahedron Lett.*, 2003, **44**, 8315–8319; (k) P.-Q. Zhao, L.-W. Xu and C.-G. Xia, *Synlett*, 2004, 846–850; (l) R.-H. Fan and X.-L. Hou, *J. Org. Chem.*, 2003, **68**, 726–730; (m) A. Kamal, R. Ramu, M. Amerudin Azhar and G. B. Ramesh Khanna, *Tetrahedron Lett.*, 2005, **46**, 2675–2677; (n) F. Carree, R. Gil and J. Collin, *Tetrahedron Lett.*, 2004, **45**, 7749–7751; (o) G. Sundrarajan, K. Vijayakrishna and B. Varghese, *Tetrahedron Lett.*, 2004, **45**, 8253–8256; (p) J. R. Rodriguez and A. Navarro, *Tetrahedron Lett.*, 2004, **45**, 7495–7498; (q) M. M. Mojtahedi, M. R. Saidi and M. Bolourchian, *J. Chem. Res., Synop.*, 1999, 128–129; (r) U. Das, B. Crousse, V. Kesavan, D. Bonnet-Delpon and J. -P. Bégue, *J. Org. Chem.*, 2000, **65**, 6749–6751; (s) J. S. Yadav, B. V. S. Reddy, A. K. Basak and A. V. Narsaiah, *Tetrahedron Lett.*, 2003, **44**, 1047–1050; (t) T. Ollevier and G. Lavie-Compin, *Tetrahedron Lett.*, 2004, **45**, 49–52; (u) A. K. Chakraborti and A. Kondaskar, *Tetrahedron Lett.*, 2003, **44**, 8315–8319; (v) A. K. Chakraborti, S. Rudrawar and A. Kondaskar, *Org. Biomol. Chem.*, 2004, **2**, 1277–1280.
- (a) D. R. Burfield, S. Gan and R. H. Smithers, *J. Chem. Soc., Perkin Trans. 1*, 1977, 666–671; (b) P. K. Sundaram and M. M. Sharma, *Bull. Chem. Soc. Jpn.*, 1969, **42**, 3141–3147; (c) M. Azizi and M. R. Saidi, *Org. Lett.*, 2005, **7**, 3649–3651; (d) J. Wu and H. -G. Xia, *Green Chem.*, 2005, **7**, 708–710; (e) K. Surendra, N. S. Krishnaveni and K. R. Rao, *Synlett*, 2005, 506–510.
- For recent papers see: (a) F. Fringuelli, F. Pizzo, M. Rucci and L. Vaccaro, *J. Org. Chem.*, 2003, **68**, 7041–7045; (b) F. Fringuelli, F. Pizzo, S. Tortoioli and L. Vaccaro, *J. Org. Chem.*, 2003, **68**, 8248–8251; (c) D. Amantini, F. Fringuelli, F. Pizzo, S. Tortoioli and L. Vaccaro, *Synlett*, 2003, **68**, 2292–2296; (d) F. Fringuelli, F. Pizzo and L. Vaccaro, *J. Org. Chem.*, 2004, **69**, 2315–2321; (e)

F. Fringuelli, F. Pizzo, S. Tortoioli and L. Vaccaro, *Org. Lett.*, 2005, **7**, 4411–4414.

6 (a) F. Fringuelli, F. Pizzo, S. Tortoioli and L. Vaccaro, *J. Org. Chem.*, 2004, **69**, 7745–7747; (b) F. Fringuelli, F. Pizzo, S. Tortoioli and L. Vaccaro, *J. Org. Chem.*, 2004, **69**, 8780–8785; (c) F. Fringuelli, F. Pizzo, C. Vittoriani and L. Vaccaro, *Chem.*

Commun., 2004, 2756–2757; (d) F. Fringuelli, F. Pizzo, S. Tortoioli, C. Zuccaccia and L. Vaccaro, *Green Chem.*, 2006, **8**, 191–196.

7 At pH 4.2 the azidolysis of 1,2-epoxides is strongly catalyzed and generally gives a C- α regioselectivity, indicating that the process proceeds on the protonated oxirane-ring: F. Fringuelli, F. Pizzo and L. Vaccaro, *J. Org. Chem.*, 1999, **64**, 6094–6096.

Find a SOLUTION

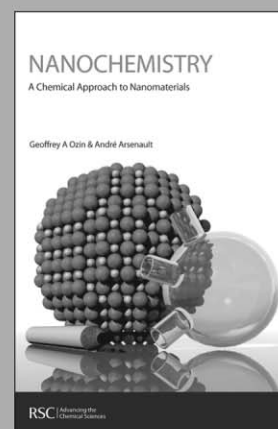
... with books from the RSC

Choose from exciting textbooks, research level books or reference books in a wide range of subject areas, including:

- Biological science
- Food and nutrition
- Materials and nanoscience
- Analytical and environmental sciences
- Organic, inorganic and physical chemistry

Look out for 3 new series coming soon ...

- RSC Nanoscience & Nanotechnology Series
- Issues in Toxicology
- RSC Biomolecular Sciences Series



28040542

RSC | Advancing the
Chemical Sciences

www.rsc.org/books

Formation and catalytic activity of Pd nanoparticles on silica in supercritical CO₂

Shohreh Saffarzadeh-Matin,^{ac} Francesca M. Kerton,^{*b} Jason M. Lynam^a and Christopher M. Rayner^c

Received 19th May 2006, Accepted 18th July 2006

First published as an Advance Article on the web 14th August 2006

DOI: 10.1039/b607118j

Metal complexes of polydimethylsiloxane-derived ligands can be adsorbed onto silica and subsequently reduced *in-situ* in supercritical CO₂ (scCO₂) to generate metal nanoparticles. Pd nanoparticles on silica, generated during C–C coupling reactions in scCO₂, can be recycled several times without any loss in activity. Focusing on Heck and Suzuki coupling reactions, the products showed no contamination of the organic products with Pd using quantitative ICP emission spectroscopy. The use of scCO₂ prevents the desorption of the Pd nanoparticles from their support. Build-up of ammonium salts as by-products in these coupling reactions leads to reduced activity for these heterogeneous catalysts after four runs.

Introduction

Palladium catalysed coupling reactions have been the subject of intensive research over the last twenty years.^{1–3} The main use of these reactions is to create biaryls. The Suzuki reaction, reaction of aryl or vinyl halides or triflates with boronic acids, is of particular importance to the pharmaceutical and agrochemical industries. For example, it is used in the industrial production of Losartan, a Merck antihypertensive drug.⁴ The Heck reaction, which results in C–C bond formation between alkenes and aromatic rings, is used in at least five commercial processes on a scale in excess of 1 ton per year.⁵ Attempts to perform these reactions more cleanly can be divided into two areas, the use of supported/recyclable catalysts and the use of environmentally benign media.

Recent reports on palladium based heterogeneous catalysts for these reactions include Suzuki couplings using Pd/C in DMF/water,⁶ continuous Heck and Suzuki reactions using Pd(0) within ion-exchange resins using *N*-methylpyrrolidinone or DMF/water as the solvent, biomaterial supported Pd in xylene for Suzuki and Heck reactions,^{7,8} and nanosized Pd particles in silica or carbon aerogels for Heck reactions in acetonitrile.⁹

A number of groups have performed ‘ligand-free’ Pd catalysed Suzuki reactions in water.^{10,11} Suzuki reactions have also been performed in PEG-400 and ionic liquids/water.^{12,13} Since the first reported Pd catalysed C–C bond forming reactions in scCO₂,^{14,15} a wide range of substrates and substances have been transformed in this medium using Pd.^{16,17} Recent examples include cyclotrimerization reactions and C–N bond formations.^{18,19}

More recently researchers have combined these areas of green chemistry and have performed reactions using heterogeneous catalysts in benign media. For example, “solventless” Suzuki coupling reactions have been conducted using palladium-doped potassium fluoride alumina,²⁰ Pd/C has been used as a recyclable catalyst in Suzuki cross-coupling reactions in water,²¹ and polyurea-encapsulated Pd has been used in Heck, Stille and Suzuki reactions in scCO₂.^{22,23}

In this paper, we describe the *in situ* preparation of Pd nanoparticles on silica in scCO₂ and the use of this material as a recyclable catalyst for C–C bond forming reactions in scCO₂.

Experimental

Reagents were purchased from Aldrich or Lancaster. Palladium salts were purchased from Precious Metals Online Ltd (Australia). Polydimethylsiloxane monocarbinol and phenyl(*tri-n*-butyl)tin were purchased from ABCR Gelest. Liquid reagents were deoxygenated by three freeze–pump–thaw cycles prior to use. PDMS-PPh₂, Fig. 1, Pd(PDMS-PPh₂)₂Cl₂ and Pd(PDMS-PPh₂)₂Cl₂ on silica (supported pre-catalyst), Fig. 2, were prepared according to literature procedures.²⁴

Toluene was dried over sodium-benzophenone, distilled under argon and subsequently stored in ampoules under nitrogen. Deuterated chloroform was dried over CaH₂, distilled and then stored under nitrogen in the presence of molecular sieves.

Reaction mixtures and products were analysed on a Jeol EX 270 or a Bruker AMX-500 NMR spectrometer. ¹H NMR spectra were referenced to residual protons in the deuterated solvent. DRIFT spectra were obtained on a IR Bruker Equinox 55 equipped with a Specac Diffuse Reflectance accessory. TEM was performed on a Tecnai 12 BIO TWIN operating at 120 kV in the Biology Department at the University of York. Simultaneous TGA, differential TGA (DTGA) and DSC were conducted using a Stanton Redcroft STA 625 GTA under a nitrogen atmosphere. ICP analyses was performed on a UNICAM 701 Series Emission Spectrometer by the Advanced Chemical and Materials Analysis service of

^aDepartment of Chemistry, University of York, Heslington, York, UK YO10 5DD. Fax: +44 (0)1904 432516

^bGreen Chemistry and Catalysis Group, Department of Chemistry, Memorial University of Newfoundland, St. John's, NL, A1B 3X7, Canada. E-mail: fkerton@mum.ca; Fax: +1 709 7373702; Tel: +1 709 7378089

^cCleaner Synthesis Group, Department of Chemistry, University of Leeds, Leeds, UK LS2 9JT. Fax: +44 (0)113 3436565

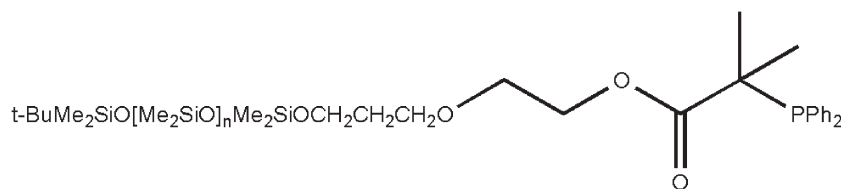


Fig. 1 Poly(dimethylsiloxane)-derived phosphine ligand, PDMS-PPh₂.

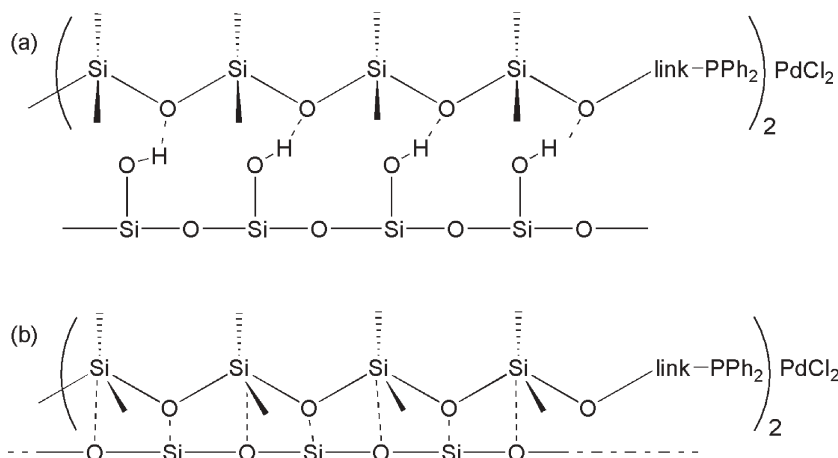


Fig. 2 Proposed adsorption mechanism of PDMS-PPh₂ complexes on silica through (a) hydrogen-bonding and (b) van der Waals interactions.

the University of Newcastle. Elemental analyses were performed by Elemental Microanalysis Ltd, Devon.

In order to check the reproducibility of the catalytic reactions and the recyclability of the catalyst, they were performed at least twice. The average conversions from the experiments are reported, Table 1.

Heck reaction using supported catalyst in toluene

A Schlenk tube was charged with the supported pre-catalyst (0.80 g, 2 mol% Pd), toluene (18 mL), 4-iodotoluene (0.26 g, 1.2 mmol), methyl acrylate (0.50 g, 5 mmol), and *N,N*-diisopropylethylamine (0.23 g, 1.78 mmol). The reaction mixture was stirred for 3 h at 75 °C. Once cooled to room temperature, the mixture was filtered under nitrogen, the siliceous material retained for reuse and the solvent removed under vacuum. The product-containing mixture was analyzed by ¹H NMR spectroscopy. The isolated orange-brown silica was reused under the same conditions. Conversions were 96% in run 1, 85% in run 2, 65% in run 3 and 10% in run 4.

Heck reaction using supported catalyst in scCO₂

Using a glovebox or a Schlenk line, the supported pre-catalyst (0.80 g, 2 mol% Pd), 4-iodotoluene (0.27 g, 1.2 mmol), methyl acrylate (0.50 g, 5 mmol), *N,N*-diisopropylethylamine (0.23 g, 1.78 mmol) and a stir bar were placed in a 25 mL stainless steel pressure vessel (Thar technologies). The vessel was sealed and heated to 75 °C and stirred for 10 minutes. It was then pressurised to 100 bar with carbon dioxide.† This temperature

† As with all processes under high pressure, appropriate safety precautions must be taken.

and pressure were maintained for 18 h. The vessel was allowed to cool and was then vented into toluene (10 mL) under nitrogen, washed with dry toluene and the contents filtered inside the glovebox. The catalyst was dried under vacuum and reused whilst avoiding contact with the air. Conversions were 98% in run 1 (or 55% if the reaction time was reduced to 3 h), 96% in run 2, 92% in run 3, 92% in run 4 and 48% in run 5. If the reactions were worked-up in air, the conversion in run 2 was reduced to 41%.

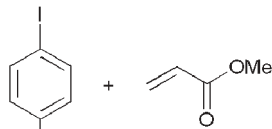
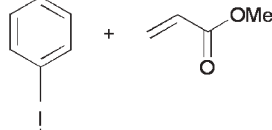
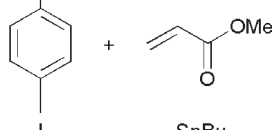
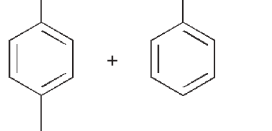
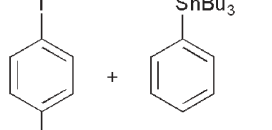
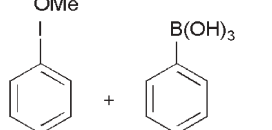
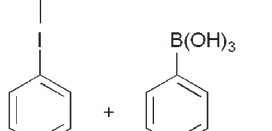
Stille reaction using supported catalyst in toluene

A Schlenk tube was charged with the supported pre-catalyst (0.40 g, 2 mol% Pd), toluene (18 mL), 4-aryl iodide (0.6 mmol), phenyl(tri-*n*-butyl)tin (0.25 g, 0.6 mmol). The reaction mixture was stirred for 3 h at 75 °C. Upon cooling to room temperature, the mixture was filtered under nitrogen, the siliceous material retained for reuse and the solvent was removed under vacuum. The product-containing mixture was analyzed by ¹H NMR spectroscopy. The isolated orange-brown silica was reused under the same conditions. Conversions were 100% in run 1 and 96.5% in run 2 with iodotoluene, and 100% in run 1 and 100% in run 2 for iodoanisole.

Suzuki reaction using supported catalyst in toluene

A Schlenk tube was charged with the supported pre-catalyst (0.80 g, 2 mol% Pd), toluene (18 mL), 4-iodotoluene (0.26 g, 1.2 mmol), phenylboronic acid (0.24 g, 2.5 mmol) and *N,N*-diisopropylethylamine (0.23 g, 1.78 mmol). The reaction mixture was stirred for 18 h at 75 °C. Upon cooling to room temperature, the mixture was filtered and the solvent was removed under vacuum. The product-containing mixture was

Table 1 Coupling reactions and effect of catalyst recycling on conversions

Entry	Substrates	Reaction conditions	Conversion
1		Toluene, 75 °C, 3 h, recycled under N ₂	Run 1–96% Run 2–85% Run 3–65% Run 4–10%
2		CO ₂ , 75 °C, 100 bar, 18 h, recycled under N ₂	Run 1–98% Run 2–96% Run 3–92% Run 4–92% Run 5–48%
3		CO ₂ , 75 °C, 100 bar, 18 h, recycled in air	Run 1–98% Run 2–41%
4		Toluene, 75 °C, 3 h, recycled under N ₂	Run 1–100% Run 2–97%
5		Toluene, 75 °C, 3 h, recycled under N ₂	Run 1–100% Run 2–100%
6		Toluene, 75 °C, 3 h, recycled under N ₂	Run 1–95% Run 2–63%
7		CO ₂ , 75 °C, 100 bar, 18 h, recycled under N ₂	Run 1–96% Run 2–93% Run 3–93% Run 4–91% Run 5–52% Run 6–38% Run 7–12%

analyzed by ¹H NMR spectroscopy. The isolated orange-brown silica was reused under the same conditions. Conversions were 95% in run 1 and 62.5% in run 2.

Suzuki reaction using supported catalyst in scCO₂

The reactions were performed under similar conditions to the Heck reaction using the supported catalyst in scCO₂. However, phenylboronic acid (0.24 g, 2.5 mmol) was used instead of methyl acrylate. Conversions were 96% in run 1, 93% in run 2, 93% in run 3, 91% in run 4, 52% in run 5, 38% in run 6 and 12% in run 7.

Results and discussion

We have previously reported the synthesis of a range of polydimethylsiloxane derived phosphine and phosphinite

ligands.²⁴ These ligands are soluble in scCO₂ and can be used to catalyse C–C bond forming reactions in this medium. During the course of this research, we discovered that these ligands and their complexes adsorbed onto silica to afford free-flowing powders and this provided an easy way to store and manipulate these oily materials. The ligands adsorb onto silica through the mechanisms previously reported for siloxane based polymers, Fig. 2.^{25–28} Upon addition of oven-dried silica to an orange hexane solution of complex Pd(PDMS-PPh₂)₂Cl₂, the solvent becomes colourless and the silica turns yellow. Typically, 0.200 g of complex are adsorbed onto 2.00 g of silica. No free ligand or complex are present in the supernatant solvent when analysed by ¹H NMR, ³¹P NMR and FT-IR spectroscopies. Upon changing the solvents, the complex remains adsorbed in non-polar solvents such as hydrocarbons, whereas it quantitatively desorbs in ethers, alcohols and acetonitrile.

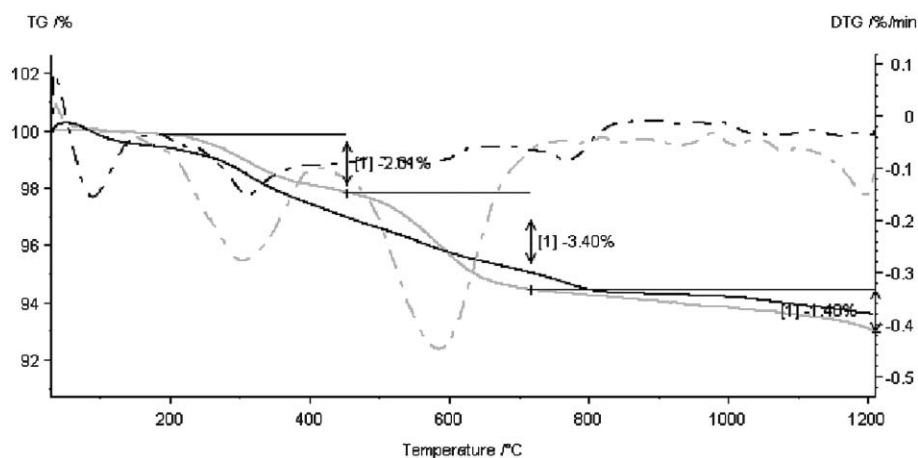


Fig. 3 TGA, DTGA (light grey graphs) and DSC thermographs (black graphs) of supported pre-catalyst.

Herein, we report on the thermal stability of the adsorbed complex. Fig. 3 displays the TGA and differential TGA (DTGA) (light grey solid and dotted curves respectively) for the Pd supported pre-catalyst. The solid line is a mass loss curve and the dotted line is the derivative of the mass loss curve with respect to time. The derivative curve indicates that there are two main mass loss events. The first is centred at about 305 °C and the second at about 600 °C with weight losses of 2.01 and 3.40% respectively. These peaks correspond to the exothermic decomposition of the organic components in the supported pre-catalyst. Since the catalyst loading on silica, in this case, was 100 mg g⁻¹, this result shows that the pre-catalyst degrades thermally to give Pd and silica. The thermal weight loss corresponds to all the phosphorus, carbon, hydrogen and chlorine degrading by this point. This correlates with the results obtained from the elemental analysis of Pd(PDMS-PPh₂)₂Cl₂ (C, 39.91; H, 7.92; Cl, 1.87; O, 17.72; P, 1.63; Pd, 2.81; Si, 28.14). This curve also indicates that the supported pre-catalyst is thermally stable at temperatures lower than 300 °C.

The differential scanning calorimetric (DSC) results for the supported pre-catalyst are also shown in Fig. 3 (black graphs). There are two endotherms observed for the hybrid catalyst in the 100 to 300 °C regions. There are a few smaller ones after this temperature. The first endotherm at about 100 °C is due to evaporation of trace water. The second endotherm at 300 °C in the DSC correlates with the first large weight loss in the TGA. However, the DSC and TGA events do not seem to tie in at around 600 °C, where the major weight loss (3.4%) is seen. For this weight loss, no corresponding endotherm on the differential DSC trace is observed. We propose that ligand degradation is occurring at the lower temperature (around 300 °C). However, the gaseous products remain physisorbed onto the surface of the metal and silica and then desorb (endothermic event) at the higher temperature. At the same time, the crystallization of the Pd into microdomains/nanoparticles (exothermic event) is taking place and therefore, these two processes cancel each other out in the DSC trace.

Pd(PDMS-PPh₂)₂Cl₂ is an air-stable species; no change in its spectroscopic data, particularly its ³¹P NMR spectrum, was observed over a six month period when exposed to the air.

Therefore, the adsorbed species on silica can also be considered air-stable prior to reaction. Pd(PDMS-PPh₂)₂Cl₂ on silica (supported pre-catalyst) was screened in Heck, Suzuki and Stille reactions in toluene and scCO₂, as described in the Experimental section.

When mixtures from Heck reactions performed in toluene were filtered in air, the catalyst gave negligible conversions when reused under the same conditions. The conversions were 45% in run 1, 3% in run 2, and 2% in run 3. ¹H NMR spectra of the crude product showed that some ligand leaching occurred. Also, the low conversions using the recycled catalyst indicated that the active species formed *in situ* was air-sensitive. Therefore, the Heck reaction experiments in toluene were repeated under a nitrogen atmosphere. The conversions were improved; 96% in run 1, 85% in run 2, 65% in run 3 and 10% in run 4. However, ligand leaching was still evident, indicating that the active catalyst does not have the PDMS-derived phosphine bound. Although the conversions decreased significantly during catalyst recycling, no palladium black precipitate was seen in the products or in the silica.

For reactions in scCO₂, the pressure vessel was loaded with the silica supported pre-catalyst and reagents in a glovebox or using a Schlenk line. The vessel was sealed, pressurised and heated to the required temperature, Table 1. Upon cooling, the vessel was vented into toluene under nitrogen using a Schlenk line. Then, the vessel and its contents were washed with dry toluene. The silica-based material was dried and reused. In the Heck reaction, the conversions were 98% in run 1, 96% in run 2, 92% in run 3, 92% in run 4 and 48% in run 5. The diisopropylethylammonium iodide salt is not soluble in toluene; therefore, it gradually built up on the supported catalyst after each run and the weight of the recovered silica increased. The colour of the catalyst changed from yellow to grey during the third run and by the fifth run, it was white. The dramatic drop in conversion for the fifth run can be attributed to the covering of active sites on the Pd/silica catalyst with diisopropylethylammonium iodide. The Pd particles became inaccessible to the reagents and led to a considerable loss of activity. DRIFT spectra, Fig. 5, confirmed the build up of the ammonium salt. Attempts to remove this salt build up by washing the catalyst with degassed and dried polar solvents

such as ethanol or acetone led to leaching of the Pd out of the silica. After washing the catalyst with these solvents, Pd black particles immediately started to precipitate from the mixture and the resulting colourless silica did not show any catalytic activity.

ICP analysis of the products was used to assess the extent of any Pd leaching. The crude products from each run were stirred with 10% HCl and were analysed using ICP for Pd content. No Pd was detected. In previously reported examples of supported Pd catalysts, preconditioning washing steps were essential to remove loosely bound Pd and avoid Pd leaching during the course of reaction.^{7,29,30} Therefore, it is particularly noteworthy that no Pd leaching occurred in this study. We propose that this is a result of using scCO_2 as the solvent, as it will have minimal interactions with the silica surface and therefore, will not displace the Pd. However, the stabilization of the nanoparticles on the silica by ammonium salts, as has been reported for phosphine-free Pd catalysts,³¹ cannot be ruled out.

The Suzuki reaction was also performed under similar conditions to the Heck reaction above, but with phenylboronic acid instead of methyl acrylate. The conversions were 96% in run 1, 93% in run 2, 93% in run 3, 91% in run 4, 52% in run 5, 38% in run 6 and 12% in run 7. Similarly to the Heck reaction, a considerable drop in yield was observed after the 4th run, which can be attributed to the blocking of active sites. Again, quantitative ICP analysis did not show any Pd in the products. Stille couplings were also performed but only in toluene to further demonstrate the utility of this system. Interestingly, conversions remained high upon reuse, thus providing further evidence for ammonium salts blocking active sites, as no ancillary base is used in these catalytic reactions. However, as the tin reagents used in these reactions are toxic, and therefore not green, Stille couplings were not performed in scCO_2 .

As there was evidence for leached ligand in the crude products, Si–Me environments in the ^1H NMR spectra, and no leached palladium, it was likely that Pd nanoparticles had formed and were catalysing the reactions. The leached ligand can be adsorbed onto fresh silica when purifying the organic products and can be reused if kept under a nitrogen atmosphere. PDMS-PPH₂ is air-sensitive and will oxidize to the corresponding phosphine-oxide if exposed to air.

Recently, there have been significant advances in the use of scCO_2 in materials preparation and processing, particularly in the production of metal nanoparticles.^{32–39} Practically, CO_2 -soluble metal precursors are generally sprayed into a CO_2 receiving solution containing a reducing agent such as $\text{NaBH}(\text{OAc})_3$ or H_2 and fluorocarbon stabilizing ligands to produce metallic nanoparticles with sizes ranging from 1 to 15 nm, and TEM has been used widely to determine the range and variation in particle size.³⁶ TEM has also been used in analyzing reaction mixtures for Pd nanoparticles in other catalysed reactions.^{8,9,31,35,40–42} As it appeared that during the course of the catalytic reactions, Pd nanoparticles were produced and were stabilised on the silica support, TEM analysis was performed on the recovered catalyst, Fig. 4. Unfortunately, the particles overlap with each other and it is therefore difficult to measure the size of the particles, but by a

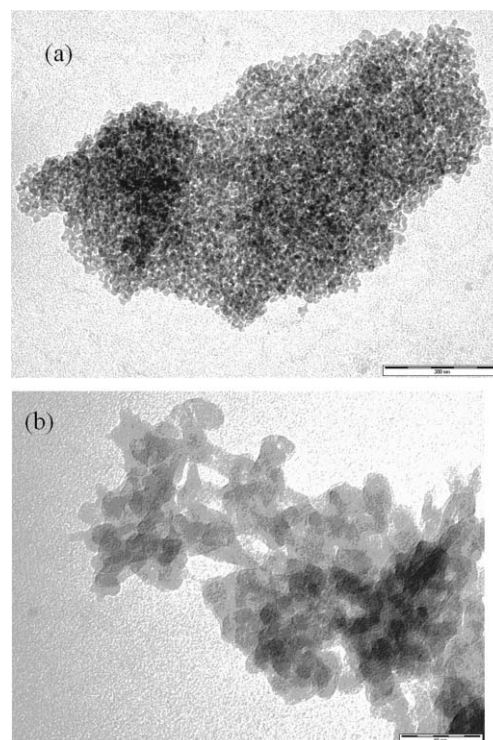


Fig. 4 Representative TEM microphotographs of recovered catalyst, scale (a) 200 nm (b) 50 nm.

careful inspection of particles near the edges of the image, an approximate diameter of 10 nm can be assigned. Despite the overlapping nature of the particles, Fig. 4 clearly illustrates the homogeneous dispersion of the particles throughout the silica. TEM analysis of the supported pre-catalyst before reaction at high and low magnifications showed no Pd particles. On a stereomicroscope, the silica particles in the pre-catalyst are visible with a homogeneous smooth yellow layer on their surface.

DRIFT spectroscopy was conducted on the supported pre-catalyst and recovered catalyst after the first through to third runs of the Heck reaction in scCO_2 . The DRIFT spectrum, Fig. 5, of the pre-catalyst shows a strong O–H stretching vibration at 3656 cm^{-1} assigned to free silanol residues, hydrogen bonded OH groups between $3600\text{--}3100\text{ cm}^{-1}$, aromatic C–H stretching bands (attributed to Ph groups of the ligand) at 2985 cm^{-1} , C=O stretching band (also within the ligand, Fig. 1) at 1640 cm^{-1} and Si–O stretching band centered at 1049 cm^{-1} . A decrease in the number of strongly and weakly hydrogen-bonded groups on the silica surface during the course of the reaction was clearly observed in the region $3600\text{--}3100\text{ cm}^{-1}$ in the DRIFT spectrum of the recovered silica samples. The same observation has been made during the heat treatment of silica supported catalysts.⁴³ The intensity of the C=O band at 1640 cm^{-1} decreased after the first run and disappeared after the third run. This provides additional confirmation of ligand leaching during the different runs, in addition to ^1H NMR data. The appearance of a C–N stretching band for aliphatic ammonium salts at 1380 cm^{-1} after the first run indicates the build up of diisopropylethylammonium iodide and its intensity increases considerably

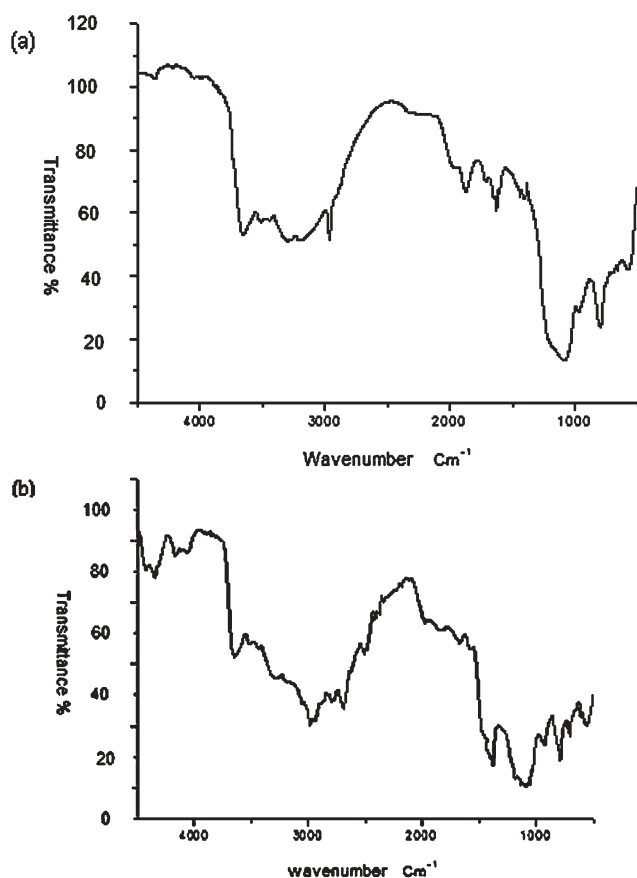


Fig. 5 (a) DRIFT spectrum of the silica supported pre-catalyst (b) DRIFT spectrum of recovered catalyst from run 3 (Heck reaction in scCO_2).

with each run. Elemental analysis of the used catalysts also indicated an increase in N levels consistent with the deposition of ammonium salts.

Conclusions

$\text{Pd}(\text{PDMS-PPH}_2)_2\text{Cl}_2$ on silica as a pre-catalyst to dispersed palladium nanoparticles on silica gave reproducible results during the course of Heck and Suzuki reactions and could be recovered and re-used for four times without substantial activity drops. TEM analysis shows the presence of Pd nanoparticles. These are probably responsible for the catalysis and the considerable drop in conversions after four runs is likely a result of quaternary ammonium salts depositing on the catalyst surface thereby blocking the active catalytic sites. The presence of these salts was proved using elemental analysis and DRIFT experiments. Additional experiments, such as XPS, would prove the presence of Pd(0) nanoparticles. Although the activity of these materials is not very high, this research provides further evidence for active Pd nanoparticles in C–C bond forming catalysis and indicates that, in this case, the use of scCO_2 in batch reactions for recycling such species is superior to conventional solvents. Future work will involve the use of a continuous flow-reactor to produce catalytic metal nanoparticles and performing other catalytic reactions.

Acknowledgements

The authors would like to thank the Green Chemistry Group at York, in particular Dr Duncan Macquarrie and Mr Paul Elliott for their advice and assistance with DRIFT, TGA and DSC. Meg Stark in the York biology department is also gratefully acknowledged for TEM micrographs. The Universities of Leeds and York are acknowledged for their financial support. F. M. K. thanks the Royal Society for a University Research Fellowship during the course of this research.

References

- 1 P. Espinet and A. M. Echavarren, *Angew. Chem., Int. Ed.*, 2004, **43**, 4704.
- 2 F. Bellina, A. Carpita and R. Rossi, *Synthesis*, 2004, 2419.
- 3 N. T. S. Phan, M. Van Der Sluys and C. W. Jones, *Adv. Synth. Catal.*, 2006, **348**, 609.
- 4 G. B. Smith, G. C. Dezeny, D. L. Hughes, A. O. King and T. R. Verhoeven, *J. Org. Chem.*, 1994, **59**, 8151.
- 5 J. G. de Vries, *Can. J. Chem.*, 2001, **79**, 1086.
- 6 D. A. Conlon, B. Pipik, S. Ferdinand, C. R. LeBlond, J. R. Sowa, B. Izzo, P. Collins, G. J. Ho, J. M. Williams, Y. J. Shi and Y. K. Sun, *Adv. Synth. Catal.*, 2003, **345**, 931.
- 7 J. J. E. Hardy, S. Hubert, D. J. Macquarrie and A. J. Wilson, *Green Chem.*, 2004, **6**, 53.
- 8 M. J. Gronnow, R. Luque, D. J. Macquarrie and J. H. Clark, *Green Chem.*, 2005, **7**, 552.
- 9 S. Martinez, A. Vallribera, C. L. Cotet, M. Popovici, L. Martin, A. Roig, M. Moreno-Manas and E. Molins, *New J. Chem.*, 2005, **29**, 1342.
- 10 D. Badone, M. Baroni, R. Cardamone, A. Ielmini and U. Guzzi, *J. Org. Chem.*, 1997, **62**, 7170.
- 11 N. E. Leadbeater, *Chem. Commun.*, 2005, 2881.
- 12 W. J. Liu, Y. X. Xie, L. A. Yun and J. H. Li, *Synthesis*, 2006, 860.
- 13 B. W. Xin, Y. H. Zhang, L. F. Liu and Y. G. Wang, *Synlett*, 2005, 3083.
- 14 D. K. Morita, D. R. Pesiri, S. A. David, W. H. Glazec and W. Tumas, *Chem. Commun.*, 1998, 1397.
- 15 M. A. Carroll and A. B. Holmes, *Chem. Commun.*, 1998, 1395.
- 16 N. Shezad, A. A. Clifford and C. T. Rayner, *Green Chem.*, 2002, **4**, 64.
- 17 B. M. Bhanage, S. Fujita and M. Arai, *J. Organomet. Chem.*, 2003, **687**, 211.
- 18 J. S. Cheng and H. F. Jiang, *Eur. J. Org. Chem.*, 2004, 643.
- 19 C. J. Smith, M. W. S. Tsang, A. B. Holmes, R. L. Danheiser and J. W. Tester, *Org. Biomol. Chem.*, 2005, **3**, 3767.
- 20 G. W. Kabalka, L. Wang, R. M. Pagni, C. M. Hair and V. Namboodiri, *Synthesis*, 2003, 217.
- 21 M. Lysen and K. Kohler, *Synthesis*, 2006, 692.
- 22 S. V. Ley, C. Ramarao, R. S. Gordon, A. B. Holmes, A. J. Morrison, I. F. McConvey, I. M. Shirley, S. C. Smith and M. D. Smith, *Chem. Commun.*, 2002, 1134.
- 23 C. K. Y. Lee, A. B. Holmes, S. V. Ley, I. F. McConvey, B. Al-Duri, G. A. Leeke, R. C. D. Santos and J. P. K. Seville, *Chem. Commun.*, 2005, 2175.
- 24 S. Saffarzadeh-Matin, C. J. Chuck, F. M. Kerton and C. M. Rayner, *Organometallics*, 2004, **23**, 5176.
- 25 A. Patel, T. Cosgrove and J. A. Semlyen, *Polymer*, 1991, **32**, 1313.
- 26 T. M. Roshchina, N. K. Shonia, A. A. Kazmina, K. B. Gurevich and A. Y. Fadeev, *J. Chromatogr., A*, 2001, **931**, 119.
- 27 B. J. Stanley and G. Guiochon, *Langmuir*, 1995, **11**, 1735.
- 28 H. Barthel and E. Nikitina, *Silicon Chem.*, 2002, **1**, 261.
- 29 E. B. Mobufu, J. H. Clark and D. J. Macquarrie, *Green Chem.*, 2001, **3**, 23.
- 30 R. B. Bedford, C. S. J. Cazin, M. B. Hursthouse, M. E. Light and S. Wimperis, *J. Organomet. Chem.*, 2001, **633**, 173.
- 31 M. T. Reetz and E. Westermann, *Angew. Chem., Int. Ed.*, 2000, **39**, 165.
- 32 K. P. Johnston and P. S. Shah, *Science*, 2004, **303**, 482.

- 33 K. S. Morley, P. Licence, P. C. Marr, J. R. Hyde, P. D. Brown, R. Mokaya, Y. D. Xia and S. M. Howdle, *J. Mater. Chem.*, 2004, **14**, 1212.
- 34 K. S. Morley, P. C. Marr, P. B. Webb, A. R. Berry, F. J. Allison, G. Moldovan, P. D. Brown and S. M. Howdle, *J. Mater. Chem.*, 2002, **12**, 1898.
- 35 P. Meric, K. M. Yu and S. C. Tsang, *Langmuir*, 2004, **20**, 8537.
- 36 M. C. McLeod, W. F. Gale and C. B. Roberts, *Langmuir*, 2004, **20**, 7078.
- 37 H. M. Woods, M. C. G. Silva, C. Nouvel, K. M. Shakesheff and S. M. Howdle, *J. Mater. Chem.*, 2004, **14**, 1663.
- 38 Y. Wang, R. Pfeffer, R. Dave and R. Enick, *AIChE J.*, 2005, **51**, 440.
- 39 H. Ohde, M. Ohde and C. M. Wai, *Chem. Commun.*, 2004, 930.
- 40 P. Meric, K. M. K. Yu, A. T. S. Kong and S. C. Tsang, *J. Catal.*, 2006, **237**, 330.
- 41 H. Ohde, C. M. Wai, H. Kim, J. Kim and M. Ohde, *J. Am. Chem. Soc.*, 2002, **124**, 4540.
- 42 Z. Hou, N. Theysen, A. Brinkmann and W. Leitner, *Angew. Chem., Int. Ed.*, 2005, **44**, 1346.
- 43 S. Ek, E. I. Iiskola and L. Niinistö, *Langmuir*, 2003, **19**, 3461.



STOP!

searching...

Save valuable time searching for that elusive piece of vital chemical information.

Let us do it for you at the Library and Information Centre of the RSC.

We are your chemical information support, providing:

- Chemical enquiry helpdesk
- Remote access chemical information resources
- Speedy response
- Expert chemical information specialist staff

Tap into the foremost source of chemical knowledge in Europe and send your enquiries to

library@rsc.org

RSCPublishing

www.rsc.org/library

12120515

Immobilized metal complexes in porous hosts: catalytic oxidation of substituted phenols in CO₂ media

Sarika Sharma,^{ac} Boris Kerler,^b Bala Subramaniam^{*ab} and A. S. Borovik^{*ac}

Received 27th February 2006, Accepted 19th July 2006

First published as an Advance Article on the web 14th August 2006

DOI: 10.1039/b602965e

Development of processes that utilize heterogeneous catalysis in environmentally beneficial media is of fundamental and practical importance. The oxidation of 2,6-di-*tert*-butylphenol (DTBP) to 2,6-di-*tert*-butyl-1,4-benzoquinone (DTBQ) and 3,5,3',5'-tetra-*tert*-butyl-4,4'-diphenylquinone (TTBDQ) has been investigated to evaluate the factors necessary to achieve high product conversion and selectivity in various media. A series of porous materials with immobilized Co(II) complexes served as catalysts and their reactivities using O₂ as the terminal oxidant were screened in neat acetonitrile, supercritical carbon dioxide (*sc*CO₂), and CO₂-expanded acetonitrile. The highest conversions were found with the catalysts that had high affinity for dioxygen. Moreover, the greatest conversions (~60%) were obtained when reactions were done in *sc*CO₂, which is attributed to improved mass transfer of O₂ and substrates through the porous catalysts. Furthermore, the heterogeneous catalysts can be recycled with some loss of activity (~30%) after three cycles; nonetheless these results suggest that the polymer hosts efficiently protect the immobilized catalytic sites from destructive bimolecular routes.

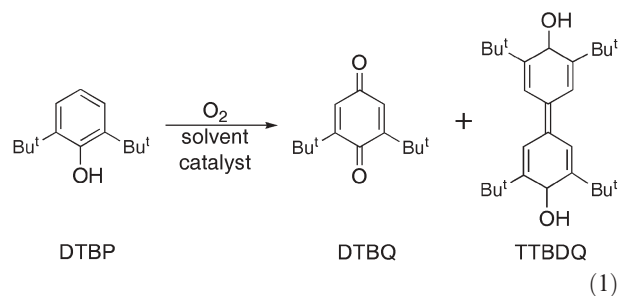
Introduction

Materials as heterogeneous catalysts have received considerable attention because of their possible use in a wide variety of reactions, convenient post-reaction separation, and reusability.^{1–3} This has led to methods for incorporating catalytic centers on solid supports, including those for immobilization of metal complexes into porous hosts. However, many of these methods produce heterogeneous catalysts that have limited function, in part, because the properties of the supported catalysts differ from those of their homogenous counterparts. It is therefore necessary to integrate catalyst preparation with specific reaction conditions in order to obtain optimal activity.

We have found that template copolymerization is an effective method for immobilizing metal complexes within porous organic host.^{4–6} Formation of the immobilized sites occurs during polymerization, using a substitutionally inert metal complex as the template—this allows each site to have similar structural properties that are related to those of the template compound. Materials produced with this methodology have high site accessibility and control of ligand positions around the immobilized metal centers. Moreover the immobilized sites are isolated from each other, producing functional materials for the reversible binding of CO, NO, and O₂. Four of these materials, P-1[Co^{II}], P-1[Co^{II}(py)], P-1-py[Co^{II}], and P-2[Co^{II}] are shown schematically in Scheme 1.

The high degree of dioxygen binding to the immobilized Co^{II} complexes in these porous materials (90% for P-1-py[Co^{II}])

suggested that they might function as heterogeneous oxidation catalysts. To evaluate this possibility, we have investigated the catalytic activity of P-1[Co^{II}], P-1[Co^{II}(py)], P-1-py[Co^{II}], and P-2[Co^{II}] to oxidize 2,6-di-*tert*-butylphenol (DTBP) to 2,6-di-*tert*-butyl-1,4-benzoquinone (DTBQ) and 3,5,3',5'-tetra-*tert*-butyl-4,4'-diphenylquinone (TTBDQ) (eqn 1).



This reaction has been thoroughly studied for homogenous catalysts using conventional organic solvents and dioxygen as the oxidant. We reasoned that conventional conditions might not be suitable for catalysis with our porous materials; in particular, catalysis may be limited by the solubility of dissolved dioxygen in organic solvents, which could hinder mass transfer to the catalytic sites.

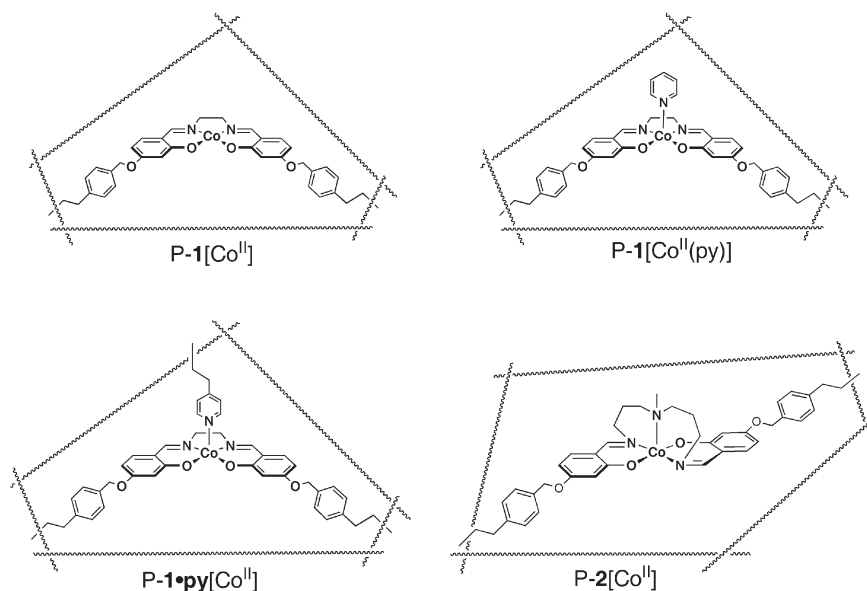
One way to circumvent this problem is to perform the reaction in CO₂-containing media. Supercritical carbon dioxide (*sc*CO₂)^{7,8} has several beneficial attributes for oxidative processes,⁹ including complete miscibility with O₂, resistance to oxidation, and tunable transport properties. Other potentially useful solvent systems are the CO₂-expanded liquids (CXLs), which can have a large portion (up to 80%) of a conventional organic solvent replaced by dense phase CO₂.^{10–15} CXLs are advantageous because they combine the beneficial properties of organic solvents (which solubilize catalysts and substrates easily) with those of dense CO₂ (better O₂ miscibility

^aNSF Engineering Research Center for Environmentally Beneficial Catalysis, University of Kansas, Lawrence, KS 66045.

E-mail: bsubramaniam@ku.edu; aborovik@ku.edu

^bDepartment of Chemical and Petroleum Engineering, University of Kansas, Lawrence, KS 66045

^cDepartment of Chemistry, University of Kansas, Lawrence, KS 66045



Scheme 1 Depictions of the immobilized metal sites in P-1[Co^{II}], P-1[Co^{II}(py)], P-1·py[Co^{II}], and P-2[Co^{II}].

compared to neat organic solvents). Taking advantage of these properties, recent studies showed that the homogenous oxidation of DTBP with Co(salen') catalysts [salen', *N,N'*-bis(3,5-di-*tert*-butylsalicylidene)-1,2-ethylenediaminato(2-)] in CXLs significantly increased the rate of oxidation compared to reactions done in either conventional organic solvents or *sc*CO₂.¹⁰ We report herein results for the oxidation of DTBP with the heterogeneous catalysts P-1[Co^{II}], P-1[Co^{II}(py)], P-1·py[Co^{II}], and P-2[Co^{II}] in CH₃CN, CO₂-expanded CH₃CN, and *sc*CO₂. In contrast to the homogeneous case, our findings demonstrate that *sc*CO₂ as reaction medium provides better conversion compared to either the neat organic solvent or the CO₂-expanded organic solvent with the heterogenized Co complex. We attribute this behavior to a combination of complete O₂ miscibility and improved pore diffusion rates with *sc*CO₂ which cumulatively offset the tunable dielectric constant afforded by CO₂-based mixtures. Oxidation is also correlated to the dioxygen affinity of the materials and the fraction of CO₂ used as the reaction solvent.

Experimental

All chemicals and solvents used in the catalyst synthesis were purchased from either Aldrich or Fisher Scientific and used without further treatment. Coolant grade liquid CO₂, filled in cylinders with dip-tubes, and cylinders of ultrahigh purity oxygen (99.94%) were purchased from Airgas Inc.

Synthesis

The synthesis of the air-sensitive complexes and polymers were conducted in a Vacuum Atmospheres dry box under argon atmosphere. Standard Schlenk type glassware under N₂ was used to work up reactions outside the drybox. The compounds 2-hydroxy-4-(4-vinylbenzyl-methoxy)benzaldehyde¹⁶ and bis[2-hydroxy-4-(4-vinylbenzylmethoxy)benzaldehyde]ethylenediimine (H₂I)¹⁷ were synthesized following literature procedures. Detailed preparative routes to

P-1[Co^{II}], P-1[Co^{II}(py)], and P-2[Co^{II}] have been reported previously.^{4,18,19} Note that the polymer, P-1[Co^{II}(py)] was generated *in situ* by addition of pyridine to suspensions of P-1[Co^{II}].

P-1·py[Co^{II}] was prepared as described previously¹⁸ with the following modifications: after copolymerization and reduction, P-1·py[Co^{II}(dmap)] (0.30 g) was placed into a 100 mL flask and treated with 20 mL of 0.10 M Na₂EDTA solution in deionized water. The mixture was refluxed for 24 h, after which it was allowed to cool to room temperature and the resulting polymer was collected on a medium porosity glass frit. The polymer was washed with five 5 mL portions of deionized water, three 3 mL portions of diethyl ether, and dried under vacuum for 6 h to yield 0.275 g of a polymer formulated as P-1_{sal}·py. Elemental analyses suggested that hydrolysis to salicylaldehydes moieties has occurred. Anal Calcd for P-1·py[Co^{III}(dmap)]: Co, 145 μmol Co per g of polymer and 998 μmol N per g of polymer; Anal Calcd for P-1_{sal}·py: Co, 50.1 μmol Co per g of polymer and N, 282 μmol of N per g of polymer.

The salen ligand was reformed by treating P-1_{sal}·py with ethylenediamine (5.5 μL, 4.97 mg, 0.81 mmol) in 10 mL of methanol. After 6 h of stirring, the polymer was collected on a medium porosity glass frit, washed twice with 3 mL portions each of methanol and diethyl ether, then dried under vacuum for 6 h to yield 0.250 g of P-1·py. This yellow polymeric material was mechanically crushed to particles with an average size of approximately 150 μm and then treated with Co(OAc)₂ in 10 mL of methanol to afford 0.23 g of P-1·py[Co^{II}], having 150 μmol Co per g of polymer.

Instruments

All proton nuclear magnetic spectra (¹H NMR) were collected on a Bruker DRX400 spectrometer equipped with an SGI INDY workstation to characterize the template complexes. EPR spectra were collected using a Bruker EMX spectrometer

equipped with an ER4102SR cavity. The instrument was previously calibrated using DPPH. The spectra for the Co^{II} samples were collected at the following settings: attenuation = 25 dB, microwave power = 0.64 mW, frequency = 9.34 GHz, sweep width = 5000 G, modulation amplitude = 10.02 Gpp, gain = 5.00×10^{-3} , conversion time = 81.92 ms, time constant = 655.36 ms, and resolution = 1024 points. Elemental analyses of the fresh and used catalyst were performed at Desert Analytics (Tucson, AZ). BET surface area and pore volume were measured with a Gemini 237011 surface area analyzer employing N₂ physisorption. A Hewlett-Packard gas chromatograph (HP 5890) with a FID detector was used for the routine analysis for compound identification. The instrument was equipped with a 30 m HP 5 MS column crosslinked 5% PH- methylsiloxane film.

Solvent expansion by CO₂

These studies were conducted in a 100 mL high-pressure Jurgeson view cell ($P_{\max} = 400$ bar, $T_{\max} = 100$ °C) described elsewhere.¹⁰ Volumetric expansion of acetonitrile by dense CO₂²⁰ and the solubility limits of [Co^{II}(salen)] complexes in CO₂-acetonitrile CXLs have previously been reported.¹⁰ The expansion ratio is defined as the ratio of the volume of the equilibrated CO₂-expanded liquid phase at pressure P and temperature T [$V(P,T)$] to the initial volume of the neat solvent at atmospheric pressure and temperature $T[V_0(P_0,T)]$. Complementary expansion data were obtained in this study at different temperatures ($T = 35$ – 80 °C). The results from these studies provided guidance for the choice of pressure and temperature used in the catalytic runs.

Catalytic conversion studies

General operational procedures and details of experimental set-up can be found elsewhere.¹⁰ In brief, the oxidation studies of 2,6 di-*tert*-butylphenol (eqn 1) in neat organic solvent, CO₂ expanded solvent and *sc*CO₂ were carried out in a 15 mL stainless steel reactor ($p_{\max} = 400$ bar, $T_{\max} = 300$ °C; Thar Designs) equipped with two sapphire windows. A computer controlled data acquisition system (Camile TG) was used for monitoring the reaction temperature and pressure. To facilitate comparison, the reactor operating conditions for the heterogeneous catalysis studies were chosen to be similar to those employed in the homogeneous catalytic runs as follows: catalyst : substrate : O₂ molar ratio of 1 : 80 : 800, and a reaction time of 21 h at various temperatures (35–80 °C). Molecular oxygen was used as an oxidant in all the reactions. The catalysts were housed within a stainless steel cage (mesh per inch = 325 × 325) with a stirrer bar affixed to the bottom of the cage. This set-up confined the catalysts within the cage throughout the reactions, obviating post-reaction catalyst separation. Catalysts were prepared for reuse studies by simply washing the cage with acetonitrile and purging with N₂. The reactions with the organic solvents (acetonitrile and acetonitrile-pyridine) were initiated by addition of the dioxygen. In runs involving CXLs and *sc*CO₂, the O₂ was admitted following CO₂ addition to achieve either the desired expansion ratio or pressure, respectively. Following a batch run, the reactor was gradually depressurized over a period of 2 h and

the contents were led to a cold trap containing 5 mL of acetonitrile. Aliquots of diluted samples were analyzed for reaction products. Experiments were done at $T = 35$ °C, 50 °C and 80 °C in neat acetonitrile, CXLs ($V/V_0 = 1.4$ and 3), and *sc*CO₂.

The following experiments were performed to evaluate whether catalysis occurred from substances leached from the heterogeneous catalysts. Following the procedure described above, catalytic reactions were run for 4 h, following which an aliquot was removed and analyzed for products. The cage containing the catalysts was then removed from the reaction mixture by simple filtration, and the resulting homogeneous mixtures were further stirred for 17 h with aliquots removed and analyzed for products every 4 h. No additional products were detected after the removal of the catalyst cage.

Results and discussion

Expansion studies

The volumetric expansions of solvents (acetonitrile and pyridine) by addition of CO₂ were determined at various temperatures (25 °C,²⁰ 50 °C,²⁰ 80 °C) prior to the catalytic studies. Fig. 1 shows the isothermal volumetric expansion ratio (V/V_0) of acetonitrile with CO₂ mixtures at various temperatures. The volume of the CO₂-expanded liquid phase expands exponentially as the CO₂ critical pressure is approached. This is to be expected since CO₂ is highly compressible in the vicinity of its critical point (31.1 °C and 72.8 atm) causing the density (and therefore the miscibility with organic solvents) to increase sensitively with pressure. Note from Fig. 1 that at a given pressure, higher temperatures decrease the expansion ratio due to a reduction in CO₂ density. Hence, increased CO₂ pressures were needed to provide the same expansion ratio. For instance, at the expansion ratio of $V/V_0 = 1.4$ for acetonitrile, 23 bar of CO₂ is needed at 25 °C, compared to 58 bar of CO₂ at 80 °C. Clearly, the expansion data are essential for determining reaction operating conditions when employing CXLs as reaction media.

Properties of the catalysts

The materials used in this study contain immobilized cobalt complexes dispersed throughout the porous poly(methacrylate) hosts. The sites where the metal complexes are housed

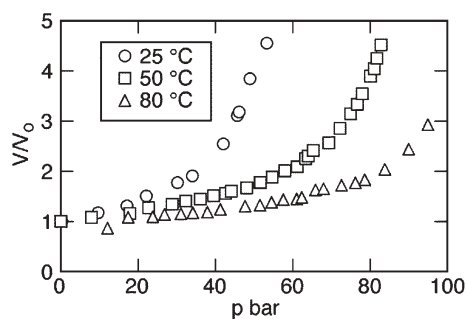


Fig. 1 Volumetric expansion ratio V/V_0 of pure acetonitrile vs. CO₂ expansion pressure at 25 °C, 50 °C, and 80 °C measured in the Jurgeson high pressure cell.

were formed during copolymerization from monomeric Co(III) template complexes and have approximately the same size and shape as the metal template. We have found that styryloxy groups, appended from the aromatic rings, serve as good linkers for covalent attachment of the metal complexes to the polymer backbone. All polymers¹⁸ were mesoporous with average pore diameters ranging from 25 to 50 Å. Our previous investigations found that each porous material binds dioxygen at atmospheric pressure, although with different affinities. P-1[Co^{II}] has a relatively low affinity for dioxygen with less than 10% of the immobilized site forming Co–O₂ adducts. Treating suspensions of P-1[Co^{II}] with excess pyridine forms P-1[Co(py)], a porous polymer with immobilized sites containing five-coordinate Co^{II} complexes. In solution, monomeric five-coordinate [Co^{II}salen(py)] complexes are known to have substantially greater thermodynamic affinity for dioxygen than their four-coordinate [Co^{II}salen] counterparts.²¹ We observed a similar trend in our porous polymers—nearly 60% of the cobalt sites bind dioxygen in P-1[Co(py)]. The two additional polymers, P-1·py[Co^{II}] and P-2[Co^{II}], have architectures that promote formation of five-coordinate Co(II) complexes and show the greatest affinity for dioxygen: 90% of the immobilized sites reversibly bind O₂ in P-1·py[Co^{II}] and P-2[Co^{II}]. It is important to note that the metal sites in all these porous materials are sufficiently isolated so that unwanted and detrimental intermolecular interactions between metal complexes are prevented.

P-1[Co^{II}] as an oxidation catalyst

Table 1 lists results for the oxidation of DTBP with P-1[Co^{II}] in various media. In neat acetonitrile at 35 °C, only 11% conversion to oxidized products was observed, with a large preference for the quinone, DTBQ (*S* = 86%), over the coupled product TTBDQ (*S* = 14%).²² Only small changes in conversion were found upon increasing the reaction temperature; for instance, a 20% conversion was found at 80 °C.

Reactions done in CO₂-expanded acetonitrile (*V/V*₀ = 1.4) at 35 and 50 °C had similar conversions as those done in acetonitrile. However, a significant difference was seen at 80 °C where the conversion to products increased to 43% with *S* = 77% for DTBQ. Larger conversions were found at all temperatures when reactions were done under supercritical conditions. For example, at 80 °C in *sc*CO₂, conversion to products reached 50% with a slight drop in selectivity for DTBQ to *S* = 70%. Note that at all temperatures the selectivity

Table 1 Substrate conversion and selectivity results for catalyst P-1[Co^{II}] catalyst for 35 °C and 80 °C in various reaction media (error limits in parentheses)

Solvent	<i>x</i> (CO ₂)	<i>T</i> /°C	% <i>X</i>	% <i>S</i>	
				DTBQ	TTBDQ
Neat CH ₃ CN	0	35	11(1)	80	20
CXL	0.695	35	11(1)	77	23
<i>sc</i> CO ₂	0.979	35	17(2)	74	26
Neat CH ₃ CN	0	80	30(2)	81	19
CXL	0.695	80	43(2)	77	23
<i>sc</i> CO ₂	0.979	80	50(2)	70	30

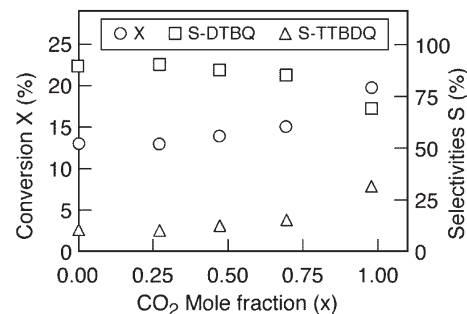


Fig. 2 Substrate conversion (*X*) of 2,6-di-*tert*-butyl phenol and selectivities (*S*) towards DTBQ and TTBDQ vs. mole fraction of CO₂ (*x*) with P-1[Co^{II}] catalyst at 50 °C. Reaction conditions: total pressure 1 bar in neat solvent, 125 bar in *sc*CO₂ and 50–80 bar in CO₂-expanded solvent, catalyst : substrate : oxygen ratio = 1 : 80 : 800, *t* = 21 h, *T* = 50 °C, *V* = 15 mL.

for DTBQ decrease as the amount of CO₂ in the media increases (Fig. 2), a trend that is not yet understood.

P-1[Co^{II}(py)] as an oxidation catalyst

The above results suggested that increased dioxygen concentrations within the reaction medium leads to higher conversion of products. Further improvements in catalysis could occur by increasing the dioxygen affinity of the catalyst. We thus explored the reactivity of the P-1[Co^{II}(py)] generated *in situ* by addition of excess pyridine to the reaction mixture. Formation of P-1[Co^{II}(py)] is achieved by treating acetonitrile suspensions of P-1[Co^{II}] with 20 equivalents of pyridine (relative to the Co(II) sites within the suspended polymer). Comparisons between the performance of P-1[Co^{II}(py)] and P-1[Co^{II}] shows small enhancements in conversions when using P-1[Co^{II}(py)]. In neat acetonitrile and CO₂-expanded acetonitrile–pyridine mixture a nearly 5% increase was observed. Unfortunately, the need to have pyridine present in the reaction medium prevents further studies of this polymer in *sc*CO₂.

P-1·py[Co^{II}] and P-2[Co^{II}] as oxidation catalysts

The use of pyridine to generate high affinity O₂-binding sites needed for catalysis was circumvented by employing P-1·py[Co^{II}] and P-2[Co^{II}] as catalysts. These polymers have immobilized sites containing the requisite five endogenous donors around the Co(II) ions required for O₂ binding.²³ Similar catalytic results were obtained for each polymer (Table 2) and will be discussed using P-1·py[Co^{II}]. In all cases, higher conversions were observed for P-1·py[Co^{II}] and P-2[Co^{II}] as catalysts compared to those that used P-1[Co^{II}]. For instance, an 8% increase in conversion was observed using P-1[Co^{II}] at 80 °C in neat acetonitrile. At all temperatures, maximum conversion was observed for reactions done in *sc*CO₂. Fig. 3 shows plots of conversions vs. temperature for reactions using P-1·py[Co^{II}] as the oxidation catalyst. Only modest improvement in catalytic performance was found in CO₂-expanded acetonitrile, while at all temperatures, maximum conversion was observed for reactions in *sc*CO₂. Moreover, in *sc*CO₂ at 80 °C, 60% phenol conversion was

Table 2 Substrate conversion and selectivity results for catalysts P-1·py[Co^{II}] and P-2[Co^{II}] at 35 °C, 50 °C, and 80 °C in various reaction media (error limits in parentheses)

Solvent	Catalyst	$x(\text{CO}_2)$	$T/^\circ\text{C}$	%X	%S	
					DTBQ	TTBDQ
Neat CH ₃ CN	P-1·py[Co ^{II}]	0	35	17(2)	79	21
<i>sc</i> CO ₂	P-1·py[Co ^{II}]	0.979	35	23(3)	74	26
Neat CH ₃ CN	P-1·py[Co ^{II}]	0	50	19(1)	75	26
CXL	P-1·py[Co ^{II}]	0.695	50	18(1)	82	18
<i>sc</i> CO ₂	P-1·py[Co ^{II}]	0.979	50	31(2)	69	31
Neat CH ₃ CN	P-1·py[Co ^{II}]	0	80	28(1)	78	22
<i>sc</i> CO ₂	P-1·py[Co ^{II}]	0.979	80	60(2)	70	30
Neat CH ₃ CN	P-2[Co ^{II}]	0	50	26(1)	80	20
CXL	P-2[Co ^{II}]	0.695	50	33(1)	82	18
<i>sc</i> CO ₂	P-2[Co ^{II}]	0.979	50	49(2)	67	23
Neat CH ₃ CN	P-2[Co ^{II}]	0	80	29(2)	79	21
CXL	P-2[Co ^{II}]	0.695	80	39(2)	70	30
<i>sc</i> CO ₂	P-2[Co ^{II}]	0.979	80	65(3)	63	37

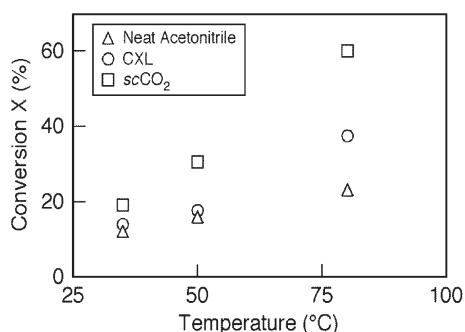


Fig. 3 Substrate conversion of 2,6-di-*tert*-butyl phenol as a function of temperature with P-1·py[Co^{II}] as catalyst in various reaction media: neat acetonitrile, CXL and *sc*CO₂.

observed, a value comparable to that found for homogeneous Co(II) catalysts.¹⁰

The increased conversions in *sc*CO₂ relative to CXL is in contrast to the behavior observed using related homogeneous catalysts under similar reaction conditions. With a homogeneous [Co^{II}salen] catalyst, higher phenol conversions were reported in CO₂-expanded acetonitrile mixtures, which provides complete catalyst solubility (due to the presence of the organic solvent) and significantly better O₂ solubility (relative to the organic solvent at atmospheric pressure). For the heterogeneous catalysts, P-1·py[Co^{II}] and P-2[Co^{II}], the O₂ miscibility in the reaction medium and pore diffusion rates to the immobilized catalytic sites dictate the overall rate. In *sc*CO₂, the dioxygen miscibility is complete and the pore diffusion rates at certain pressures can be tuned to be significantly better than with either the organic medium or CO₂-expanded liquids. Thus, in the case of the heterogeneous catalysts, *sc*CO₂ provides the maximum conversion of substrate to products, as well as having the greatest environmental benefit.

The reusability of the catalyst P-1·py[Co^{II}] was also evaluated in neat acetonitrile, CXLs, and *sc*CO₂. All three media gave similar results, which are illustrated in Fig. 4 for reactions done in CXL ($V/V_0 = 3$) and *sc*CO₂ at $T = 50$ °C. There is a small drop in conversions between the first and

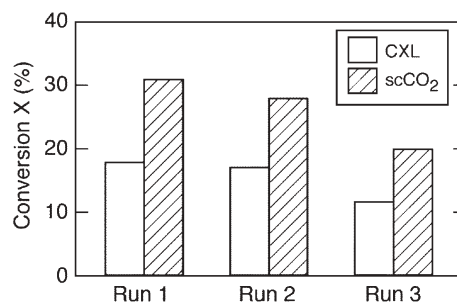


Fig. 4 Recycling experiments using P-1·py[Co^{II}] in CXL ($V/V_0 = 3$ in acetonitrile, unfilled rectangles) and *sc*CO₂ (filled rectangles).

second cycles, whereas an approximately 30% decrease in conversion occurred between the first and third experiments. ICP analyses indicate that the catalyst used over three cycles showed a decrease in the cobalt content (115 μmol Co per g of polymer) compared to the freshly prepared polymer (150 μmol Co per g of polymer). Between the initial and final cycles, the selectivity decreased to approximately 60% for DTBQ and increased to approximately 40% for TTBDQ, a trend which is not currently understood. Nevertheless, these reusability studies indicate that P-1·py[Co^{II}] retains a majority of its activity over several cycles.

Conclusions

We have demonstrated that immobilized [Co(salen)] complexes within porous polymers are effective catalysts for the oxidation of substituted phenols. The best conversions were obtained with reactions done in *sc*CO₂, findings that contrast with those reported for analogous homogeneous systems where reactions done in CXLs gave the best results. The higher conversions obtained in CXLs for homogeneous reactions have been partially credited to the presence of organic solvent that increases catalyst solubility and greater O₂ concentrations compared to neat organic solvent. For the heterogeneous catalysts described here, the complete miscibility of dioxygen in *sc*CO₂ yields substantially larger amounts O₂ in the reaction medium while improved mass transport through the pores to the immobilized catalytic sites is achieved. Thus, *sc*CO₂ can be the optimum solvent for heterogeneous oxidation catalysis where dioxygen is the terminal oxidant. Furthermore, our studies underscore the need to “match” reaction conditions with the type of catalyst to obtain maximum activity.

The maximum conversions of $X \approx 60\%$ were found with catalysts P-1·py[Co^{II}] and P-2[Co^{II}], polymers that have relatively high affinities for dioxygen—these conversion values approach those reported for related homogeneous catalysts. Moreover, substantial activity for the P-1·py[Co^{II}] is maintained over several reactions, indicating improved catalyst lifetime is achieved. We attributed this enhanced activity to prevention, by the polymer host, of destructive bimolecular pathways that often are prevalent in metal ion mediated oxidative transformations. The ability to modulate the architecture of the immobilized catalytic sites in polymers prepared by template copolymerization methods provides an effective means to tune reactivity. Taken together, our results

clearly illustrate the potential of this approach in preparing heterogenized oxidation catalysts and the benefits of coupling their function with *sc*CO₂ reaction media.

Acknowledgements

The financial support for this work was provided by the NSF-ERC program (NSF-EEC 0310689), the NIH (GM58680 to A.S.B.), and the postdoctoral programme of the German Academic Exchange Service (DAAD to B.K.).

References

- 1 P. T. Anastas, M. M. Kirchhoff and T. C. Williamson, *Appl. Catal., A*, 2001, **221**, 3.
- 2 J. H. Golden, H. Deng, F. J. DiSalvo, J. M. J. Fréchet and P. M. Thompson, *Science*, 1995, **268**, 1463.
- 3 (a) S. J. Shuttleworth, S. M. Allin and P. K. Sharma, *Synthesis*, 1997, 1217; (b) A. Choplin and F. Quignard, *Coord. Chem. Rev.*, 1998, **178–180**, 1679.
- 4 K. M. Padden, J. F. Krebs, C. E. MacBeth, R. C. Scarrow and A. S. Borovik, *J. Am. Chem. Soc.*, 2001, **123**, 1072.
- 5 P. K. Dhal and F. H. Arnold, *Macromolecules*, 1992, **25**, 7051.
- 6 J. F. Krebs and A. S. Borovik, *J. Am. Chem. Soc.*, 1995, **117**, 10593.
- 7 G. T. Musie, M. Wei, B. Subramaniam and D. H. Busch, *Coord. Chem. Rev.*, 2001, **789**, 219.
- 8 Y. Arai, T. Sako and Y. Takebayashi, *Supercritical Fluids. Molecular Interactions, Physical Properties, and New Applications*, Springer-Verlag, Berlin, 2002.
- 9 G. T. Musie, M. Wei, B. Subramaniam and D. H. Busch, *Inorg. Chem.*, 2001, **40**, 3336.
- 10 M. Wei, G. T. Musie, D. H. Busch and B. Subramaniam, *J. Am. Chem. Soc.*, 2002, **124**, 2513.
- 11 (a) C. A. Eckert, D. Bush, J. S. Brown and C. L. Liotta, *Ind. Eng. Chem. Res.*, 2000, **39**, 4615; (b) C. A. Eckert, C. L. Liotta, D. Bush, J. S. Brown and J. P. Hallett, *J. Phys. Chem. B*, 2004, **108**, 18108; (c) D. Xu, R. G. Carbonell, D. J. Kiserow and G. W. Roberts, *Ind. Eng. Chem. Res.*, 2005, **44**, 6164.
- 12 M. Wei, G. T. Musie, D. H. Busch and B. Subramaniam, *Green Chem.*, 2004, **8**, 387.
- 13 K. K. Kapellen, C. D. Mistele and J. M. DeSimone, *Macromolecules*, 1996, **29**, 495.
- 14 B. Rajagopalan, M. Wei, G. T. Musie, B. Subramaniam and D. H. Busch, *Ind. Eng. Chem. Res.*, 2003, **42**, 6505.
- 15 J. C. De la Fuente Badilla, C. J. Peters and J. de Swaan Arons, *J. Supercrit. Fluids*, 2000, **17**, 13.
- 16 (a) J. Daly, L. Horner and B. Witkop, *J. Am. Chem. Soc.*, 1961, **83**, 4787.
- 17 J. F. Krebs and A. S. Borovik, *Chem. Commun.*, 1998, 553.
- 18 A. C. Sharma and A. S. Borovik, *J. Am. Chem. Soc.*, 2000, **122**, 8946.
- 19 J. F. Krebs, PhD Thesis, Kansas State University, 1998.
- 20 B. Kerler, R. E. Robinson, A. S. Borovik and B. Subramaniam, *Appl. Catal., B*, 2004, **49**, 91.
- 21 (a) R. D. Jones, D. A. Summerville and F. Basolo, *Chem. Rev.*, 1979, **79**, 139 and references therein; (b) E. C. Niederhoffer, J. H. Timmons and A. E. Martell, *Chem. Rev.*, 1984, **84**, 137.
- 22 Percent conversion: $X = (\text{moles of quinone products}/\text{moles of substrate}) \times 100$ and percent selectivity: $S = (\text{moles of quinone product (either DTBQ or TTBDQ)}/\text{total moles of products}) \times 100$.
- 23 J. A. Norman, G. P. Pez and D. A. Roberts, in *Oxygen Complexes and Oxygen Activation by Transition Metal Metals*, ed. A. E. Martell and D. T. Sawyer, Plenum Press, New York, 1988, pp. 107–127.

Phase behavior of novel fluorinated surfactants in supercritical carbon dioxide

Zhao-Tie Liu,^{*a} Jin Wu,^a Ling Liu,^a Liping Song,^a Ziwei Gao,^a Wensheng Dong^a and Jian Lu^{ab}

Received 13th February 2006, Accepted 2nd August 2006

First published as an Advance Article on the web 16th August 2006

DOI: 10.1039/b602105k

A series of novel fluorinated analogues of sodium bis(2-ethylhexyl) sulfosuccinate (AOT) surfactants, the sodium salt of bis(3,3,4,4,5,5,6,6,6-nonafluoro-1-hexanol) sulfosuccinate ($\text{CF}_3(\text{CF}_2)_3\text{CH}_2\text{CH}_2\text{OOCCH}_2\text{CH}(\text{SO}_3\text{Na})\text{COOCH}_2\text{CH}_2(\text{CF}_2)_3\text{CF}_3$, di-HCF5), the sodium salt of bis(2,2,3,4,4,4-hexafluoro-1-butanol) sulfosuccinate ($\text{CF}_3\text{CFHCF}_2\text{CH}_2\text{OOCCH}_2\text{CH}(\text{SO}_3\text{Na})\text{COOCH}_2\text{CF}_2\text{CFHCF}_3$, di-HCF3), the sodium salt of bis(2,2,3,3-tetrafluoro-1-propanol) sulfosuccinate ($\text{HCF}_2\text{CF}_2\text{CH}_2\text{OOCCH}_2\text{CH}(\text{SO}_3\text{Na})\text{COOCH}_2\text{CF}_2\text{CF}_2\text{H}$, di-HCF2), and the sodium salt of bis(2,2,3,3-pentafluoro-1-propanol) sulfosuccinate ($\text{CF}_3\text{CF}_2\text{CH}_2\text{OOCCH}_2\text{CH}(\text{SO}_3\text{Na})\text{COOCH}_2\text{CF}_2\text{CF}_3$, di-CF2), were synthesized and characterized by ^1H NMR, ^{13}C NMR, ^{19}F NMR and FT-IR spectroscopy, melting point, and elemental analysis. The pressure–temperature phase behavior for water-in- CO_2 microemulsions stabilized by the four surfactants was tested and the P – T diagrams were determined. In the phase behavior experiments, pressures up to 35 MPa, temperatures up to 65 °C, and water-to-surfactant molar ratios (W_o) from 10 to 30 were tested. The cloud-point pressure in microemulsions stabilized by the four fluorinated surfactants increased with increasing temperature, and at a fixed temperature, the cloud-point pressure increased with increasing W_o . However, the cloud-point pressure was only slightly affected by an increase in the concentration of surfactant at a settled W_o . The phase behavior for water-in- CO_2 microemulsions at different $\text{Cd}(\text{NO}_3)_2$ concentrations in the aqueous phase with the surfactant di-HCF5 was also determined, which is useful for the formation of CdS nanoparticles in our future studies.

Introduction

In recent years, supercritical fluids (SCFs) have offered a great opportunity to replace conventional organic solvents in a variety of applications, especially supercritical carbon dioxide (scCO_2), because it is inexpensive, nontoxic, nonflammable, readily available in a large quantity and good quality, has a low surface tension, low viscosity, and a moderate critical temperature and pressure (31.1 °C and 7.38 MPa). Meanwhile, some properties of scCO_2 , such as its density, dielectric constant, diffusion coefficient, and solubility parameter can be tuned continuously by changing pressure and temperature. Therefore, these unique properties provide advantages in a wide range of applications including extraction,¹ polymer processing,² phase transfer reactions and catalysis,³ enzymatic catalysis,⁴ processing of microelectronic devices,⁵ and the synthesis of nanoparticles.^{6–10}

Water-in- CO_2 microemulsions have been investigated recently as a nano-reactor for synthesizing nanoparticles. A microemulsion is a thermodynamically stable state with at least three components: two immiscible components and a surfactant. Surfactants with a high solubility in CO_2 and which

are able to form water-in- CO_2 microemulsions are in demand. Consani and Smith¹¹ reported that most industrially available surfactants are incapable of forming stable microemulsions in CO_2 because of their negligible solubilities. However, under certain conditions the problems have been overcome by employing peculiar fluorinated surfactants to stabilize water-in- CO_2 microemulsions.^{12,13} Several research groups have reported on water-in- CO_2 microemulsions and phase behavior supported by fluorinated surfactants having two fluorocarbon chains,^{12,14,15} some hybrid type surfactants having both hydrocarbon and fluorocarbon chains within one molecule,^{16,17} as well as other fluorinated surfactants such as ammonium carboxylate perfluoropolyether (PFPE),^{13,18} Furthermore, some phosphate fluorosurfactants have been demonstrated to have a high activity at the water and CO_2 interface and therefore, can stabilize water-in- CO_2 microemulsions.^{19–21} There are a limited number of non-fluorous surfactants that can also form small hydrated reverse micelles in scCO_2 .^{22–25}

In water-in- CO_2 microemulsions, the aqueous phase is dispersed as nanosized droplets surrounded by a monolayer of surfactant molecules in the continuous CO_2 phase. The nanosized water droplets, when acting as nanoreactors, can facilitate the nanoparticle synthesis and a wide range of chemical transformations.^{14,26} The radii of the nanosized water droplets are determined by the water-to-surfactant ratio (W_o), therefore, the size of the nanoparticles synthesized in water-in- CO_2 microemulsions can be controlled by the W_o value.⁸ However, it should be noted that the amount of water used in

^aKey Laboratory for Macromolecular Science of Shaanxi Province, School of Chemistry and Materials Science, Shaanxi Normal University, Xi'an, 710062, People's Rep. China. E-mail: ztliu@snnu.edu.cn; Fax: +86-29-85303682; Tel: +86-29-85303682

^bXi'an Modern Chemistry Research Institute, Xi'an, 710065, People's Rep. China

these experiments as given in W_o is the total water added minus the water dissolved in bulk scCO_2 , due to the fact that water is slightly soluble in scCO_2 as reported by Wiebe and Gaddy.²⁷ The water dissolved in bulk scCO_2 could not form a microemulsion.

Phase behavior measurements are important when studying nanoparticle formation in water-in- CO_2 microemulsions. In this study, the synthesis, characterization, and phase behavior measurements of a series of novel fluorinated analogues of AOT surfactants are investigated. The phase behavior for water-in- CO_2 microemulsions with $\text{Cd}(\text{NO}_3)_2$ at different concentrations is also presented, which is useful for the synthesis of CuS nanoparticles in our future studies.

Experimental

Materials and instruments

3,3,4,4,5,5,6,6,6-Nonafluoro-1-hexanol (97%), 2,2,3,3-tetrafluoro-1-propanol (98%), 2,2,3,3,3-pentafluoro-1-propanol (97%), 2,2,3,4,4,4-hexafluoro-1-butanol (95%) were purchased from Aldrich (WI, USA). *p*-Toluenesulfonic acid monohydrate (99%), 1,4-dioxane (99%), maleic anhydride (99.5%) were obtained from Sinopharm Group Chemical Reagent Co. (Shanghai, China). Sodium hydrogen sulfite (SO_2 : 65.0%), $\text{Cd}(\text{NO}_3)_2$, acetone and toluene were obtained from Xi'an Chemical Reagent Factory (99%, Xi'an, China). Acetone- d_6 was obtained from Beijing Chemical Reagent Factory (Beijing, China). Water was taken from Millipore Milli-Q Plus system, and CO_2 (99.99%, Xi'an Yatai Liquid Gas Co., China) was used as received. The chemical reagents used were all AR grade.

The schematic diagram of the experimental apparatus for phase behavior measurements is given in Fig. 1. The macroscopic phase behavior of surfactant aggregations in scCO_2 was investigated by using a high-pressure vessel (Beijing, Sihe Chuangzhi Keji Corporation, SF-400), which has a maximum pressure of 40 MPa, a maximum temperature of 80 °C, an internal volume of 60 cm^3 and is equipped with two sapphire windows (diameter = 25 mm, thickness = 20 mm). The windows are sealed on both sides with poly(ether-ether-ketone) (PEEK) seals.

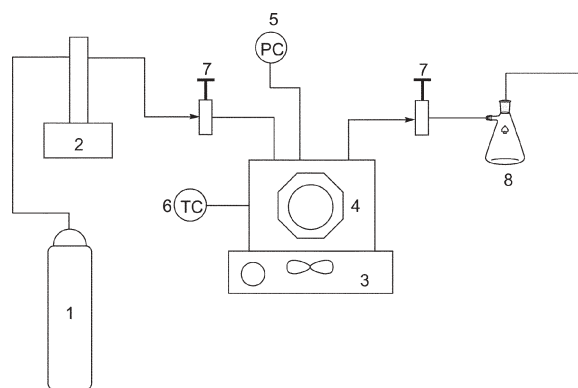


Fig. 1 Schematic diagram for studying phase behavior: 1. Carbon dioxide cylinder; 2. Isco model 260D syringe pump; 3. magnetic stir device; 4. SF-400 high-pressure vessel; 5. pressure transducer; 6. thermocouple assembly; 7. valve; 8. recycle vase.

^1H NMR and ^{13}C NMR spectra were recorded on a super-conducting Fourier digital NMR spectrometer (Bruker, AVANCF300 MHz). ^{19}F NMR spectra were recorded on a super-conducting Fourier digital NMR spectrometer (Bruker, AVANCF500 MHz). FT-IR spectra were recorded on a Fourier transform infrared spectrometer (Bruker, EQUINX55). The melting point of the surfactants was measured with a digital melting point apparatus (WRS-1B, Shanghai). The elemental analysis was done using an elemental analyzer (Vario EL III, Germany).

Surfactant synthesis

The surfactants were synthesized by a certain modification of the procedures given by Liu and Erkey,¹⁴ Yoshino *et al.*,²⁸ Downer *et al.*²⁹ and Nave *et al.*³⁰ The sodium salts of bis(3,3,4,4,5,5,6,6,6-nonafluoro-1-hexanol) sulfosuccinate, bis(2,2,3,3-tetrafluoro-1-propanol) sulfosuccinate, bis(2,2,3,3,3-pentafluoro-1-propanol) sulfosuccinate, and bis(2,2,3,4,4,4-hexafluoro-1-butanol) sulfosuccinate were synthesized in our laboratory by esterification and sulfonation reactions.

A mixture of fluorinated alcohol, maleic anhydride, and *p*-toluenesulfonic acid monohydrate as the catalyst in toluene was refluxed under stirring and the liberated water was removed azeotropically from the reaction system to shift the equilibrium of the esterification. The reaction was stopped when approximately 90% of the theoretical amount of water was collected in the trap and the solvent was evaporated using a rotary apparatus, the raw product was washed with hot water (60 °C) to remove *p*-toluenesulfonic acid monohydrate and excess maleic anhydride, and after purification by vacuum distillation a pure corresponding diester was obtained. Subsequently, the diester was dissolved in the mixture of 1,4-dioxane and aqueous sodium hydrogen sulfite. Then the mixture was refluxed under stirring for several hours. After the reaction, the solvent of 1,4-dioxane was evaporated using a rotary apparatus and the remaining mixture was treated by purification and recrystallization. A white solid was obtained after drying under vacuum overnight.

The surfactants were characterized by ^1H NMR, ^{13}C NMR, ^{19}F NMR and FT-IR spectroscopy, melting point, and elemental analysis.

Water-in-carbon dioxide phase behavior measurements

In the experimental measurements of phase behavior,^{10,14,31} a certain amount of surfactant, water and a magnetic stir bar were placed in the vessel, which was then sealed. The vessel was placed on a magnetic stir plate and heated to the desired temperature by a controllable heater. The vessel was charged very slowly with CO_2 from an ISCO syringe pump (model 260D) equipped with a cooling jacket, and the mixtures were stirred and equilibrated for several minutes. When an optically transparent single-phase solution was obtained, the pump was stopped.

Phase transition was determined visually by adjusting the pressure at a fixed temperature.³² When the pressure was higher than the cloud-point pressure, a clear single phase was observed. When the temperature and/or the pressure decreased

a little, the mixture in the vessel became cloudy again. Then, increasing the pressure until the optically transparent one-phase was obtained, the pressure and temperature were recorded. The temperature was controlled during each experiment with a variation of ± 0.5 °C. The pressure was measured using a pressure transducer.

Using the same approach, the phase behavior for water-in-CO₂ microemulsions at different Cd(NO₃)₂ concentrations in the aqueous phase with the surfactant di-HCF5 was also measured. The only difference is that an aqueous solution of cadmium nitrate or an aqueous solution of sodium sulfide was placed in the high-pressure vessel simultaneously with the surfactant.

Results and discussion

The characterization of surfactants

The structures of surfactants synthesized are shown in Fig. 2.

(1) ¹H NMR of surfactants

di-HCF5: CF₃(CF₂)₃CH₂^aCH₂^bOOCCH₂^cCH^d(SO₃Na)-COOCH₂^eCH₂^f(CF₂)₃CF₃, ¹H NMR (acetone-*d*₆): δ = 2.60–2.75 (a and f, m, J = 6.18 Hz, 4H), 3.01–3.17 (c, m, J = 7.95 Hz, 2H), 3.97–4.01 (d, m, J = 6.87 Hz, 1H), 4.39–4.54 (b and e, m, J = 6.21 Hz, 4H).

di-HCF3: CF₃CFH^aCF₂CH₂^bOOCCH₂^cCH^d(SO₃Na)COOCH₂^eCF₂CFH^fCF₃, ¹H NMR (acetone-*d*₆): δ = 3.20–3.33 (c, m, J = 3.82 Hz, 2H), 4.11–4.16 (d, m, J = 2.99 Hz, 1H), 4.57–4.68 (b and e, m, J = 2.19 Hz, 1H), 5.79–5.96 (a and f, m, J = 5.74 Hz, 2H).

di-HCF2: CF₂H^aCF₂CH₂^bOOCCH₂^cCH^d(SO₃Na)COOCH₂^eCF₂CF₂H^f, ¹H NMR (acetone-*d*₆): δ = 6.46–6.58 (a and f, m, J = 35.94 Hz, 2H), 4.46–4.73 (b and e, m, J = 12.40 Hz, 4H), 3.10–3.18 (c, m, J = 4.83 Hz, 2H), 4.04–4.05 (d, m, J = 4.74 Hz, 1H).

di-CF2: CF₃CF₂CH₂^aOOCCH₂^bCH^c(SO₃Na)COOCH₂^dCF₂CF₃, ¹H NMR (acetone-*d*₆): δ = 3.18–3.34 (b, m, J = 4.53 Hz, 2H), 4.11–4.16 (c, m, J = 4.71 Hz, 1H), 4.68–4.92 (a and d, m, J = 5.91 Hz, 4H).

(2) ¹⁹F NMR of surfactants

di-HCF5: CF₃^aCF₂^bCF₂^cCF₂^d(CH₂)₂OOCCH₂CH(SO₃Na)COO(CH₂)₂CF₂^eCF₂^fCF₂^gCF₃^h, (acetone-*d*₆): δ = –80.25 to –80.42 (a and h, t, J = 30.50 Hz, 6F), –112.35 to –112.71 (b and g, m, J = 16.00 Hz, 4F), –123.11 to –123.34 (c and f, d, J = 59.50 Hz, 4F), –124.91 to –125.07 (d and e, m, J = 15.50 Hz, 4F).

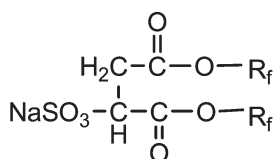


Fig. 2 Surfactants synthesized and used to form water-in-CO₂ microemulsions: (1) di-HCF5: sodium salt of bis(3,3,4,4,5,5,6,6,6-nonafluoro-1-hexanol) sulfosuccinate, R_fOH = CF₃(CF₂)₃CH₂CH₂-OH; (2) di-HCF3: sodium salt of bis(2,2,3,4,4,4-hexafluoro-1-butanol) sulfosuccinate, R_fOH = CF₃CFHCF₂CH₂OH; (3) di-HCF2: sodium salt of bis(2,2,3,3-tetrafluoro-1-propanol) sulfosuccinate, R_fOH = CF₂HCF₂CH₂OH; (4) di-CF2: sodium salt of bis(2,2,3,3,3-pentafluoro-1-propanol) sulfosuccinate, R_fOH = CF₃CF₂CH₂OH.

di-HCF3: CF₃^aCFH^bCF₂^cCH₂OOCCH₂CH(SO₃Na)COOCH₂CF₂^dCFH^eCF₃^f, (acetone-*d*₆): δ = –74.74 to –74.96 (a and f, t, J = 28.50 Hz, 6F), –115.31 to –120.34 (c and d, m, J = 112.00 Hz, 4F), –212.85 to –213.27 (b and e, m, J = 23.50 Hz, 2F).

di-HCF2: CF₂^aHCF₂^bCH₂OOCCH₂CH(SO₃Na)COOCH₂CF₂^cCF₂^dH, (acetone-*d*₆): δ = –123.80 to –124.68 (b and c, m, J = 70.00 Hz, 4F), –138.00 to –139.41 (a and d, q, J = 73.5 Hz, 4F).

di-CF2: CF₃^aCF₂^bCH₂OOCCH₂CH(SO₃Na)COOCH₂CF₂^cCF₃^d, (acetone-*d*₆): δ = –82.77 to –82.85 (a and d, t, J = 38.5 Hz, 6F), –121.97 to –122.26 (b and c, m, J = 12.5 Hz, 4F).

(3) ¹³C NMR of surfactants

di-HCF5: C^aF₃C^bF₂C^cF₂C^dF₂C^eH₂C^fH₂OOC^gC^hH₂CⁱH-(SO₃Na)C^jOOC^kH₂C^lH₂C^mF₂CⁿF₂-C^oF₂C^pF₃, (acetone-*d*₆): δ = 33.99 (h, 1C), 62.29 (i, 1C), 169.72 (g, 1C), 173.40 (j, 1C), 54.61–58.41 (f and k, 2C), 34.50–35.60 (e and l, 2C), 115.95–116.84 (d and m, 2C), 120.65–122.15 (c and n, 2C), 109.98–111.23 (b and o, 2C), 118.69–119.20 (a and p, 2C).

di-HCF3: C^aF₃C^bFHC^cF₂C^dH₂OOC^eC^fH₂C^gH(SO₃Na)C^hO-OCⁱH₂C^jF₂C^kFHC^lF₃, (acetone-*d*₆): δ = 33.95 (f, 1C), 61.86–62.27 (g, 1C), 168.36 (e, 1C), 170.98 (h, 1C), 83.11–85.76 (d and i, 2C), 110.03–110.58 (c and j, 2C), 118.32–118.46 (b and k, 2C), 115.21–115.43 (a and l, 2C).

di-HCF2: C^aF₂H^bCF₂^cCH₂OOC^dC^eH₂C^fH(SO₃Na)C^gOO-C^hH₂CⁱF₂C^jF₂H, (acetone-*d*₆): δ = 33.94 (e, 1C), 60.43–61.41 (c and h, 2C), 112.95–115.42 (b and i, 2C), 129.31–130.78 (a and j, 2C), 168.44 (d, 1C), 170.91 (g, 1C), 65.85 (f, 1C).

di-CF2: C^aF₃C^bF₂C^cH₂OOC^dC^eH₂C^fH(SO₃Na)C^gOO-C^hH₂-CⁱF₂C^jF₃, (acetone-*d*₆): δ = 34.03 (e, 1C), 59.54–60.55 (c and h, 2C), 61.69 (f, 1C), 117.62–119.26 (b and i, 2C), 121.41–123.46 (a and j, 2C), 168.53 (h, 1C), 170.59 (g, 1C).

(4) Elemental analysis of surfactants

di-HCF5: Anal. Calcd: C, 26.95; H, 1.54; S, 4.60. Found: C, 26.93; H, 1.60; S, 4.66.

di-HCF3: Anal. Calcd: C, 26.68; H, 1.64; S, 5.84. Found: C, C, 26.71; H, 1.69; S, 5.91.

di-HCF2: Anal. Calcd: C, 26.77; H, 2.01; S, 7.14. Found: C, 26.79; H, 2.09; S, 7.21.

di-CF2: Anal. Calcd: C, 24.78; H, 1.45; S, 6.61. Found: C, 24.69; H, 1.51; S, 6.72.

(5) Melting point of surfactants

di-HCF5: 261.3–263.5 °C; di-HCF3: 141.1–144.6 °C; di-HCF2: 140.1–142.5 °C; di-CF2: 238.7–239.7 °C.

(6) FT-IR (KBr) spectra of the four surfactants are shown in Fig. 3. Curves (a)–(d) correspond to di-CF2, di-HCF3, di-HCF2 and di-HCF5, respectively. The acyl group (O–C=O) vibrations at 1752 cm^{–1} and –C–F group at 1100–1200 cm^{–1} are observed. The increase in intensity of the –CH₂ group at 2990 cm^{–1} is attributed to the increasing number of H atoms in these surfactants. Moreover, the intensity of –C–F increases with the increasing number of F atoms in the surfactants.

The study of phase behavior

The pressure–temperature phase diagrams for water-in-CO₂ microemulsions formed with di-HCF5 at different W_o are shown in Fig. 4. At a surfactant concentration of 0.005 M and

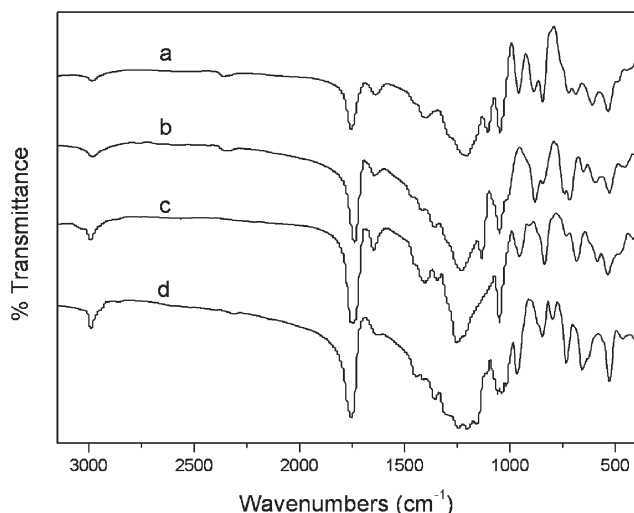


Fig. 3 FT-IR of surfactants (a: di-CF₂, b: di-HCF₃, c: di-HCF₂, d: di-HCF₅).

W_o from 10–30, the cloud-point pressure increases with increasing W_o at a fixed temperature, and increases with increasing temperature, which has also been observed for water-in-CO₂ microemulsions reported in other articles.^{11,14,17,18,33–35} The water-in-CO₂ microemulsions swell when the water is added. The swelling reinforces the attraction between microemulsion particles. Therefore, high pressure is required to make the system become transparent. However, water-in-CO₂ microemulsions cannot be obtained at this surfactant concentration under W_o of 40, because the micelle–micelle interaction is stronger than the interaction between water and the polar head of surfactant. The surfactant cannot aggregate more water in the microemulsion and the system cannot be stabilized, which means that the maximum value of W_o for di-HCF₅ cannot reach 40 for this system. Without any water added, the di-HCF₅ surfactant is not soluble in CO₂ in the absence of water.

The pressure–temperature phase diagrams at $W_o = 10$ for different concentrations of di-HCF₅ are shown in Fig. 5. At a fixed temperature, while the surfactant concentration

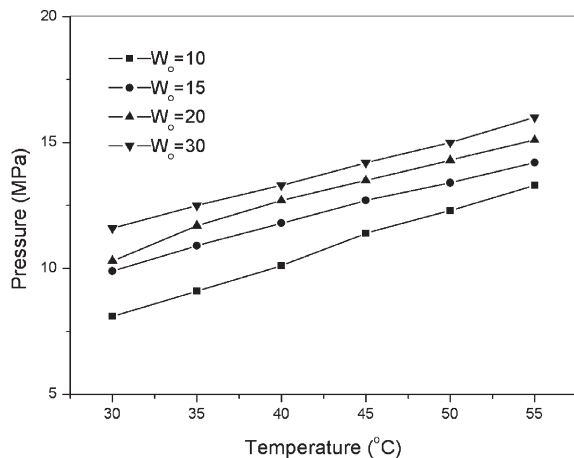


Fig. 4 Pressure–temperature phase diagram for W/CO₂ microemulsions at [di-HCF₅] = 0.005 M.

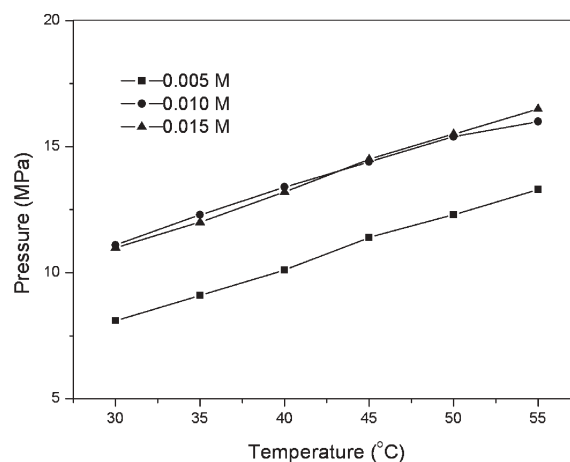


Fig. 5 Effect of surfactant concentration on the pressure–temperature phase diagram for water-in-CO₂ microemulsions supported by di-HCF₅ at $W_o = 10$.

increases from 0.005 to 0.01 M, there is a visible cloud-point pressure increase. However, when the surfactant concentration increases from 0.01 to 0.015 M, there is no appreciable increase in cloud-point pressure. The amount of water dissolved in the microemulsion increases when the surfactant concentration increases, so in order to keep the size of the microemulsion the same, the cloud pressure must be increased. However, while the surfactant concentration increases from 0.01 to 0.015 M, the concentration of water in the water-droplet pool also increases, so the interaction force or hydrogen-bond force increases between water molecules, which is favorable for keeping the same size of microemulsion, therefore the increasing trend of cloud pressure will decrease as shown in Fig. 5 when the surfactant concentration increases from 0.01 to 0.015 M. It indicates that the micelle size is little affected by the concentration of surfactant, and the cloud-point pressure changes unobviously.

The pressure–temperature phase diagrams for water-in-CO₂ microemulsions stabilized by different surfactants (di-HCF₅, di-HCF₃ and di-HCF₄) are given in Fig. 6. The cloud-point pressure data of di-HCF₄ are cited from the results reported by Liu and Erkey.¹⁴ The concentrations of these surfactants are 0.0154 M with $W_o = 10$. At the same concentration and W_o , the cloud-point pressure of di-HCF₃ and di-HCF₄ is distinctly higher than that of di-HCF₅. It can be seen that the cloud-point pressure is affected by the length of the CO₂-philicity tail, and the surfactant with the longest fluoroalkyl chain has the lowest cloud point pressure. Attributed to the strong interaction forces between CO₂ and the nonpolar tails of di-HCF₅, the stability of reverse micelles supported by di-HCF₅ is the best compared with that of others. However, at concentrations of 0.003 M, 0.01 M and 0.015 M, water-in-CO₂ microemulsions cannot be formed with di-HCF₂ surfactant. The CO₂-philicity of the tail group may be too little and the tail–solvent interactions are too weak to compensate for attractive micelle–micelle interactions. It is also an influence of the different surface tension between the H–CF₂-tipped surfactants and F–CF₂-tipped surfactants. This result is consistent with the findings reported by Eastoe *et al.*³⁴

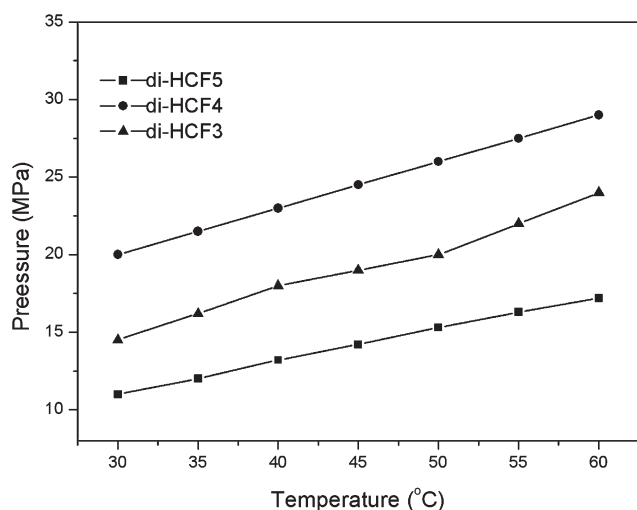


Fig. 6 Comparison of a pressure–temperature phase diagram for water-in-CO₂ microemulsions for different surfactants at $W_o = 10$ and a concentration of 0.015 M.

The pressure–temperature phase diagrams for water-in-CO₂ microemulsions at different Cd(NO₃)₂ concentrations in the aqueous phase are illustrated in Fig. 7. It was found that the probability of forming stable microemulsions at these electrolyte concentrations was promising for other applications. At concentrations of 0–3.46 mM, the presence of Cd(NO₃)₂ had a noteworthy effect on the cloud point compared with the absence of Cd(NO₃)₂ when the critical temperature is higher than 35 °C. While Cd(NO₃)₂ concentration increased to 4.61 mM, the cloud-point pressure increased just a little compared with that of 3.46 mM. However, for microemulsions supported by PFPE, the presence of Cd(NO₃)₂ even at a concentration of 10 mM was found to decrease the cloud-point pressures.³⁶ For microemulsions supported by di-HCF4 (HF₂C(CF₂)₃CH₂OOCH₂CH(SO₃Na)COOCH₂(CF₂)₃CF₂H), the cloud-point pressure decreases when Cu(NO₃)₂ is present at a concentration of 195.3 mM, whereas at concentrations of 7.8 mM and 39.1 mM, the presence of Cu(NO₃)₂ had no

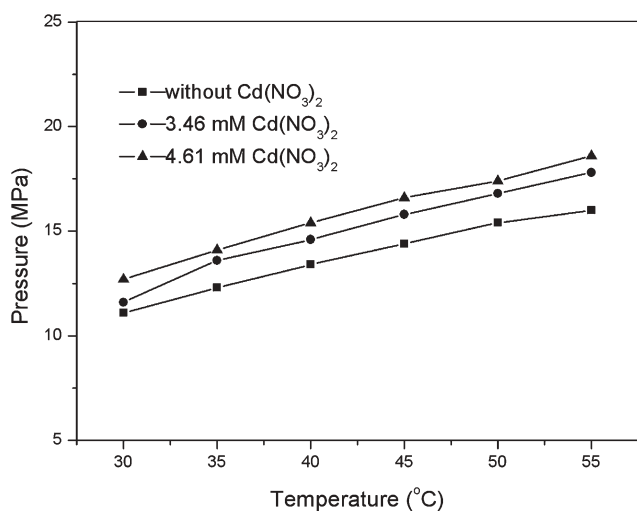


Fig. 7 Pressure–temperature phase diagram for water-in-CO₂ microemulsions with Cd(NO₃)₂ at [di-HCF5] = 0.01 M and $W_o = 10$.

significant effect on the cloud-point.¹⁰ This was attributed to a change in charge screening such as Cd²⁺ or Cu²⁺ between surfactant headgroups, which increased the surfactant membrane rigidity in the micellar interfacial region, and thus the cloud-point pressure increased. The difference in behavior between these systems might be indicative of the effect of the cation on the phase behavior.¹⁰

Conclusions

Four different fluorinated analogues of AOT surfactants were synthesized and characterized. The phase behavior in water-in-CO₂ microemulsions stabilized by these fluorinated surfactants was investigated. We have presented their phase behavior as a function of temperature, pressure, concentration of the surfactants, and water-to-surfactant ratio. The phase behavior for water-in-CO₂ microemulsions at various Cd(NO₃)₂ concentrations in the aqueous phase with the surfactant of di-HCF5 was also tested and determined. The phase behavior study of these surfactants is the basis of our future research work, which aims to synthesize nanoparticles in water-in-carbon dioxide or water-in-fluoroethane with various fluorinated surfactants.

Acknowledgements

The authors gratefully acknowledge financial support from the National Natural Science Foundation of China (NSFC) (Grant No. 20473051) and the Special Project of National Grand Fundamental Research Pre-973 Program of China (Program/Grant 2004CCA00700). We also appreciate the support provided by the Natural Science Foundation of Shaanxi Province (2004B12).

References

- C. A. Eckert, B. L. Knutson and P. G. Debenedetti, *Nature*, 1996, **383**, 313.
- A. I. Cooper, *J. Mater. Chem.*, 2000, **10**, 207.
- A. K. Dillow, S. L. Yun, D. S. Suleiman, D. L. Boatright, C. L. Liotta and C. A. Eckert, *Ind. Eng. Chem. Res.*, 1996, **35**, 1801.
- J. D. Holmes, D. C. Steytler, G. D. Rees and B. H. Robinson, *Langmuir*, 1998, **14**, 6371.
- N. Sundararajan, S. Yang, K. Ogino, S. Valiyaveetil, J. Wang, X. Zhou, C. K. Ober, S. K. Obendorf and R. D. Allen, *Chem. Mater.*, 2000, **12**, 41.
- M. Ji, X. Chen, C. M. Wai and J. L. Fulton, *J. Am. Chem. Soc.*, 1999, **121**, 2631.
- H. Ohde, F. Hunt and C. M. Wai, *Chem. Mater.*, 2001, **13**, 4130.
- H. Ohde, M. Ohde, F. Bailey, H. Kim and C. M. Wai, *Nano Lett.*, 2002, **2**, 721.
- H. Ohde, J. M. Rodriguez, X. R. Ye and C. M. Wai, *Chem. Commun.*, 2000, **23**, 2353.
- X. Dong, D. Potter and C. Erkey, *Ind. Eng. Chem. Res.*, 2002, **41**, 4489.
- K. A. Consani and R. D. Smith, *J. Supercrit. Fluids*, 1990, **3**, 51.
- J. Eastoe, A. Dupont and D. C. Steytler, *Curr. Opin. Colloid Interface Sci.*, 2003, **8**, 267.
- K. P. Johnston, K. L. Harrison, M. J. Clarke, S. M. Howdle, M. P. Heitz, F. V. Bright, C. Carlier and T. W. Randolph, *Science*, 1996, **271**, 624.
- Z. T. Liu and C. Erkey, *Langmuir*, 2001, **17**, 274.
- J. Eastoe, B. M. H. Cazelles, D. C. Steytler, J. D. Holmes, A. R. Pitt, T. J. Wear and R. K. Heenan, *Langmuir*, 1997, **13**, 6980.
- M. Sagisaka, S. Yoda, Y. Takebayashi, K. Otake, B. Kitiyanan and Y. Kondo, *Langmuir*, 2003, **19**, 220.

- 17 K. L. Harrison, J. Goveas, K. P. Johnston and E. A. O'Rear, *Langmuir*, 1994, **10**, 3536.
- 18 M. P. Heitz, C. Carlier, J. DeGrazia, K. L. Harrison, K. P. Johnston, T. W. Randolph and F. V. Bright, *J. Phys. Chem. B*, 1997, **101**, 6707.
- 19 J. S. Keiper, R. Simhan, J. M. DeSimone, G. D. Wignall, Y. B. Melnichenko and H. Frielinghaus, *J. Am. Chem. Soc.*, 2002, **124**, 1834.
- 20 D. C. Steytler, E. Rumsey, M. Thorpe, J. Eastoe, A. Paul and R. K. Heenan, *Langmuir*, 2001, **17**, 7984.
- 21 J. S. Keiper, J. A. Behles, T. L. Bucholz, R. Simhan and J. M. DeSimone, *Langmuir*, 2004, **20**, 1065.
- 22 J. Eastoe, A. Paul, S. Nave, D. C. Steytler, B. H. Robinson, E. Rumsey, M. Thorpe and R. K. Heenan, *J. Am. Chem. Soc.*, 2001, **123**, 988.
- 23 J. C. Liu, B. X. Han, J. L. Zhang, G. Z. Li, X. G. Zhang, J. Wang and B. Z. Dong, *Chem.-Eur. J.*, 2002, **8**, 1356.
- 24 J. C. Liu, B. X. Han, G. Z. Li, X. G. Zhang, J. He and Z. M. Liu, *Langmuir*, 2001, **17**, 8040.
- 25 J. C. Liu, J. L. Zhang, T. C. Mu and B. X. Han, *J. Supercrit. Fluids*, 2003, **26**, 275.
- 26 C. T. Lee, W. Ryoo, P. G. Smith, J. Arellano, D. R. Mitchell, R. J. Lagow, S. E. Webber and K. P. Johnston, *J. Am. Chem. Soc.*, 2003, **125**, 3181.
- 27 R. Wiebe and V. L. Gaddy, *J. Am. Chem. Soc.*, 1941, **63**, 475.
- 28 N. Yoshino, N. Komine, J. Suzuki, Y. Arima and H. Hirai, *Bull. Chem. Soc. Jpn.*, 1991, **64**, 3262.
- 29 A. Downer, J. Eastoe, A. R. Pitt, E. A. Simister and J. Penfold, *Langmuir*, 1999, **15**, 7591.
- 30 S. Nave, J. Eastoe and J. Penfold, *Langmuir*, 2000, **16**, 8733.
- 31 X. Dong, C. Erkey, H. J. Dai, H. C. Li, H. D. Cochran and J. S. Lin, *Ind. Eng. Chem. Res.*, 2002, **41**, 1038.
- 32 J. Eastoe, A. Paul, A. Downer, D. C. Steytler and E. Rumsey, *Langmuir*, 2002, **18**, 3014.
- 33 J. Y. Park, J. S. Lim, C. H. Yoon, C. H. Lee and K. P. Park, *J. Chem. Eng. Data*, 2005, **50**, 299.
- 34 J. Eastoe, A. Paul, A. Downer, D. C. Steytler and E. Rumsey, *Langmuir*, 2002, **18**, 3014.
- 35 M. Sagisaka, S. Yoda, Y. Takebayashi, K. Otake, Y. Kondo, N. Yoshino, H. Sakai and M. Abe, *Langmuir*, 2003, **19**, 8161.
- 36 J. D. Holmes, P. A. Bhargava, B. A. Korgel and K. P. Johnston, *Langmuir*, 1999, **15**, 6613.

Textbooks from the RSC

The RSC publishes a wide selection of textbooks for chemical science students. From the bestselling *Crime Scene to Court*, 2nd edition to groundbreaking books such as *Nanochemistry: A Chemical Approach to Nanomaterials*, to primers on individual topics from our successful *Tutorial Chemistry Texts series*, we can cater for all of your study needs.

Find out more at www.rsc.org/books

Lecturers can request inspection copies – please contact sales@rsc.org for further information.



Registered Charity No. 207890

RSC Publishing

www.rsc.org/books

Novel debromination method for flame-retardant high impact polystyrene (HIPS-Br) by ammonia treatment

Mihai Brebu†* and Yusaku Sakata

Received 10th March 2006, Accepted 28th July 2006

First published as an Advance Article on the web 21st August 2006

DOI: 10.1039/b603584a

Debromination of flame-retardant brominated high impact polystyrene (HIPS-Br) was performed at 450 °C by ammonia treatment. All inorganic and most organic Br compounds were successfully removed and converted to inorganic NH_4Br powder, which allows easy bromine recovery. The liquid degradation products are rich in benzene derivatives and can be used as feedstock or fuel.

Introduction

Plastics are attractive materials extensively used in our daily life but create large amounts of waste with serious environmental problems. Pyrolysis is one of the best options for treatment of plastic waste as it allows both energy and material recovery. This is obtained by breaking down polymers at high temperatures into petrochemical feedstock components from which they originate. Polymers or plastic additives might contain heteroatoms that have undesired effects during thermal treatment of waste streams.

Brominated flame retardants (Br-FRs), such as polybrominated diphenyl ethers (PBDEs), polybrominated biphenyls (PBBs) and tetrabromobisphenol A (TBBPA), in combination with antimony oxide synergist (Sb_2O_3), have special interest and wide use in plastic materials because they ensure higher fire safety for lower quantities of additive. However, they are of high environmental concern, especially after the widespread contamination with PBB in Michigan, 1973.^{1,2} Studies have shown that Br-FRs are ubiquitous in sediment and biota, with rapidly increasing levels and risk of adverse effects in wildlife and human populations. Several reviews were published on bromine (Br) distribution in plastic products and waste streams, Br-FRs in the environment, their metabolism and potential toxicity in organisms.^{3–5} Br-FRs can generate polybrominated dibenzodioxins and dibenzofurans during thermal processes (*e.g.* in accidental fires, plastic production or recycling).^{4,6,7} PBDEs are the most discussed Br-FRs, for dioxin formation and because they are long-lived, fat-seeking and bioaccumulate in animal tissue. Their market is decreasing after a regulation change especially in Europe.⁸ Polybrominated diphenylethanes are considered instead of PBDEs, as the oxygen atom in the molecule is replaced by an ethane structure.

We previously reported that Br-FRs interact with polymers to form Br-organic compounds in degradation oils.⁹ Bromophenol and 1-bromoethylbenzene were the main organic Br-compounds produced by epoxy-type and PBDE-type Br-FRs, respectively.^{10,11} Sb_2O_3 initiates the degradation

of Br-FR and the plastic and gives inorganic SbBr_3 , soluble in oil products.¹² Various debromination methods, using calcium- or iron oxide- based carbon composites as dehalogenation catalysts/sorbents,^{13–15} polymers as reductive sources for dehalogenation,^{16,17} hydrothermal and alkaline debromination in autoclaves,^{18,19} debromination with subcritical water²⁰ or Br recycling from municipal solid waste combustion facilities,²¹ were reported. Studies on alkaline debromination in aqueous or organic solutions,^{22,23} alkaline pre-treatment of plastic waste with hydroxides or carbonates²⁴ and co-pyrolysis of components from electronic scrap with alkaline inorganic solids²⁵ were also performed. Alkaline treatment was found to be effective for epoxy resins but less effective for Br-styrenic polymers that contain mainly PBDEs.²⁶ However, none of these studies envisaged both debromination and material recovery for feedstock recycling. A report on adding ammonia to the fluidizing gas during pyrolysis of chlorine-containing materials showed successful removal of chlorine from pyrolysis products and no difficulties related to mass streams that usually appeared in conventional treatment using limestone.²⁷

In the present investigation we propose a novel method to remove the Br content of flame-retardant high impact polystyrene (HIPS-Br) by thermal degradation in a gaseous ammonia flow. HIPS with two types of Br-FRs and Sb_2O_3 as synergist was considered for this study. The material and Br distribution in the products as well as qualitative and quantitative analysis of compounds in the degradation oil is discussed.

Results and discussion

Debromination of HIPS-Br (POPS and PEPS samples: see Experimental) containing two types of Br-FRs and Sb_2O_3 as synergist was performed by thermal degradation at 450 °C in an ammonia flow using a semi-batch process. Nitrogen flow was used in reference experiments to maintain similar retention times of products inside the reactor. The degradation products were classified as residue (remaining at the bottom of reactor), powder (coated on the walls of reactor in the colder region between the furnace and reactor outlet), oil (liquid product condensed in the condenser and accumulated in the graduated cylinder) and gases (collected in the Teflon bag). The material balance and bromine concentration in the degradation products of HIPS-Br is presented in Fig. 1.

Department of Applied Chemistry, Faculty of Engineering, Okayama University, 3-1-1 Tsushima Naka, Okayama, 700-8530, Japan

† Permanent address: "Petru Poni" Institute of Macromolecular Chemistry, 41A Grigore Ghica Voda Alley, 700487 Iasi, Romania, Tel.: +40 232 217454, Fax: +40 232 211299, E-mail: bmihai@icmpp.ro

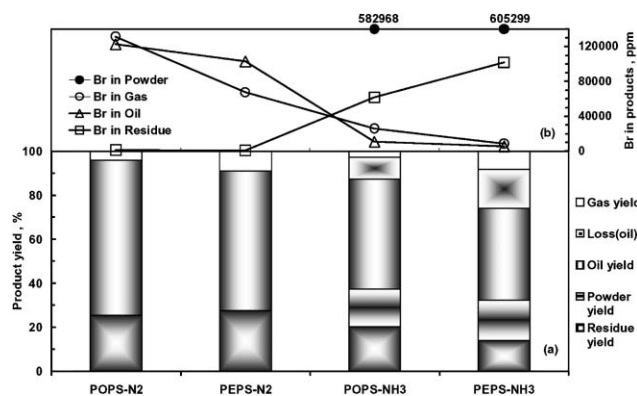


Fig. 1 (a) Product yield and (b) Br amount in products for degradation of HIPS-Br in nitrogen and ammonia flow.

Thermal degradation at 450 °C converts 60–70 wt% of HIPS-Br into oils with a density of 0.9–1.0 g cm⁻³ and a Br amount dependent on sample and especially on the degradation atmosphere. Less than 9 wt% was represented by gases, while the carbonaceous residue was below 28 wt%. Most of the initial Br in the plastic was found in the oil products after degradation in nitrogen flow. The Br concentration in the oil was higher than 100 000 ppm in this case, as determined by a combustion flask coupled with ion chromatography. The Br in the oil was mainly in the form of inorganic antimony bromide (SbBr₃) that comes from the interaction between the brominated flame retardant and the Sb₂O₃.¹¹

Ammonia treatment decreased the Br amount in oil to below 10 000 ppm, which represents less than 5 wt% of initial Br in samples. The oil density is decreased, suggesting that heavy SbBr₃ might be removed. A powder laid on the cold walls of reactor was observed. This was highly concentrated in Br (60 wt%) and trapped more than 90 wt% of the initial Br in HIPS-Br. XRD analysis showed a main phase of inorganic ammonium bromide (NH₄Br) in powder, but also Sb₂O₃ and antimony oxo-bromides as minor phases. This explains the lower Br concentration in the powder compared to pure NH₄Br, which contains 81.6 wt% Br. Gaseous products and their Br concentration were decreased. This is explained by reaction between hydrogen bromide and ammonia to form powdered NH₄Br. Less carbonaceous residue remained inside the reactor suggesting that ammonia favors the conversion of HIPS into oils. However, carbon residue seems to contain more Br than in the nitrogen case, but this is due to contamination with some NH₄Br powder that fell to the bottom of the reactor at the end of the experiment. The differences caused by the type of flame retardant in HIPS-Br consisted of a higher gas yield, lower oil density and lower Br concentration in the gas and oil products obtained in presence of decabromodiphenylethane (PEPS sample).

The composition of HIPS-Br degradation oils was characterized using C–NP-grams (C-stands for carbon and NP stands for normal paraffin), shown in Fig. 2. These curves were obtained by plotting the weight percent of the hydrocarbons (determined from gas chromatographic analysis) versus the carbon number of the normal paraffin having equivalent retention time in the chromatogram.²⁸ The hydrocarbons leave a non-polar chromatographic column in order of their

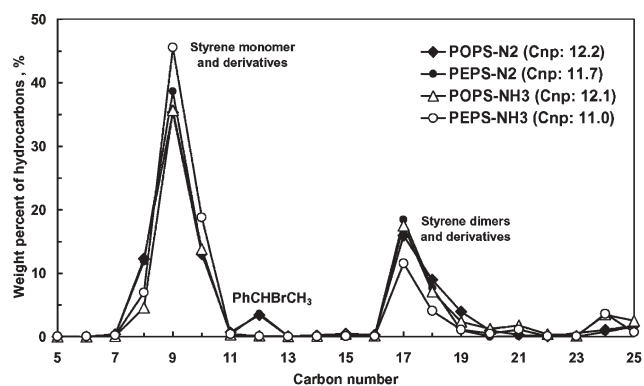


Fig. 2 C–NP-gram of liquid products from HIPS-Br degradation in nitrogen and ammonia flow (C_{np}: average carbon number).

increasing boiling points, therefore higher retention times indicate compounds with higher molecular weight and boiling points (*i.e.* higher carbon number).

Most of the HIPS-Br degradation oil consists of aromatic compounds such as toluene, ethylbenzene, styrene, isopropylbenzene and α -methylstyrene (at n-C₈–n-C₁₀ in Fig. 2). This was expected, since it is known that thermal degradation of polystyrene occurs mainly by depolymerization, leading to the styrene monomer and its derivatives. About 30 wt% of the oil consists of the styrene dimers at n-C₁₇–n-C₁₉, and small amounts (below 5 wt%) correspond to styrene trimers at n-C₂₄ and higher. The oil composition changed with sample type and degradation atmosphere. PEPS and ammonia treatment gave a smaller average carbon number of oil compared to POPS and nitrogen treatment. The greatest effect was observed in cumulative conditions, namely for ammonia treated PEPS. Ethylbenzene and isopropylbenzene were the main hydrocarbons obtained in nitrogen, while ammonia treatment strongly increased the amounts of styrene and α -methylstyrene, especially for PEPS. That means ammonia favors depolymerization of HIPS. PEPS gave more unsaturated aromatic compounds (styrene, α -methylstyrene, propenylbenzene) compared to POPS, probably due to the fragmentation of C_{aliphatic}–C_{aromatic} bond in the flame retardant

A peak was present at n-C₁₂ in the C–NP-gram of the oils obtained in nitrogen flow but was not found after ammonia treatment. This peak counts for about 3.5 wt% of the oils and corresponds to 1-bromoethylbenzene, the main organic Br compound in oil that comes from interaction between Br from the flame retardant and styrene fragments from HIPS. Detailed analysis of Br- and O-containing compounds in oils was performed by GC-MSD and the identified compounds are listed in Table 1. HIPS-Br degradation oils have a complex composition, and most Br- and O- compounds were found in peaks smaller than 0.01% of the total peak area of the chromatogram. Their quantitative determination was difficult to obtain and they are represented by a compound code in Table 1. However some compounds in higher amounts could be quantitatively determined and have the peak area shown in Table 1.

The formation of Br- and O- compounds in HIPS-Br degradation oil depends on the type of the flame retardant and especially on the degradation condition. Inorganic Br

Table 1 Br- and O-compounds (GC-MSD area% or compound code) identified in degradation oils of HIPS-Br^{a,b}

Compound group	Molecular formula	POPS ^g		PEPS ^g	
		N ₂	N ₂	NH ₃	NH ₃
a: Inorganic Br	HBr	0.24	0.28	—	—
	SbBr ₃	4.52	4.46	—	—
b: Alkyl Br ^c	C _n H _{2n+1} Br	C ₁₋₆	C ₁₋₆	C _{1,2}	C _{1,2}
c: Phenyl-alkyl Br ^d	PhC _n H _{2n} Br	C ₁₋₃	C ₁₋₃	C _{1,2}	C ₂
	1-Br-Ethylbenzene (PhCHBrCH ₃)	3.98	4.51	*	*
	Brominated Styrene dimers	1.26	0.42	—	—
d: Br-FR fragments and derivatives ^e	BrPhC _n	C ₁₋₃	C ₁₋₃	C ₁₋₃	C ₁₋₃
	Br _n Ph	Br ₁₋₃	Br _{1,3}	Br ₁₋₃	Br ₁
	Br _n Anthracene	—	Br _{a1,a2}	—	Br _{a1,a2}
e: O-FR fragments and derivatives ^f	C _n H _{2n+1} PhOH	C _{0,1}	C _{0,1}	C _{0-2,6}	C _{0-2,6}
	Br _n PhOH	Br _{1,2}	—	Br _{1,2}	—
	Br _n Ph-O-PhBr _n	Br _{e0,e2}	—	Br _{e0,e2}	—
f: Others	Dibenzofuran	0.25	—	0.06	—

^a —: Not identified. ^b *: Identified in small amounts but no quantitative data. ^c Group b: Br-methane(C₁), Br-ethane(C₂), 2-Br-propane(C₃), 2-Br-isobutane(C₄), 3-Br-pentane(C₅), Br-hexane(C₆), Br-cyclohexane(C₆). ^d Group c: Br-methylbenzene(C₁), 2-Br-ethylbenzene(C₂), 2-Br-propylbenzene(C₃). ^e Group d: 1-Br-3-methylbenzene(C₁), 1-Br-2-ethylbenzene(C₂), 1-Br-4-ethenylbenzene(C₂), 1-Br-2-isopropylbenzene(C₃); Br-benzene(Br₁), diBr-benzene(Br₂), triBr-benzene(Br₃); Br-anthracene or Br-phenanthrene(Br_{a1}), diBr-anthracene or diBr-phenanthrene (Br_{a2}). ^f Group e: phenol(C₀), 4-methylphenol(C₁), 2-ethylphenol(C₂), 3,5-bisopropylphenol(C₆); Br-phenol(Br₁), diBr-phenol(Br₂); diphenylether(Br_{e0}), diBr-diphenylether(Br_{e2}). ^g See Experimental for definition of POPS and PEPS samples.

compounds (group a in Table 1) are represented by hydrobromic acid (HBr) and SbBr₃. It was confirmed by the values of the peak area that SbBr₃ was the main Br- compound in HIPS-Br oil obtained in nitrogen flow. HBr and SbBr₃ are formed by interaction of Br radicals from degradation of the flame retardant with the H radicals from the plastic and with the Sb₂O₃ synergist, respectively, and they were totally removed from oil by ammonia treatment.

The alkyl bromides and the phenyl-alkyl bromides (group b and c) are formed by interaction between Br radicals and alkyl fragments or alkyl side chains of the aromatic derivatives from degradation of HIPS. Ammonia treatment removed the Br-compounds with alkyl chains longer than 2 atoms of carbon. It is important to note that 1-bromoethylbenzene, the main organic Br- compound, and the second highest in amount after SbBr₃, was almost totally removed by ammonia treatment. Two brominated styrene dimer isomers were found in significant amounts after degradation in nitrogen flow (Table 1) but they were totally removed by ammonia treatment.

The compounds of group d are fragments and their derivatives from the flame retardant after scission of Ph-O-Ph or Ph-C-C-Ph bonds but without total debromination of aromatic ring. They were not removed by ammonia treatment. We found that up to three atoms of Br remained bonded on the aromatic ring in our experimental conditions. Bromoanthracenes or bromophenanthrenes (it was difficult to identify the structure unambiguously) were observed for PEPS samples, and they are formed by cyclisation of Ph-C-C-Ph from the flame retardant.

The group e in Table 1 contains totally or partially debrominated O- compounds that remain from Ph-O-Ph structure in POPS. They are alkyl- and brominated-phenols and brominated or debrominated diphenylether and they were not removed by ammonia treatment. Alkylphenols were surprisingly found in PEPS oils suggesting possible contamination or partial degradation during storage of PEPS.

Dibenzofuran (group f) was found in POPS oil in a significant amount compared to the other Br- and O- compounds. It

was formed by cyclisation of totally debrominated Ph-O-Ph units and its amount was decreased by ammonia treatment.

Experimental

Materials

Commercially available HIPS-Br containing decabromodiphenyl oxide and decabromodiphenyl ethane brominated flame retardants (POPS and PEPS sample respectively) with 10.8 wt% Br content and 4.5 wt% Sb₂O₃ synergist were used in the present study.

Degradation procedure

The degradation experiments were performed in a glass reactor by semi-batch operation (Fig. 3).

A 10 g amount of HIPS-Br was used for each experiment. The plastic was laid on a stainless steel net covered by quartz wool and placed about 5 mm from the bottom of the reactor. A metal line for gas flow was placed with the outlet at the bottom of reactor below the plastic layer to assure nitrogen or

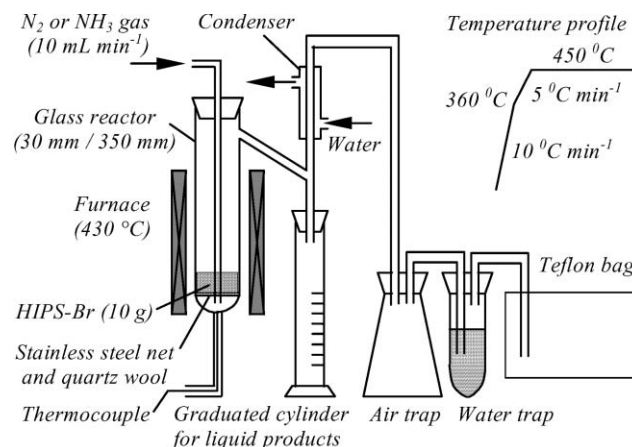


Fig. 3 Schematic experimental setup for ammonia treatment of HIPS-Br at 450 °C.

ammonia atmosphere in the reacting zone. A 10 mL min⁻¹ flow rate of gases was used.

A degradation temperature of 450 °C and a heating program shown in Fig. 3 was chosen based on our previous studies on thermal degradation of plastic. The plastic was rapidly heated by 10 °C min⁻¹ up to 360 °C, when HIPS degradation starts, then a slower heating of 5 °C min⁻¹ up to the final degradation temperature of 450 °C was used to avoid an excessive increase of reaction rate. Practically, oil products started to accumulate in the cylinder about 40 min from the beginning of experiments when temperature inside reactor was around 380 °C, and about 70% of oil volume was collected before reaching 450 °C. A powder on the cold walls of reactor was observed for ammonia treatment. The powder adsorbed a part of the oil product, therefore vacuum filtration was necessary to separate solid and liquid. Light compounds from the oil that evaporated during vacuum filtration could not be recovered and were classified as loss; however they can be counted as oil in the mass balance. Small amounts of powder fell to the bottom of reactor and contaminated the residue.

Analysis procedure

The Br content in the aqueous solution from the water trap was measured using an ion chromatograph (DIONEX, DX-120 Ion Chromatograph). The Br content in the solid residue, powder and oils was determined by combusting about 10 mg material in a Pyrex combustion flask, adsorbing the gaseous products in 25 mL of water containing H₂O₂ (0.3 mL), and analyzing the solution by ion chromatography. Qualitative and quantitative analyses of liquid products were performed by gas chromatographic analysis using various types of detectors (GC-AED: HP G2350A, GC-MSD: HP5973). Details on the analysis parameters were presented elsewhere.¹⁰

Conclusions

Ammonia treatment at 450 °C is an attractive method to remove bromine from flame-retardant high impact polystyrene (HIPS-Br). This debromination method allows the recovery of 60–70 wt% of the organic content as liquid products rich in benzene derivatives and suitable for feedstock recycling. Simultaneously more than 90 wt% Br can be recovered as inorganic NH₄Br powder. Ammonia treatment is simpler than catalytic upgrading of the degradation oil that requires dehalogenation of the gaseous products from regeneration of deactivated catalyst or sorbent. Also ammonia treatment has less environmental impact as it concentrates the bromine into an inorganic solid form that is easy to handle compared to gaseous emissions. Ammonia traps the Br radicals formed by thermal debromination of the flame retardant, and hence it suppresses the secondary reactions leading to SbBr₃ and alkyl- or phenylalkyl- bromides in liquid products. However, ammonia can not remove the aromatic bromine that remained as flame retardant fragments in our experimental conditions. It seems that more severe degradation conditions are necessary for total debromination of the flame retardant in order to produce “green” bromine-free degradation oil by ammonia treatment.

Acknowledgements

The authors gratefully acknowledge the Japan Society for the Promotion of Science for supporting M. Brebu by JSPS post-doctoral fellowship No. P04706. Financial support from MEXT Japan, on subject No. 15651031 (Houga) is appreciated. We are grateful to Dr Emma Jakob for support in analysing GC-MSD data, to Prof. Jun Takada for help with XRD analysis and to Dr Cornelia Vasile, Dr Akinori Muto and Dr Thallada Bhaskar for their valuable discussions.

References

- 1 M. R. Reich, *Am. J. Public Health*, 1983, **73**, 302–313.
- 2 K. Kay, *Environ. Res.*, 1977, **13**, 74–93.
- 3 A. Tohka and R. Zevenhoven, *Processing Wastes and Waste-Derived Fuels Containing Brominated Flame Retardants*, Final Report TKK-ENY-7, Espoo, 2002.
- 4 C. A. de Wit, *Chemosphere*, 2002, **46**, 583–624.
- 5 H. Hakk and R. J. Letcher, *Environ. Int.*, 2003, **29**, 801–828.
- 6 R. Weber and B. Kuch, *Environ. Int.*, 2003, **29**, 699–710.
- 7 R. Luijk, H. Wever, K. Olie, H. A. J. Govers and J. J. Boon, *Chemosphere*, 1999, **23**, 1173–1183.
- 8 Proposal for a directive COM (2000) 347 – C5-0415/2000 – 2000/0159(COD).
- 9 M. Brebu, T. Bhaskar, K. Murai, A. Muto, Y. Sakata and M. A. Uddin, *Fuel*, 2004, **83**, 2021–2028.
- 10 M. Brebu, T. Bhaskar, K. Murai, A. Muto, Y. Sakata and M. A. Uddin, *Chemosphere*, 2004, **56**, 433–440.
- 11 T. Bhaskar, T. Matsui, M. A. Uddin, J. Kaneko, A. Muto and Y. Sakata, *Appl. Catal., B*, 2003, **43**, 229–241.
- 12 E. Jakob, M. A. Uddin, T. Bhaskar and Y. Sakata, *J. Anal. Appl. Pyrolysis*, 2003, **68–69**, 83–99.
- 13 T. Bhaskar, T. Matsui, J. Kaneko, M. A. Uddin, A. Muto and Y. Sakata, *Green Chem.*, 2002, **4**, 372–375.
- 14 T. Bhaskar, K. Murai, M. Brebu, T. Matsui, M. A. Uddin, A. Muto and Y. Sakata, *Green Chem.*, 2004, **4**, 603–606.
- 15 M. Brebu, T. Bhaskar, K. Murai, A. Muto, Y. Sakata and M. A. Uddin, *Polym. Degrad. Stab.*, 2005, **87**, 225–230.
- 16 A. Hornung, A. I. Balabanovich, S. Donner and H. Seifert, *J. Anal. Appl. Pyrolysis*, 2003, **70**, 723–733.
- 17 A. Hornung, S. Donner, A. Balabanovich and H. Seifert, *J. Clean. Prod.*, 2005, **13**, 525–530.
- 18 M. A. Uddin, T. Bhaskar, T. Kusaba, K. Hamano, A. Muto and Y. Sakata, *Green Chem.*, 2003, **5**, 260–263.
- 19 M. Brebu, T. Bhaskar, A. Muto and Y. Sakata, *Chemosphere*, 2006, **64**, 1021–1025.
- 20 I. Okajima, T. Sugeta and T. Sako, *Kobunshi Ronbunshu*, 2001, **58**, 692–696.
- 21 J. Vehlow, B. Bergfeldt, H. Hunsinger, K. Jay, F. E. Mark, L. Tange, D. Drohmann and H. Fisch, *Recycling of Bromine from Plastics Containing Brominated Flame Retardants in State-of-the-art Combustion Facilities*, Technical report from APME, Brussels, 2001.
- 22 M. Uchida, M. Furusawa and A. Okuwaki, *J. Hazard. Mater.*, 2003, **A101**, 213–238.
- 23 K. Mackenzie and F. D. Kopinke, *Chemosphere*, 1996, **33**, 2423–2430.
- 24 M. P. Luda, G. Camino, A. I. Balabanovich and A. Hornung, *Macromol. Symp.*, 2002, **180**, 141–151.
- 25 M. Blazsó, Zs. Czégény and Cs. Csoma, *J. Anal. Appl. Pyrolysis*, 2002, **64**, 249–261.
- 26 M. P. Luda, N. Euringer, U. Moratti and M. Zanetti, *Waste Manage.*, 2005, **25**, 203–208.
- 27 B. Hinz, M. Hoffmocker, K. Pohlmann, S. Schaedel, I. Schimmel and H. Sinn, *J. Anal. Appl. Pyrolysis*, 1994, **30**, 35–46.
- 28 K. Murata, Y. Hirano, Y. Sakata and M. A. Uddin, *J. Anal. Appl. Pyrolysis*, 2002, **65**, 71–90.

Limiting thermodynamic efficiencies of thermochemical cycles used for hydrogen generation

B. C. R. Ewan* and R. W. K. Allen

Received 27th January 2006, Accepted 24th July 2006

First published as an Advance Article on the web 23rd August 2006

DOI: 10.1039/b601361a

Thermochemical cycles can provide a transformation mechanism for highly endothermic reactions at moderate temperatures and worthwhile yields but without the generation of waste streams. These have a general applicability but have been predominantly used for energy transformation from heat to stored chemical free energy in the form of hydrogen, with a view to a future hydrogen economy. Thermal efficiency is a key parameter in such a transformation, and the study presents a simple methodology for the determination of the limiting efficiency available, for the purpose of decision making in further cycle implementation and to develop consistency with other heat-to-work processes. The method is applied to 21 previously reported cycles, for which no such efficiency information has been reported, and discusses the features of the cycles which give rise to high and low efficiencies.

Introduction

The present revival in interest in thermochemical cycles (TC's) as a means of producing hydrogen reflects the increasing expectation of the contribution which 'CO₂-free' sources of process heat will make to a hydrogen economy. This includes, in particular, heat from solar furnaces and high temperature nuclear reactors, where heat will be available at temperatures in the range of 1200–1700 K. Thermochemical cycles offer the potential of providing the cleanest chemical route to hydrogen by the creation of a completely closed set of reactions with input and output material streams being only water and H₂/O₂ gases respectively.

Recent re-assessments of the broad range of possible cycles first proposed in the 1980s has generated a number of publications which present flowsheet improvements for existing processes as well as additional cycles for consideration. In all of these, the thermodynamically calculated overall process efficiency is a key parameter. Unfortunately, there remains considerable variability in the way in which this parameter is defined. Variations in process flowsheets and a lack of consistency in the way in which process efficiency is calculated can lead to significant uncertainties over the relative values of different cycles and makes comparison difficult. This suggests that adoption of a more consistent approach would be useful in order to enable a strategic view to be taken of the potential contribution of TC's to future energy scenarios.

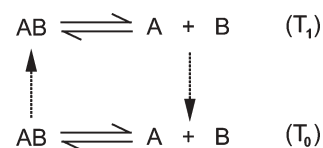
The value of a Carnot efficiency for determining the limiting efficiency of a thermal process producing work is taken for granted in power engineering and a similar approach for TC's would aid in the assessment of the maximum, or ideal, efficiency achievable, assuming perfect implementation. Any subsequent flowsheet variations will mean a performance drop from this ideal value. The present work sets out a basis for

representing such ideal efficiencies, based on a step by step examination of each stage of the cycle in terms of its free energy change and heat requirements. The maximum thermodynamically allowed internal heat transfer is used to minimise external heat input and an overall efficiency is calculated based on the residual free energies and heat requirements, including the recombination of hydrogen and oxygen.

In this way, the thermochemical cycle is viewed as a mechanism for converting heat into work, as represented by the combination of stored chemical free energy and any additional work which the intermediate reactions can produce. The examination of the maximum theoretical efficiency of cycles in this way provides a useful starting point for any comparison between cycles and also allows identification of the strengths and weaknesses within cycles.

Carnot efficiency equivalence

For the simplest cycle, this consists of an endothermic thermal decomposition at high temperature (T_1) combined with a work recovery step at low temperature (T_0).



For the reactions from left to right, assuming to a first approximation that enthalpy and entropy changes are independent of temperature, the overall Gibbs free energy change for reactants and products at their reference condition, is

$$\Delta G_{\text{overall}} = (\Delta G_1 - \Delta G_0) = (T_0 - T_1)\Delta S \quad (1)$$

i.e. the cycle will provide work output ($\Delta G_{\text{overall}} = -ve$) if ΔS for the decomposition is a +ve quantity. In this case ΔG at the

Department of Chemical & Process Engineering, University of Sheffield, Mappin St, Sheffield, UK S1 3JD. E-mail: b.c.ewan@sheffield.ac.uk

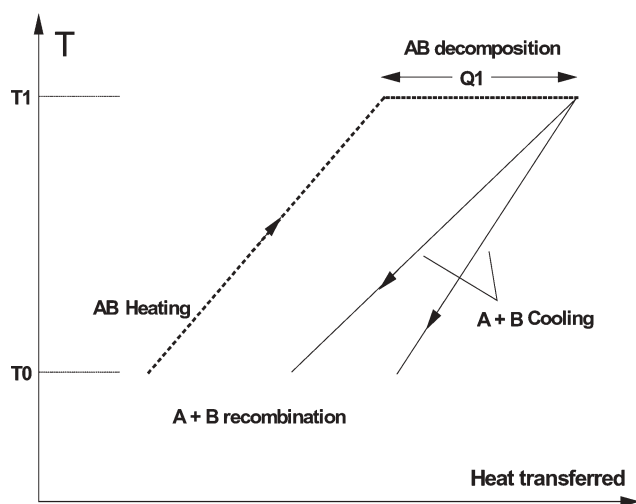


Fig. 1 Heating and cooling behaviour for simple AB decomposition.

higher temperature is numerically lower, becoming zero at the decomposition temperature.

The heat balance for a simple AB decomposition can be usefully represented on a pinch diagram as shown in Fig. 1. Here it is assumed that the specific heats for AB heating and A + B cooling are independent of temperature.

The possibility for internal heat balancing is represented by two possible product cooling lines, showing both a shortfall in cooling heat with respect to the heating line and an excess of cooling heat leading to heat rejection. When standard states are used to represent the free energy and enthalpy changes, the work efficiency for the cycle is given by:

$$\eta = -\frac{\Delta G_{\text{overall}}}{Q} = \frac{\Delta G_0^{\circ} - \Delta G_1^{\circ}}{Q1 + \text{heat mismatch}} \quad (2)$$

where $Q1$ is the heat input at decomposition and 'heat mismatch' represents the heat transfer shortfall between A + B cooling and AB heating.

In the special case where the specific heat functions of products and reactants are identical, *i.e.* $C_p(\text{A} + \text{B}, T) = C_p(\text{AB}, T)$, then both the entropy changes and enthalpy changes are independent of temperature and exact heat matching results.

In this case, $\Delta H_0^{\circ} = \Delta H_1^{\circ}$ and $\Delta S_0^{\circ} = \Delta S_1^{\circ}$ and the efficiency then becomes:

$$\eta = \frac{\Delta G_0^{\circ} - \Delta G_1^{\circ}}{\Delta H_1^{\circ} - \Delta G_1^{\circ}} = \frac{\Delta H_0^{\circ} - T_0 \Delta S_0^{\circ} - \Delta H_1^{\circ} + T_1 \Delta S_1^{\circ}}{T_1 \Delta S_1^{\circ}} = 1 - \frac{T_0}{T_1} \quad (3)$$

For this special case, heat is added only at the upper temperature T_1 , and such simple cycles can provide the Carnot efficiency for converting heat into chemical free energy.

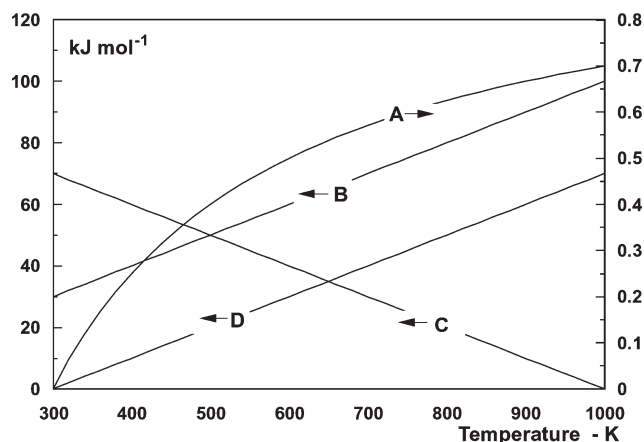


Fig. 2 Variation of heat, work and efficiency with temperature for cycle with matched heating and cooling load. A = η , B = Q , C = ΔG_1 , D = $\Delta G_0 - \Delta G_1$.

Fig. 2 shows the variation of the parameters of eqn 3 with temperature for the hypothetical case of a system with $\Delta H = 100 \text{ kJ mol}^{-1}$ and $\Delta S = 100 \text{ J (mol K)}^{-1}$.

As a result of the entropy and enthalpy independence with temperature, the cycle will provide the Carnot efficiency throughout the temperature range. At the decomposition temperature (1000 K), $\Delta G_1 = 0$ and only heat is required to effect the conversion of 1 mol of reactants to products at the standard state.

Several decompositions of simple molecules approximate quite closely to this condition as shown for some examples in Table 1. In these cases, $T_0 = 298 \text{ K}$ and Q is the greater of ΔH_0° and ΔH_1° .

Maximum efficiency methodology

Since thermochemical reactions form a closed set, comparison of the work efficiency for different cycles can usefully be assessed by referring the reactants and products to the standard state of 1 bar pressure for each of the steps in a cycle. This is equivalent to equating the total work produced as the algebraic sum of the standard free energy changes for each reaction, excluding any separation work. Due to the closed nature of the system, species have a dual identity as both a reactant and product, and therefore changing a species' initial or final pressure will produce additional work terms which cancel due to their having opposite signs, resulting in

$$\Delta G_{\text{overall}} = \sum_k^{\text{reactions}} \Delta G_k^{\circ} \quad (4)$$

This also applies to the generation of hydrogen at higher pressures, which will require an additional amount of work,

Table 1 Comparison of cycle and Carnot efficiencies for some simple decompositions based on the decomposition temperature

Decomposition species	$\Delta H_1^{\circ}/\text{kJ}$	$\Delta H_0^{\circ}/\text{kJ}$	$\Delta G_0^{\circ}/\text{kJ}$	T_1/K	η/Carnot	$\Delta G_0^{\circ}/Q$
$\text{SO}_3 \rightarrow \text{SO}_2 + \frac{1}{2}\text{O}_2$	97.3	98.9	70.9	1055	0.717	0.716
$\text{H}_2\text{O} \rightarrow \text{H}_2 + \frac{1}{2}\text{O}_2$	251.2	241.8	228.5	4346	0.931	0.909
$\text{CO}_2 \rightarrow \text{CO} + \frac{1}{2}\text{O}_2$	271.0	282.9	257.29	3340	0.911	0.908
$\text{CaCO}_3 \rightarrow \text{CaO} + \text{CO}_2$	165.8	178.2	130.5	1160	0.743	0.732

which will become available again on recombination with oxygen.

For the simple cycle depicted above, the operation of the decomposition at a temperature where $\Delta G_1^{\circ} = 0$, is particularly useful since no external work is required to take the reactants to products at the standard state defined. As part of the objective of comparing the ability of a number of thermochemical cycles to convert heat into work, an initial approach has been taken to establish the maximum efficiency possible for these. Since the underlying interest is in the use of heat to effect chemical changes, for reactions involving +ve values for both ΔH and ΔS , an operating temperature is chosen which results in $\Delta G^{\circ} = 0$, thus limiting any additional work required to bring the products to standard pressure. In some cases, the reaction temperature chosen in this way would exceed those of practical process conditions, and therefore an upper limit operating temperature of 1700 K has been imposed for all cycles. For those endothermic reactions with -ve values for ΔS , the quoted literature value for the operating temperature has been chosen. Literature values for the operating temperature have also been chosen for any exothermic reactions in a cycle.

The main features of the analysis are described as follows:

1. Each cycle is closed and includes the recombination of the H_2 and O_2 produced to liquid water at the standard state (1 bar) and at 298 K.

2. Reactions involving only heat inputs are carried out under equilibrium conditions and temperatures are chosen to satisfy $\Delta G^{\circ} = 0$, when possible, subject to a limit temperature of 1700 K.

3. Heat balancing is carried out between all of the heating and cooling branches of the process, with the constraint that the heat transfer temperature difference ΔT is greater than or equal to zero.

4. Enthalpy changes are calculated using the HSC 5.1 chemistry package.¹ Enthalpy and entropy values for some species have been updated in the database where necessary from published sources.

5. Efficiency is calculated through a combination of the work terms arising within the cycle and the total heat added.

The work components of the cycle are the Gibbs free energy changes for each of the fundamental steps required to complete the cycle, and are taken as:

(a) Free energy work available from recombination, at the standard state and 298 K, of $H_2/1/2 O_2$ produced by the cycle ($\Delta G_{298}^{\circ}(H_2/O_2)$). This is taken as $-237 \text{ kJ} (\text{mol } H_2)^{-1}$.

(b) Free energy work available from certain reactions within the set at the standard state, characterised by -ve ΔG° values, $\Delta G^{\circ}(-)$

(c) Free energy work consumed by certain reactions within the set at the standard state, characterised by +ve ΔG° values, $\Delta G^{\circ}(+)$

(d) Free energy work associated with the separation of reaction products. This is calculated as the negative of the mixing free energy

$$\Delta G_{\text{sep}} = -R T \sum_i n_i \ln(x_i) \quad (5)$$

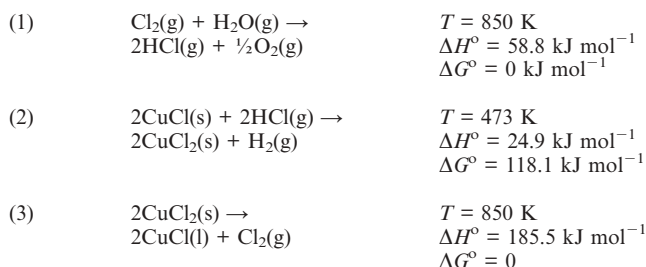
where n_i and x_i are the number of moles and mole fraction of species i in the mixture respectively. This is a +ve quantity, consistent with the sign of the other work terms.

In representing an efficiency (η) for the cycle, all free energy components providing output work, $\Delta G^{\circ}(-)$ and $\Delta G_{298}^{\circ}(H_2/O_2)$, and consuming input work, $\Delta G^{\circ}(+)$ and $\Delta G_{\text{sep}}^{\circ}$, are considered equivalent. The efficiency thus becomes defined by:

$$\eta = \frac{[\Delta G_{298}^{\circ}(H_2/O_2) + \sum \Delta G^{\circ}(-) + \sum \Delta G^{\circ}(+) + \sum \Delta G_{\text{sep}}^{\circ}]}{\text{heat input}} \quad (6)$$

It is noted that the above definition of efficiency differs from those often used in the thermochemical cycle literature where the HHV of hydrogen is frequently used in the numerator and any work capability of some reactions ($\Delta G^{\circ}(-)$) is ignored. In some cases eqn 6 may be a less generous definition, although it is believed that it provides consistency for comparisons with the normal calculation of a Carnot efficiency.

The representation of a cycle by a series of elementary steps is demonstrated for the case of the US Chlorine cycle,² which involves the following three reactions:



The elementary steps required to evaluate a limiting efficiency are shown in Fig. 3.

Reaction (2) has a negative value for ΔS and therefore does not provide the possibility of equilibrium at the standard state

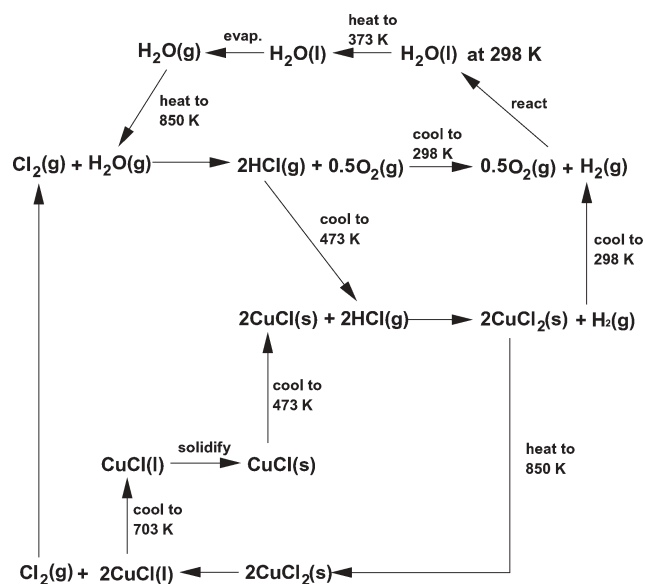


Fig. 3 US Chlorine cycle for hydrogen production.

Table 2 Steps required to complete the US Chlorine cycle

Step no.	US Chlorine cycle	T_0/K	T_1/K	$\Delta G^\circ/kJ$	Q_{\pm}/kJ
1	$Cl_2(g) + H_2O(g) \rightarrow 2HCl(g) + \frac{1}{2}O_2(g)$ 2HCl and $\frac{1}{2}O_2$ separation at 473 K	850	850	0 4.92	58.8
2	$2CuCl_2 \rightarrow 2CuCl(l) + Cl_2(g)$	850	850	0	185.5
3	$2CuCl_2(s) \rightarrow 2CuCl_2(s)$	473	850		62.46
4	$H_2O(l) \rightarrow H_2O(l)$	298	373		7.5
5	$H_2O(l) \rightarrow H_2O(g)$	373	373		40.9
6	$H_2O(g) \rightarrow H_2O(g)$	373	850		17.5
7	$2CuCl(l) \rightarrow 2CuCl(l)$	850	703		-17.8
8	$2HCl(g) \rightarrow 2HCl(g)$	850	473		-22.54
9	$2CuCl(l) \rightarrow 2CuCl(s)$	703	703		-14.2
10	$2CuCl(s) \rightarrow 2CuCl(s)$	703	473		-55.7
11	$\frac{1}{2}O_2(g) \rightarrow \frac{1}{2}O_2(g)$	850	298		-17.5
12	$2CuCl + 2HCl(g) \rightarrow 2CuCl_2 + H_2(g)$	473	473	118.1	-93.2
13	$H_2(g) \rightarrow H_2(g)$	473	298		-5.0

for reactant and products, resulting in a positive ΔG value in the temperature range of interest.

Table 2. summarises the individual steps representing the operation of the cycle. T_0 and T_1 define the starting and finishing temperatures of each step, ΔG° represents the standard Gibbs free energy change for the reactions and any work required to separate components for a further reaction step, and Q_{\pm} is the heat change involved with the step (+ve when heat is added). Separation work terms are not included when reaction products exist in different phases. All of the thermochemical cycles considered are dealt with in the same way, *i.e.* heating, reaction, phase change and cooling.

For each cycle it is confirmed that an overall energy balance is satisfied, *i.e.*,

$$\sum_i \Delta G_i^\circ(\text{reactions}) = \sum_i Q_i$$

This also includes the reaction free energy and additional heat rejected at 298 K when the hydrogen and oxygen are recombined ($-48.6 \text{ kJ mol}^{-1}$). For an efficiency calculation, it is necessary to know the overall heat input requirement and this is evaluated on the basis of the maximum possible heat transfer from the cooling side to the heating side of the process. This is most easily calculated using a pinch diagram for each of the cycles. These are constructed for the limiting case of a heat transfer temperature difference $\Delta T = 0$ degrees, and refer to the production of 1 mol of H_2 . The pinch diagram for the US Chlorine cycle corresponding to Table 2 is shown in Fig. 4.

Results and discussion

A number of preferred thermochemical cycles, aimed at hydrogen generation, were identified by Brown *et al.*³ on the basis of a range of performance measures, and these cycles have since been the focus of attention for workers in the field. Efficiency was excluded from such measures due to a lack of published data, and this is now addressed using the framework described above for most of the cycles originally selected.

The operating conditions and thermodynamic parameters at the standard state for each reaction considered are collected together in Table 3.

In the same way as described for the US Chlorine cycle above, a detailed heating and cooling scheme for the cycles of Table 3 has been derived, based on the needs of individual

species involved, transforming from products of one reaction to reactants of another. The pinch diagram for each of these enables the minimum heat input and heat rejection to be determined.

The representation of the cycle efficiencies is concerned specifically with the ability of cycles to produce work in the form of chemical free energy from a heat source. The principal component of the free energy produced is the H_2/O_2 recombination energy, which however, carries the same importance as other $\Delta G^\circ(-)$ and $\Delta G^\circ(+)$ terms in eqn 6. The efficiency therefore represents that of the cycle as a whole, and the calculated values can only be used to represent maximum 'hydrogen production efficiencies' when the additional ΔG terms (+ve and -ve) are coupled with one another, through choice of process conditions, or with the hydrogen generation process. The equivalence of such ΔG terms with that of the $\Delta G_{298}^\circ(H_2/O_2)$ term ensures that when such coupling is achieved, the calculated maximum efficiency value for the cycle can be used to represent the efficiency for hydrogen production. One such example of coupling would be to operate $\Delta G^\circ(-)$ reactions at high product partial pressures and $\Delta G^\circ(+)$ reactions, involving the same gaseous species, at high reactant partial pressure.

The examination of the simple cycle of Fig. 1 indicates that good matching of heating and cooling, combined with overall

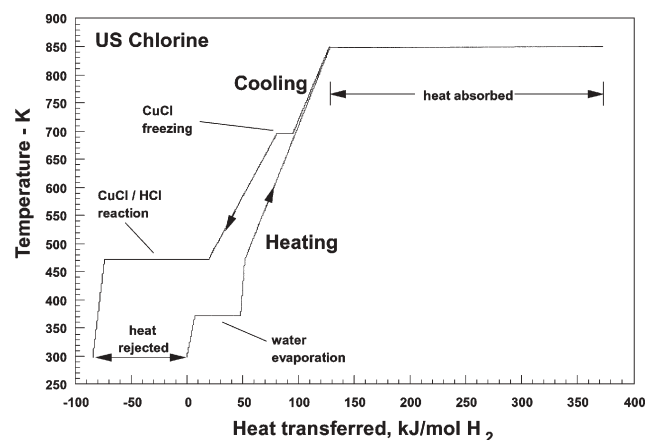


Fig. 4 Pinch diagram for US Chlorine cycle (excluding H_2/O_2 recombination).

Table 4 Principal heat and work components of the cycles. (Nett work input excludes H₂/O₂ recombination work)

Cycle No.	Process	Heat input/kJ (mol H ₂) ⁻¹	Heat rejection/kJ (mol H ₂) ⁻¹	Nett work input/kJ (mol H ₂) ⁻¹	η
1	Ispra Mark 1C	354.3	108.6	-9.0	0.69
2	Ispra Mark 7A	480.6	143.6	-84.2	0.67
3	Vanadium chloride	415.5	144.6	-33.6	0.65
4	Univ Aachen 1972	387.0	138.6	-9.15	0.64
5	Ispra Mark 4	174.4	63.8	129.7	0.62
6	Westinghouse	246.0	84.8	87.7	0.61
7	Nickel ferrite	249.3	76.6	97.7	0.56
8	Zinc oxide	341.7	143.1	47.3	0.56
9	Ispra Mark 9	476.6	208.6	-13.3	0.53
10	Sulfur-iodine	192.0	85.6	179.3	0.51
11	Julich EOS	483.6	243.6	4.3	0.48
12	Hallett 1965	92.1	54.6	194.0	0.47
13	US Chlorine	258.9	132.6	123.0	0.44
14	Ispra CO/Mn ₃ O ₄	104.3	48.6	192.6	0.43
15	Ispra Mark 3	91.5	48.6	199.0	0.42
16	LASL U	321.9	186.6	102.1	0.42
17	UT-3	375.5	160.0	94.0	0.38
18	Ispra Mark 6C	516.8	346.6	73.3	0.32
19	Ispra Mark 6	272.0	235.6	153.8	0.31
20	Ispra Mark 7B	337.7	196.6	135.8	0.30
21	Gaz de France	219.8	303.6	319.6	0

heat addition at the maximum temperature will maximise the cycle efficiency.

For an ideal cycle this is also associated with the minimum heat rejection but may involve additional work input, which acts to reduce the heat requirement, thus having little effect on the efficiency. Real cycles with multiple reactions include several phase changes, as products undergo the necessary temperature transitions to their next reaction. Maintaining efficiency for these requires that such steps permit heat transfer from the cooling to the heating side. Where process conditions exclude this possibility, large heat rejection and efficiency losses can result.

Heat rejection can also result from -ve entropy changes for one or more reaction steps and, while this may be matched by a heat absorption transition, thus benefiting the system heat balancing, such a heat rejection is associated with the input of work to the system. Such $\Delta G^{\circ}(+)$ terms reduce the magnitude of the numerator in the efficiency estimation and are a primary factor in lowering the efficiency for some of the cycles presented. Heat rejection due to phase changes, however, are associated with equilibrium processes for which $\Delta G = 0$ and their effect on efficiency depends only on the extent to which the heating curve can absorb the rejected heat.

Table 4 presents the calculated efficiencies for the cycles of Table 3 as well as the aggregated heat input, output and work input terms.

Heat input represents the nett input after the maximum allowable internal heat balancing. Heat rejection is the unavoidable expelled heat from the system including that from H₂/O₂ recombination to complete the cycle. The work input is the algebraic sum of the $\Delta G^{\circ}(+)$, $\Delta G^{\circ}(-)$ and ΔG_{sep} terms. This excludes the main work output term of the cycle (*i.e.* $\Delta G_{298}^{\circ}(\text{H}_2/\text{O}_2)$) and provides an indication of (a) the extent to which the nett work output of the cycle arises from the other reactions and (b) the need for external work input to the cycle. In principle, when this latter term is +ve, a proportion of the available hydrogen free energy should be recycled and coupled to the system reactions.

Table 4 orders the cycles in terms of maximum efficiency, and the underlying reasons for high or low efficiency provide some insight into the necessary attributes of cycles for design purposes.

Examination of the top group of cycles (1–6) indicates that heat rejection is around 1/3 of the nett heat input. The higher the effective temperatures at which heat is input is achieved, the greater will be the efficiency which can finally be achieved, and for the top two cycles, when the maximum heat balancing has been applied, this is in the range 1400–1573 K and 1000–1450 K. For cycles 3–6 these range from 1200–1300 K down to 600–1000 K. For cycles 1–4 there is also some nett work produced in addition to the H₂/O₂ recombination work, indicating that some useful work is produced from the higher heat inputs associated with these cycles. For cycles 5 and 6 there is a nett work input, but a corresponding reduction in heat input, indicating that the input work is contributing to enthalpy increase within the system, rather than heat rejection.

The low efficiencies for the bottom group (16–21) can be rationalised in a similar way. The nett heat input range for cycle 16 is lower at 440–950 K and for cycles 17–21 the range is 850–1100 K. This latter range suggests the possibility of good efficiencies, however, for these cycles, large work inputs reduce the overall work outputs of the cycles, and these are associated with correspondingly large heat rejection stages. These can be identified with one or more unfavourable reactions, with large, -ve entropy changes. In the worst case for cycle 21, the overall work output is -ve, including H₂/O₂ recombination work, resulting in zero efficiency. This can be traced to the K₂O decomposition and K/KOH reactions, where the equilibrium lies strongly to the left.

The above approach has a number of features which are useful in making comparisons among thermochemical cycles and with other heat-work processes. Some of these include:

- an evaluation, without the use of process flowsheeting, of the maximum or ideal thermal efficiency which a cycle can provide.

- an indication of the relative contributions of the hydrogen and non-hydrogen related work terms to the overall efficiency. This is particularly relevant when cycles are being viewed as production routes for hydrogen.

- the provision of a starting point for process optimisation, identifying the main geometrical needs for heat transfer. This becomes important in specifying system design and layout to enable the prescribed heat transfer.

- assessment of the relative efficiencies of heat–electricity cycles and thermochemical cycles for use with hybrid cycles. This provides useful information on the contribution which the electrical conversion step makes to overall thermochemical cycle efficiency.

- the basis for improvement of existing cycles through chemicals selection and better positioning of isothermal heat processes.

Whilst the procedure described sets out to determine the maximum efficiencies available, it does not deal with the practical difficulties and new challenges in realising these.

Examination of Table 3 for the highest efficiency cycles indicates that some of this derives from $\Delta G(-)$ terms, and work must therefore be extracted from these to realise the efficiency indicated.

In some cases this may be set directly against $\Delta G(+)$ terms, e.g. through the operation pressure for a common gas species, or by means of an established electrochemical pathway for electricity generation, which can then be coupled to hydrogen generation.

In other cases, no clear work production pathway or coupling route is evident, an example being the solid reaction of $\text{CuBr}_2\text{--CaO}$ in Cycle 1.

Fuel cells and a new range of membrane technologies provide new opportunities in these areas e.g. $\text{H}_2\text{--O}_2$ fuel cells for electrical input to hybrid cycles and reverse concentration cells for electrochemical pumping and separation, and therefore new fuel cell combinations and ion transport media may eventually provide implementation routes for those cycles involving ‘difficult’ reactions. A number of practical design features also limit achievable efficiencies,^{12–14} examples being:

- the need for finite approach temperatures in heat transfer equipment (in contrast to a $\Delta T = 0$ condition)

- the overall thermal efficiency arising from electrical pumping to raise product pressures. This may involve thermal to electrical efficiencies of 40% and pump mechanical efficiencies of 70%.

- large energy losses arising from separations, an example being the use of phosphoric acid to break the $\text{HI--H}_2\text{O}$ azeotrope in cycle 10.

- the use of excess solvents to improve reaction conversions. The use of solvation energy can improve product yield but at the expense of subsequent separation energy.

Conclusion

The aim of the analysis has been to provide a method which yields the best achievable efficiency, as a basis for decision making on the value of further study.

In addition, in view of the importance of the thermal efficiency parameter in judging the value of heat–work processes, the procedure for thermochemical cycles has sought to define their efficiency in such a way that their limiting efficiency can tend to the Carnot value in the same way as for other thermal processes. This consistency is particularly important when comparisons are made with other heat utilisation processes, such as electricity generation by different routes, and overcomes definitions involving the higher and lower heating values for hydrogen (hhv, lhv) such as the following:

$$\eta = \frac{\Delta H(\text{hhv})}{Q(\text{per mol H}_2)} \quad , \quad \eta = \frac{\Delta H(\text{lhv})}{Q(\text{per mol H}_2)} \quad ,$$

$$\eta = \frac{\Delta H(\text{hhv})}{Q(\text{per mol H}_2) + \text{Elect.work}/\eta_{\text{el}}}$$

where η_{el} is the thermal to electrical conversion efficiency for electricity generation, assuming that work input terms can be achieved using an electrochemical process.

This simple, but useful approach may encourage others to review some of the many other cycles which have been identified for hydrogen production, from a limiting efficiency perspective, and re-evaluate their feasibility.

References

- 1 HSC Chemistry v 5.1, Outokumpu Research, Finland, 2002.
- 2 L. O. Williams, *Hydrogen Power*, Pergamon, 1980.
- 3 J. H. Norman, G. E. Besenbruch, L. C. Brown, D. R. O’Keefe and L. C. Allen, General Atomics Final Report GA-A16713, May 1982.
- 4 L. E. Brecher, S. Spewock and C. J. Warde, *Int. J. Hydrogen Energy*, 1977, **2**, 7–15.
- 5 H. Engels and K. F. Knoche, Vapor pressures of the system $\text{HI}/\text{H}_2\text{O}/\text{I}_2$ and H_2 , *Int. J. Hydrogen Energy*, 1986, **12**(11), 703–707.
- 6 C. E. Bamberger, *Cryogenics*, 1978, **18**, 170–183.
- 7 A. Steinfeld, *Int. J. Hydrogen Energy*, 2002, **27**(6), 611–619.
- 8 K. F. Knoche and P. Schuster, *Int. J. Hydrogen Energy*, 1984, **9**, 457–472.
- 9 G. E. Beghi, *Int. J. Hydrogen Energy*, 1986, **11**, 761–771.
- 10 Y. Tamaura, A. Steinfeld, P. Kuhn and K. Ehrensberger, *Energy*, 1995, **20**(4), 325–330.
- 11 J. K. Funk and R. M. Reinstorm, *Ind. Eng. Chem. Proc. Des. Dev.*, 1966, **5**, 336–342.
- 12 M. Sakurai, E. Bilgen, A. Tsutsumi and K. Yoshida, *Sol. Energy*, 1996, **57**(1), 51–58.
- 13 E. D. Teo, N. P. Brandon, E. Vos and G. J. Kramer, *Int. J. Hydrogen Energy*, 2005, **30**, 559–564.
- 14 S. Goldstein, J.-M. Borgard and X. Vitart, *Int. J. Hydrogen Energy*, 2005, **30**, 619–629.

CO₂ absorption by aqueous NH₃ solutions: speciation of ammonium carbamate, bicarbonate and carbonate by a ¹³C NMR study

Fabrizio Mani,^{*a} Maurizio Peruzzini^b and Piero Stoppioni^a

Received 10th February 2006, Accepted 7th August 2006

First published as an Advance Article on the web 31st August 2006

DOI: 10.1039/b602051h

The absorption of CO₂ in aqueous NH₃ solutions occurs with high efficiency and loading capacity at room temperature and atmospheric pressure producing the ammonium salts of bicarbonate (HCO₃⁻), carbonate (CO₃²⁻), and carbamate (NH₂CO₂⁻) anions. ¹³C NMR spectroscopy at room temperature has been proven to be a simple and reliable method to investigate the speciation in solution of these three ionic species. Fast equilibration of HCO₃⁻/CO₃²⁻ anions results in a single NMR peak whose chemical shift depends on the relative concentration of the two species. A method has been developed to correlate the chemical shift of this carbon resonance to the ratio of the two anionic species. Integration of the carbamate carbon peak provided the relative amount of this species with respect to HCO₃⁻/CO₃²⁻ pair. No other species was detected in solution by ¹³C NMR, and no solid compounds separated out under our experimental conditions. Finally, the relative amount of HCO₃⁻, CO₃²⁻, and NH₂CO₂⁻ in solution have been correlated to the molar ratio between free ammonia in solution and absorbed CO₂.

Introduction

There is a growing consensus among the governments, scientists, and industrial organisations of the most developed countries about the threat of climate changes due to the greenhouse effect caused by the huge introduction of anthropogenic CO₂ in the atmosphere.^{1,2} A variety of strategies can be adopted to limit and reduce CO₂ emissions. These include improving the efficiency of energy production, substituting carbon rich fossil fuels, such as coal and oil, with natural gas and other energy sources, and developing technologies to capture CO₂ in view of reutilization and/or sequestration.³ Concerning this latter approach, there is a range of potentially attractive technologies for CO₂ capture based on physical⁴ and chemical absorption⁵ methods, cryogenic and membrane separation processes,⁶ and biological fixation.⁷ Chemical capture processes based on amine scrubbing have received particular attention.⁸ The method is currently utilized for CO₂ recovery from exhaust gases in US Navy submarines, in NASA space shuttles and, in pilot plants, for CO₂ separation in flue gases from power generation stations and refineries. Monoethanolamine (MEA) or other hindered amines are used as efficient absorbents.⁹ In this process, diluted CO₂ (5–15%) is chemically captured at low temperature and then released essentially pure at higher temperature, while the regenerated amine can be recycled for further CO₂ uptake. The method however suffers from several drawbacks, such as the high cost of chemicals due to amine degradation in the absorption–desorption cycles, the high corrosion of the technical equipment, the energy costs for the amine regeneration step, and the relatively low loading capacity of CO₂. Alternative inorganic

systems using sodium or potassium carbonates¹⁰ and aqueous ammonia^{11,12} as absorbents have been proposed. The ammonia scrubbing process provides the advantage of higher CO₂ loading capacity, no absorbent degradation problems and, therefore, lower material costs. However, although the process for regenerating the chemical absorbent needs a lower heat of reaction in comparison to amine technology, the regeneration of NH₃ by heating large volumes of dilute aqueous solutions and the separation of NH₃ from pure CO₂ are still highly energy consuming steps.

Speciation of the products which are formed in aqueous solution during the reaction between ammonia and carbon dioxide under different experimental conditions is of paramount importance to optimize the process in term of loading capacity, reaction temperature, and ammonia concentration. Several studies have been carried out on the capture of carbon dioxide by aqueous ammonia, and the results of either model calculations¹¹ or experimental investigations¹² have been reported.

Absorption and reaction kinetics occurring when CO₂ is absorbed into aqueous ammonia solutions are rather complex, and the speciation products have been poorly understood. Moreover, no satisfactory method has been so far described to rapidly evaluate the relative amount of the species occurring in the CO₂/NH₃/H₂O system.¹³

In this paper we report on the ¹³C NMR spectroscopic investigation of the species distribution which occurs during CO₂ absorption into aqueous ammonia at 293 K using different NH₃ concentrations and during the reaction progress. The results reported here indicate that ¹³C NMR spectroscopy provides a straightforward and reliable method to evaluate the reaction products between CO₂ and NH₃ in aqueous solution.

To the best of our knowledge, and in spite of the practical importance of this system, this kind of NMR study has never been carried out systematically on the CO₂/NH₃/H₂O system

^aUniversity of Florence, Department of Chemistry, via della Lastruccia, 3, 50019, Sesto Fiorentino, Firenze, Italy. E-mail: fabrizio.mani@unifi.it

^bICCOM CNR, via Madonna del Piano, 10, 50019, Sesto Fiorentino, Firenze, Italy

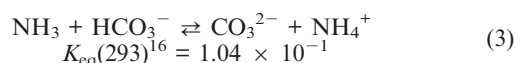
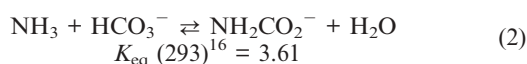
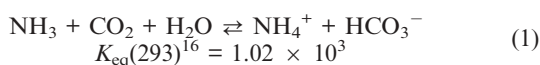
and only sparse results have reported on the ^{13}C NMR spectra of the solid compounds which form in the gaseous $\text{CO}_2/\text{NH}_3/\text{H}_2\text{O}$ reaction.¹⁴ The ^{13}C NMR analysis of D_2O solutions of ammonium carbonate and ammonium carbamate has been also reported.^{13a} Finally, speciation of the CO_2/amine aqueous systems has been reported by ^1H and ^{13}C NMR spectroscopy.¹⁵

Results and discussion

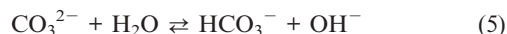
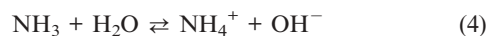
Speciation of the $\text{CO}_2/\text{NH}_3/\text{H}_2\text{O}$ systems

Our absorption experiments were carried out at 293 K using a glass absorber filled with 0.240 dm^3 of 2.50 M NH_3 (4.3% w/w) solution and equipped with a thermometer and a pH electrode. The flue gas was simulated by a mixture of 10% (v/v) CO_2 diluted with N_2 . During each absorption experiment the NH_3 solution was not circulated while the CO_2/N_2 gas mixture was continuously flowing at the bottom of the absorbent through a sintered glass diffuser until CO_2 absorption stopped. The flow of the gas mixture was maintained constant at the rate of $15\text{ dm}^3\text{ h}^{-1}$. As the reaction of CO_2 with aqueous NH_3 is exothermic, the absorber was immersed in a thermostatted water bath to keep the temperature constant. The outlet gas was dried by flowing through activated molecular sieves, anhydrous CaSO_4 and, finally, passed through a gas purification tower filled with P_2O_5 . The mass change of P_2O_5 allowed us to evaluate the amount of gaseous NH_3 that had escaped from the absorbing solution. In the whole series of experiments the loss of ammonia from the 2.50 M NH_3 absorbing solution never exceeded 1.3% (on a molar basis) at 293 K. For the entire duration of each absorption experiment, a sample of the solution (0.5 ml) was withdrawn from the absorber every hour at increasing amounts of absorbed CO_2 (a total of 7–8 samples were analysed) and checked by ^{13}C NMR spectroscopy. Changes of pH were also measured, and steadily decreasing values between 10.5 and 8.5 were recorded as more CO_2 was absorbed. At the lowest pH values no more than 15–20% of CO_2 is absorbed by the residual ammonia. Each absorption experiment was repeated in triplicate showing a high reproducibility of the results with changes in the percentage of each species never higher than 2 units during the different NMR experiments.

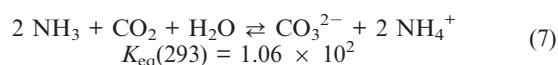
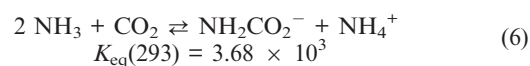
The reaction of the weak acid CO_2 ($K_a(293) = 4.08 \times 10^{-7}$)¹⁶ with the weak base NH_3 ($K_b(293) = 1.71 \times 10^{-5}$)¹⁶ in water is characterized by several chemical equilibria, which complicate representing the overall picture of the system. However, such complex thermodynamic behaviour can be much simplified by neglecting unimportant reaction equilibria featuring comparatively much smaller equilibrium constants. The main reactions to be taken into account when CO_2 reacts with aqueous ammonia are:



The pH of this system is, in part, controlled by the ammonia–ammonium and carbonate–bicarbonate buffers



The composition of the solution depends on the ratio between free NH_3 and absorbed CO_2 which, in turn, determines the pH of the solution. When the reaction occurs between comparable amounts of CO_2 and NH_3 , the equilibrium (1) prevails and ammonium bicarbonate is the main species in solution. The same is even more true when an excess of CO_2 is loaded into the solution. In contrast, an excess of NH_3 , with respect to the absorbed CO_2 , increases the amount of ammonium carbamate and, to a lesser extent, of carbonate according to reactions (2) and (3), respectively. If an excess of NH_3 is maintained in the system, the overall reactions can be rewritten as



Due to the very high solubility of the ammonium salts of carbonate ($320\text{ g dm}^{-3}\text{ H}_2\text{O}$),¹⁷ carbamate ($790\text{ g dm}^{-3}\text{ H}_2\text{O}$),¹⁷ and bicarbonate ($220\text{ g dm}^{-3}\text{ H}_2\text{O}$),¹⁷ no solid compound is expected to separate out under the present experimental conditions and, consequently, no heterogeneous equilibrium involving solid salts has to be taken into account in the present description of the aqueous CO_2/NH_3 system. As a matter of fact, no solid was found to separate out from these solutions under the adopted experimental conditions.

In order to evaluate the species present in solution, we recorded ^{13}C NMR spectra of several NH_3 solutions at increasing CO_2 loading and decreasing pH values. The ^{13}C NMR spectra of the investigated solutions are quite simple (Fig. 1) and exhibit two distinct resonances.

The signal at *ca.* 166 ppm is attributed to the carbamate ion, while the other resonance, slightly shifted to lower frequencies, in the range $165.23 \leq \delta \leq 161.50$, is ascribed to the carbon atoms of the carbonate and bicarbonate ions which are fast exchanging on the NMR time scale *via* proton scrambling. No detectable amounts of any other species was evident from inspection of the NMR spectra. Remarkably, while the NH_2CO_2^- carbamate resonance is practically unaffected by pH changes, the resonance due to the freely exchanging $\text{HCO}_3^-/\text{CO}_3^{2-}$ pair steadily moves high-field by decreasing the pH, *i.e.* by increasing the CO_2 absorption by the ammonia solution. As all the species in solution contain only one carbon atom and these are likely relaxing with comparable rates,¹⁸ the relative amounts of carbamate and of overall $\text{HCO}_3^-/\text{CO}_3^{2-}$ species may be reasonably determined by NMR integration of the corresponding signals. NMR integration of test spectra of solutions, prepared by dissolving in a known volume of D_2O weighted amounts of potassium carbonate, bicarbonate and carbamate, adds high confidence to this procedure showing that the integration of the NMR signals parallels the change in

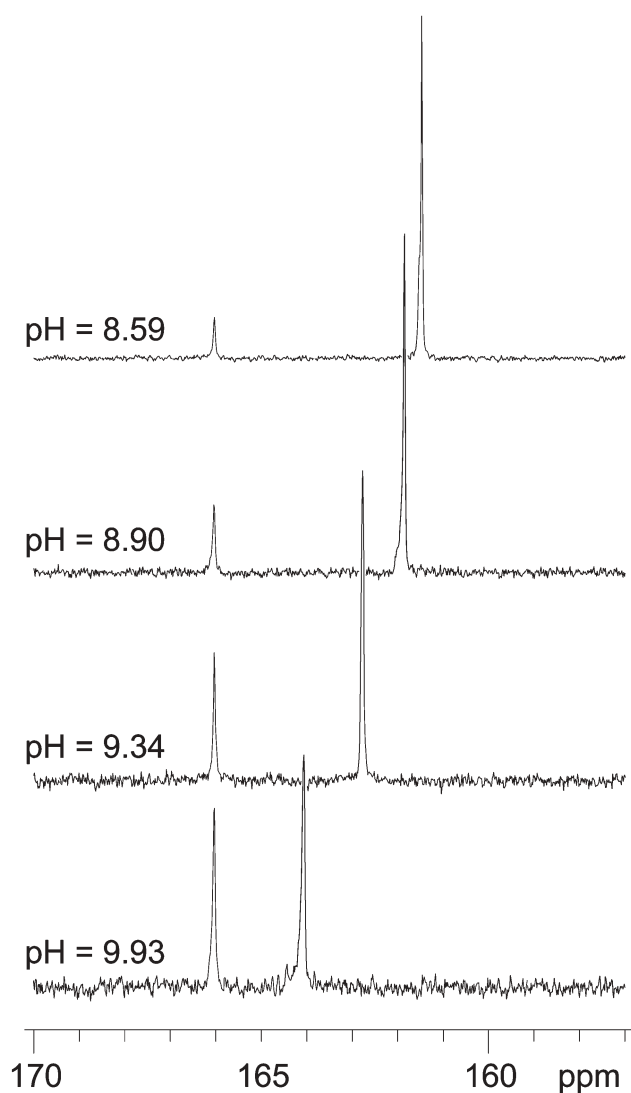
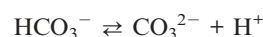


Fig. 1 ^{13}C NMR spectra showing the NH_2CO_2^- and $\text{HCO}_3^-/\text{CO}_3^{2-}$ carbon resonances at different pH in four NH_3 solutions at increasing CO_2 loading.

the experimentally known composition of the solution. The results (Table 1) indicate that the carbamate is an important species in the aqueous NH_3/CO_2 system and its concentration progressively decreases, as expected, at higher CO_2 loading when the CO_2/NH_3 ratio increases or, in other words, when the pH of the solution decreases.

Much more intriguing is to know whether the relative amounts of fast equilibrating HCO_3^- and CO_3^{2-} ions may be quantified by NMR analysis. To this purpose we have carried

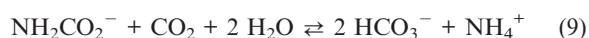
out a quantitative ^{13}C NMR study on D_2O standard solutions of neat KHCO_3 and K_2CO_3 , and of mixtures of the two salts accurately prepared by dissolving weighted amounts of the two salts in different molar ratios (see experimental). Plotting of the chemical shift of each single ^{13}C -resonance due to $\text{HCO}_3^-/\text{CO}_3^{2-}$ equilibration against the relative concentrations of the two salts provides a straight line with limiting values assigned to pure KHCO_3 (δ 160.82) and 98.6% (on molar basis) K_2CO_3 (δ 168.24). Hydrolysis of KHCO_3 is negligible for the concentrations used, whereas a 1.4% hydrolysis of K_2CO_3 is computed and taken into account. The straight line featuring this plot suggests that the resonance frequency due to carbon atoms in the acid/base



equilibrium is proportional to the relative concentration of the two ions and allows for a facile extrapolation of the $[\text{HCO}_3^-]/[\text{CO}_3^{2-}]$ value.

The use of potassium salts instead of ammonium salts does not affect the reliability of the method.† In keeping with this hypothesis, we found that the ^{13}C NMR behaviour of KHCO_3 and NH_4HCO_3 solutions in D_2O is essentially unchanged. The occurrence of a linear plot for the resonance of the carbonate and bicarbonate pair as a function of their relative amounts allows one to estimate the relative concentrations of the two HCO_3^- and CO_3^{2-} species in solution from the measured chemical shift of the ^{13}C NMR spectra.

The result of a typical experiment is reported in Table 1. In Fig. 2 the relative concentration of NH_2CO_2^- , HCO_3^- and CO_3^{2-} is plotted *versus* the pH value at increasing amount of absorbed CO_2 . In each step of CO_2 absorption, carbamate is more abundant than carbonate, as expected from the comparison of the equilibrium constants for the two pairs of reactions (2), (6) and (3), (7). Both species decrease with pH, while a simultaneous increase of bicarbonate occurs. These results are easily explained on the basis of the equilibria (8) and (9) which gradually move to the right as the CO_2 absorption increases.



† It was not possible to use standard solutions of the ammonium carbonate and bicarbonate mainly because commercially available $(\text{NH}_4)_2\text{CO}_3$ is a mixture of ammonium carbamate and bicarbonate and also because NH_4^+ from NH_4HCO_3 reacts with CO_3^{2-} solution in the salt mixtures.

Table 1 Chemical shifts (δ , ppm), pH and relative amounts (% on molar scale) of carbamate, bicarbonate and carbonate at increasing loading steps of CO_2 in the 2.5 M solution of aqueous ammonia

Absorption step	1	2	3	4	5	6	7	8
pH	10.31	9.93	9.65	9.34	9.12	8.90	8.64	8.59
$\delta(\text{NH}_2\text{CO}_2^-)$	166.03	166.02	166.04	166.01	166.03	166.05	166.03	166.04
$\delta(\text{HCO}_3^-/\text{CO}_3^{2-})$	165.23	164.13	163.54	162.83	162.27	161.86	161.59	161.50
%(NH_2CO_2^-)	43.3	36.8	31.5	27.8	23.1	19.5	15.4	14.7
%(HCO_3^-)	22.5	34.1	42.3	51.3	60.2	67.5	74.5	75.7
%(CO_3^{2-})	34.2	29.1	26.2	20.9	16.7	13.1	10.1	9.6

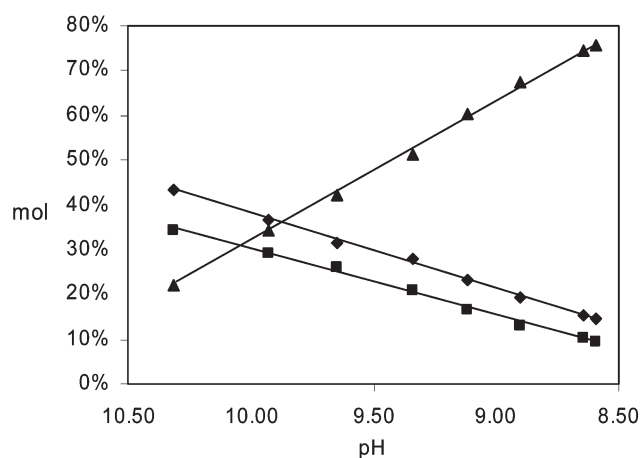


Fig. 2 Variation of the relative amounts (% on molar scale) of carbamate (◆), carbonate (■), and bicarbonate (▲) as a function of pH.

Furthermore, the more the concentration of free NH_3 decreases and that of NH_4^+ increases, the more the backward reactions (2) and (3) occur, thus resulting in further formation of bicarbonate at the expenses of both carbamate and carbonate. Finally, reaction (1) between CO_2 and residual NH_3 contributes to the increase the concentration of bicarbonate. At the end of the absorption reaction, when the pH is around 8.6, the solution contains more than 75% of HCO_3^- . Triplicate CO_2 absorption experiments confirmed that differences in the experimentally determined percentages of the carbon species originated from carbon dioxide absorption were never higher than 1–2 units. Although the results presented here from the analysis of the ^{13}C NMR spectra in aqueous ammonia solutions at different CO_2 loading may be easily explained in the light of the simultaneous equilibria (1)–(9) specifically applied to the present experimental conditions and absorption methods, the unobserved formation of any solid compounds during our CO_2 absorption tests deserves a few additional comments. In any case, at the end of the absorption experiment, the maximum amount of the less soluble salt, *i.e.* NH_4HCO_3 , *ca.* 32 g in 0.240 dm^3 , is largely below its solubility limit (22 g per 0.100 dm^3). Slow evaporation at room temperature and pressure of the final solutions containing NH_4^+ , HCO_3^- , CO_3^{2-} , NH_2COO^- , leads to complete decomposition to NH_3 and CO_2 with no residue remaining. In this respect, we cannot confirm the formation of solid compounds as reported previously even in more dilute NH_3 solution ($<1 \text{ M}$).¹⁹

To evaluate the effects of NH_3 concentration on the speciation of CO_2 absorption products by ammonia solutions, a series of separate experiments were carried out with comparable amounts (about 0.10 mol) of CO_2 loading by increasing the concentration of the absorbing ammonia solution (0.85 M, 2.50 M, 5.08 M, 7.50 M; 10.0 M). The results are reported in Fig. 3, where the relative amounts of NH_2CO_2^- , HCO_3^- and CO_3^{2-} are plotted with respect to the molar ratio of $\text{NH}_3/\text{NH}_4^+$ which increases with the NH_3 concentration. The maximum formation of NH_2CO_2^- (*ca.* 78%) occurs in the 10 M NH_3 solution and decreases in less

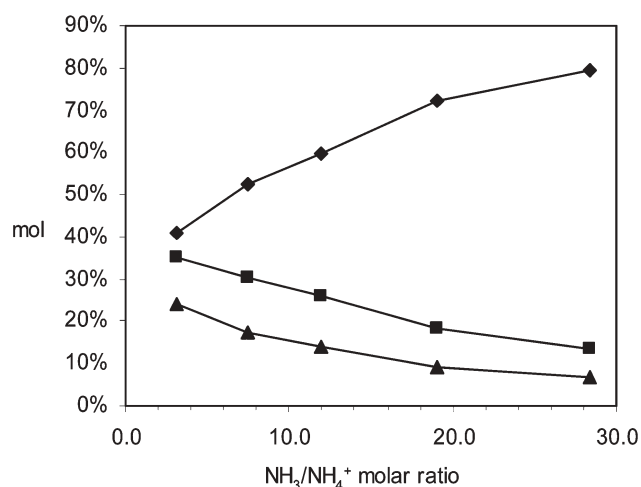


Fig. 3 Variation of the concentration (% on molar scale) of carbamate (◆), carbonate (■), and bicarbonate (▲) as a function of the $\text{NH}_3/\text{NH}_4^+$ molar ratio.

concentrated NH_3 solutions. As expected, the growth of bicarbonate follows the opposite direction with respect to carbamate, whereas changes in carbonate concentration exhibit a less foreseeable behaviour. Overall, these results agree with the equilibrium constants ruling the equilibria (1)–(3), (6), and (7).

To determine how the concentration of the different species varies with time, ^{13}C NMR spectra were taken again three times after 30 day periods after keeping the samples at room temperature in the NMR tubes. The results of a few tests carried out at high pH values (≥ 9.6) [*i.e.* with high $\text{NH}_3(\text{free})/\text{CO}_2(\text{absorbed})$ molar ratio (≥ 2)] indicate that the concentration of NH_2CO_2^- is increased (10–20% in different experiments) to the detriment of both HCO_3^- and CO_3^{2-} . In contrast, at lower pH, the concentrations of NH_2CO_2^- is decreased or does not change appreciably with time. The ^{13}C NMR spectra of the two solutions featuring the highest $\text{NH}_3(\text{free})/\text{CO}_2(\text{absorbed})$ molar ratio (≥ 13) exhibit only one resonance at 166.03 ppm imputable to the sole NH_2CO_2^- . These results suggest that the reaction (2) is slower than reactions (1) and (3) and completes only when a large excess of NH_3 with respect to the absorbed CO_2 is admitted into the solution. To confirm this hypothesis, we have recorded the ^{13}C NMR spectrum of neat NH_4HCO_3 in D_2O which exhibits a unique resonances at 160.87 ppm due to HCO_3^- . Adding NH_3 to the previous solution causes the appearance of a new resonance in the ^{13}C NMR spectrum (δ 165.92) which is assigned to carbamate. The relative amounts of HCO_3^- and NH_2CO_2^- depend on the $\text{NH}_3/\text{HCO}_3^-$ ratio and a large excess of ammonia completely transforms HCO_3^- into NH_2CO_2^- according to reaction (2). Conversely, the hydrolysis of NH_2CO_2^- occurs at lower pH according to the reverse of reaction (2).

Removal of CO_2 by aqueous ammonia solutions

It is well known that ammonia solutions shows a high CO_2 removal efficiency and absorption capacity at room temperature.¹² In general, solutions with a high NH_3 concentration

enable higher CO₂ absorptions, but also cause a greater loss of gaseous NH₃ from the solution. We have found that a 2.5 M NH₃ (4.3% by mass) solution represents the better compromise between CO₂ loading capacity and ammonia loss. In our experiments using a 2.5 M NH₃ solution (0.600 mol) and a 10% (v/v; total flue gas kept at 15 dm³ h⁻¹) inlet CO₂ concentration, the maximum removal efficiency was near 100% at room temperature in the first two analytical runs due to the large excess of NH₃ with respect to the CO₂ admitted into the solution. The absorption capacity decreased with increasing of the absorbed CO₂. The loss of NH₃ from the absorber is lower than 0.5% (v/v) in the first steps of absorption going down to *ca.* 0.1% when the amount of free NH₃ in solutions is reduced to 50%. The CO₂ absorption experiments were stopped when no more than 15–20% of CO₂ is absorbed by the residual ammonia and pH values are in the range 8.5–8.7. In a typical experiment 0.600 mol of NH₃ absorbed a total amount of 0.404 mol of CO₂ (0.404 ± 0.04 in triplicate experiments) with a 64% (v/v) average removal efficiency; from these figures an absorption capacity of 1.76 kg CO₂ per kg NH₃ may be calculated. For comparison purposes, the maximum absorption capacity of MEA was reported to be 0.55–0.58 kg CO₂ per kg MEA.²⁰

The CO₂ capture by ammonia scrubbing requires thermal regeneration of NH₃ followed by its separation from pure CO₂, which must be sequestered.²¹ Both processes are energy consuming and make this technique economically unattractive in spite of the high absorption efficiency and loading capacity of ammonia solutions. The separation from the absorbed solution of solid products worth of profit-making, such as NH₄HCO₃ or NH₄CO₂NH₂, might lower the costs of the process avoiding the costly steps of NH₃ regeneration/CO₂ sequestration. In the present system, however, no solid compound crystallized out during our absorption tests due to the high water solubility of these ammonium salts. Further studies aimed at exploiting the process to recover valuable solid products from the absorption solutions are in progress and will be reported in due time.

Experimental

All reagents were reagent grade. NH₄HCO₃, KHCO₃, NH₄CO₂NH₂, K₂CO₃ (Sigma–Aldrich) were used as received. Standard NH₃ solution 5.08 M and 14.8 M (Sigma–Aldrich) were used to prepare the absorbent solutions. Pure CO₂ and N₂ (Rivoira) were used to simulate flue gas. pH measurements were carried out with a Crison GLP 22.02 model pH-meter calibrated with standard buffer solutions at pH 7.0 and 9.0. Flow rates of N₂ and CO₂ were measured with 150 mm flowmeters equipped with gas controllers (Cole Parmer). The inlet and outlet CO₂ concentrations in the flue gas mixture were measured with a Varian CP-4900 gas chromatograph calibrated with a 10% v/v CO₂/N₂ reference gas (Rivoira).

The absorber was a glass cylinder with a diameter of 56 mm and height 300 mm fitted with a thermometer and a combined pH electrode and containing 0.240 dm³ of the absorbent solution. CO₂ absorption experiments were carried out with 0.85 M (1.46% w/w), 2.50 M (4.34% w/w), 5.08 M (9.00% w/w) 7.50 M (13.5% w/w), 10.0 M (18.1% w/w) NH₃ solutions. The

temperature of the absorber was kept constant by means of a water bath thermostat (Julabo model F33-MC refrigerated bath) regulated at 293 K. To mimic flue gas, a gas mixture containing 10% (v/v) CO₂ in N₂, was continuously fed into the absorber through a sintered glass diffuser (16–40 μm pores) at the bottom of the absorbent solution with a flow rate of 15 dm³ h⁻¹. The vent gas exited from the top of the absorber. The inlet gas mixture was humidified by bubbling it through water before it flowed into the absorbent reactor.

The ¹³C NMR spectra were obtained with a Varian Gemini g300bb spectrometer operating at 75.46 MHz. Chemical shifts are to high frequency relative to tetramethylsilane as external standard at 0.00 ppm. CD₃CN was used as internal reference. The H₂O solutions of the reactants were added with 15% (v/v) D₂O (Aldrich) contained in a sealed capillary to provide enough signal for the deuterium lock system without changes in the concentration of the solutions. NMR spectra were recorded after each absorption step and repeated on the same samples again three times after 30 day periods. Reference solutions for calibrating the ¹³C NMR spectra were prepared by dissolving in D₂O pure K₂CO₃, KHCO₃, and accurately weighted mixtures of the two salts in different percentages. Chemical shifts of reference solutions are in ppm and percentages of KHCO₃, in parenthesis, are on molar basis. ¹³C NMR: δ 168.24 (neat K₂CO₃), 167.44 (11.0), 166.63 (21.7), 166.01 (29.6), 165.74 (33.0), 165.14 (40.3), 164.98 (43.1), 163.92 (56.9), 163.36 (63.7), 162.54 (74.5), 162.20 (79.8), 161.67 (86.4), 161.59 (88.1), 160.82 (neat KHCO₃).

Conclusions

We have shown that ¹³C NMR spectroscopy provides an efficient, reliable and straightforward method to evaluate the relative amounts of NH₂CO₂⁻, HCO₃⁻, and CO₃²⁻ which form from the reaction of CO₂ with aqueous ammonia at 293 K. In agreement with the equilibria governing the CO₂/NH₃/H₂O system, NH₂CO₂⁻ is the main species in solution in the presence of excess NH₃ with respect to absorbed CO₂. In contrast, HCO₃⁻ prevails when most of NH₃ has reacted with CO₂ and the pH lowers. Finally, the CO₃²⁻ anion is always present in solution but at a concentration always lower than carbamate. No other species has been detected in solution by NMR spectroscopy and no solid compound separated out during the absorption experiments.

In conclusion, the present study deals with the CO₂ removal by aqueous NH₃ solutions and confirms the advantage of this process in terms of CO₂ loading capacity and absorption efficiency. Of course, the problem of CO₂ capture is far from being resolved by our preliminary studies and further investigations are required for an extensive application of NH₃ scrubbing process. We are currently orienting our work towards the design of chemical processes capable of converting the captured CO₂ into useful solid products by means of inexpensive and recyclable chemicals. Such an accomplishment could overcome the expensive steps of NH₃ regeneration and separation from pure CO₂. In this perspective, an in-depth knowledge of the ¹³C NMR behaviour of the CO₂/NH₃ system is mandatory to quickly test both reaction conditions and experimental methods aimed at improving the selectivity and

the yield of the species formed in liquid phase with minimum loss of NH₃ and minimal energy requirements. This research is now in progress in our laboratory and the results will be reported elsewhere.

Acknowledgements

Financial support from MIUR (Rome, Italy) and Ente Cassa di Risparmio di Firenze (Florence, Italy), through Florence Hydrolab Project, is gratefully acknowledged.

References

- J. Hansen, M. Sato, R. Ruedy, A. Lacis and V. Oinas, *Proc. Natl. Acad. Sci. U. S. A.*, 2000, **97**, 9875; D. M. Haseltine, *Chem. Eng. Prog.*, 2000, **75**; B. Hileman, *Chem. Eng. News*, 1999, **77**, 16.
- The Science of Climate Change*, ed. J. T. Houghton, L. G. Meira Filho, B. A. Callender, N. Harris, A. Kattenberg and K. Maskell, Cambridge University Press, Cambridge, UK, 1995, pp. 572.
- H. J. Herzog, *Environ. Sci. Technol.*, 2001, **148A**; H. J. Herzog, B. Eliasson and O. Kaarstad, *Sci. Am.*, 2000, **282**(2), 72; C. Hanisch, *Environ. Sci. Technol.*, 1999, **66A**.
- R. V. Siriwardane, M. Shen and E. P. Fisher, *Energy Fuels*, 2005, **19**, 1153; M. Casarin, D. Falconer and A. Vittadini, *Surf. Sci.*, 2004, **556–558**, 890; M. T. Izquierdo, B. Rubio, C. Mayoral and J. M. Andres, *Fuel*, 2003, **82**, 147; S. Kaneco, N. Hiei, Y. Xing, H. Katsumata, H. Hohnishi, T. Suzuki and K. Ohta, *Electrochim. Acta*, 2002, **48**, 51; R. V. Siriwardane, M. Shen and E. P. Fisher, *Energy Fuels*, 2001, **15**, 279.
- Z. Li, N. Lai, Y. Huang and H. Han, *Energy Fuels*, 2005, **19**, 1447; T. Koljionen, H. Siikavirta, R. Zevenhoven and I. Savolainen, *Energy*, 2004, **29**, 1521; Y. Soong, A. L. Goodman, J. R. McCarthy-Jones and H. P. Baltrus, *Energy Convers. Manage.*, 2004, **45**, 1845; H. P. Huang, Y. Shi, W. Li and S. G. Chang, *Energy Fuels*, 2001, **15**, 263; G. H. Rau and K. Caldeira, *Energy Convers. Manage.*, 1999, **40**, 1803; T. Kojima, A. Nagamine, N. Ueno and S. Uemiya, *Energy Convers. Manage.*, 1997, **38**, S461; K. S. Lackner, C. H. Wendt, D. P. Butt, E. L. Joyce and D. H. Sharp, *Energy*, 1995, **20**, 1153.
- M. Mavraudi, S. P. Kaldis and G. P. Sakellaropoulos, *Fuel*, 2003, **82**, 2153; L. Xu, L. Zhang and H. Chen, *Desalination*, 2002, **148**, 309.
- C. Stewart and M. Hessami, *Energy Convers. Manage.*, 2005, **46**, 403; S. M. Klara and R. D. Srivastava, *Environ. Prog.*, 2004, **21**, 247.
- M. Koji, I. Yoshikatsu, H. Masahiro and F. Harno, *Tetrahedron*, 2005, **61**, 213; Y. Tang, W. S. Kassel, L. N. Zakharov, A. L. Rheingold and R. A. Kemp, *Inorg. Chem.*, 2005, **44**, 359; C. Alie, L. Backham, E. Croiset and P. L. Douglas, *Energy Convers. Manage.*, 2005, **46**, 475; N. Danashvar, M. T. Zaaferani Moattor, M. A. Abedinzadegan Abi and S. Aber, *Sep. Purif. Technol.*, 2004, **37**, 135; B. P. Mandal, A. K. Biswas and S. S. Bandyopadhyay, *Chem. Eng. Sci.*, 2003, **58**, 4137; D. Bonefant, M. Mimeault and R. Hausler, *Ind. Eng. Chem. Res.*, 2003, **42**, 3179; J. Y. Park, S. J. Yoon and H. Lee, *Environ. Sci. Technol.*, 2003, **37**, 1670; A. Dibenedetto, M. Aresta, C. Fragale and M. Marracci, *Green Chem.*, 2002, **4**, 439; J. T. Yeh and H. W. Pennline, *Energy Fuels*, 2001, **15**, 274.
- E. D. Bates, R. D. Nayton, I. Ntai and J. H. Davis, *J. Am. Chem. Soc.*, 2002, **124**, 926; B. P. Mandal, M. Guha, A. K. Biswas and S. S. Bandyopadhyay, *Chem. Eng. Sci.*, 2001, **56**, 6217; S. H. Lin and C. T. Shyu, *Waste Manage.*, 1999, **19**, 255; A. K. Chakravorthy, G. Astarita and G. Bishoff, *Chem. Eng. Sci.*, 1986, **41**, 997.
- J. T. Culliname and G. T. Rochelle, *Fluid Phase Equilib.*, 2005, **227**, 197.
- O. Brettschneider, R. Thiele, R. Faber, H. Thielert and G. Wozny, *Sep. Purif. Technol.*, 2004, **39**, 139; A. Corti and L. Lombardi, *Intern. J. Thermodynamics*, 1999, **7**, 173; K. Thomsen and P. Rasmussen, *Chem. Eng. Sci.*, 1999, **54**, 1787.
- J. T. Yeh, K. P. Resnik, K. Rygle and H. W. Pennline, *Fuel Process. Technol.*, 2005, **86**, 1531; K. P. Resnik, J. T. Yeh and H. W. Pennline, *Int. J. Environ. Technol. Manage.*, 2004, **4**, 89; J. W. Lee and R. F. Li, *Energy Convers. Manage.*, 2003, **44**, 1535; H. Huang and S. G. Chang, *Energy Fuels*, 2002, **16**, 904; A. Perez-Salado Kamps, R. Sing, B. Rumpf and G. Maurer, *J. Chem. Eng. Data*, 2000, **45**, 796; A. C. Yeh and H. Bai, *Sci. Tot. Environ.*, 1999, **228**, 121; H. Bai and A. C. Yeh, *Ind. Eng. Chem. Res.*, 1997, **36**, 2490.
- (a) N. Wen and M. H. Brooker, *J. Phys. Chem.*, 1995, **99**, 359; (b) J. E. Pelkie, P. J. Concannon, D. B. Manley and B. E. Poling, *Ind. Eng. Chem. Res.*, 1992, **31**, 2209.
- X. Li, E. Hagaman, C. Tsouris and J. W. Lee, *Energy Fuels*, 2003, **17**, 69.
- V. Ermatchkov, A. Perez-Salado Kamps and G. Maurer, *J. Chem. Thermodyn.*, 2003, 1277; J. Y. Park, S. J. Yoon and H. Lee, *Environ. Sci. Technol.*, 2003, **37**, 1670; T. Suda, T. Iwaki and T. Mimura, *Chem. Lett.*, 1996, 777.
- T. J. Edwards, J. Newman and J. M. Prausnitz, *Ind. Eng. Chem. Fundam.*, 1978, 17.
- Merck Chemical Database. www.de.chemdat.info.
- E. Breitmaier and W. Voelter, *Carbon-13 NMR spectroscopy*, 3rd ed., VCH-Weinheim, Germany, 1990.
- Y. F. Diao, X. Y. Zheng, B. S. He, C. H. Chen and X. C. Xu, *Energy Convers. Manage.*, 2004, **45**, 2283.
- D. Bonefant, M. Mimeault and R. Hausler, *Ind. Eng. Chem. Res.*, 2003, **42**, 3179; R. J. Hook, *Ind. Eng. Chem. Res.*, 1997, **36**, 1779.
- D. Yang, P. Tontiwachwuthikul and Y. Gu, *Energy Fuels*, 2005, **19**, 216; C. M. White, H. D. Smith, K. L. Jones, A. L. Goodman, S. A. Jikich, R. B. LaCount, S. B. DuBose, E. Ozdemir, B. I. Morsi and K. T. Schroeder, *Energy Fuels*, 2005, **19**, 659; S. Bachu, J. J. Adams, S. H. Stevens and J. Gale, *Oil Gas*, 2000, **5**, 40.

Solvent-free bromination of 1,3-diketones and β -keto esters with NBS

Igor Pravst,^a Marko Zupan^{ab} and Stojan Stavber^{*b}

Received 15th June 2006, Accepted 18th August 2006

First published as an Advance Article on the web 5th September 2006

DOI: 10.1039/b608446j

Trituration of *N*-bromosuccinimide at room temperature with several liquid or solid 1,3-diketones and β -keto esters resulted in high yield conversion to the monobrominated derivatives, and a work-up procedure using only water to remove succinimide was employed. The entire process uses no organic solvent and is therefore more ecologically desirable.

Introduction

In the face of demands for sustainable and ecologically friendly organic syntheses,¹ solvent-free strategies² are an important alternative to the use of organic solvents in synthetic reactions. In the absence of solvent, however, reaction pathways, as well as the products formed, may be modified significantly.

Solvent-free halogenation has not been extensively studied,^{2a} but it is known that some brominations can be carried out under such conditions. Selective solid-state brominations of alkenes and aromatic compounds have been achieved with gaseous bromine^{3–7} or with the recyclable ditribromide reagent (1,2-dipyridiniumditribromide-ethane), which has also been used for functionalisation of ketones.⁸ *N*-Bromosuccinimide (NBS) has been used for solvent-free bromination of aromatics and in many cases the crystallinity of substrates was crucial for product selectivity.^{9–11} Allylic¹² and α -carbonyl¹³ brominations with NBS have also been reported recently. In all these cases, although the reaction involved no solvent, organic solvents were used for work-up procedures, and thus the overall protocols were not completely organic solvent-free.

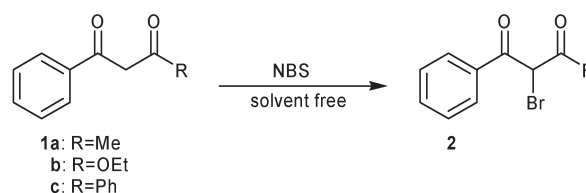
Due to their high reactivity, monobrominated 1,3-dicarbonyl compounds are valuable building blocks in organic synthesis.¹⁴ It has been reported that bromination at the reactive position in a 1,3-keto compound enhances bioactivity, particularly cytotoxicity against breast cancer 1A9 cells, with respect to the unsubstituted compound.¹⁵ Bromination of 1,3-diketones and β -keto esters has been accomplished with various reagents, including molecular bromine and its complexes,¹⁶ potassium bromide with oxidising agents,¹⁷ sodium hypobromite,¹⁸ CuBr₂ with Koser's reagent,¹⁹ ammonium bromide in combination with vanadium pentoxide and hydrogen peroxide,²⁰ NBS alone²¹ or in combination with sodium hydride,²² triethylamine,²³ magnesium perchlorate,²⁴ silica-supported sodium hydrogen sulfate,²⁵ Amberlyst-15²⁶ and ammonium acetate.²⁷ The reactions were usually performed in organic solvents although ionic liquids have also

been used.²⁸ Nevertheless, selective monobromination of 1,3-diketones and β -keto esters remains a challenge since these reactions in many cases result in a mixture of mono and dibrominated products.²¹

Further disadvantages of the established methods include their use of hazardous reaction chemicals, complicated work-up methods, organic solvents or uncommon and expensive chemicals and solvents. Molecular bromine, the simplest brominating agent, suffers from several drawbacks: it is hazardous and difficult to handle and use. On the contrary, NBS is an easily accessible, easy to handle and inexpensive brominating agent, which could be employed for ecologically acceptable bromination of 1,3-dicarbonyl compounds. Organic solvents are generally used as reaction media and/or for isolation procedures, even when ionic liquids were employed. We now report an efficient solvent-free bromination of 1,3-diketones and β -keto esters with NBS (Scheme 1). This can be performed successfully at room temperature without the use of organic solvents, catalysts or drying agents.

Results and discussion

It is known that the aggregate state of both substrate and reagent play important roles in molecular migration and thus have significant influence on the transformation. Reactions where both partners are solid are especially problematic but much better contact between reagent and target substrate can be established in case of liquid–liquid and liquid–solid systems. In addition to the reaction conditions employed in the bromination, the structure of the 1,3-diketones and β -keto esters exert a significant influence on the reactivity and the selectivity of bromine introduction. This effects the distribution of possible products: monobromo derivatives in keto or enol form and dibromo products. With both of these factors in mind we chose three target compounds as model substrates: 1-phenylbutane-1,3-dione (**1a**), a solid;



Scheme 1

^aFaculty of Chemistry and Chemical Technology, University of Ljubljana, Aškerčeva 5, SI-1000 Ljubljana, Slovenia.
E-mail: igor.pravst@ijs.si; marko.zupan@fkt.uni-lj.si

^bLaboratory for Organic and Bioorganic Chemistry, "Jozef Stefan" Institute, Jamova 39, SI-1000 Ljubljana, Slovenia.
E-mail: stojan.stavber@ijs.si

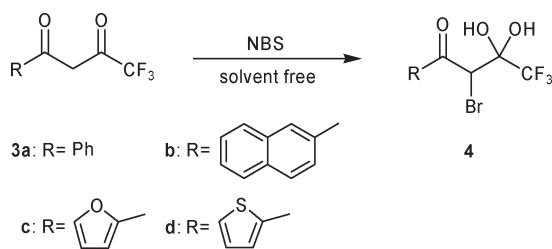
3-oxo-3-phenylpropionic acid ethyl ester (**1b**), a liquid; and 1,3-diphenylpropane-1,3-dione (**1c**), a solid (Scheme 1).

Trituration of an equimolar mixture of solid diketone **1a** with NBS in a porcelain mortar at room temperature resulted in formation of a liquid paste, and selective conversion to monobrominated product **1b** was shown to have occurred. No dibromination was detected even when using a 100% excess of NBS. A similar reaction was observed with the liquid β -keto ester **1b** and the solid phenyl substituted diketone **1c**, which afforded quantitative yields of the monobrominated ester **2b** or diketone **2c**, respectively.

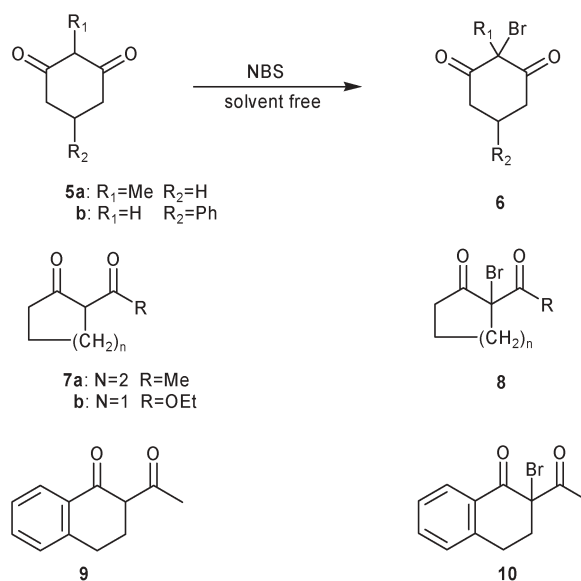
In most cases a desirable green approach to synthetic protocols is not followed by environmentally friendly isolation and purification procedures. In our case, we have been aware of this pitfall and have avoided it by taking advantage of the high solubility (33 g per 100 mL²⁹) of succinimide in water. In our hands, all reaction mixtures were washed with water and separated by decantation, in the case of **2a** and **2b**, or filtration, in the case of the solid product **2c**. After drying in a desiccator overnight all products were isolated in good yields (**2a**: 92%, **2b**: 95%, **2c**: 98%), and their purity was established by NMR analysis to be over 95%. A further useful point is that regeneration of NBS from the aqueous succinimide solution is also possible.³⁰

We have investigated the effect of the trifluoromethyl group and heteroaromatic rings on the solvent-free bromination reactions (Scheme 2). The phenyl diketone **3a**, a solid, the naphthalenyl **3b**, and thiophenyl **3d** diketones, both solids, and liquid furanyl diketone **3c** were effectively brominated at room temperature after 10 minutes by applying the solvent-free procedure described above. NMR analysis of the crude reaction mixture from **3a** showed that in addition to succinimide, two products, the monobrominated ketone and its hydrate **4a** were formed in equal proportions. Work-up of the reaction using water, however, gave only stable solid 2-bromo-4,4,4-trifluoro-3,3-dihydroxybutan-1-ones in high yield (**4a**, 91%; **4b**, 90%; **4c**, 86%; **4d**, 93%).

In order to determine the limitations of the method we tested it on several additional substrates (Scheme 3), including cyclohexane-1,3-dienones (**5**), 2-substituted cycloalkanones (**7**) and 2-substituted derivatives of 1-tetralone (**9**). Bromination of both solid 2-methylcyclohexane-1,3-dione (**5a**) and 4-phenylcyclohexane-1,3-diones (**5b**) was successful; the monobrominated ketones **6a** (liquid) and **6b** (solid) were formed selectively and were isolated in high yield (98% and 88%, respectively). Bromination of the 2-acetylcyclohexanone (**7a**) also proceeded quantitatively giving the 2-bromo product **8a**, isolated as a liquid in 98% yield. The reaction with 2-acetylcyclohexanone



Scheme 2



Scheme 3

(**7b**) was not quantitative. Although this substrate is a liquid, the final reaction mixture contained only 90% of the brominated compound **8b**, thus necessitating purification by column chromatography in order to obtain pure 2-acetyl-2-bromocyclohexanone (**8b**: liquid, 84%). Functionalisation of the solid tetralone derivative **9** under these conditions resulted in only 68% conversion of starting material to the brominated product **10**, but quantitative yield of **10** was obtained under slightly changed reaction conditions. If the crude reaction mixture in water emulsion was allowed to stand for 30 minutes at room temperature, filtration then gave pure 2-acetyl-2-bromo-3,4-dihydro-2*H*-naphthalen-1-one (**10**) in 93% yield.

Conclusions

Solid and liquid 1,3-diketones and β -keto esters can be successfully and selectively brominated with NBS at room temperature with no solvent. After reactions lasting between 10 and 60 minutes, high yields of the α -monobromo products were achieved. Organic solvent-free conditions, a feature of the green chemistry concept, were successfully used not only for these reactions but also for the isolation of the products. The purity of the products was, in all but a single case, in excess of 95% and no further purification was necessary. The brominated trifluoromethyl substituted 1,3-diketones **3a–d** underwent water addition during the procedure forming the 1-substituted 2-bromo-4,4,4-trifluoro-3,3-dihydroxybutan-1-ones (**4a–d**). Solvent-free bromination of 1,3-diketones and β -keto esters with NBS was found to be very successful for various types of substrates.

Experimental

Melting points were determined on a Büchi 535 apparatus. NMR spectra were recorded on a Varian INOVA 300 spectrometer at 300 MHz for ¹H and at 76 MHz for the ¹³C nucleus. Chemical shifts are reported in ppm from TMS as the internal standard. ¹⁹F NMR spectra were recorded on the

same instrument at 285 MHz and chemical shifts are reported in ppm from CCl_3F as the internal standard. IR spectra were obtained with a Bio-Rad FTS 3000MX. Standard KBr pellet procedures were used to obtain IR spectra of solids, while a film of neat material was used to obtain IR spectra of liquid products. Mass spectra were obtained on an Autospec Q instrument under electron impact (EI) conditions at 70 eV. Elemental analyses were carried out on a Perkin Elmer 2400 Series II CHNS/O Analyzer. *N*-Bromosuccinimide (Merck) and starting materials (Sigma–Aldrich, Fluka) were used as received. ACS grade solvents were used. Isolated compounds were identified on the basis of spectroscopic data, elemental microanalysis and high resolution MS spectroscopy, while in case of known compounds comparison with literature data was made. In cases where the comparative physical constant can not be found, spectroscopic data are in accordance to previously reported data.

Bromination of 1,3-diketones **1c**, **3a–d**, **5b** and **9**; typical procedure where a solid reaction mixture was formed

Ketone **1c** (897 mg, 4 mmol) and *N*-bromosuccinimide (NBS, 712 mg, 4 mmol) were triturated together in a porcelain mortar for 5 minutes, and after 1 hour water (4 mL) was added and the mixture converted into a paste. After filtration and additional washing with water, the crude product was dried overnight in a desiccator under reduced pressure and yielded 1.187 g (98%) of pure product **2c**. The purity of the isolated product was over 95%, determined by ^1H NMR spectroscopy.

2-Bromo-1,3-diphenylpropane-1,3-dione¹⁷ (**2c**)

Isolated yield 98% as colourless crystals, mp 91 °C (from EtOH) (lit.,³¹ 93 °C), $\nu_{\text{max}}(\text{KBr})/\text{cm}^{-1}$ 1673, 1587, 1445, 1285, 1186, 995 and 686; $\delta_{\text{H}}(300 \text{ MHz}; \text{CDCl}_3; \text{Me}_4\text{Si})$ 6.57 (s, 1H, CHBr), 7.44–7.49 (m, 4H, ArH), 7.57–7.62 (m, 2H, ArH) and 7.98–8.00 (m, 4H, ArH); $\delta_{\text{C}}(76 \text{ MHz}; \text{CDCl}_3; \text{Me}_4\text{Si})$ 52.6 (CHBr), 129.0 (ArCH), 129.9 (ArCH), 133.8 (ArC), 134.2 (ArCH) and 188.9 (CO); m/z (EI, 70 eV) 304 (1%, $\text{M}^+ + 2$), 303 (1%, $\text{M}^+ - \text{H} + 2$), 302 (1%, M^+), 301 (1%, $\text{M}^+ - \text{H}$), 223 (25%), 105 (100%) and 77 (52%).

2-Bromo-4,4,4-trifluoro-3,3-dihydroxy-1-phenylbutan-1-one (**4a**)

This was prepared by the same procedure with reaction time 10 minutes and isolated as white crystals in 91% yield; mp 91–92 °C (from CHCl_3) (Found: C, 38.10; H, 2.61. $\text{C}_{10}\text{H}_8\text{BrF}_3\text{O}_3$ requires C, 38.36; H, 2.58); $\nu_{\text{max}}(\text{KBr})/\text{cm}^{-1}$ 3381 (OH), 3306 (OH), 1665, 1593, 1337, 1175, 1080, 1007, 968, 818, 682 and 623; $\delta_{\text{H}}(300 \text{ MHz}; \text{CDCl}_3; \text{Me}_4\text{Si})$ 5.18 (s, 1H, OH), 5.24 (s, 1H, OH), 5.41 (s, 1H, CHBr), 7.53–7.58 (m, 2H, ArH), 7.68–7.73 (m, 1H, ArH) and 8.00 (d, *J* 8.0 Hz, 2H, ArH); $\delta_{\text{F}}(285.05 \text{ MHz}; \text{CDCl}_3; \text{CCl}_3\text{F})$ –82.5 (s, CF_3); m/z (EI, 70 eV) 312.9694 (0.1%, MH^+), $\text{C}_{10}\text{H}_9\text{BrF}_3\text{O}_3$ requires 312.9687), 315 (0.1%, $\text{MH}^+ + 2$), 105 (100%) and 77 (43%).

2-Bromo-4,4,4-trifluoro-3,3-dihydroxy-1-thiophen-2-yl-butan-1-one¹⁷ (**4b**)

This was prepared by the same procedure with reaction time 10 minutes and isolated as light yellow crystals in 90% yield;

mp 102–104 °C (from CHCl_3) (lit.,¹⁷ 97–100 °C); $\nu_{\text{max}}(\text{KBr})/\text{cm}^{-1}$ 3339 (OH), 3233 (OH), 1641, 1510, 1409, 1204, 1175, 1082, 1001, 864, 733 and 630; $\delta_{\text{H}}(300 \text{ MHz}; \text{CDCl}_3; \text{Me}_4\text{Si})$, 5.13 (s, 1H, OH), 5.15 (s, 1H, OH), 5.24 (s, 1H, CHBr), 7.23–7.26 (m, 1H, ArH) and 7.87–7.90 (m, 2H, ArH); $\delta_{\text{F}}(285.05 \text{ MHz}; \text{CDCl}_3; \text{CCl}_3\text{F})$ –82.5 (s, CF_3); m/z (EI, 70 eV) 317.9182 (3%, M^+), $\text{C}_8\text{H}_6\text{BrF}_3\text{O}_3\text{S}$ requires 317.9173), 320 (3%, $\text{M}^+ + 2$), 206 (8%), 204 (8%) and 111 (100%).

2-Bromo-4,4,4-trifluoro-1-furan-2-yl-3,3-dihydroxybutan-1-one (**4c**)

This was prepared by the same procedure with reaction time 10 minutes and isolated as white crystals in 86% yield; mp 98–100 °C (from CHCl_3) (Found: C, 32.20; H, 2.11. $\text{C}_8\text{H}_6\text{BrF}_3\text{O}_4$ requires C, 31.71; H, 2.00); $\nu_{\text{max}}(\text{KBr})/\text{cm}^{-1}$ 3352 (OH), 3279 (OH), 3011, 1656, 1568, 1463, 1327, 1210, 1176, 1131, 1084, 986, 778 and 656; $\delta_{\text{H}}(300 \text{ MHz}; \text{CDCl}_3; \text{Me}_4\text{Si})$ 5.00 (s, 1H, OH), 5.04 (s, 1H, OH), 5.32 (s, 1H, CHBr), 6.70 (dd, *J* 3.7 and 1.6 Hz; 1H, ArH), 7.50 (d, *J* 3.7 Hz, 1H, ArH) and 7.76 (d, *J* 1.6 Hz, 1H, ArH); $\delta_{\text{F}}(285.05 \text{ MHz}; \text{CDCl}_3; \text{CCl}_3\text{F})$ –82.7 (s, CF_3); m/z (EI, 70 eV) 301.9409 (3%, M^+), $\text{C}_8\text{H}_6\text{BrF}_3\text{O}_4$ requires 301.9402); 190 (15%), 188 (15%), 95 (100%).

2-Bromo-4,4,4-trifluoro-3,3-dihydroxy-1-naphthalen-2-yl-butan-1-one (**4d**)

This was prepared by the same procedure with reaction time 10 minutes and isolated as white crystals in 93% yield; mp 113–114 °C (from CH_2Cl_2) (Found: C, 46.28; H, 2.86. $\text{C}_{14}\text{H}_{10}\text{BrF}_3\text{O}_3$ requires C, 46.31; H, 2.78); $\nu_{\text{max}}(\text{KBr})/\text{cm}^{-1}$ 3340, 3222, 3065, 1651, 1624, 1449, 1268, 1196, 1179, 1075, 1005, 866, 735, 662 and 592; $\delta_{\text{H}}(300 \text{ MHz}; \text{CDCl}_3; \text{Me}_4\text{Si})$ 5.23 (m, 2H, OH), 5.58 (s, 1H, CHBr), 7.59–7.72 (m, 2H, ArH), 7.90–8.04 (m, 4H, ArH) and 8.53 (s, 1H, ArH); $\delta_{\text{F}}(285.05 \text{ MHz}; \text{CDCl}_3; \text{CCl}_3\text{F})$ –83.3 (s, CF_3); m/z (EI, 70 eV) 361.9777 (1%, M^+), $\text{C}_{14}\text{H}_{10}\text{BrF}_3\text{O}_3$ requires 361.9765), 362 (1%), 266 (20%), 155 (100%), 127 (60%), 69 (25%).

2-Bromo-5-phenylcyclohexane-1,3-dione³² (**6b**)

This was prepared by the same procedure and isolated as white crystals in 88% yield; mp 176–178 °C (dec., from EtOH) (lit.³² 177 °C), $\nu_{\text{max}}(\text{KBr})/\text{cm}^{-1}$ 2523, 1566, 1295, 1248, 1146, 999, 951, 762, 698 and 524; $\delta_{\text{H}}(300 \text{ MHz}; \text{CDCl}_3; \text{Me}_4\text{Si})$ 2.70–2.90 (m, 4H), 3.30–3.50 (m, 1H, CHBr), 7.20–7.40 (m, 5H, ArH); $\delta_{\text{C}}(76 \text{ MHz}; \text{CDCl}_3 + \text{DMSO-}d_6; \text{Me}_4\text{Si})$ 37.7 (CH_2), 98.5, 125.9 (ArCH), 126.3 (ArCH), 128.0 (ArCH), 141.2 and 170.0 (CO); m/z (EI, 70 eV) 265.99513 (60%, M^+), $\text{C}_{12}\text{H}_{11}\text{BrO}_2$ requires 265.99424), 268 (60%, $\text{M}^+ + 2$), 187 (35%), 164 (80%), 162 (85%), 131 (60%) and 104 (100%).

2-Acetyl-2-bromo-3,4-dihydro-2H-naphthalen-1-one³³ (**10**)

This was prepared by the same procedure, but the reaction mixture containing 4 mL of water was left for 30 minutes at room temperature before filtration. The product was isolated as white crystals in 93% yield; mp 67–68 °C (from EtOH); $\nu_{\text{max}}(\text{KBr})/\text{cm}^{-1}$ 2944, 1713, 1673, 1597, 1538, 1294, 1236, 1216, 1128, 889, 813, 750 and 722; $\delta_{\text{H}}(300 \text{ MHz}; \text{CDCl}_3; \text{Me}_4\text{Si})$ 2.42–2.53 (m, 1H) 2.61 (s, 3H, CH_3) 2.78–2.90 (m, 1H)

2.99–3.11 (m, 1 H) 3.15–3.28 (m, 1 H) 7.28 (d, J 6.7 Hz, 1 H, ArH), 7.36 (t, J 7.6 Hz, 1 H, ArH), 7.55 (td, J 7.6 and 1.4 Hz, 1 H, ArH) 8.07 (dd, J 7.9 and 1.1 Hz, 1 H, ArH); δ_{C} (76 MHz; CDCl₃; Me₄Si) 26.7, 28.3, 33.7, 68.3 (CBr), 127.1 (ArCH), 128.7 (ArCH), 128.8 (ArCH), 129.8 (ArC), 134.4 (ArCH), 142.6 (ArC), 189.6 (CO) and 200.6 (CO); m/z (EI, 70 eV) 269 (5%), 267 (5%), 226 (90%), 224 (90%), 187 (92%), 145 (100%), 118 (78%), 115 (91%) and 90 (72%).

Bromination of 1,3-diketones 1a, 5a, 7a and β -keto esters 1b and 7b; typical procedure where a pasty reaction mixture was formed

The ketone 1a (12 mmol, 1.95 g) and NBS (2.13 g, 12 mmol) were triturated together in a porcelain mortar for 5 minutes. The resulting liquid paste was allowed to stand for one hour, then washed three times with 20 mL of water in a separating funnel. After each washing, the water phase was removed from the funnel by suction to avoid unnecessary product loss. The liquid organic phase was then dried overnight in a desiccator under reduced pressure and analysed. The pure product 2a which crystallized in the refrigerator and remained crystalline at room temperature was isolated with a yield of 2.651 g (92%).

2-Bromo-1-phenylbutane-1,3-dione³³ (2a)

92% as white crystals, mp 33 °C (lit.³⁴ 43–45 °C), $\nu_{\text{max}}/\text{cm}^{-1}$ 1732, 1663, 1587, 1445, 1354, 1290, 1231, 1159, 1130 and 685; δ_{H} (300 MHz; CDCl₃; Me₄Si) 2.45 (s, 3H, CH₃), 5.65 (s, 1H, CHBr), 7.48–7.53 (m, 2H, ArH), 7.61–7.66 (m, 1H, ArH), 7.96–8.00 (m, 2H, ArH); δ_{C} (76 MHz; CDCl₃; Me₄Si) 27.0 (CH₃), 52.8 (CHBr), 128.8 (ArCH), 129.0 (ArCH), 133.5 (ArC), 134.3 (ArCH), 189.8 (CO) and 197.8 (CO); m/z (EI, 70 eV) 241 (0.5%), 239 (0.5%), 200 (5%), 198 (5%), 105, (100%) and 77(40%).

2-Bromo-3-oxo-3-phenylpropionic acid ethyl ester³⁵ (2b)

This was prepared by the same procedure and isolated as a colourless oil in 95% yield; $\nu_{\text{max}}/\text{cm}^{-1}$ 2984, 1759, 1686, 1595, 1449, 1300, 1258, 1187, 1025, 999 and 688; δ_{H} (300 MHz; CDCl₃; Me₄Si) 1.25 (t, J 7.1, 3H, CH₃), 4.28 (q, J 7.1, 2H, CH₂), 5.68 (s, 1H, CHBr), 7.48–7.53 (m, 2H, ArH), 7.61–7.66 (m, 1H, ArH) and 7.98–8.01 (m, 2H, ArH); δ_{C} (76 MHz; CDCl₃; Me₄Si) 13.8, 46.3, 63.3 (CHBr), 128.9 (ArCH), 129.1 (ArCH), 133.3 (ArC), 134.2 (ArCH), 165.1 (CO) and 188.1 (CO); m/z (EI, 70 eV) 273 (2%), 271 (2%), 105 (100%) and 77 (57%).

2-Bromo-2-methylcyclohexane-1,3-dione³⁶ (6a)

This was prepared by the same procedure and isolated as a colourless oil in 98% yield; $\nu_{\text{max}}/\text{cm}^{-1}$ 2965, 1750, 1707, 1427, 1374, 1317, 1277, 1097, 1074, 1029, 682 and 733; δ_{H} (300 MHz; CDCl₃; Me₄Si) 1.65–1.90 (m, 1H), 1.83 (s, 3H, CH₃), 2.20–2.33 (m, 1H), 2.58 (dt, J 16.2 and 4.9 Hz, 2H) and 3.35 (ddd, J 16.2, 11.6 and 5.8 Hz, 2 H); δ_{C} (76 MHz; CDCl₃; Me₄Si) 17.9, 19.2, 35.6, 59.9 (CHBr), 201.0 (CO); m/z (EI, 70 eV) 204 (25%), 203 (20%), 202 (18%) 201 (22%), 125 (42%), 98 (37%), 82 (100%) and 80 (100%).

2-Acetyl-2-bromocyclohexanone³⁷ (8a)

This was prepared by the same procedure and isolated as an oily product in 98% yield; $\nu_{\text{max}}/\text{cm}^{-1}$ 2948, 2869, 1711, 1429, 1358, 1212, 1120, 1073, 913 and 733; δ_{H} (300 MHz; CDCl₃; Me₄Si) 1.75–1.88 (m, 2H, CH₂), 1.91–2.05 (m, 2H, CH₂), 2.18–2.28 (m, 1H), 2.30–2.40 (m, 1H), 2.40–2.49 (s, 3H, CH₃), 2.55–2.68 (m, 1H) and 3.05–3.20 (m, 1H); δ_{C} (76 MHz; CDCl₃; Me₄Si) 22.3, 27.0, 27.2 38.2, 38.6, 71.4 (CHBr), 200.3 (CO) and 202.7 (CO); m/z (EI, 70 eV) 218 (3%, M⁺), 220 (3%, M⁺ + 2), 178 (100%), 176 (100%), 111 (55%), 97 (80%) and 84 (73%).

1-Bromo-2-oxocyclopentanecarboxylic acid ethyl ester³⁸ (8b)

This was prepared by the same procedure, but the isolated product (conversion 90%) was additionally purified by column chromatography (SiO₂, CH₂Cl₂) to obtain 84% pure colourless liquid compound; $\nu_{\text{max}}/\text{cm}^{-1}$ 2981, 2939, 1755, 1725, 1665, 1625, 1414, 1252, 1022, 858, 784 and 735; δ_{H} (300 MHz; CDCl₃; Me₄Si) 1.32 (t, J 7.0 Hz, 3H, Me), 2.09–2.21 (m, 2H), 2.25–2.37 (m, 1H), 2.42–2.60 (m, 2H), 2.71–2.81 (m, 1H), 4.29 (q, J 7.0 Hz, 2H, CH₂); δ_{C} (76 MHz; CDCl₃; Me₄Si) 13.9 (CH₃), 19.4 (CH₂), 35.1 (CH₂), 38.7 (CH₂), 62.1, 63.2, 166.9 (CO) and 205.9 (CO); m/z (EI, 70 eV) 236 (7%), 234 (7%), 190 (15%), 188 (15) and 109 (100%).

Acknowledgements

This research was supported by the Ministry of Higher Education, Science and Technology of the Republic of Slovenia (Programme P1-0134) and the Young Researcher Programme (24300 - I.P.) of the Republic of Slovenia. We are thankful to Dr G.W.A. Milne, the staff of the National NMR Centre at the National Institute of Chemistry in Ljubljana, the staff of the Mass Spectroscopy Centre at the "Jozef Stefan" Institute in Ljubljana and to T. Stipanovič and Prof. B. Stanovnik for elemental combustion analysis.

References

- (a) *Handbook of Green Chemistry and Technology*, ed. J. Clark, and D. Macquarrie, Blackwell Science, Oxford, 2002; (b) *Chemistry In Alternative Reaction Media*, ed. D. J. Adams, P. J. Dyson and S. J. Tavener, John Wiley & Sons Ltd., Chichester, 2004; (c) *Green Separation Processes, Fundamentals and Applications*, ed. C. A. M. Afonso and J. G. Crespo, Wiley-VCH Verlag, Weinheim, 2005.
- (a) *Solvent-free Organic Synthesis*, ed. K. Tanaka, Wiley-VCH Verlag, Weinheim, 2003; (b) *Supported Reagents and Catalysts in Chemistry*, ed. B. K. Hodnett; A. P. Kybett, J. H. Clark and K. Smith, The Royal Society of Chemistry, Cambridge, 1998; (c) *Solid Supports and Catalysts In Organic Synthesis*, ed. K. Smith, Ellis Horwood Limited: New York, 1992.
- A. Schmitt, *Liebigs Ann. Chem.*, 1863, **127**, 319–332.
- G. Kaupp and D. Matthies, *Chem. Ber.*, 1987, **120**, 1897–1903.
- G. Kaup and D. Matthies, *Mol. Cryst. Liq. Cryst.*, 1988, **161**, 119–143.
- G. Kaupp and A. Kuse, *Mol. Cryst. Liq. Cryst.*, 1998, **313**, 361–366.
- F. Toda and J. Schmeyers, *Green Chem.*, 2003, **5**, 701–703.
- V. Kavala, S. Naik and B. K. Patel, *J. Org. Chem.*, 2005, **70**, 4267–4271.
- B. S. Goud and G. R. Desiraju, *J. Chem. Res.*, 1995, 244–245.
- J. A. R. P. Sarma and A. Nagaraju, *J. Chem. Soc., Perkin Trans. 2*, 2000, **6**, 1113–1118.

- 11 J. A. R. P. Sarma, A. Nagaraju, K. K. Majumdar, P. M. Samuel, I. Das, S. Roy and A. J. Mcghe, *J. Chem. Soc., Perkin Trans. 2*, 2000, **6**, 1119–1123.
- 12 A. N. M. M. Rahman, R. Bishop, R. Tan and N. Shan, *Green Chem.*, 2005, **7**, 207–209.
- 13 I. Pravst, M. Zupan and S. Stavber, *Tetrahedron Lett.*, 2006, **47**, 4707–4710.
- 14 Supplement D2. The Chemistry of Halides, Pseudo-halides and Azides, Part 1, in *The Chemistry of Functional Groups*, ed. S. Patai and Z. Rappoport, John Wiley & Sons, Chichester, 1995.
- 15 J. Ishida, H. Ohtsu, Y. Tachibana, Y. Nakanishi, K. F. Bastow, M. Nagai, H. K. Wang, H. Itokawa and K. H. Lee, *Bioorg. Med. Chem.*, 2002, **10**, 3481–3487.
- 16 R. E. Boyd, C. R. Rasmussen and J. B. Press, *Synth. Commun.*, 1995, **25**, 1045–1051.
- 17 J. Kosmrlj, M. Kocevar and S. Polanc, *Synth. Commun.*, 1996, **26**, 3583–3592.
- 18 M. L. Meketa, Y. R. Mahajan and S. M. Weinreb, *Tetrahedron Lett.*, 2005, **46**, 4749–4751.
- 19 S. J. Coats and H. H. Wasserman, *Tetrahedron Lett.*, 1995, **36**, 7735–7738.
- 20 A. T. Khan, P. Goswami and L. H. Choudhury, *Tetrahedron Lett.*, 2006, **47**, 2751–2754.
- 21 R. V. Hoffman, W. S. Weiner and N. Maslough, *J. Org. Chem.*, 2001, **66**, 5790–5795.
- 22 D. P. Curran, E. Bosch, J. Kaplan and M. Newcomb, *J. Org. Chem.*, 1989, **54**, 1826–1831.
- 23 S. Karimi, K. G. Grohmann and L. Todaro, *J. Org. Chem.*, 1995, **60**, 554–559.
- 24 D. Yang, Y. L. Yan and B. Lui, *J. Org. Chem.*, 2002, **67**, 7429–7431.
- 25 B. Das, K. Venkateswarlu, G. Mahender and I. Mahender, *Tetrahedron Lett.*, 2005, **46**, 3041–3044.
- 26 H. M. Meshram, P. N. Reddy, K. Sadashiv and J. S. Yadav, *Tetrahedron Lett.*, 2005, **46**, 623–626.
- 27 K. Tanemura, T. Suzuki, Y. Nishida, K. Satsumabayashi and T. Horaguchi, *Chem. Commun.*, 2004, 470–471.
- 28 H. M. Meshram, P. N. Reddy, P. Vishnu, K. Sadashiv and J. S. Yadav, *Tetrahedron Lett.*, 2006, **47**, 991–995.
- 29 *The Merck Index* ed. M. Windholz, S. Budavari, R. F. Blumetti and E. S. Otterbein, Merck & Co., Inc., Rahway, N.J., USA, 10th edn, 1983.
- 30 F. Lengfeld and J. Stieglitz, *Am. Chem. J.*, 1893, **15**, 215–224.
- 31 H. G. Garg, *J. Org. Chem.*, 1961, **26**, 948–949.
- 32 A. J. Boyd, P. H. Clifford and M. E. Probert, *J. Chem. Soc.*, 1920, **117**, 1383–1390.
- 33 H. Y. Choi and D. Y. Chi, *Org. Lett.*, 2003, **5**, 411–414.
- 34 G. T. Morgan and H. D. K. Drew, *J. Chem. Soc.*, 1924, **125**, 372–381.
- 35 W. T. Ashton, S. M. Hutchins, W. J. Greenlee, G. A. Doss, R. S. L. Chang, V. J. Lotti, K. A. Faust, T. B. Chen, G. J. Zingaro, S. D. Kivlighn and P. K. S. Siegl, *J. Med. Chem.*, 1993, **36**, 3595–3605.
- 36 T. Wakui, Y. Otsuji and E. Imoto, *Bull. Chem. Soc. Jpn.*, 1974, **47**, 1522–1526.
- 37 A. A. Akhrem and A. M. Moiseenkova, *Izv. Akad. Nauk Sssr, Ser. Khim.*, 1968, 1345–1346.
- 38 N. K. Levchenko, G. M. Segal and I. V. Torgov, *Izv. Akad. Nauk Sssr, Ser. Khim.*, 1973, 1086–1090.



Journal of Environmental Monitoring

Comprehensive, high quality coverage of multidisciplinary, international research relating to the measurement, pathways, impact and management of contaminants in all environments.

- Dedicated to the analytical measurement of environmental pollution
- Assessing exposure and associated health risks
- Fast times to publication
- Impact factor: 1.578
- High visibility - cited in MEDLINE



Environmental Science Books

Issues in Environmental Science & Technology

Series Editors:

R E Hester and R M Harrison

Format: **Hardback**

Price: **£45.00**

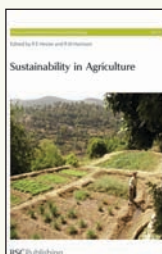
RSC Member Price: **£29.25**

Written by leading experts, this series presents a multidisciplinary approach to pollution and the environment. Focussing on the science and broader issues including economic, legal and political considerations.

Sustainability in Agriculture Vol. No. 21

Discusses the key factors impacting on global agricultural practices including fair trade, the use of pesticides, GM products and government policy.

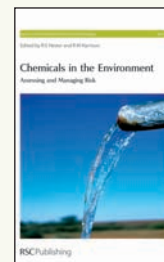
2005 | xiv+130 pages | ISBN-10: 0 85404 201 6
ISBN-13: 978 0 85404 201 2



Chemicals in the Environment Assessing and Managing Risk Vol. No. 22

Beginning with a review of the current legislation, the book goes on to discuss scientific and technical issues relating to chemicals in the environment and future developments.

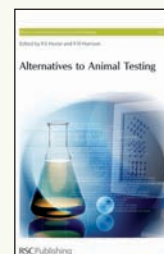
2006 | xvi+158 pages | ISBN-10: 0 85404 206 7
ISBN-13: 978 0 85404 206 7



Alternatives to Animal Testing Vol. No. 23

Provides an up-to-date discussion on the development of alternatives to animal testing including; international validation, safety evaluation, alternative tests and the regulatory framework.

2006 | xii+118 pages | ISBN-10: 0 85404 211 3
ISBN-13: 978 0 85404 211 1

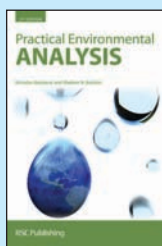


Practical Environmental Analysis 2nd Edition

By *M Radojevic and V N Bashkin*

A new edition textbook providing an up-to-date guide to practical environmental analysis. Ideal for students and technicians as well as lecturers wishing to teach the subject.

Hardback | 2006 | xxiv+458 pages | £39.95 | RSC member price
£25.75 | ISBN-10: 0 85404 679 8 | ISBN-13: 978 0 85404 679 9



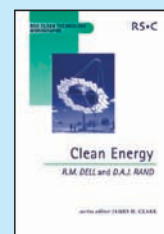
Clean Energy (RSC Clean Technology Monographs)

By *R M Dell and D A J Rand*

Series Editor *J H Clark*

Covering a broad spectrum of energy problems, this highly accessible book discusses in detail strategies for the world's future energy supply.

Hardback | 2004 | xxxvi+322 pages | £89.95 | RSC Member Price
£58.25 | ISBN-10: 0 85404 546 5 | ISBN-13: 978 0 85404 546 4



An Introduction to Pollution Science

By *R M Harrison*

A student textbook looking at pollution and its impact on human health and the environment. Covering a wide range of topics including pollution in the atmosphere, water and soil, and strategies for pollution management.

Hardback | 2006 | ca xii+322 pages | £24.95 | RSC Member Price
£16.50 | ISBN-10: 0 85404 829 4 | ISBN-13: 978 0 85404 829 8

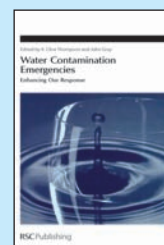


Water Contamination Emergencies Enhancing Our Response

By *J Gray and K C Thompson*

A look at the impact and response of contaminated water supplies including the threat of chemical, biological, radiological and nuclear (CBRN) events.

Hardback | 2006 | x+372 pages | £99.95 | RSC Member Price
£64.75 | ISBN-10: 0 85404 658 5 | ISBN-13: 978 0 85404 658 4

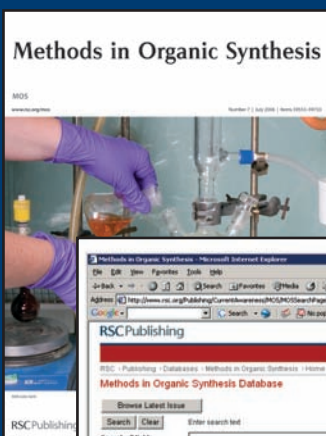


Specialised searching

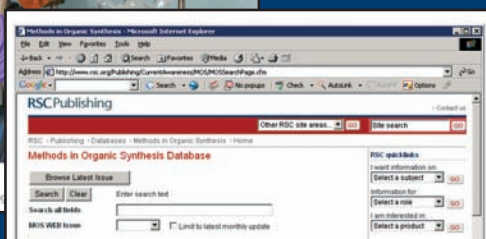


The graphical abstracting services at the RSC are an indispensable tool to help you search the literature. Focussing on specific areas of research they review key primary journals for novel and interesting chemistry.

requires specialised tools



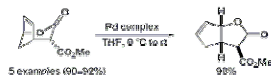
Methods in Organic Synthesis provides information on reaction schemes, new reactions and new methods. Topics include functional group changes, the introduction of chiral centres, and enzyme and biological transformations.



The online database has excellent functionality. Search by: authors, products, reaction, reactants and reagents.

59453 Tandem radical rearrangement/Pd-catalysed translocation of bicyclo[2.2.2]lactones. An efficient access to the oxatriquinane core structure
J.-H. Liao; N. Maulide; B. Augustyns; I. E. Marko*

Org. Biomol. Chem., 2006, 4(8), 1464-1467



With Methods in Organic Synthesis you can find exactly what you need. Search results include diagrams of reaction schemes. Also available as a print bulletin.